Structural and geo-environmental applications of waste quarry dust

PhD Thesis

Martins Pilegis

2014

DECLARATION

This work has not been submitted in substance for any other degree or award at this or any other university or place of learning, nor is being submitted concurrently in candidature for any degree or other award.

Signed:…… (candidate) Date: ……..

STATEMENT 1

This thesis is being submitted in partial fulfilment of the requirements for the degree of PhD.

Signed:…… (candidate) Date: ……..

STATEMENT 2

This thesis is the result of my own independent work/investigation, except where otherwise stated. Other sources are acknowledged by explicit references. The views expressed are my own.

Signed:…… (candidate) Date: ……..

STATEMENT 3

I hereby give consent for my thesis, if accepted, to be available for photocopying and for inter-library loan, and for the title and summary to be made available to outside organisations.

Signed:…… (candidate) Date: ……..

Acknowledgements

I would like to thank everyone who has helped and supported me during the PhD course.

First of all I would like to thank my family and friends for their support throughout these years.

I would like to thank my supervisors Bob Lark, Diane Gardner and Devin Sapsford for their guidance and encouragement. Also I would like to acknowledge all the laboratory staff in Cardiff University School of Engineering for the help with experimental work, Carl, Ian, Steffan, Len, Jeff, Ravi, Harry, Des.

I would like to thank industrial partners Damian Lusty and Andi Lusty from Kayasand Ltd. for their technical support, provision of manufactured sands and solving logistics issues.

I would like to acknowledge CEMEX, AI and Grace Construction Products for the technical support and guidance.

Summary

This thesis presents a study of the characterisation of fine aggregates manufactured from waste quarry material and their use in concrete supported by artificial neural network models of the fresh and hardened concrete properties. The reutilization of rock filler, a by-product of the sand manufacturing process, as a soil liming material is explored.

A set of tests and techniques were identified to characterise fine aggregates manufactured from quarry dusts via a dry processing system. Granite, limestone, sandstone and basalt manufactured sands and their unprocessed counterparts "feed quarry dusts" were characterised with respect to their shape and texture, grading and quality of fines (presence of clays). The results showed that the reprocessing of quarry dusts improves the particle shape and grading irrespective of rock mineralogy.

Plasticised and non-plasticised concrete mixes were developed and the fresh and hardened properties tested. Concrete consistency, compressive and flexural strength is correlated with the fine aggregate characterisation test results. The manufactured fine aggregates showed a higher water demand when compared with natural sand whereas compressive and flexural strengths were enhanced.

Artificial neural network models were developed to enable the prediction of the consistency and compressive strength of concrete. These models used the fine aggregate properties and mix composition parameters as input variables and were validated using a separate testing dataset, additional concrete mixes and numerical evaluation. Artificial neural network models were shown to be able to predict fresh and hardened concrete properties based on the fine aggregate characteristics.

The excess fillers created in the sand manufacturing process were evaluated for soil liming potential through standard tests and a soil incubation study. The main finding

was that materials with high silicate content exhibit a potential for liming, however, a higher dosage is required when compared to the dosage of high purity limestone to achieve the same liming potential.

Table of Contents

List of Tables

List of Figures

Glossary

The terms defined in this section will be used throughout the thesis. These might differ from the ones employed in national standards, used by industry experts or used in scientific literature due to their ambiguous perception in various fields.

Aggregate - granular material used in construction as a constituent material of concrete or mortar.

Fine aggregate (FA) – aggregate, most of which passes through a 4 mm sieve.

Coarse aggregate (CA) – aggregate, most of which is retained on a 4 mm sieve.

Filler aggregate - aggregate, most of which passes a 0.063 mm sieve, which can be added to construction materials to provide certain properties.

Fines – particle size fraction of an aggregate which passes the 0.063 mm sieve.

Natural aggregate - aggregate obtained by dredging and screening from seabed, riverbed or won from land based sand and gravel pits and that has not undergone a crushing process.

Crushed aggregate - aggregate produced by crushing and screening of rocks.

Natural sand (NS) –natural fine aggregate.

Quarry dust – rock particles that are created as a by-product in crushed coarse aggregate production.

Manufactured fine aggregate (MFA) – aggregate material passing the 4 mm sieve, processed from crushed rock or gravel with intention to be used in concrete or mortar.

Rock filler – rock particles, most of which pass a 0.063 mm sieve and that were created by crushing or milling of aggregates.

d/D mm – aggregate particle size fraction where d represents lower sieve on which the aggregate particles are retained and D is the sieve size that majority of particles pass.

1 Introduction

According to United States Geological Survey (USGS 2013) the global cement production has risen from 1.24 billion tonnes in 1992 to 3.7 billion tonnes in 2012. As the main use of cement is in concrete applications, it can be assumed that concrete production has followed a similar trend. Thus, it can be inferred that the demand for concrete aggregates has also increased.

Due to the extensive use of natural sand and gravel, deposits for aggregates in many places are being exhausted, for example, in parts of Australia (Thomas et al. 2007) and Norway (Manning 2004). Marine sand dredging in Japan was banned in 2000 followed by the halting of sand import from China in 2006 thus making Western Japan dependent on manufactured fine aggregate for concrete applications (Kaya et al. 2009). Some parts of the UK, such as in the vicinity of London and South Wales, rely on the marine dredged aggregates for construction purposes, as the demand exceeds the supply of land-won sand and gravel (Highley et al. 2007). Thus, there is a need for crushed rock aggregates around the world to address both the lack of natural reserves and to diversify the aggregate supply.

However, the production of crushed coarse aggregate is unsustainable as non-renewable materials are used and approximately 20-35% of the crushed rock ends up as fine waste or “quarry dust”. This fine waste is unsaleable or unsatisfactory for use in concrete and is stockpiled in quarries (Harrison et al. 2000). According to Mitchell et al. (2008) UK quarries annually produce 55.1 million tonnes of quarry dust. This dust increases the cost of quarry operations as the stockpiles have to be managed, moved around to access the rock below them or transported to a landfill. This imposes extra costs as well as a

negative environmental impact due to both the fuel consumed during the transportation and the airborne dust generated with this activity.

The current practice in the UK in order to deal with quarry dust is to blend it with land-won or marine dredged sand, thereby - modifying the particle size distribution until it is acceptable for concrete applications (Harrison et al. 2000). The rounded natural sand particles aid the workability of concrete which is otherwise reduced by highly angular quarry dust. However, the natural sand has to be extracted and transported to the required location. This increases the environmental impact of dredging sites and areas surrounding them and also incurs extra transportation costs. Another practice is to wash the quarry dust, thus removing the fines from it and making it compliant to the relevant technical standards with respect to particle size distribution. The fine aggregate obtained by such methods still has to be blended with fine natural sand to aid concrete workability and finishability which deteriorates due to the quarry dust particle angularity. The washing of quarry dust uses water, which in some parts of the UK is seasonally restricted due to droughts, furthermore, settling ponds have to be installed in the quarry to capture the silt and clay removed during the washing process.

In the UK Mitchell et al. (2008) recommend minimising the production of quarry dust by quarry optimisation and using crushers at settings that reduce the quantity of fines generated. However, they note that using crushers at these settings can negatively affect the shape of aggregates. Such a solution might reduce the quarry dust production, however, the resulting aggregates are generally of poorer shape and have a negative effect on the quality and workability of concrete. Thus, the concrete industry has to look for remedies for poor quality aggregates, which in turn may increase the cost of the end product.

In summary, the presence and use of crushed aggregates in the UK is unavoidable due to the demand from the construction industry and the lack of alternative substitute for concrete aggregates. The quarrying industry generates quarry dust which is typically 20 to 35 % of the raw rock feed weight. This dust has low economic value and is sometimes considered as waste. The management and utilization of this waste increases the costs as well as having negative impacts on the environment. Following current practice, utilization of the quarry dust in concrete requires natural sand for blending.

However, the negative impacts could be minimised by reprocessing the quarry waste into a quality fine aggregate for use in concrete. Such a solution has the potential to reduce the waste and increase the efficiency of the quarry industry as well as reduce the demand and thus the environmental impact of natural sand extraction.

Faced with a ban on marine sand dredging a Japanese company KEMCO has designed a dry sand manufacturing system that is claimed to produce well shaped and graded sand from quarry dusts irrespective of the type of rock. The sand produced is deemed to be usable in production of concrete without blending with natural sand. This could provide an opportunity to reuse the quarry waste, reduce natural sand demand and increase the yield from quarries, resulting in economic and environmental benefits.

1.1 Aims and objectives

This study focused on the use of manufactured fine aggregate (MFA) as a fine aggregate in concrete as a complete replacement for natural sand and sand blends. It also examined the geo-environmental applications of the rock filler generated in the production of the MFA.

The MFAs are reluctantly accepted in the concrete industry, primarily due to their inferior shape and grading when compared to a marine dredged natural sand, as well as the potential presence of clays and silt. However, there may be beneficial effects in terms of concrete strength, durability and a more sustainable quarrying and concrete industry. Thus, it is necessary to be able to define and measure the physical and chemical properties of MFA and correlate them to concrete performance. This leads to the first aim of the study:

To identify techniques that can be used to characterise the physical and chemical properties of MFAs.

This aim was achieved through the following objectives of the study:

- To identify and select appropriate tests which describe the properties of fine aggregates.
- To carry out selected tests and evaluate the results for sands with varying mineralogy.

In order to correlate the fine aggregate characterisation test results with concrete performance, concrete mixtures had to be made and tested for relevant parameters. Thus, the second aim of the study was:

To investigate the fresh and hardened properties of concrete made with MFA.

In order to do this, the following objectives were established for the study:

- To investigate the performance of MFA concrete mixtures made with constant slump (Stage I).
- To investigate the performance of MFA concrete mixtures made with constant w/c ratio (Stage II).
- To evaluate the performance of MFA concrete with respect to the characterisation test results.

Acknowledging the fact that it was impossible to test every possible mineralogy and type of MFAs, there was a need to extrapolate the identified correlations and interrelationships between aggregate properties and concrete performance to a wider range of MFAs. This allowed both concrete producers and the quarry industry to evaluate the feasibility of particular quarry dust or MFA to be used in concrete applications. Three major parameters of concrete were of particular interest – consistency, compressive strength and durability. It may be assumed that if the quarry produces coarse aggregates that have been successfully used in concrete, then the corresponding quarry dust should not pose a threat to concrete durability. Other durability issues could be addressed by appropriate cement blend selection. Therefore consistency and compressive strength were the main parameters of interest. Therefore, the third aim of the study was:

To develop a model which predicts compressive strength and consistency of MFA concrete mixture.

The following objectives were set in order to achieve the above mentioned aim:

- To identify and select an appropriate modelling technique and relevant input and output variables.
- To develop and validate the model with existing data and trial mixtures.
- To numerically evaluate the model's predictions with known theoretical relationships.

During the manufacture of sand by reprocessing a quarry dust a very fine powder or rock filler, in which majority of particles passed a 63 micron sieve, was produced. This was a waste material and had to be disposed of or reutilized. In order to make the sand manufacture process more efficient and environmentally sustainable, finding a potential

application for large quantities of rock powder was essential. Thus, the fourth aim of the study was:

To identify and evaluate the feasibility of a geo-environmental application of waste rock filler.

This aim was achieved through following objectives:

- To identify a potential application for large quantities of rock filler.
- To characterise rock fillers with respect to relevant physical and chemical properties for particular application.
- To investigate efficiency of the fillers for potential application in laboratory trials.

1.2 Thesis outline

This thesis is divided into seven chapters with five appendices. Chapter 2 reviews the current literature on the influence of aggregate characteristics on fresh and hardened properties of concrete. It also covers the manufacture, requirements and use of MFA in concrete applications and associated effects on strength, consistency and durability of the resulting concrete. A review of modelling of concrete properties based on aggregate characteristics and mix composition is presented.

Chapter 3 presents a detailed overview of the methods and results of the MFA characterisation study. It compares the properties of MFAs to those of natural sand and quarry dusts and discusses the expected effects of the MFA characteristics on fresh and hardened properties of concrete.

The methodology and results of the MFA concrete study are presented in Chapter 4. Constant slump and constant w/c ratio concrete mixes are investigated and the fresh and

hardened concrete properties are discussed with respect to the characterisation test results and with reference back to published literature regarding the use of MFAs in concrete.

Chapter 5 presents the development and validation of artificial neural network (ANN) models that predict 28 day compressive strength and slump values for concrete mixtures. These models use the fine aggregate properties and concrete mix composition presented in Chapters 3 and 4 as input parameters. The models are validated with data which was not employed in the model development and additional concrete mixes created specifically for this purpose. Finally, the predictions of these models are evaluated numerically with respect to relationships between the input parameters, consistency and compressive strength, as identified in Chapter 2.

An evaluation of the feasibility of using rock filler as a soil liming material is presented in Chapter 6. It starts with a literature review of soil pH and liming with conventional liming materials as well as rock powders. This is followed by an overview of test methods and results of filler characterisation. The effects on soil pH are investigated through 28 day soil incubation experiments and the results presented and discussed.

Finally, conclusions are drawn from the studies performed in the thesis and a number of recommendations for future work are given in Chapter 7.

2 Literature review

Concrete is a composite material usually made from cement, inert aggregate and water. In most applications around 70% of concrete is composed of aggregate. Therefore, it is not surprising that the aggregate greatly influences the performance of concrete. Aggregates may not only limit the strength of concrete but its properties affect the durability and structural performance of concrete (Neville 1995). Aggregate is generally considered as a cheap and inert material and is incorporated within the concrete mix due to economic considerations. However, there are other benefits of using aggregates within concrete such as increased volume stability and better durability than that of cement paste alone.

Usually the aggregates are divided into three categories: coarse, fine and filler aggregate. Within the British Standards BS EN 12620:2002 these fractions are defined by aggregate particle sizes. The majority of coarse aggregate particles should not pass the 4mm sieve, whilst the major proportion of fine aggregate particles pass through 4mm sieves and filler aggregate consists of aggregate most of which passes the 0.063mm sieve. In other countries the limits for these fractions differ slightly, for example, in the USA filler aggregate is defined as passing the 0.075mm sieve and the division between coarse and fine aggregate is made at 4.75mm. This division is imposed as the various aggregate size fractions might influence the concrete in different ways.

In order to ensure the quality of the resulting concrete, a series of specifications for aggregates have been developed and provided within various national standards. However, it is not always true that an aggregate which does not conform to the

specifications makes poor concrete, but an aggregate found to be unsound in more than one parameter is unlikely to make satisfactory concrete (Neville 1995).

Another division between aggregates is whether they are natural or crushed. Natural aggregates are usually dredged sand or quarried gravel from existing deposits, whereas crushed aggregates are made from rocks mechanically broken down to the desired size. The most obvious differences between them are particle shape and texture. Natural aggregates tend to be rounded in shape and have a smooth surface as they have undergone long weathering and abrasion processes, whereas crushed rocks tend to be angular and rough due to the mechanical crushing process. These and other characteristics of aggregates influence the consistency, strength and durability of concrete.

This literature review will explore various properties of aggregates and their effects on concrete performance and compile the views expressed in scientific papers. Furthermore it will summarise the requirements and recommended tests for MFA presented in European Standards, published documents and research reports. Also modelling techniques that have been used to link aggregate properties to concrete performance will be reviewed.

2.1 Aggregate characteristics and their effects on concrete properties

2.1.1 Shape and texture

It is hard to describe the shape of three dimensional objects and therefore it is convenient to define certain geometrical characteristics of such bodies. These are usually roundness, sphericity and form.

Roundness measures the relative sharpness or angularity of the edges and corners of a particle. It is largely controlled by the strength and abrasion resistance of the parent rock as well as the wear to which the particle has been subjected (Neville 1995). In the former British Standard BS 812:Part 1:1975, a broad classification of roundness was specified which is reproduced in Table 2.1.1. However, in the European standards this classification has been withdrawn and the test most commonly used is the shape index for coarse aggregate (BS EN 933-4:2008), which is the mass of particles with a ratio of length to thickness more than three expressed as a percentage of the total dry mass of particles tested. The particle shape classification sometimes used in the United States according to Neville (1995) is presented in Table 2.1.2.

Table 2.1.1 Particle Shape Classification of BS 812:Part 1:1975

Classification	Description
Rounded	Fully water-worn or completely shaped by attrition
Irregular	Naturally irregular, or partly shaped by attrition and having round edges
Flaky	Material of which the thickness is small relative to the other two dimensions
Angular	Possessing well-defined edges formed at the intersection of roughly planar faces
Elongated	Material, usually angular, in which the length is considerably larger than the other two dimensions
Flaky and elongated	Material having the length considerably larger than the width, and the width considerably larger than the thickness

Table 2.1.2 Particle shape classification sometimes used in US (Neville 1995)

Classification	Description
Well-rounded	No original faces left
Rounded	Faces almost gone
Subrounded	Considerable wear, faces reduced in area
Subangular	Some wear but faces untouched
Angular	Little evidence of wear

Sphericity is defined as the function of the ratio of the surface area of the particle to its volume. It is related to the bedding and cleavage of the parent rock, and is also influenced by the crushing equipment when the size of particles has been artificially reduced (Neville 1995).

The surface texture of aggregates depends on the hardness, grain size and pore characteristics of the parent material, as well as the degree of wear or other forces which have been acting on the particle (Neville 1995). Visual estimation of surface roughness is quite reliable and a classification of this is been given in BS 812:Part 1:1975 (reproduced in Table 2.1.3). However, the former standard has been superseded by European standards which do not include this classification.

Table 2.1.3 Surface Texture of Aggregates from BS 812: Part 1: 1975

Surface Texture	Characteristics
Glassy	Conchoidal fracture
Smooth	Water-worn, or smooth due to fracture of laminated or fine-grained rock
Granular	Fracture showing more or less uniform rounded grains
Rough	Rough fracture of fine- or medium- grained rock containing no easily visible crystalline constituents
Crystalline	Containing easily visible crystalline constituents
Honeycombed	With visible pores and cavities

The shape of aggregate can affect water demand and consistency, bleeding, finishability and strength. According to Newman and Choo (2003) coarse aggregates with equidimensional (possessing comparable dimensions in three axes e.g. sphere or cube) particle shape are preferred as particles deviating from this shape have a larger surface area and pack in an anisotropic manner. Flaky and elongated particles especially tend to reduce the consistency, increase the water demand for constant consistency and may also have a negative effect on durability as bleed water and air bubbles tend to form underneath them.

Marek (1995) reported that, especially in high strength concrete, angular particles will produce higher strength as opposed to spherical aggregate particles. This is attributed to the fact that angular particles possess a larger surface area, therefore, allowing a higher adhesive force to develop between the aggregate particles and the cement matrix. Similar observations were made by Özturan and Cecen (1997). They found that for high strength concrete an angular crushed aggregate produced higher compressive and flexural strengths than coarse gravel aggregate. The positive effects on compressive strength due to angularity and rough surface texture are also shown by Newman and Choo (2003). They reported that for higher strength concretes the best results are achieved with increased angularity of coarse aggregate. However, they also stated that for the low and medium cement contents, the smooth and rounded marine gravel exhibited a lower water demand for a given consistency than crushed rock due to it having a smaller surface area to wet, thus allowing a lower water to cement ratio for the same consistency, which in turn would result in higher strength.

In terms of fine aggregates, it was shown by Korjakins et al. (2008) that increasing the levels of replacement of rounded natural sand with angular dolomite sand resulted in

lower slump values for mortar and normal strength concrete mixes. However, even with increased water to cement ratios the strength of the mortar and concrete was the same or higher. These findings for normal strength concrete are contradicted by Donza et al. (2002, p. 1756) who stated "The effect of shape and surface texture of fine aggregates on mechanical properties is often not a factor in conventional concretes (30–40 MPa), although these properties may cause an increase in the water demand. For these concretes, the hydrated cement paste and the transition zone around the aggregate are relatively weak. Consequently, the water/cement (w/c) ratio controls the mechanical properties of concrete for the same degree of hydration."

According to Neville (1995) angular fine aggregate particles increase the water demand for a given consistency as the surface area of particles is greater than that of equidimensional ones, therefore, more water is required to wet the entire surface of the aggregate. The surface texture of the aggregate affects its bond to the cement paste and also influences the water demand of the mix, especially in the case of fine aggregate.

In a study by Jackson and Brown (1996) the particle shape of the fine aggregate was found to influence the void space in the aggregate. As the particles become more non-spherical, the void space increases. Thus, they suggested that the potentially adverse consequences of crushed particles can be overcome by increasing the fines content in the fine aggregate. These in turn fill the voids between the angular particles and lubricate the mix.

Most researchers are in agreement that angular and rough particles decrease the consistency of the concrete mix and exhibit increased water demand due to higher voids content and surface area when compared to rounded aggregates. However, the

compressive and flexural strength is expected to be higher due to better particle interlock and a larger bond area between the aggregate and the cement matrix. Equidimensional or nearly cubical particles are preferred as these have a balance between surface area and angularity.

It has to be noted that even though the particle shape of fine aggregate influences the properties of concrete, an objective method for measuring and expressing shape is not yet available according to Neville (1995). Thus, the effects on the strength or water demand cannot be quantified in terms of aggregate shape. Recent attempts by Cepurits et al. (2014) have shown that some techniques show promise for filler and fine aggregate shape characterisation, for example, Dynamic Image Analysis and X-ray microcomputer tomography combined with spherical harmonic analysis, however, these require specialised equipment and software.

2.1.2 Particle size distribution

Particle size distribution, also known as grading, is the division of aggregate particles according to various size fractions. Usually this is evaluated using a set of sieves with defined aperture sizes and a shaker. According to the European standard BS EN 933-1:1997 there are two methods, wet and dry sieving using a standard set of sieves. The results are usually plotted on a graph with a logarithmic scale where the abscissa is the sieve size and the ordinate is the percentage of aggregate particles passing this sieve size.

There is a distinction between continuously and gap graded aggregate. This is shown in Figure 2.1.1. A gap grading can be defined as a grading where one or more intermediate size fractions are omitted, whereas in continuous grading all particle size fractions are present (Neville 1995).

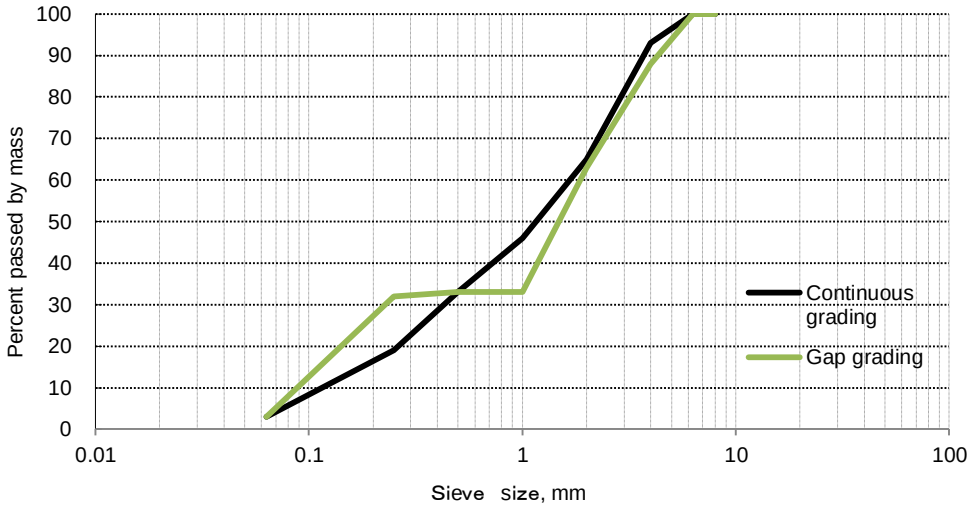

Figure 2.1.1 Continuous and gap grading curves

The grading or particle size distribution of the aggregate affects the consistency of concrete, which, in turn, influences water and cement requirements, controls segregation and has some effect on the bleeding, placing and finishing of the concrete. These characteristics of fresh concrete affect the strength, shrinkage and durability of hardened concrete. Segregation and bleeding are hindered by interlocking of larger aggregate particles and surface forces of attraction for smaller particles. Therefore, the major causes of segregation and bleeding are poorly graded aggregates and excessive water contents (Newman and Choo 2003).

Meddah et al. (2010) concluded that in normal strength concrete the highest strength can be achieved by continuous grading for the same aggregate content. This was attributed to the higher compactness of the aggregate particles as opposed to a gap grading. However, better strength in high strength concrete was obtained by a gap graded aggregate.

Variations in grading can influence the voids content of the fine aggregate, therefore affecting the paste volume necessary to fill the voids and additional amounts to float the

coarser aggregate particles, thereby providing consistency to the mixture (Marek 1992). Marek also concluded that if a grading suitable for relatively spherical particles is employed for an aggregate containing a high volume of non-spherical particles the resulting concrete might perform less satisfactorily than expected. Therefore, concrete should be designed to have a minimum amount of voids in the aggregate combination employed to minimize the water requirement, shrinkage and provide maximum strength.

According to Neville (1995) grading requirements should depend on shape and surface texture of the aggregates. For sharp and angular particles slightly finer grading should be employed to reduce the interlocking possibility and compensate the high friction between particles. Also higher amounts of fine aggregate should be used if a crushed and angular coarse aggregate is present in the mix. It follows that for a fine grading of fine aggregate the fine to coarse aggregate ratio should be decreased.

It appears that there are general guidelines for grading of aggregates, however, the exact grading and combination of aggregates should be estimated based on the properties of aggregates such as shape, texture and packing density as well as on the experience obtained from using a particular aggregate in concrete. Thus, the concrete mix proportioning requires a trial and error approach.

2.1.3 Maximum aggregate size

The larger the aggregate particles, the smaller the surface area to be wetted and covered by cement paste in a concrete mix. Therefore, an increase in aggregate size causes a reduction in the water requirement for a specified consistency and cement content. This in turn results in a lower water to cement ratio, increasing the strength of the concrete. However, experimental results show that for cement contents larger than 300 kg/m^3 the best results are achieved when the maximum size of the aggregate is around 38 mm, as

the benefit from the water requirement reduction is offset by a smaller surface area. For leaner mixes the increase in maximum aggregate size results in a higher strength, but there are limitations in maximum aggregate size for structural concrete related to the thickness of the section and spacing of reinforcement (Neville 1995, Newman and Choo 2003).

In a study by Meddah et al. (2010) when a constant cement content was used it was found that the compressive strength of normal strength concrete was increased by allowing a larger maximum size aggregate to be incorporated in the mix, although for high strength concrete an opposite trend was observed. It is speculated that for normal strength concrete the weakest part of the material is the transition zone between the aggregate and cement paste. Therefore, a larger maximum size aggregate reduces the surface area and transition zone decreasing the volume of the weakest phase within the mix. In high strength concrete the weakest phase is considered to be the aggregate bulk. Thus, larger coarse aggregate particles result in a higher probability of crack initiation through them and consequently a reduced compressive strength.

2.1.4 Absorption and water content of aggregate

The water absorption of aggregate is defined as the moisture content that the aggregate can hold within its pores to reach a saturated but surface dry state. The water content of the aggregate is the amount of water which is held within the particle pores as well as that which adheres to the surface of the aggregate. Figure 2.1.2 illustrates the different moisture states of aggregates. The absorption and water content is important for concrete mixes as they influence the effective water to cement ratio as well as consistency. In BS EN 1097-6:2000 the water absorption and content is expressed as a percentage of oven dry aggregate mass.

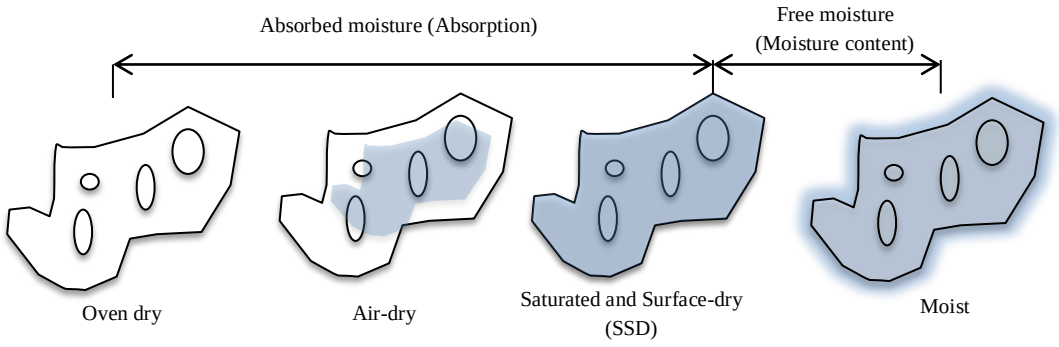

Figure 2.1.2 Diagrammatic representation of moisture in aggregate.

It is traditionally assumed that the aggregate in a concrete mix achieves a saturated and surface dry state (SSD) (Neville 1995). Therefore if an aggregate in an oven dried (OD) state is used in concrete, additional water will be required to achieve the given water to cement ratio as some of the water will be absorbed into the aggregate from the mix. Moreover this water absorption will result in a small decrease in consistency. On the other hand an aggregate with a water content larger than the absorption capacity will increase the effective water to cement ratio in the mix and consequently increases its consistency and decreases strength. Due to these considerations the amount of water added to the mix has to be modified according to the water content and absorption capacity of the aggregate. However, the absorption of water by dry aggregate within the mix is slowed down or stopped due to the coating of particles with cement paste. Such behaviour is most common with coarse aggregate as water has to travel a larger distance in order to saturate the larger particles.

Poon et al. (2004) investigated the influence of different aggregate moisture states on the consistency measured via the slump test and compressive strength of concrete. It was found that the initial slump of the mix depended on the free moisture within the mix. The initial slump of the concrete with oven dried aggregates was higher than that of air dry or saturated and surface dry aggregates. This was attributed to the fact that

extra water was added to the mix to compensate for the absorption capacity of the aggregate, but the rate of absorption is a time dependent process and therefore a large portion of the additional water contributed to the mix consistency.

The compressive strength at 28 days was found to be similar for air dry and SSD aggregate but for OD aggregate it was much lower. This may have been due to the higher initial w/c ratio in conjunction with a blockage of absorption by a coating of cement paste. Another hypothesis is that a better bond is developed between the cement matrix and aggregates in SSD conditions. Similar results were obtained by Alhozaimy (2009) who investigated the effects of absorption and water content in limestone aggregates. He concluded that the initial slump was increased for higher levels of initial free water. Furthermore, it was found that most of the absorption takes place during the first 15 minutes after mixing and the limestone aggregate in this case absorbed 75% of their capacity. Also the strength of the concrete was lower for dry aggregates in comparison with wet ones and this was attributed to the higher effective water/cement ratio as the extra water was not fully absorbed.

In a study by Lo et al. (2008) the effects of lightweight aggregates with a high water absorption capacity on the interfacial zone in concrete was investigated. It was concluded that lightweight aggregate with a greater absorption capacity will result in a more porous interfacial zone which eventually negatively affects the concrete strength. Furthermore, it was found that an increase in w/c ratio from 0.4 to 0.48 did not affect the pore size in the transition zone.

It can be concluded that care should be exercised regarding the water content and absorption capacity during the concrete mixture proportioning and mixing as these aggregate parameters can influence the fresh and hardened concrete properties. The

effects of different moisture states could be overcome by adding some of the mixing water to the aggregates prior to the addition of cement into the mixer, thus saturating them to the SSD state before they are covered in cement paste.

2.1.5 Mineralogy and coatings

Aggregates with different mineralogy can produce concretes with a variety of properties. The type of the parent rock will influence the physical and chemical properties of the aggregate as well as particle shape and texture if a crusher is employed to reduce its size. The mineralogical description of the aggregates cannot be used alone to estimate whether it will produce a good concrete or not as there are many other factors which in some cases have a more dominant effect (Neville 1995). However, the chemical and mineralogical composition can be used as a tool to identify minerals which might interfere with the hydration of cement or cause alkali-silica or alkali-carbonate reactions. The mineralogical composition can also be used to identify the presence of clay minerals.

Aggregate particles might be covered by clay, silt or crushing dust coatings. These can inhibit the bond between the aggregates and cement paste as well as increase the water demand. These will be discussed in more detail in section 2.1.7. However, if the coatings are physically and chemically stable and do not pose a threat to concrete properties, there is no objection to using such aggregates (Neville 1995).

2.1.6 Bulk density and voids content

Bulk density is the mass of aggregate particles filling a container of unit volume. It depends on the particle shape, grading, surface texture and compaction of the aggregate. The higher the bulk density, the less voids are present in the aggregate. The voids ratio for given aggregate can be expressed by formula given in equation 2.1.1.

$$voids\ ratio = 1 - \frac{bulk\ density}{specific\ gravity \times unit\ mass\ of\ water}$$ Equation 2.1.1

The voids content shows how much free volume is present in an aggregate for a given compaction. In a concrete mix the voids have to be filled with cement paste or smaller aggregate particles. More angular particles usually result in higher voids contents (Neville 1995). Concrete should be designed to have a minimum amount of void space in fine and coarse aggregate combinations in order to reduce the water requirement, minimise concrete shrinkage, and provide maximum flexural and compressive strength for a given cement content (Marek 1992).

Inclusion of a high percentage of suitably graded particles with a good shape and size less than 0.075mm allows for higher aggregate packing and results in a denser concrete mix. Denser concrete will be more durable and less permeable due to the filling and closing of capillary channels with fine particles (Hudson 1997). However, concrete mixtures designed for maximum packing density are very coarse, prone to segregation and present poor consistency. A more desirable mixture has a uniform grading while maintaining a high packing density (Quiroga 2003).

2.1.7 Fines content

Fines in BS EN 12620:2002 are defined as aggregate particle size fraction passing the 0.063 mm sieve. In aggregates these can be very fine sand, silt, dust or clay. According to Newman and Choo (2003) a moderate fines content is beneficial in concrete as it fills the voids in the mix and aids cohesion and finishability. However, excessive fines content can increase the water demand and reduce the aggregate-cement paste bond which in turn results in reduced strength. It is said that especially clay and silt particles within the aggregate are detrimental to the concrete as they can form coatings on aggregate particles inhibiting the bond between the aggregate and the cement paste reducing the strength and durability of the concrete. Also, due to their intrinsic large

specific surface area, silt and clay increase the amount of water necessary to wet all particles in the mix. Furthermore, some clays exhibit an expansive nature when in contact with water. This detrimentally affects the hardening of concrete and its strength (Neville 1995).

Norvell et al. (2007) investigated different types of clay and clay-sized particles replacing up to 4% of the fine aggregate in mortars and reported the corresponding effects on consistency and strength. It was concluded that clays increase water and superplasticiser demand in accordance with their interlayer absorption and cation exchange capacity, whereas clay-sized particles do not significantly affect the water and admixture demand at the levels studied. Montmorillonite (smectite) was found to have the highest absorption, followed by illite and kaolinite clays. At the same w/c ratio illite and kaolinite did not affect the compressive strength of mortars as opposed to montmorillonite clay which resulted in a much lower compressive strength, although this might have been side effect of an excessive dose of superplasticiser to achieve constant slump, thus delaying the cement hydration. Partial replacement of the fine aggregate with clay-sized particles did not affect the compressive strength.

Similar conclusions were made by Fernandes et al. (2007) who investigated clay contaminated sands on concrete strength and consistency. It was found that all types of clay increased the water demand for constant consistency and the compressive strength depended on the corresponding increase in w/c ratio, except for montmorillonite clay. It was suggested that this type of clay has an effect on the fundamental strength of hydrated paste. However, it was found that at higher w/c ratio satisfactory concrete blocks or mortar not requiring coarse aggregates can be made.

Clay and silt are often present in natural sand or gravel aggregates. In various national standards there are limits of the amount of fines content in aggregate and historically they have been imposed to limit the clay and silt particles in aggregates. However, within a crushed rock coarse aggregate or sand the smaller particles tend to be dust created during the manufacturing process which is not necessarily detrimental to the concrete. A substantial amount of research has been carried out to investigate the effects of crushed mineral fines on concrete and demonstrate that higher permissible levels of fines could be allowed in national standards. However, the published information is sometimes contradictory and results vary from paper to paper. This is discussed in more detail in the following paragraphs.

Kronlöf (1994) obtained some interesting results on the effects of fines in concrete with a maximum aggregate size of 6mm. It was concluded that mixes with low binder amount, irregularly shaped aggregates, and large superplasticiser dosages benefited the most from the addition of the fines. The resulting effects were found to be reduced water requirement due to improved particle packing, increased strength due to smaller water requirement and improved interaction between paste and aggregate, decreased porosity and better consistency, especially in very lean mixtures. Lean mixes are defined as having a cement content less than 275 kg/m^3. Similar conclusions were presented by Jackson and Brown (1996) where the use of higher fines in Portland cement concrete was discussed and investigated. They concluded that the material passing the 75 micron sieve provides additional paste in lean mixes making them more workable and finishable.

Celik and Marar (1996) examined the effects of crushed stone filler aggregate replacing part of the fine aggregate in a concrete mix. It was observed that the slump decreased

with increased filler aggregate content. This was attributed to the increase in fineness and total surface area of the aggregate requiring more water for a specific consistency. Compressive and flexural strengths were at a maximum for inclusions of 10% of filler aggregate in the mix. The increase was attributed to the void filling capacity of the fines, whereas for higher replacement levels there was insufficient paste to cover all the aggregate particles leading to lower strength. Drying shrinkage was found to follow the trends of concrete strength – increasing and decreasing with strength respectively. However, the coefficient of permeability was found to decrease with higher amounts of filler aggregate content due to blockage of the capillary pores in the hardened concrete. It has to be noted that the concrete mix contained 420 kg/m^3 of cement with a constant w/c ratio of 0.5, therefore, is strictly not a lean mix, where according to Kronlöf (1994) most of the benefit of the filler aggregate can be seen.

In a similar study, Topçu and Uurlu (2003) replaced up to 15 % of fine aggregate by a limestone filler aggregate in 3 mixes with cement contents of 200, 275 and 350 kg/m^3. The slump was kept constant and a higher water demand was observed with the addition of filler aggregate irrespective of cement content which contradicts the findings of Kronlöf (1994). The paper did not include any discussion on the reasons behind such behaviour, but it is proposed that this could be due to the increased specific surface area of the aggregate combination. The best compressive and flexural strength results were obtained for replacement levels of 7 and 10% of filler aggregate irrespective of cement content and increased w/c ratios. The permeability of concrete was decreased as the level of fines increased.

In a study by Quiroga (2003) it was concluded that the amount of fines had a very important effect on mortar and concrete consistency. In general, the higher the fines

content, the higher the water demand as reported by Topçu and Uurlu (2003) and Celik and Marar (1996). All identified that the type of fines had an effect on the fresh and hardened properties of concrete. In Quiroga's study limestone fines led to a lower water demand in comparison to granite and trap rock (basaltic igneous rock) fines whereas the concrete strength was the highest for trap rock fines.

A study by Jones et al. (2003) explored the filler aggregate content requirements in order to reduce the voids content in concrete by laboratory trials and theoretical calculations using particle packing models. It was found that the quantity of filler aggregate content that led to the lowest water content is less than the quantity of filler aggregate content that gives the minimum voids ratio calculated by the packing models. This is attributed to the agglomeration of the filler aggregate particles and the effects of increased specific surface area. They also found that the void reduction or increase and the subsequent effect on water demand in the cement and aggregate systems depends on several factors: original cement content of the mixture, shape of the filler aggregate particles, particle size distribution of the filler aggregates and usage of plasticisers. Their conclusions somewhat explain the contradictions in the findings of other researchers, although they suggest that further research efforts in this area are still required.

In summary, the inclusion of very fine aggregate particles in lean concrete mixes made with highly angular aggregate particles is beneficial for the consistency and packing density, and result in improved strength and permeability characteristics. However, there is an optimum content beyond which the increased relative surface area of the aggregates outweighs these beneficial effects and leads to higher water and cement paste demand. In high strength and cement rich concretes the optimum value of fines

content is relatively small compared to lean mixes. However, if the fines contain clay particles, then even small quantities of fines lead to significantly increased water demand and can affect compressive strength depending on the clay type.

2.2 Manufactured fine aggregates

This section will look at the production of MFAs, research which has investigated the performance of MFA and its effects on fresh and hardened properties of concrete and mortars. It will be divided into sub sections covering various properties of concrete presenting and discussing the observations and conclusions of different research studies.

Fine aggregate for concrete can be broadly divided in three groups – natural, manufactured and recycled. Natural fine aggregates or natural sands are usually obtained from marine dredging or won from land-based sand pits and have not undergone a crushing process. Manufactured fine aggregate (MFA) is obtained through mechanical crushing of rocks. Here it will be defined as aggregate material passing the 4 mm sieve, processed from crushed rock or gravel with intention to be used in concrete or mortar. Recycled aggregates are usually obtained by crushing of demolition waste. These definitions differ from the ones provided in BS EN 12620 and are deliberately chosen for the purposes of this thesis.

As natural resources are being depleted or a resistance to the usage of dredged sand due to environmental concerns is met, an alternative source of fine aggregate has to be found. One such source is the crushed rock material from stone quarries. However, the material produced differs in characteristics from natural sands. The major variations are shape and texture, grading and amount of fines. These are common characteristics which can detrimentally affect concrete as discussed previously in this chapter, therefore MFAs are only reluctantly accepted within the industry (Harrison et al. 2000).

The shape typically is highly angular, elongated or flaky. As discussed in section 2.1.1 this characteristic highly influences the fresh and therefore hardened properties of concrete. MFA shape depends on the parent rock and to large extent on the crushing method (Ahn and Fowler 1999, Manning 2004).

Typical gradings of quarry dusts do not conform to the requirements of national standards. These types of aggregate can produce harsh mixes with bleeding problems if it is washed and screened to fit into the prescribed limits (Harrison et al. 2000). This is mainly due to an excess of fine particles passing the 63µm sieve and a deficiency of particles in the size range 0.3mm to 1mm. Thus quarry dusts are commonly used in blends with fine natural sands to improve the consistency of concrete mixes. Limitations and requirements for MFAs by national standards will be briefly discussed in section 2.3.1

Manufactured fine aggregates typically contain 10 to 20% of material passing the 75µm sieve (Ahn et al. 2001). As discussed in section 2.1.7 fines affect fresh and hardened properties of concrete and can be both beneficial and detrimental. Historically national standards limited the permissible level of fines as most commonly these were clays and silts in natural sands. However, the fines present in MFA are usually the dust of fracture (Hudson 1997).

2.2.1 Aggregate production

Hard rock quarries are the main source of coarse aggregates for various construction applications. The main product particle sizes usually are in range from 4 to 40mm. Production of the coarse aggregate generates quarry dust. These quarry dusts usually pass 4 mm sieves and the particles are with angular shape and large proportion fines.

Due to these properties this material is hard to sell and use in the construction industry without further processing, classification, washing or blending.

A typical quarry setup will have three or four subsequent crushing and screening stages in order to reduce and classify the rock into the required size fractions. The individual setup and choice of crushers will vary based on the type and properties of the rock, volume to be produced, required size fractions, layout of the quarry and decisions made by the quarrying company regarding quality of end products and economy. Table 2.2.1 shows the typical crushers employed in each crushing stage, feed and product size ranges.

Two important parameters for crushers are reduction ratio and feed conditions. Reduction ratio is the ratio between the feed and crushed product size. The calculation uses particle sizes which are larger than 80% of feed and crushed product material. The reduction ratio affects the amount of quarry dust produced as well as the shape of the crushed aggregate. A smaller reduction ratio will lead to less quarry dust and usually better shape, however, in order to acquire the required size fractions more crushing stages are necessary. Thus the efficiency of such a setup is questionable due to power consumption and quarry dust production in the subsequent crushing stages. Feed conditions can be classified as either “choke feeding”, whereby the operation of the crusher occurs with the crusher chamber being completely full, or “trickle feeding” or “starve-fed” where the crusher chamber is not fully filled with rock fragments. Feeding conditions affect the shape and amount of quarry dust produced.

Table 2.2.1 Typical crusher types by stage, feed and product size range (Mitchell et al. 2008)

Crushing stage	Crushing equipment	Maximum feed size (mm)	Maximum crushed product size (mm)
Primary	Jaw crusher Gyratory crusher	700-1000	100-300
Secondary	Cone crusher HSI crusher	100-250	20-100
Tertiary	Cone crusher VSI crusher	14-100	10-50
Quaternary and subsequent stages	VSI crusher Cone crusher	10-40	10-20

Jaw crushers consist of two plates between which the crushing of aggregates takes place. One is fixed while the other opens and shuts thus exerting a compressive force on the rock while it travels in a downward motion as shown in Figure 2.2.1. This type of crusher is employed in the primary crushing stage. The optimum conditions for the jaw crusher is a reduction ratio of 6:1 operating in a choke-fed mode (Mitchell 2007). The best particle shape is obtained for particle sizes near that of the closed side setting (the gap at the bottom of the crushing chamber).

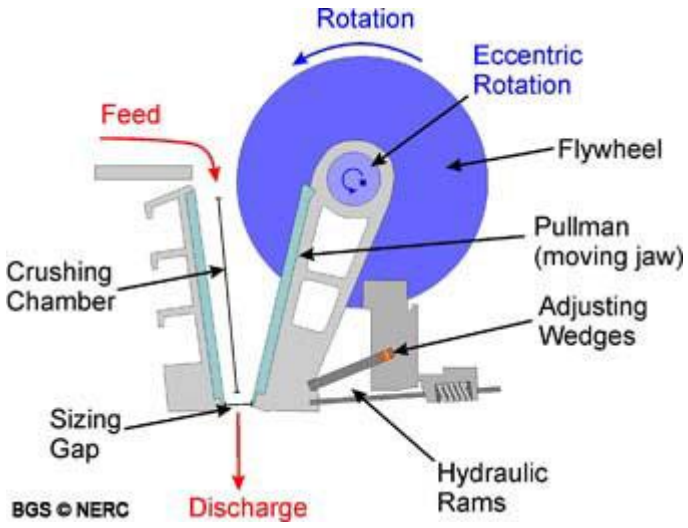

Figure 2.2.1 Diagram of jaw crusher (BGS 2013)

Gyratory crushers consist of an eccentric steel cone and fixed mantle and are similar to cone crushers with an operational principle as shown in Figure 2.2.2. The rotation of the cone causes the gap between the mantle and the cone to open and close thus crushing the feed material which travels downwards until the size is sufficiently reduced to exit the crusher (Manning 2004). These are typically used in primary crushing stage.

Cone crushers use the same principle as gyratory crushers but with smaller cone, larger "throw" (travel distance between the cone and fixed sides) and higher operational speed (Manning 2004). These crushers are usually used in secondary and tertiary crushing stages due to their ability to produce cubical shape aggregates with less fines in comparison to impact crushers when choke fed. However, the shape from cone crushed material becomes more irregular for particle sizes further away from the closed side setting (Gonçalves et al. 2007).

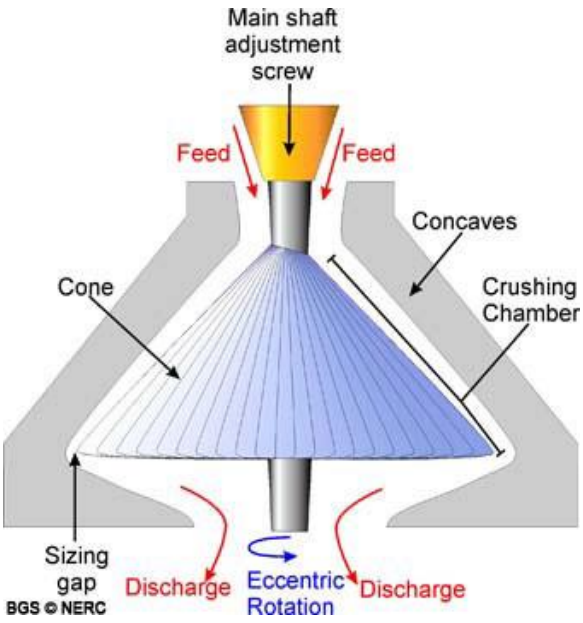

Figure 2.2.2 Diagram of cone crusher (BGS 2013)

Impact crushers propel aggregate particles at metal plates or into a cloud of rock particles in the crushing chamber thus inducing crushing of the particles along the natural cleavage planes as well as attrition. The operational principles are shown in

Figures 2.2.3 and 2.2.4 for horizontal shaft impact (HSI) and vertical shaft impact (VSI) crushers, respectively. These crushers are commonly used in tertiary and subsequent stages when good particle shape is required, however, the improvement in shape comes at a cost of increased fines production. The rotor speed in these crushers dictates the reduction ratio, particle shape as well as the amount of fines produced. Higher speeds will lead to a higher reduction ratio and more rounded, equi-dimensional particles simultaneously increasing the fines output. Thus, it is important to have a balance between the desirable particle shape and amount of fines.

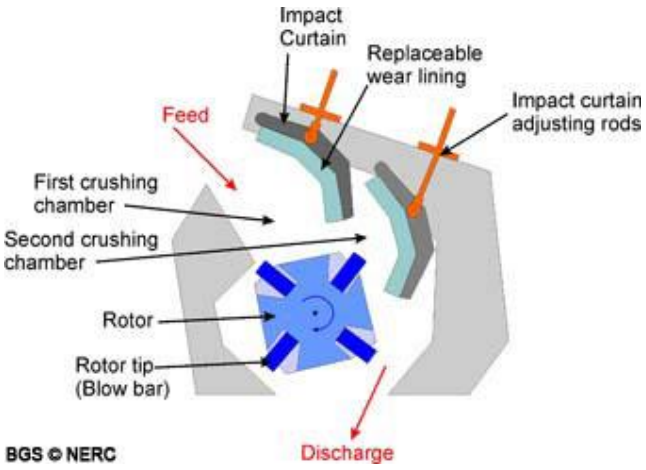

Figure 2.2.3 Diagram of HSI crusher (BGS 2013)

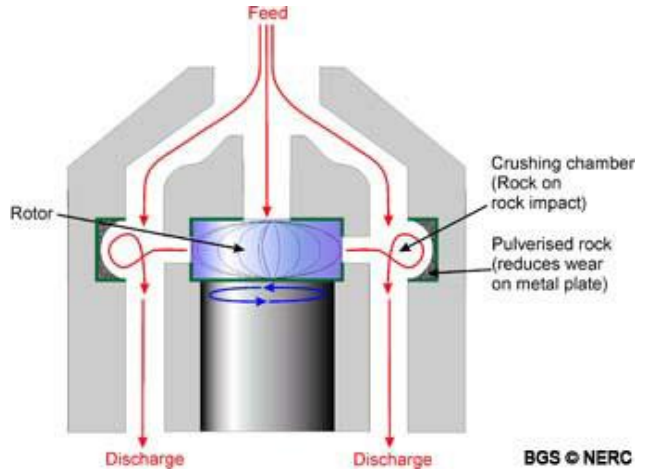

Figure 2.2.4 Diagram of VSI crusher (BGS 2013)

The production of MFAs mainly takes part in the tertiary and any following crushing stages using VSI and cone crushers. If the quarry is focusing on sales of the MFA for construction purposes then the shape and grading of the small particles is important, thus the type of crusher and means of screening the particles for desired grading in the final crushing stages have to be considered. Usually the quarry dust is washed or fed to an air classifier so that the resulting MFA conforms to the required grading requirements set out in various national standards.

2.2.2 V7 Process

The MFA's used in this study were processed in an industry scale V7 dry sand manufacturing system, a brief overview of which is provided in this section. It can be considered as a subsequent crushing and screening stage in a quarry which aims to produce MFA for construction purposes.

The V7 was developed by KEMCO (Kotobuki Engineering & Manufacturing Company) in Japan and introduced to the market in 2001 (Lusty 2008). The plant is intended to produce well graded and shaped MFA from surplus quarry dust allowing for precise control on the particle size distribution in a closed circuit.

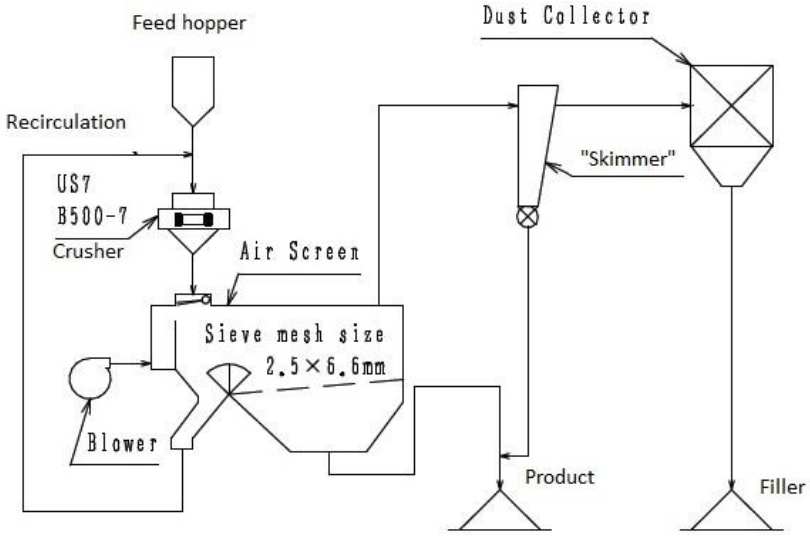

Figure 2.2.5 Schematic representation of the V7 plant

Figure 2.2.5 shows the schematic representation of the plant. The system consists of a feeder, modified VSI crusher, air screen, "skimmer" and dust collector. Usually the feed material is quarry dust which has been through several crushing stages in the quarry with the largest particle size of 10mm and water content of less than 1.5%. Typically the processing results in a sand product with maximum size of 4mm and a fine dry rock filler with 70 – 90% passing a 0.5mm sieve. Usually the division between the sand and rock filler is around 80% and 20%, respectively; however, it depends on the amount of fines in the feed material as well as the parent rock properties.

The feed material is fed to a modified Barmac VSI crusher incorporating a milling function, using tungsten carbide impact members, and a restriction on the crushing chamber outlet, thus forcing the material into a zone of powerful attrition. This allows for better shaping of the particles and a reduction in the rotor speed if compared to autogenous VSI crushers (Kaya et al. 2009).

The crushed particles are then run through an air screen which allows for oversize and some of the coarser particles to be recirculated, the required particle sizes are delivered as a product sand and the rock filler is separated with the air flow. The amount of recirculation and removed rock filler is controlled by a damper and blower speed in the air screen.

The rock filler is run through a "skimmer" right after the air screen. This part of the process allows the separation of coarser particles up to 300 micron size and a part of fines from the rock filler which goes to a bag filter. The separated (skimmed) particles are added to the final sand product, thus increasing the yield of the plant and improving

the sand particle size distribution. The amount of skimmed particles, similarly to the air screen recirculation, is controlled by a damper and the air flow speed.

The rock filler is forwarded to a bag filter or a silo, whereas the sand and the “skimmed” particles are mixed in a drum mixer, where the water content is increased to around 3% in order to avoid segregation during stockpiling and transportation of the final sand product.

Figure 2.2.6 shows an example of particle size distributions of a granite feed material and corresponding products from V7 processing. The addition of the “skimmer” particles to the product shows that the sand becomes more evenly graded by increasing the proportion of 0.1 to 0.3 mm particle sizes.

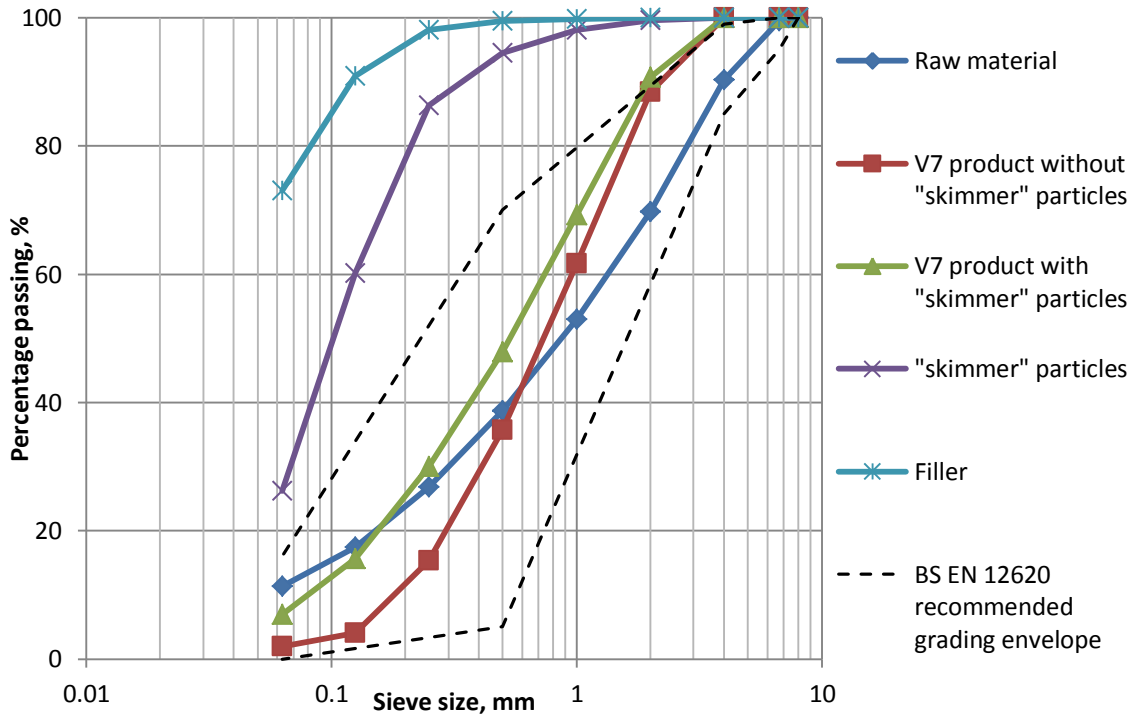

Figure 2.2.6 Particle size distributions of granite feed material and V7 process products

2.2.3 Effects of MFA on consistency and water requirement

Acknowledging the differences in the MFAs and natural sands the following sections will review the research efforts which have been aimed at investigating the combined effects of shape and texture, grading and type of MFAs with respect to concrete and mortar consistency, compressive and flexural strength.

Marek (1992) reports that with the same grading MFAs result in higher voids content when compared with natural sands due to angular shape. As the voids content in fine aggregates rises, the water requirement for constant slump flow of mortars on a drop table increases. However, inclusion of fines in the mix does not change or even reduce the water requirement for some MFAs. He explains this by the reduced voids content of the fine aggregate and noted that as more dust of fracture is included in the fine aggregate, more water is tied up in the system, but at the same time the fines themselves lubricate the mixture and offset the reduction in consistency resulting from less free water in the system. Similar findings were made by Hudson (1997) who showed that the water requirement for constant slump flow of MFA mortar incorporating up to 20% fines is reduced as the level of fines increases. This effect is attributed to the void filling, lubricating effect of the fines.

An opposite trend was found by Celik and Marar (1996) who showed that partial replacement of MFA with limestone quarry dust passing the 75 micron sieve decreases the slump. Such behaviour was explained by the need for more water to lubricate all particles as the relative surface area of the aggregate increases by increasing the dust percentage. This is supported by the work of Quiroga et al. (2006) where they concluded that there is a tendency of MFA with high fines to increase the concrete water demand.

The differences in observations could be explained by the concrete or mortar mix composition as discussed in section 2.1.7 and as shown by researchers with MFA concrete mixtures. Li et al. (2009) concluded that the consistency is increased in low strength MFA concrete by the addition of up to 15% of limestone filler. However, in high strength concrete inclusion of filler up to 7% did not change the slump whereas higher levels resulted in decreased consistency. The effects of fines in MFAs being dependent on mixture composition are also supported by the findings of Gonçalves et al. (2007). They showed that increased levels of fines improved the consistency of MFA mortars at w/c ratio of 0.4. However, there were no significant differences in consistency at a w/c ratio of 0.5. Similar observations suggesting an optimum fines content were reported by Kroh (2010) who found that inclusion of limestone quarry dust fines in a MFA mortar at 10% of fine aggregate increased the consistency while a fines content of 15% resulted in reduced consistency. This behaviour was attributed to the fact that up to 10% replacement level of fines lubricates the mixture whereas further addition of dust increases the surface area which has to be covered by the paste. These findings as stated by Jones et al. (2003) are due to combined effects of mixture composition, filler and aggregate shape, grading and packing.

If the MFA shape and texture is considered, then it has been observed by Donza et al. (2002) that the granite and dolomite sands were angular and crystalline as opposed to rounded and smooth natural sand. The slump of concrete mixes was found to be lower for the granite MFA and a higher dose of superplasticiser was required to achieve the same consistency as that of natural sand. Dolomite aggregate possessed high amounts of elongated particles and resulted in an unworkable concrete mix prone to bleeding.

A more elaborate study regarding MFA shape was conducted by Cortes et al. (2008). They tested two natural silica and two manufactured granite and limestone sands with the same grading in mortars with fixed w/c and fine aggregate/cement ratios. It was observed that MFAs are more angular and elongated resulting in lower sphericity, roundness, higher maximum voids ratio and angle of repose. In mortar flowability tests two distinct cases were observed – dry and wet flow. These were defined by continuous slurry surface for wet flow; breaking and spreading in granulated form for dry flow. The results suggested a distinction between these cases when the ratio of volume of paste to volume of fine aggregates reached a value of 1.1 times the maximum void ratio. It was concluded that the loosest packing density of fine aggregate depends on particle shape. Therefore, a larger volume of paste will be required to attain adequate flowability when angular crushed fine aggregates are used instead of natural round aggregates of the same grain size distribution.

Hudson (1997) emphasized that the shape of the MFAs affects the consistency and water requirement, especially in the range of 300µm to 2.36mm of particle size. The shape of the MFA is influenced by the manufacturing process and it was shown by Gonçalves et al. (2007) that cone crushed sands display poorer consistency compared to ones produced using a VSI crusher.

Quiroga et al. (2006) reported the negative effects of the MFA shape and fines content as well as grading on concrete workability. Furthermore, they stated that the slump test alone might not be adequate to assess the workability of concrete with high fines, thus the use of dynamic tests such as the flow test was recommended for this type of concrete. They suggested that the negative effects of MFA could be counteracted by means of proper grading, plasticisers, or fly ash (as replacement of cement due to the

rounded particle shape). However, an exact method for estimating these parameters that provide optimum consistence for the particular concrete mix and MFA were not presented.

In summary, the consistency of MFA concrete depends on the combined effects of type, shape and texture, grading and the amount of fines of the aggregate as well as the concrete mix composition. In general, MFA tends to be angular, elongated with a rough surface texture which leads to an increased voids content and higher water demand for a specified consistency. Inclusion of fines sometimes can reduce the water demand and lubricate the mixture due to a reduction in voids in the aggregate and concrete up to an optimum content for particular mix and MFA. Exceeding this optimum value will decrease the consistency as the benefit in voids reduction is offset by an increase in surface area. However, there is no method for estimation of the optimum content of fines other than that of trial and error. Nevertheless, the research efforts have shown that workable concretes can be produced with a variety of MFAs by appropriate grading, use of admixtures and mixture proportioning.

2.2.4 Effects of MFA on compressive and flexural strength

Marek (1992) reported that the strength of MFA mortar increases as the amount of fines is raised due to a lower voids content within the aggregate. Therefore, it is concluded that concrete should be designed to have a minimum amount of void space present in the aggregate to provide maximum strength for a given cement content. Consequently, the voids content of the manufactured aggregate should be evaluated for the grading used in the concrete mix. However, Marek's results for concrete with high and low fines MFA gradings at constant water and cement contents exhibited almost identical 28 day compressive strengths. Hudson (1997) stated that the compressive strength of MFA concrete is increased as the level of fines increases. This was explained by the void

filling role of the fines. In contrast to these findings are observations of Kroh (2010) who showed that the compressive strength of MFA mortars decrease with an increase in the level of fines. In this case this was attributed to the absorption of water from the mix by the fines, resulting in delayed hydration of the cement paste.

Celik and Marar (1996) reported that in MFA concrete where limestone quarry dust replaced a part of the fine aggregate, the compressive and flexural strength was increased with a dust content up to 10%, but with higher dust contents the strength was gradually decreased. Such trends are attributed to a lack of cement paste to cover all of the aggregate as the dust content is increased above an optimum level. A similar study by Topçu and Uurlu (2003) showed that a fines content of 7 to 10% improved the compressive and flexural strength of MFA and river sand concrete. If the replacement level exceeded 10% concrete properties either remained constant or were negatively influenced. Similar variations were shown by Kenai et al. (2008), who found that MFA mortar showed a slight increase in strength up to 10% fines content. Further addition of the fines up to 20% reduced the mortar strength to approximately the same level as without the fines and the decrease in strength was attributed to the dilution effect of the fines. This effect is a reduction in the strength of cement paste resulting from inert filler occupying a volume of paste that previously was taken up by cement particles (Zollinger and Sarkar 2001).

Optimum values for fines content that yield the highest compressive strength are also reported by Li et al. (2009) as shown in figure 2.2.7. However, the explanations for this behaviour were different to those of the researchers discussed in the paragraphs above.

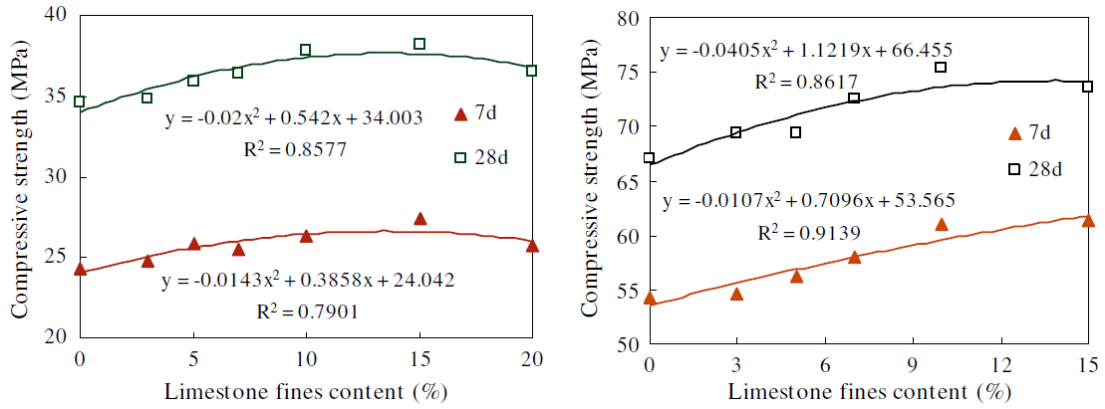

Figure 2.2.7 Variation of compressive strength with fines content. Low strength on the left, high strength on the right (Li et al. 2009).

Li et al. (2009) suggested that the limestone fines act as nucleation sites for the hydration products at an early age and accelerated the hydration of the clinker minerals. Furthermore, they suggest that inclusion of fines increased the packing density and therefore improved the interfacial transition zone in the hardened concrete. However, increasing the level of micro-fines beyond the optimum value in a concrete mix induces a need for a larger amount of cement paste to cover all the fines. Furthermore, fines could be present at the transition zone between the cement paste and aggregate having a negative effect on the bond strength.

Similar findings were presented by Li et al. (2011). The variation of compressive and flexural strength in MFA concrete is shown in Figure 2.2.8 and apparent optimum value for compressive strength is observed at 10% fines content. Meanwhile, the rate of increase of flexural strength is diminished after the 10% level for limestone fines content. Suggested reasons for such behaviour were the increased packing of the paste as well as the enhanced hydration of cement.

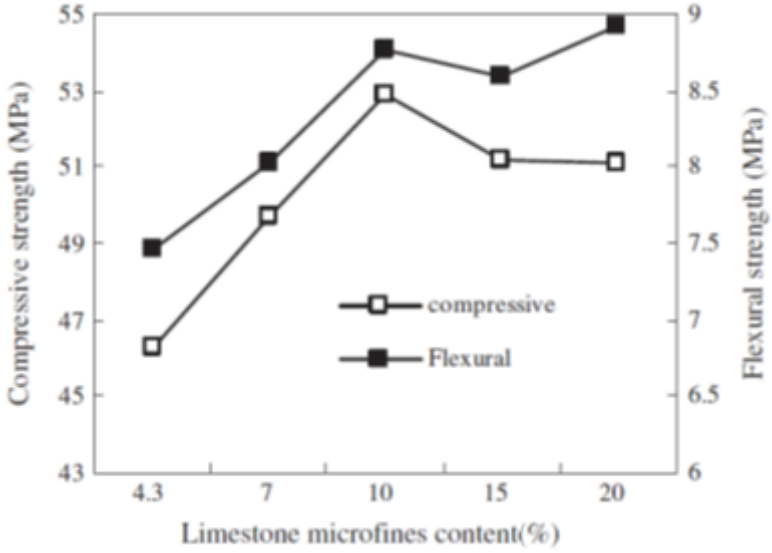

Figure 2.2.8 Variation of compressive and flexural strength of concrete with limestone fines content (Li et al. 2011)

A study by Wang et al. (2013) showed that in MFA concrete there is an optimum fines content value as noted by Topçu and Uurlu (2003), Kenai et al. (2008), Li et al. (2009), Li et al. (2011). They observed that the addition of limestone fines physically fills the voids between aggregates in fresh concrete thus increasing the free water content in the fresh mix up to an optimum fines content, after which the free water volume decreases. The variation of compressive strength follows that of the free water content which indicates the compactness of the mix.

It has to be noted that the variations in compressive strength for MFA concrete or mortar due to the changes in fines content that were observed by the abovementioned researchers were typically within a 5-10% range from the control strength. Thus, it could be assumed that the fines content of MFA has a relatively minor influence on concrete compressive strength. This is supported by the finding of Quiroga et al. (2006) that a good quality concrete can be made with MFA with quantity of fines as high as 15%. However, he noted that not all types of fines can be used in concrete and should be tested for quality beforehand due to potentially detrimental effects on consistency in

some cases. Furthermore, most of the researchers have been focusing on limestone fines, thus there is a gap in understanding of how other types of fines will affect the concrete performance.

A more prominent and beneficial effect on the compressive and flexural strength of MFA concrete due to the shape of the MFA have been demonstrated by several researchers. Dumitru et al. (1999) showed that compressive strength of concrete with basalt MFA processed in a VSI crusher is higher than that of natural sand concrete even with slightly elevated w/c ratio. This was attributed to the higher angularity of the MFA. Similarly Donza et al. (2002) found that the compressive strength of a high strength granite MFA mix was higher (10% at 1 year) than that of the natural sand mix at all stages of testing resulting from the improved interlock between the angular and rough granite particles and the cement paste. They also compared limestone, dolomite and granite MFA concretes at the same w/c ratio and cement content and came to the conclusion that the strength of the granite mixes was the highest, followed by the limestone mix and then the dolomite. This was attributed to the strength of the individual minerals and the differences in shape.

The effects on compressive strength due to variation of mineral type and corresponding differences in particle shape and surface roughness of MFA was noted by Li et al. (2011). MFAs with the same grading processed from limestone, quartzite, granite, basalt and granite gneiss rocks were tested for shape and texture using a flow time test (BS EN 933-6:2001). Concrete mixtures incorporating these sands were tested for compressive strength and the variation with flow time (roughness) is shown in Figure 2.2.9.

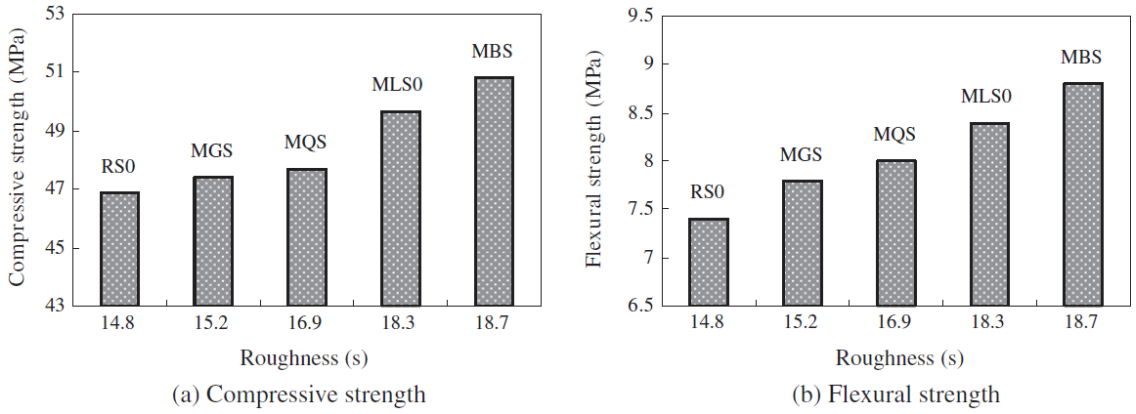

Figure 2.2.9 Variation of compressive and flexural strength with flow time (RS0 natural sand, MGS granite, MQS quartzite, MLS0 limestone, MBS basalt) (Li et al. 2011).

It shows that different mineralogy of the parent rock will result in variations in shape and texture of the MFA and that higher angularity and surface roughness, as indicated by the flow time, will result in higher compressive and flexural strengths due to better bond between aggregates and cement matrix. However, it is apparent that this relationship is non-linear.

The impact on the shape of MFA caused by the crusher type and the effects of different MFAs on mortar properties were investigated by Gonçalves et al. (2007). The shape of the sand particles was evaluated by optical microscopy and image analysis. It was found that the cone crushing resulted in more irregular and angular particles than impact crushing which produced sub-rounded particles, whereas natural sand was found to have rounded particles. Sphericity and aspect ratio of different size fractions were found to vary significantly for cone crushed material, in contrast to only small changes for natural and impact crushed sands. The mortar compressive strength for impact and cone crushed sands was found to be higher than that of natural sand at a w/c ratio of 0.4. At a w/c ratio of 0.5 the impact crushed sand mortar attained the highest strength, followed by natural sand and then cone crushed sand. These observations along with the findings of Donza et al. (2002) suggest that angular but close to equi-dimensional particles

produce concretes with higher compressive strength than irregular, elongated or rounded ones.

In summary, the compressive strength, similarly to consistency depends on the shape, texture and grading of the MFA. These properties are controlled by the parent rock as well as the crushing technique. Research shows that equi-dimensional, less angular particles in contrast to elongated and flaky ones lead to better strength values. It has been shown that there is an optimum content of fines for different mixes to attain their highest strength and it is commonly quoted that 7 – 10% fines content is optimal. However, an exact method of determining this amount for various mixes and rock types has not yet been identified. Nevertheless, most of the researchers agree that the inclusion of crusher fines in mixes made with angular crushed aggregates is beneficial in terms of aggregate packing density and concrete strength.

2.3 Review of specifications

The literature shows that the MFAs differ from natural sands and that the effects of these differences can be both detrimental and beneficial to concrete performance. Taking into account that the specifications by national standards for fine aggregates historically have been aimed at natural sands it might be expected that the limitations imposed by these would be inappropriate for MFAs. Thus, in some instances these standards could prevent the use of a specific MFA even though its performance would be satisfactory in concrete or vice versa. Furthermore, the specifications might indicate tests commonly used in industry that are able to describe MFA parameters of interest, such as shape, texture, presence of clay particles, that could be then related to the performance of concrete. Thus, this section will review the standard requirements for fine aggregates in the UK as well as research efforts aimed at providing adequate limitations and tests for MFA in other countries.

2.3.1 Specifications and tests for MFA in UK

The current British European standard BS EN 12620:2002 for aggregate properties requires the producer of the fine aggregate to declare the relevant aggregate test values and grading in prescribed categories. As a result the customer is able to specify a required category for a particular application and choose from the available supply. However, there are some specified limits included in the code itself. Published document PD 6682-1:2009 provides recommended limits for aggregates depending on the end use of the concrete in the UK.

Relevant tests for fine aggregates specified in BS EN 12620:2002 and recommended by PD6682-1:2009 for use in the UK are:

- Grading, as measured by the washing and sieving test method specified in BS EN 933-1.
- Fines content, measured as part of the washing and sieving test method specified in BS EN 933-1.
- Particle density and water absorption, measured in accordance with BS EN 1097-6.
- Bulk density, measured in accordance with BS EN 1097-3.
- Chemical requirements according to BS EN 1744-1.

The main difference to a natural fine aggregate specification is the amount of fines. The BS EN 12620:2002 specifies 4 methods by which fines can be assessed within fine aggregate to be considered as non-harmful. They are:

a) the total fines content of the fine aggregate is less than 3 % or other value according to the provisions valid in the place of use of the aggregate;

b) the sand equivalent value (SE) when tested in accordance with EN 933-8 exceeds a specified lower limit depending on country;

c) the methylene blue test (MBV) when tested in accordance with EN 933-9 gives a value less than a particular specified limit depending on country;

d) equivalence of performance with known satisfactory aggregate is established or there is evidence of satisfactory use with no experience of problems.

The limits for sand equivalent and methylene blue value are country specific. However, in PD 6682-1:2009 it is recommended that MFAs could contain up to 16% of fines or 10% for heavy duty floor finishes and be considered non-harmful provided that the materials have been processed. A further criteria for acceptability of MFAs is evidence of satisfactory use. The document also states that SE and MBV tests are not considered to be sufficiently precise for use in the UK and so no limits have been provided.

There is no distinction between crushed and natural sand with respect to grading. Figure 2.3.1 shows recommended particle size distributions for fine aggregates in the UK. The 0/4 CP envelope is for coarse grading and 0/4 MP for medium grading in the G_F85 category, meaning that 85 to 99% of particles by mass have to pass the 4 mm sieve.

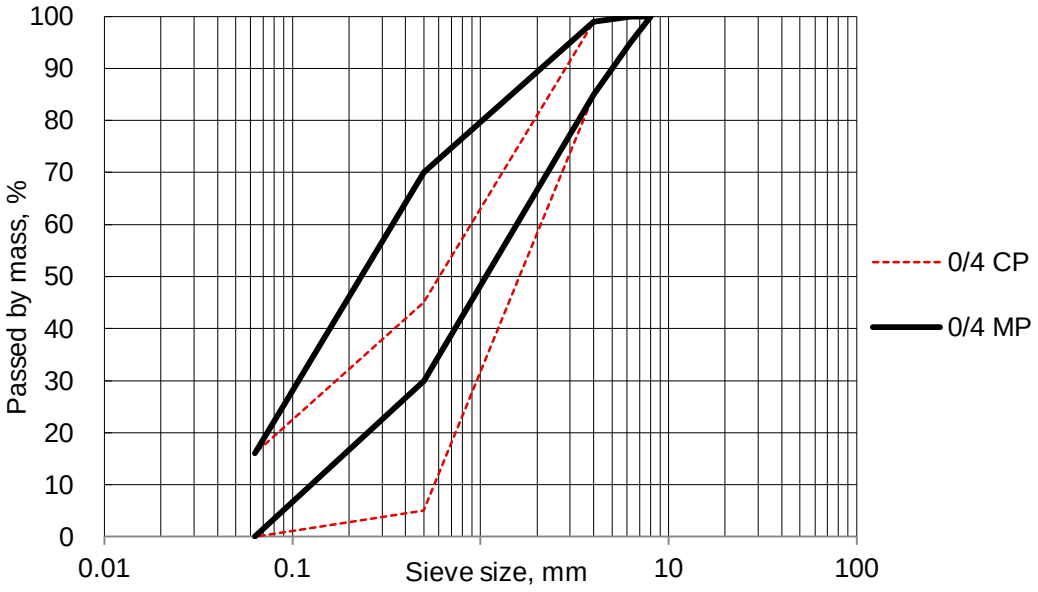

Figure 2.3.1 Recommended fine aggregate particle size distribution according to PD6682-1:2009.

Another point to note is that there are no specifications for fine aggregate shape and texture in BS EN 12620. It only refers to BS EN 1097-3, which is a test for bulk density and voids content. The voids content can give an indication of the shape, however, it is heavily influenced by the grading of the aggregate. As discussed in previous sections, shape and texture characteristics can influence the performance of concrete and the lack of guidelines makes the evaluation of fine aggregate in relation to their expected performance in a concrete mix difficult to establish.

2.3.2 Research on tests and specifications for MFA in other countries

Research intended to provide recommendations on the tests and limits for MFA in Australian standards was commissioned by the Cement, Concrete and Aggregates Australia organisation and the results of the study were reported by Thomas et al. (2007). This research used 21 sources of MFA from across Australia for characterisation and established a number of specifications. However, it states that the effects of a sand complying with the specifications on water demand, hardened and plastic properties of concrete cannot be predicted and were not addressed by any particular specification.

The following points were specified and recommended by the report:

a) Density and water absorption expressed at the SSD value should be in the range of 2.1 to 3.2 Mg/m^3

b) Particle size distribution. The report states that it is not practical to define an overall grading for MFAs due to the characteristics of the raw material and crushing equipment. The emphasis is put on consistency of the product by enforcing the producer to provide a history of grading and variations over time which should comply with a specified variation range. However, a general envelope to which the product should comply is suggested in Table 2.3.1.

Table 2.3.1 Suggested grading limits

Sieve size, mm	Cumulative percentage passing, %
4.75	90-100
0.6	15-80
0.075	0-20

c) Shape and surface texture. The New Zealand Flow cone test was evaluated and it was recommended that it should be used as a design tool to determine suitable consistency for sand blends. Although it measures shape and surface texture indirectly, it was considered impractical to design a test specification for a range of products as the grading also influences the Flow Cone results. However, it could be used as a quality control procedure on specific sources where changes in results would indicate possible changes in crushing characteristics.

d) Packing density. A test developed in France by Laboratoire Central des Ponts et Chaussees (LCPC) known as LCPC Test No. 61 (LCPC 2004). The test which evaluates the packing density was considered not to be sufficiently sensitive to act as a specification or quality control test. Nevertheless, the procedure can

generate input data for mix design and mix optimisation tool such as Betonlab (de Larrard and Sedran 2008).

e) Deleterious fines. It was recommended that the current Australian Standards limit for 2 micron size should be removed and the permissible level of the 75 micron particles modified. The specification should be based on the amount and activity of the fines, therefore it was suggested that the Methylene Blue Value (MBV) multiplied by the percentage of fines passing a 75 micron sieve should not exceed 150. The Methylene Blue Value should be determined by the procedure of the International Slurry Seal Association (ISSA) Bulletin 145 which tests only the fines from a given sample. An alternative specification procedure that was recommended was the Sand Equivalent (SE) test with a minimum limit of 60. The SE results can be in the range of 0 to 100 and the higher the percentage, the greater the proportion of sand-sized material or the lower the proportion of clay-sized materials. Higher SE values are taken to indicate better material. The use of XRD analysis as a specification tool was not recommended because of the difficulty of assessing the combined clay activity within the sample. However, it was recognized as a useful tool for investigation of the material and identification of the presence of potential deleterious mineralogy.

f) Durability.It was recommended that the durability of MFA should be measured by a degradation factor (fines) and a sodium sulphate soundness tests where specified limits should be 60 or greater (out of 100) for the degradation factor and a maximum of 6% loss of mass in the sodium sulphate soundness test. Sodium sulphate loss and degradation factor tests should be performed according to AS 1141.2 and AS 1141.25.3, respectively. The degradation factor test determines the clay and fine silts generated by vigorously agitating clean

aggregate in the presence of water. The sodium soundness test is thought to mimic freeze/thaw durability and disintegration of the rock fabric due to salt expansion in the permeable voids. These tests do not evaluate resistance to abrasion or breakdown of particles during handling or placing, therefore the Micro Deval test, based on literature, was recommended as a test for abrasion resistance.

A follow-up study (Thomas et al. 2008) targeted the specification of MFAs in Australia based on the Micro Deval test and LCPC packing density (LCPC 2004) and evaluated the performance of MFAs in cement mortars. The study concluded that the Micro Deval test for fine aggregate should be investigated further before limits or recommendation for usage of this test in Australia could be proposed as the data set generated was small. As for the LCPC packing density test, it was concluded that the test did not appear to measure any parameter that should lead to the rejection of an aggregate for use in a concrete mix. Unless the corresponding mix design software (BetonLab) was used, this test had little relevance in Australia.

In the mortar study the main conclusions with regard to specifications were that in order to control bleeding and the impact of detrimental fines, the value of MBV multiplied by the percentage of particles passing a 75 micron sieve could be limited to 100. Such a level would limit the active fines to minimise bleeding without detrimentally affecting the hardened concrete properties. Furthermore, a sand equivalent test was recommended as a screening tool as it is sensitive to the presence of illite. The clay minerals usually exhibit increased water demand, swelling or accelerate the hydration reaction of cement detrimentally affecting the fresh and hardened properties of the concrete. Indeed this

parameter was also found to be as good as X-ray diffraction for identifying potential issues due to illite or smectite clays.

The mortar properties evaluated did not appear to correlate with the sodium sulphate test or degradation factor. It was said that these tests were most likely to assess the long-term durability of concrete which was outside the scope of this study. The New Zealand Flow Cone test was not used to evaluate the suitability of different blend proportions. However, its results were found to give a good indication of those sand blends which would be suitable for mortar or concrete mixes.

In the USA a research project aimed at cement content reduction and utilization of aggregate characteristics produced recommendations for their current standards with regards to MFAs (Rached et al. 2009). These were mainly aimed at the amount of fines and grading requirements. The US standard limited fines to 7% so it was proposed that this should be modified to allow up to 20% fines where these can be tested by MBV to demonstrate their suitability if the 7% level is exceeded. Furthermore, it states: "MBV based on AASHTO Designation: TP 57 should be limited to 6 mg/g unless additional testing is performed to determine the effect on properties important for the specific application." It has to be noted that there is a difference in the MBV tests in American and British standards. In American standards only the sub 75 micron particles are tested whereas in British Standards the 0/2mm, 0/0.125mm or 0/4mm fraction is tested. Thus the MBV values measured using the American Standard will be higher due to a higher concentration of clay particles in the sub 75 micron range.

Based on the findings in the paper a recommendation for a change in the particle size distribution is provided. The proposed and current grading limits are shown in Figure

2.3.2. This recommended specification allows for a range of different particle size distributions, particularly the range for smaller particles is increased.

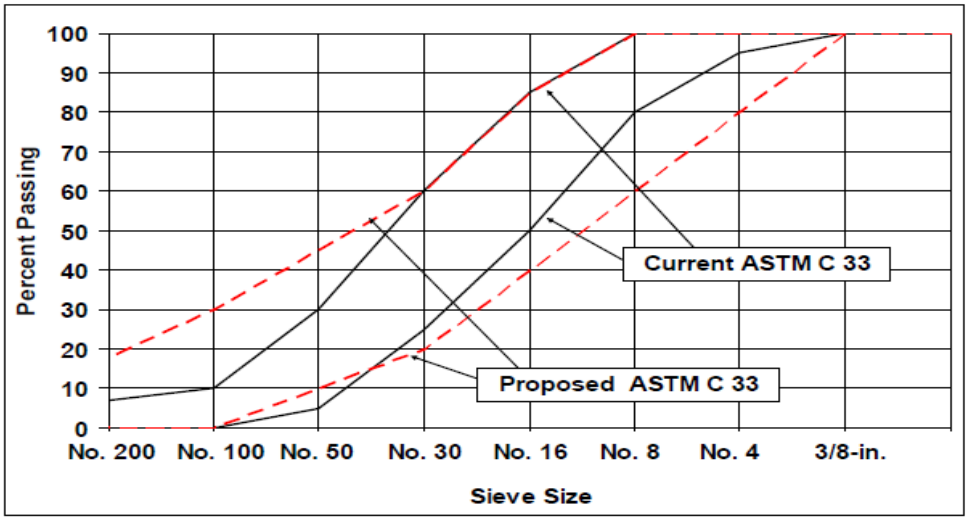

Figure 2.3.2 Proposed and current grading limits in USA reproduced from (Rached et al. 2009).

2.3.3 Summary of tests and specifications for MFAs.

The standards and published documents in the UK allow a wide range of particle size distributions for MFAs as well as allowing up to 16% fines. Similar trends are seen in Australia and USA where it is recommended that the grading requirements should be less strict as adequately performing concrete using MFAs can be produced with particle size distributions outside the prescribed limits and with higher fines contents.

The main concern is the harmful properties of the fines. Commonly suggested tests are the Methylene Blue Value and Sand Equivalent test. However, there is not a general agreement on the limits for these tests as there are major differences in the testing procedures from country to country, especially for MBV. Furthermore, MBV tests are not considered to be sufficiently precise and results are dependent on the interpretation of the operator. A suggestion of the Australian Standards that could be of interest, is to use the multiple of the MBV and the percentage fines passing the 75 micron sieve and

setting a limit for this. This could allow the influence of the combination of activity and amount of fines to be assessed. Another tool for identifying harmful fines is X-ray diffraction but it has been noted that this tool alone does not assess the activity of the harmful fines.

There are no limits regarding the shape and texture of fine aggregates and direct interpretation of these would seem difficult. However, the New Zealand Flow cone could be useful for assessing fine aggregates and blends indirectly with respect to shape and texture.

2.4 Modelling of concrete properties based on aggregate characteristics

It has been shown by the literature review that the physical and chemical characteristics of aggregates affect the fresh and hardened concrete properties and there have been numerous attempts to model these. The most obvious examples are models introduced by BRE (Teychenne et al. 1997) and the ACI (American Concrete Institute and Committee 211 1997) and provide concrete mix design procedures. These, to some extent, take into account a number of the aggregate characteristics: the particle size distribution, maximum aggregate size and aggregate type (natural or crushed). However, as these procedures are based on statistical data from many concrete mixes, the results are generalized and in the case of a specific type of aggregate, like quarry dust or MFA, might not yield the expected final concrete properties. Furthermore, the concrete compressive strength estimates are based on the w/c ratio, which might be correct in general, but with specific, very angular or very fine aggregates might prove to be an inaccurate representation of the strength. Similar effects might be applied for consistency measurements. While these models are easy to use and are appropriate for initial mix proportioning they do not provide highly accurate strength and consistency

estimations and require trial mixes and further adjustments to mix composition after the hardened concrete results are obtained.

Other attempts at concrete mix proportioning aimed at achieving the desired concrete properties have concentrated on the minimum voids content of aggregate combinations. Several models which evaluate particle packing in aggregate blends have been developed and investigated (Jones et al. 2003, Mohammed et al. 2012, Al-Ansari et al. 2012, Mangulkar and Jamkar 2013). It has been concluded that they are useful tools for modelling the aggregate blends with minimum voids contents. However, the most common assumptions in the packing models are that particles are spherical and thus the minimum voids content aggregate and cement combinations do not necessarily lead to the expected concrete mix properties. The concrete mix parameters still depend on the type, shape, grading and specific surface area of the aggregates.

Probably the most notable software for predicting concrete properties via a Compressible Packing Model (CPM) is the BetonlabPro software developed in France at LCPC (de Larrard and Sedran 2008). It comprises a collection of theoretical and semi-empirical models that evaluate the fresh and hardened concrete properties based on the level of aggregate packing and influence of various cementitious material types. In short, this collection of models is described in a paper by de Larrard and Sedran (2002). The software has been shown to be relatively accurate with a variety of aggregates, including crushed limestone sands with high filler contents, however, it tends to overestimate the consistency (Joudi-Bahri et al. 2012). It has to be noted that the packing of aggregate particles is influenced by the grading, particle shape and texture, however, in the model collection description given by de Larrard and Sedran

(2002) there is no reference to the effects of clay particles which might be present in the aggregates and affect the fresh and hardened concrete properties.

In order to achieve reasonable results using particle packing models all aggregate and cementitious materials have to be tested with a specific procedure that measures the compaction under loaded conditions of all size fractions (de Larrard and Sedran 2002). Such approach is time consuming and might be appropriate for laboratory scale but would not be employed in industry due to its complexity, time consumption and costs.

Recently researchers have applied artificial neural network (ANN) modelling to problems related to civil engineering. In particular engineering applications include concrete performance, compressive strength and consistency predictions. This is due to the ability of ANNs to model multi-variable complex problems by learning the relationships between independent variables and their corresponding results. Furthermore, once the ANN has been developed, it can be used to predict results based on the identified relationships (Hill 2006).

Ni and Wang (2000) used ANN to model concrete compressive strength using mix composition data from readymix plants. It was concluded that the 28 day compressive strength predictions based on the influence factors considered (mix composition parameters) are accurate with the absolute error not exceeding 4.5 MPa. Similar conclusions were made by Öztaş et al. (2006) regarding compressive strength and consistency of high strength concrete predictions made by ANN models based on concrete mix composition. They suggest that such ANN models would relieve the need for extensive laboratory work and yield a quick estimate of the 28 day compressive strength.

In a study by Yeh (2007) the capability of ANN and regression analysis was compared in terms of the prediction of the slump flow of high performance concrete based on the mix composition, cementitious material types and superplasticiser dosage. He demonstrated that the ANN predictions were more accurate than that of the regression analysis. Furthermore, he states that the ANN model can be used for a numerical investigation of the effects of each of the parameters under consideration on the slump flow.

A substantial number of research papers show the accuracy and value of ANN models developed for the prediction of concrete properties for a variety of concrete types, for example, strength of lightweight concrete (Alshihri et al. 2009), compressive strength of recycled aggregate concrete (Duan et al. 2013a), durability of high performance concrete (Parichatprecha and Nimityongskul 2009) and elastic modulus of recycled aggregate concrete (Duan et al. 2013b). This suggests that ANN is a feasible method for modelling concrete properties based on a variety of variables and influence factors.

Most of these studies include the major factors which influence the strength and consistency of concrete as input parameters for the ANN models, like water/cement ratio, quantities of cementitious materials and aggregates, water reducing admixture dosages. However, these studies tend to overlook the actual properties of aggregates, which, as discussed in previous sections, have been identified by researchers to influence the concrete properties, sometimes significantly. Thus, there is a value in applying and investigating the ANN technique to model concrete properties based on the aggregate characteristics along with mixture composition. Such a model could prove to be more accurate for a wider range of concrete types.

As with any models there are limitations for ANN modelling. From mathematical point of view the ANN technique was proven to be able to approximate any continuous function by Cybenko (1989). However, the accuracy of approximations depends on the topology of the neural network, training algorithms employed and training and validation data. The ANN approach is a "black box" technique where input data is fed to the ANN model and an output is provided. The output is not based on the theoretical relationships but on a function that is obtained by fitting it to previously provided training data. Therefore, care should be exercised when selecting training data and the resulting ANN models should be independently validated to ensure that what is modelled is actually the required property.

2.5 Summary

Researchers have shown that the combination of type, shape, texture, grading, amount and quality of fines of MFA influences the consistency and compressive strength of concrete. The research attention has been mostly aimed at the effects of grading and amount of fines or concentrated only on one of the parameters mentioned above. However, the combined effects of these MFA parameters are not fully understood and their quantification is difficult.

There have been attempts to develop limitations in national standards for fine aggregate characteristics as these can have a negative influence on the performance of concrete. General agreement is that a wider range of particle size distributions should be allowed as the current limitations were historically intended for natural sands and it has been shown that MFAs with gradings outside the limits of various national standards can produce acceptable concretes. However, the main concern is the limits regarding the harmful properties of the fines. The difficulty is in the accuracy of commonly used test

methods for this characteristic and sometimes the lack of correlation between the test results with concrete performance.

Recent attempts have shown the ability of ANN models to predict concrete properties based on mix composition parameters, however these do not take into account the properties of the aggregates. The development of an ANN model which accounts for both the aggregate properties and mix composition could be useful for assessing the expected performance of MFA concrete and aid the development of appropriate mix for a particular MFA.

3 Fine aggregate characterisation

3.1 Introduction

The aim of this chapter is to identify techniques that can be used to characterise the physical and chemical properties of MFAs. Therefore, the following subsections will cover the materials and notation used in the thesis, the justification for the selection of characterisation tests, the testing methods used and the corresponding results and discussion.

3.2 Materials and notation

For this study limestone, granite, basalt and gritstone quarry dusts from UK quarries were transported and processed in the KEMCO's V7 plant located in Japan. Figure 3.2.1 shows the location of these quarries. Two are located in Scotland and two in South Wales, thus, four locations and rock geologies were covered. As noted in Chapter 2, the MFA characteristics depend on the type of the parent rock and the processing technique. The use of a range of rock types allows a comparison of the effects of the V7 processing on sands with differing mineralogy as well as the effects of fine aggregate geology on concrete properties.

Figure 3.2.1 Quarry location

The V7 plant has the ability to flexibly produce different gradations that can be pre-programmed into the machine. At least four MFA gradations from each quarry dust were produced. Also the 0/4 mm fractions of the feed quarry dusts were included for comparison. Siliceous marine dredged natural sand from the Bristol channel complying with BS EN 12620:2002 was used as the control fine aggregate. Table 3.2.1 shows the notation used in the thesis for all the aggregates.

Table 3.2.1 Notation of aggregates

Description	Quarry	Fines content[1]	Type	Notation
Limestone coarse aggregate	Wenvoe	2	Crushed	CA
Marine dredged natural sand	-	1	Natural	NS
Basalt quarry dust	Duntilland	10	Crushed	B-FEED
Basalt sand	Duntilland	1	Manufactured	B-A
Basalt sand	Duntilland	2.9	Manufactured	B-B
Basalt sand	Duntilland	5.1	Manufactured	B-C
Basalt sand	Duntilland	7.4	Manufactured	B-D
Granite quarry dust	Glensanda	13	Crushed	G-FEED
Granite sand	Glensanda	2	Manufactured	G-A
Granite sand	Glensanda	2.9	Manufactured	G-B
Granite sand	Glensanda	5.1	Manufactured	G-C
Granite sand	Glensanda	6.5	Manufactured	G-D
Granite sand	Glensanda	9	Manufactured	G-E
Limestone quarry dust	Taff's Well	12	Crushed	L-FEED
Limestone sand	Taff's Well	2.8	Manufactured	L-A
Limestone sand	Taff's Well	4.9	Manufactured	L-B
Limestone sand	Taff's Well	7.1	Manufactured	L-C
Limestone sand	Taff's Well	9	Manufactured	L-D
Gritstone[2] quarry dust	Gilfach	18	Crushed	GS-FEED
Gritstone[2] sand	Gilfach	3.5	Manufactured	GS-A
Gritstone[2] sand	Gilfach	5	Manufactured	GS-B
Gritstone[2] sand	Gilfach	7	Manufactured	GS-C
Gritstone[2] sand	Gilfach	9	Manufactured	GS-D

[1]percent of aggregate by mass
[2]hard, coarse grained siliceous sandstone

3.3 Choice of tests

In order to characterise the MFA, appropriate tests were selected to cover the range of properties that are of interest regarding concrete performance. The underlying justification for the tests was that they should be simple and commonly used (standard tests) or easy to adapt, particularly if the results were to be meaningful and useful to both academia and industry.

As discussed in Chapter 2, the grading of the fine aggregate including the amount of fines (particles below 63 micron size) is an important factor influencing the performance of concrete, therefore all fine aggregates were tested for particle size distribution according to BS EN 933-1, which is a common standard test carried out routinely in industry.

Other important parameters are the shape and texture of the sand, which are more difficult to measure directly. There are imaging techniques available which can measure shape and texture, for example, optical microscopy and video recording followed by computer analysis. However, these are not commonly used for fine aggregates and can be time consuming and expensive as a result of the sophisticated equipment and software that is required. Thus, a simple indirect standard technique widely used in New Zealand and Australia was selected - the New Zealand flow cone (NZFC) test (NZS 3111-1986). This measures the flow time through a cone and un-compacted voids content of fine aggregates. The voids content in fine aggregates have been shown to correlate with the particle shape – the higher the voids content the more angular and irregular the particles are (Marek 1992). Additionally the voids content is affected by the grading of the aggregate – finer grading will result in decreased voids contents due to improved particle packing. The flow of the material is mostly affected by the shape

and surface texture of the particles (Thomas et al. 2007). Smoother and rounder particles will flow easier through an orifice than rough and angular ones. This is due to the reduced friction and interlock between the aggregate particles themselves and the cone they are flowing through as the particles get smoother and rounder. The test is an indirect measure of shape and texture and a standard envelope has been developed for natural sands based on the experiences of the New Zealand authorities regarding the performance of various natural sands in concrete. Additionally, a high resolution camera was used to take pictures of various size fractions of the fine aggregates and these were used for a visual comparison between the shape of different sands.

Also as highlighted in the previous chapter, deleterious particles like clays may have a detrimental effect on water demand and subsequent concrete performance. In order to evaluate this parameter two methylene blue (MB) value tests were selected; a standard one (BS EN 933-9 on the 0/2mm fraction) involving titration with an MB solution and one developed by Grace Construction Products (ASTM WK36804) using a pre-calibrated colorimeter allowing a direct estimation of MB solution consumption. In the thesis these tests will be referred to as MBV and GMBV respectively. These tests measure the amount of MB dye adsorbed to the surface of fine aggregate particles, therefore, it can be considered as an indirect surface area measurement. Clay particles have very high specific surface area due to their plate-like shape when compared to crushed rock or sand particles that nominally have the same diameter. This means that if two fine aggregates with the same particle distribution but one containing clays and the other without were tested, then the MB dye adsorption measurement would be notably higher for the aggregate containing clays. Therefore the purpose of the MB value tests is to indicate potential presence of clays in fine aggregates by indirect measurement of the surface area of the aggregate particles.

A sand equivalent (SE) test (BS EN 933-8 on the 0/2mm fraction) was also adopted, which evaluates the proportion of very fine and clay sized particles in the whole sample. The test involves rough agitation of fine aggregate in a flocculating solution. The agitation suspends very fine sand particles as well as silt and clay above the coarser aggregate fractions where they flocculate and slowly settle. After the agitation the suspension is let to settle for set amount of time and the ratio of the volume of coarser particles to the volume of flocculated and the coarser ones is assessed. The clay and silt particles are considered to be in diameter less than 2 µm therefore the setting time for these is higher than that of ordinary sand or crushed rock particles. Therefore, if two aggregate samples of equal grading but one with and the other without clays are tested for sand equivalent value then after the fixed settling time the one containing clays would have a greater volume of flocculated material above the coarser aggregate particles. This would result in a lower SE value for the clay containing sample and would indicate the potential presence of clays in the aggregate sample.

The MBV, GMBV and SE tests can indicate the potential presence of clays in the fine aggregates, however, they do not provide any information of the type of the clays. Therefore, X-Ray diffraction results obtained for the study detailed in Chapter 6 were used to confirm the presence and identify the type of clays in the MFAs.

Particle density and water absorption, which are functions of the mineralogical composition of the aggregate, were determined according to BS EN 1097-6. The dry density measurement was used in the NZFC voids calculation, and the absorption capacity was used to adjust the water content of the different concrete mixes.

Other aggregate tests were also considered but it was decided not to include them in the final set of tests due to various reasons. For example, BS EN 1097-3:1998 for bulk density and BS EN 933-6:2001 for flow coefficient of aggregate measure the un-compacted voids content and flow time of fine aggregates similarly to NZFC but in two separate tests. Furthermore, there is little published information about the results and correlations of these separate test results with concrete properties as opposed by NZFC results. Fine aggregate resistance to wear and fragmentation tests were considered but it was decided that they would yield little value for the purposes of this thesis. It was assumed that, if the rocks from which the feed quarry dusts were obtained are successfully used as coarse aggregates in concrete applications, then there should not be any issues with the performance of the corresponding MFAs in concrete in terms of aggregate durability.

To summarise, seven test procedures and high resolution imaging were selected to evaluate and characterise the main properties of fine aggregates that affect concrete performance: grading, shape and texture and presence of deleterious fines. Most of these are standard tests and easy to perform. The non-standard procedures will be described in detail in the next subsection.

3.4 Test procedures

This section will describe in detail the procedures that were used for classifying and characterising the fine aggregate that are not commonly used in UK. Table 3.4.1 provides the names of the test and their corresponding standard, where appropriate, as well as where they are commonly used.

Table 3.4.1 Characterisation test names, standard numbers and notes

Test	Standard number	Notes
Particle size distribution	BS EN 933-1	Standard test in UK and Europe
New Zealand flow cone (NZFC)	NZS 3111-1986	Standard test in New Zealand and Australia
High resolution imaging	-	Ad-hoc where existing facilities allow
Methylene blue value (MBV)	BS EN 933-9	Standard test in Europe
Sand equivalent value (SE)	BS EN 933-8	Standard test in Europe
Grace methylene blue value (GMBV)	ASTM WK36804	Under consideration as a standard test for the USA
Particle density and water absorption	BS EN 1097-6	Standard test in the UK and Europe
X-ray diffraction	-	Ad-hoc where existing facilities allow

3.4.1 New Zealand flow cone

The test was carried out according to New Zealand standard NZS 3111-1986 and the apparatus is shown in Figure 3.4.1. In addition the test required scales which were able to measure mass to the nearest 0.1 g and a thermometer with an accuracy of 1°C. In order to ensure equal volume for each sample, 0.38 times the dry density (approximately 1 kg) of the fine aggregate was weighed. The cone was filled with the sand sample and the time for it to flow through the base of the cone was measured. A steel rod was used to strike off excess particles from the receiving can and its mass with the sand contained within was recorded. The sand sample was then remixed and procedure repeated three times.

The mass of the sand in the cylinder was calculated by subtracting the mass of an empty cylinder from the measurements taken during the procedure. The volume of the cylinder

was measured by filling it with water with no visible meniscus at 21±2°C, weighing it and subtracting the mass of an empty cylinder. This gave the mass of the water in the cylinder which was equal to the volume in millilitres. The flow time was the average of the three repeat tests. The voids content was calculated according to Equation 3.4.1:

$$Voids\ content, \% = \left(1 - \frac{1000B}{AD}\right) \times 100 \qquad \text{Equation 3.4.1}$$

where A was the mass in grams of water required to fill the can (equal to volume in ml), B was the mass in grams of sand contained in the receiving can and is the average of the three test repeats and D was the dry density of the sand in kg/m^3 (the '1000' on the numerator ensures dimensional correctness of the equation).

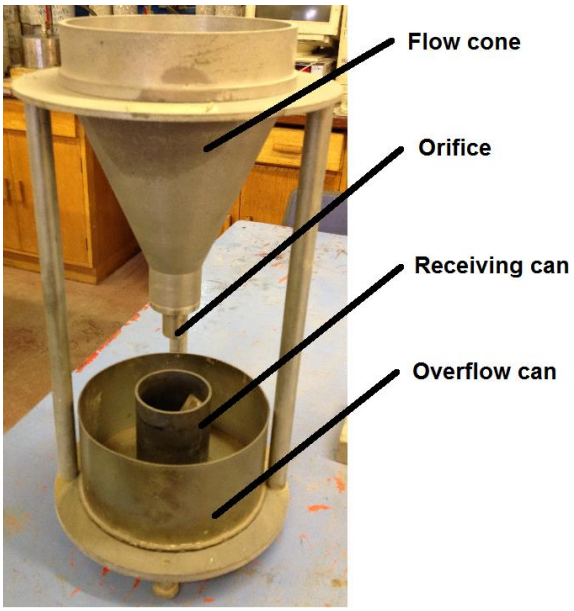

Figure 3.4.1 New Zealand flow cone

The results obtained are plotted on a graph where the abscissa is the voids content expressed as a percentage and the ordinate is the flow time in seconds. Figure 3.4.2 shows the plot including the standard envelope for natural sands from NZS 3111-1986 and labelled areas for different types of fine aggregates as reported by Goldsworthy (2005).

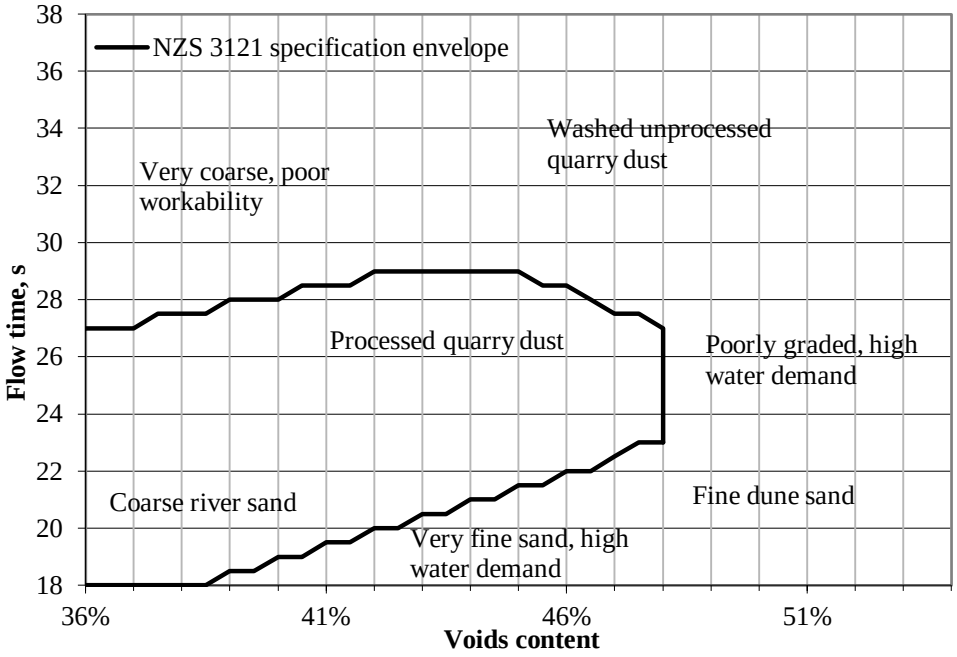

Figure 3.4.2 NZFC plot, specification envelope and labels reproduced from Goldsworthy (2005).

3.4.2 Methylene blue value

This test was performed according to BS EN 933-9 with standard methylene blue solution concentration of 10g/l and the equipment setup is shown in Figure 3.4.3. A minimum 200 g sample of oven dried 0/2 mm fraction of the fine aggregate was taken, weighed and its mass recorded as M_1. The sample and 500±5 ml of water were added to a 1 litre beaker and stirred with an agitator at 600 revs/min for 5 minutes. For the remainder of the test the speed of the agitator was set at 400 revs/min. After the initial agitation 5ml of methylene blue dye was dispensed from the burette into the suspension and a stain test was carried out after at least 1further minute of mixing. If a light blue halo around the stain was not observed a further 5 ml of dye was added and the stain test repeated after another minute of mixing. This was repeated until a halo appeared. Once a halo had appeared, the stain tests were carried out at one minute intervals without further addition of the MB dye. If the halo disappeared in the first 4 minutes, another 5 ml of the dye was added, if it disappeared in the last minute just 2ml of dye

was added. This was repeated until a blue halo persisted for 5 consecutive minutes whilst the solution was agitated.

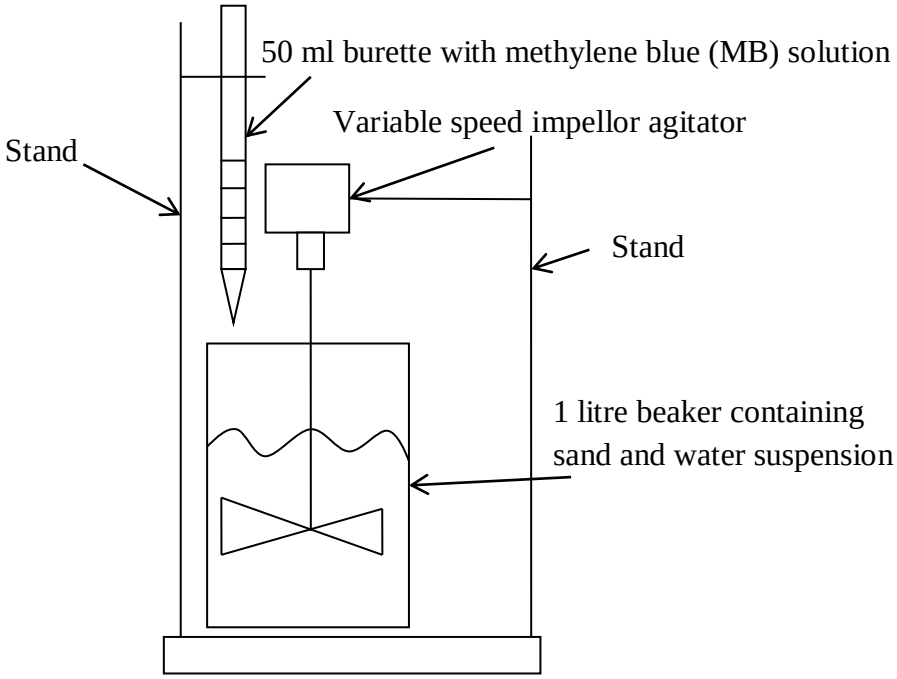

Figure 3.4.3 MBV test setup

The stain test involved dipping a glass rod into the suspension and placing a small drop on a filter paper which was placed on top of an empty beaker. This resulted in a dark stain on the filter paper with a central deposit of solids as can be seen in Figure 3.4.4. The stain marked as A does not have a light blue halo around it, thus indicating that all of the dye has been absorbed by sand particles. The stains marked as B show an approximately 1 mm wide light blue halo indicating that there is free dye present in the suspension.

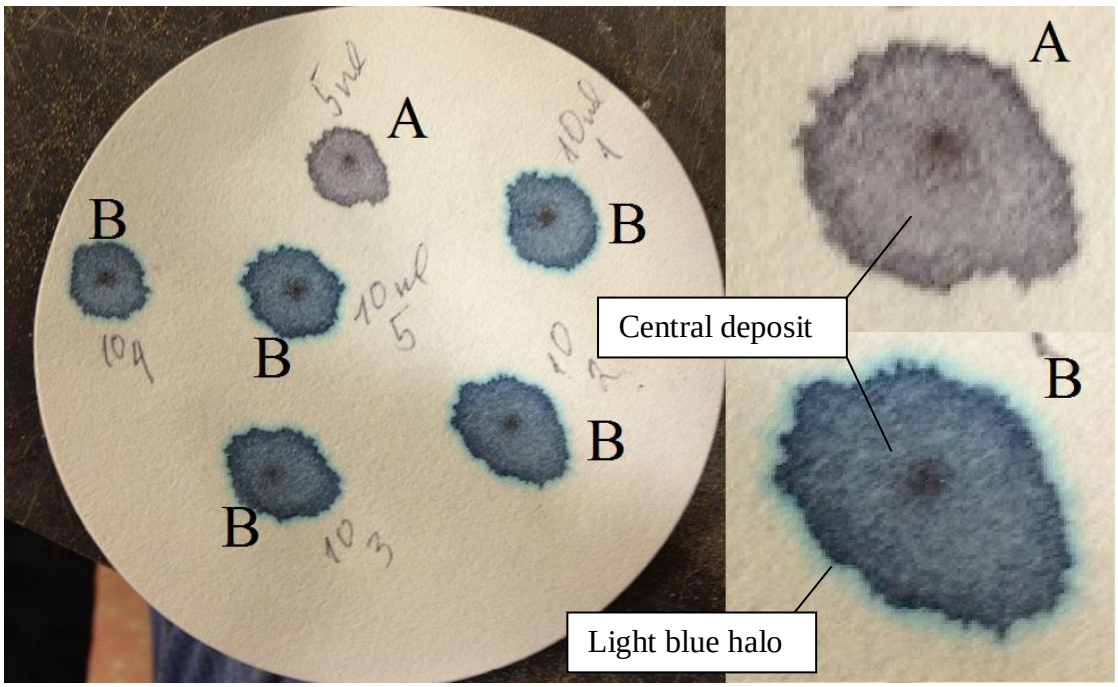

Figure 3.4.4 MBV stain tests on filter paper; A initial stain, B end-point stain

Once the halo had persisted for 5 consecutive minutes the total volume of MB dye used to the nearest 1 ml was recorded. The MB value was calculated according to the equation 3.4.2:

$$MB = \frac{V_1}{M_1} \cdot 10 \qquad \text{Equation 3.4.2}$$

where: M_1 was the mass of sand sample in grams and V_1 was the total volume of dye used in ml. The result was expressed to the nearest 0.1 grams of dye consumed per kg of 0/2 mm sand fraction.

3.4.3 Grace methylene blue value (GMBV)

The principle of this test was in essence the same as for the standard MBV test in that it aimed to measure the amount of methylene blue dye required to cover all sand and clay particles with a monomolecular layer of the chemical. However, the way in which this amount was determined was different. A pre-calibrated colorimeter was used to measure the consumed amount of MB solution after the sand had been soaked in it.

The testing equipment and procedure for this test was provided by Grace Construction Products as a "Rapid Clay Test Kit". Moreover, the method has been submitted to the ASTM International for introduction as a standard in the USA and can be found under ASTM number WK36804. A 20g sample of 0/2 sand fraction was weighed and mixed in a 45mL tube with 30 mL of MB solution with concentration of 5 g/l. The tube then was shaken for 1 minute, left to rest for 3 minutes and then shaken for another minute. From this suspension an aliquot of 130 µL was filtered into a 45mL tube and diluted with deionized water to 45mL volume. A glass test tube was filled with the diluted solution and tested in the colorimeter which showed the amount of dye consumed in miligrams of MB solution per grams of sand (it is the same as g of MB solution per kg of sand used in the standard MBV test). Additionally there are methods to account for the deviation in the initial MB solution concentration and very high MB values provided in the test kit manual.

3.4.4 Sand equivalent

The sand equivalent test was carried out according to BS EN 933-8. The test specific equipment dimensions are shown in the abovementioned standard and the test equipment setup is shown in Figure 3.4.5. A concentrated solution was made from 111g of $CaCl_2$, 480 g of glycerine and 12.5 g of formaldehyde solution diluted to 1 litre with distilled water. In addition to this, a washing solution flocculant was made by diluting 125 ml of the above concentrated solution to 5 litres volume.

Two test specimens with a mass of $\frac{120(100+w)}{100}$ were prepared, where w is the water content of the sand by mass. For this test, the 0/2 mm sand fraction with water content less than 2% was used. The washing solution was syphoned into each graduated cylinder to the lower mark to which the samples were added and left to soak for 10 minutes. After this period the cylinders were shaken for 30 seconds at a frequency of

1.5 Hz and afterwards the sand in the cylinders was agitated with the washing tube starting from the bottom to allow the fine particles to rise in the cylinders until the washing solution reached the upper mark on the graduated cylinder. These were then left for 20 minutes to settle. After this period h_1, the height of the sand and flocculated material in the cylinder relative to the base, was measured as shown in Figure 3.4.6 and then the plunger assembly was lowered into the cylinder until it rested on the sand. The distance between the top of the plunger collar and the bottom of the plunger head, marked as h_2 in Figure 3.4.6, was measured. The ratio of (h_2/h_1) multiplied by 100 was calculated for each cylinder to one decimal place and the SE value was recorded as the average of the ratios to the nearest whole number.

Figure 3.4.5 SE test kit

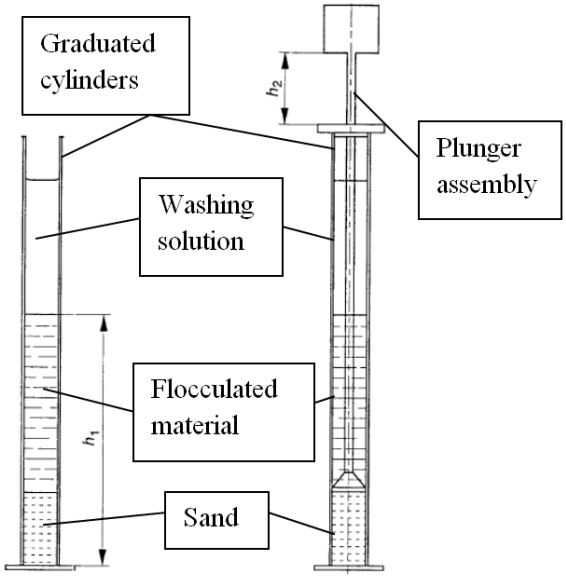

Figure 3.4.6 h_1 and h_2 measurement

3.4.5 High resolution imaging

There is no standard for high resolution imaging. However, the images were taken in a controlled manner to allow a visual comparison. Photos were taken with a Panasonic DMC-FZ28 camera. Each sand fraction was laid on a table with flat surface with a steel ruler next to it. The camera was fixed on a stand so that the distance from the table surface to the lens was 30 mm and that a graduated part of the steel ruler was visible

along with the sand particles in the viewfinder and then an image was taken. Afterwards the sample was discarded and the procedure repeated with the next sand fraction. Images were used for qualitative observations and comparison.

3.4.6 X-ray diffraction

This technique was employed to identify the minerals present in the sands. The sands were ground to a powder in a puck mill for 20 seconds. The puck mill was cleaned before grinding of each sand sample to eliminate contamination. The powders were fed into a Philips PW1710 diffractometer to identify diffraction peak and pattern data. Afterwards the data was analysed using X'pert HighScore Plus software to identify the minerals present in the powdered sands. A more detailed description of the procedure is presented in Chapter 6.

3.5 Results and discussion

In this section the fine aggregate characterisation test results are presented and discussed.

3.5.1 Particle size distribution

Figures 3.5.1 to 3.5.4 show the particle size distributions of the MFA and the corresponding 0/4 mm fractions of the feed quarry dust. Irrespective of the rock source the gradings obtained for the processed sands were all very similar.

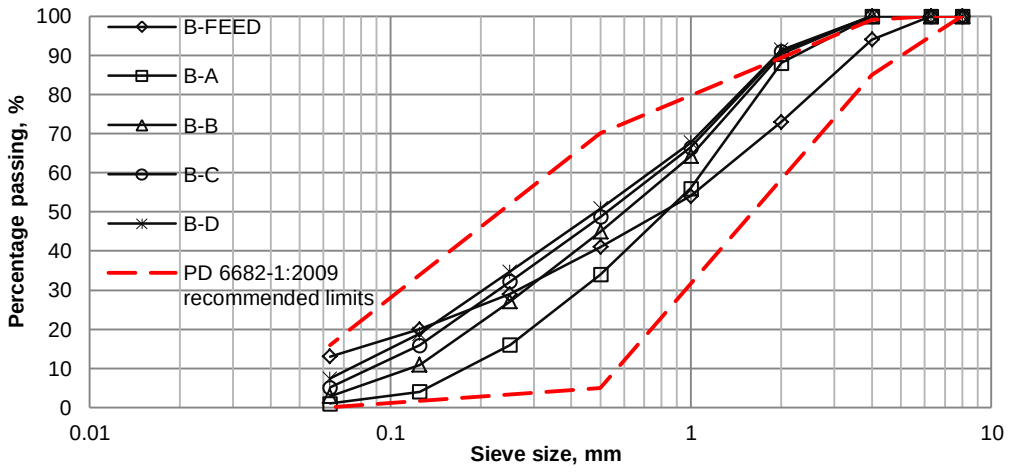

Figure 3.5.1 Basalt sand gradings

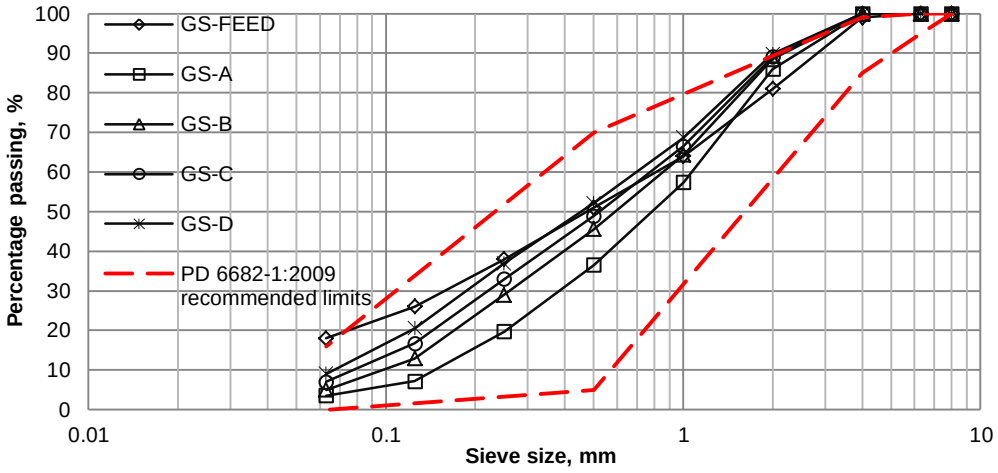

Figure 3.5.2 Gritstone sand gradings

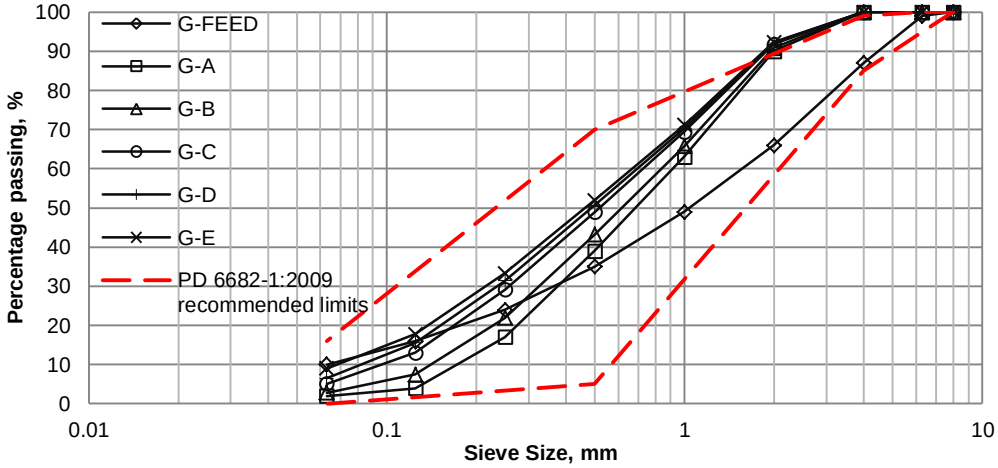

Figure 3.5.3 Granite sand gradings

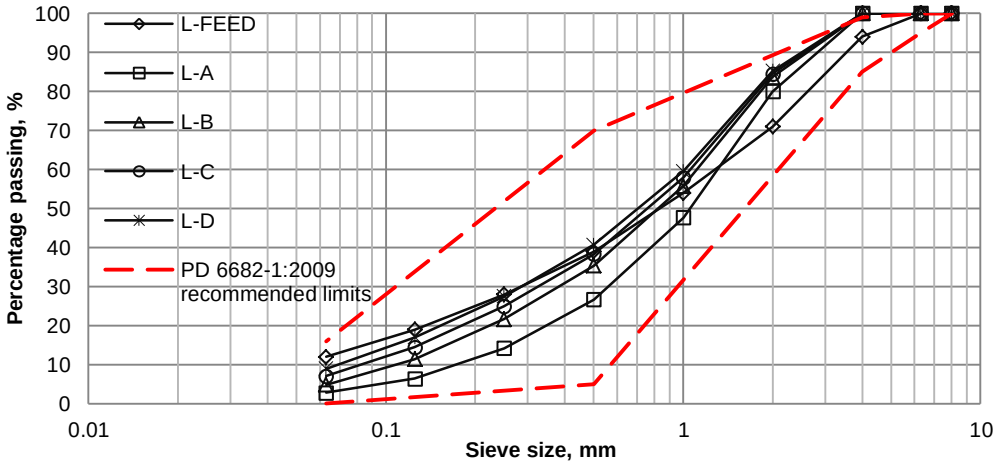

Figure 3.5.4 Limestone sand gradings

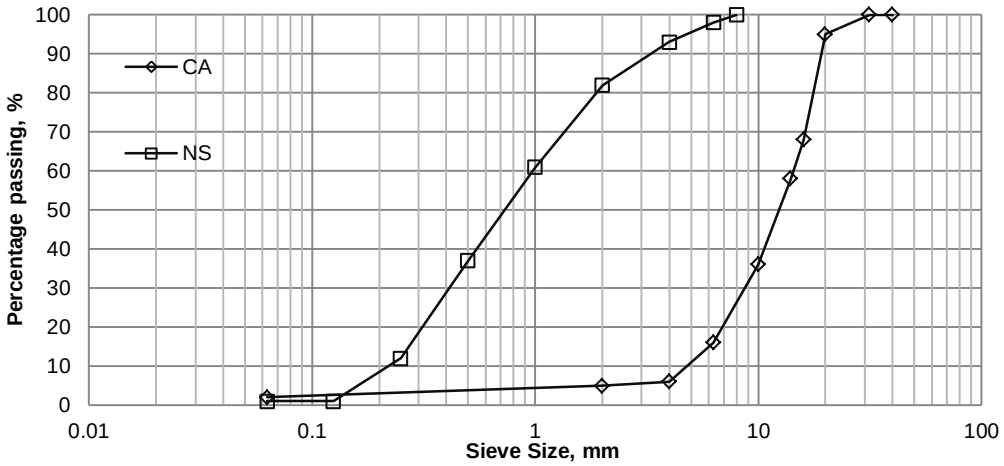

Figure 3.5.5 Coarse aggregate and NS grading

The sub 63 micron particle content of the MFA ranged from 1 to 9 percent suggesting that the air classification employed in the V7 plant has successfully and in a controlled manner removed the excess fines which were present in the feed and the materials created in the manufacturing process. In comparison with the quarry dust feed materials, the MFA had a greater quantity particles in the 0.3 to 1mm range, as indicated by the steeper gradients of the grading curves in this region. This particle size range is often deficient in quarry dusts and MFAs (Harrison et al. 2000), requiring them to be blended with fine natural sands to enable them to be suitable for use in concrete applications. Furthermore, in hardened concrete a shortage of particles passing the 1mm sieve results in high voids which increase porosity (Goldsworthy 2005). This suggests that, as far as the particle size distribution is concerned, these MFA should be suitable as fine aggregates in concrete without blending them with natural sand.

After the introduction of European Standards the grading requirements have been relaxed when compared to previous British Standards, mainly by asking the manufacturer to declare a typical grading for their product with a wide envelope for variation. This allows the customer to choose an aggregate product which suits them.

Also the aggregate producer is able to sell a wider range of particle sizes, thus minimizing waste. However, there are recommended grading limits set out in PD 6682-1:2009 for the UK. The overall upper and lower recommended grading limits are shown in Figures 3.5.1 to 3.5.4 and it can be seen that all MFAs, as well as the quarry dusts, except for the GS-FEED, lie within the envelope.

It has to be noted that the NS shown in Figure 3.5.5 contains only 1% of particles below 125 microns due to the dredging process. This greatly reduces the total surface area of the sand and in concrete mixtures should result in a lower water requirement. However, the lack of fines can lead to excessive bleeding, low cohesion and segregation of concrete mixtures (Newman and Choo 2003 and Neville 1995).

If only particle size distributions are taken into account, it might be expected that NS should have the least water requirement for constant consistency in concrete due to the larger maximum aggregate size and lower fines content of the MFA and quarry dusts. Similarly the water demand of MFA should be lower than that of feed quarry dusts due to a lower number of fine particles.

3.5.2 NZFC results

Figure 3.5.6 shows the results of the NZFC test, the specification envelope and labels of different areas in the plot describing the performance of fine aggregates based on the experience of the New Zealand and Australian authorities with natural sands (labels reproduced from Thomas et al. 2007).

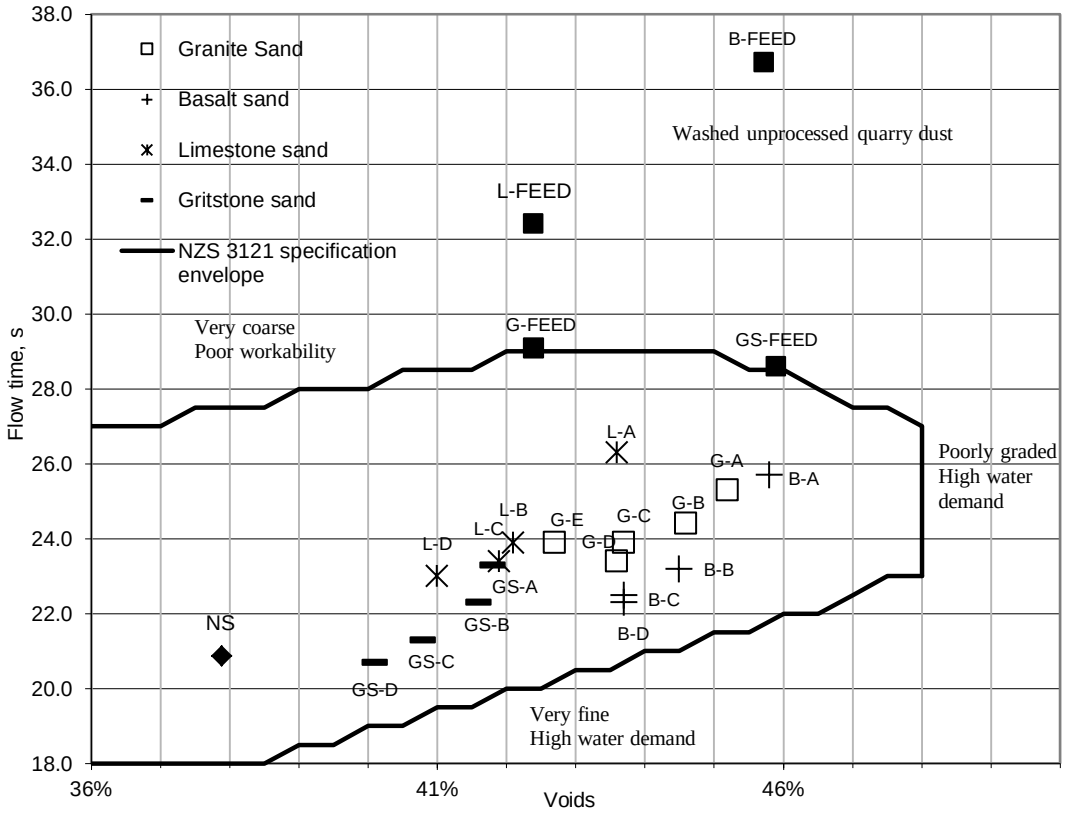

Figure 3.5.6 NZFC results

A question might arise whether this procedure is applicable to MFAs as the specification has been developed based on experience with natural sands, but Goldsworthy (2005) reported that this technique has been used extensively by New Zealand's and Australia's aggregate industries to evaluate quarry dusts as MFAs and blends with natural sand. Sand blends are tested with the flow cone and the ones falling within the standard envelope are selected for concrete and mortar trials, thus reducing the number of laboratory trials required to obtain optimal blends for particular aggregates. Furthermore, it can be argued that MFAs, in the same way as natural sands, consist of particles of different sizes and shapes and the test indirectly measures features of these particles through the flow time and voids content.

It can be seen in Figure 3.5.6 that all the MFAs used in this study fall within the New Zealand standard envelope for natural sands in contrast to their quarry dust counterparts. This suggests that the grading and shape of the MFAs should be suitable for use in concrete applications and that the reprocessing has improved the shape and grading of the feed material.

As discussed in the following sub-section the natural sand particles were smooth and rounded, whereas the quarry dusts comprised flat and elongated particles, which were angular with sharp edges. The MFAs were again angular but were more equi-dimensional and rounded than the feed quarry dusts. Thus, it can be seen from the NZFC results that the smoother and rounder the sands the lower the flow time in general.

Assuming that the governing factor for the flow time measurement is the shape and surface texture of the fine aggregate then there is evidence that the V7 process improves these characteristics as the flow time of the 0/4 mm fractions of all of the feed quarry dusts was from 28 to 37 seconds, whereas for all the MFAs it was in range of 21 to 27 seconds. If processed sands with a particular mineralogy are considered, it can be seen that the flow times were slightly reduced with an increase in the fineness of the aggregate. This reduction was typically 1 to 3 seconds for the –D gradings and therefore a major part of the flow time reduction can be attributed to particle shape improvements due to processing.

The un-compacted voids content of all the basalt and gritstone sands was lower than that of their feed material. However, the voids content of all the granite sands and the coarsest limestone sand (L-A) was greater than that of their corresponding quarry dusts. This is attributed to the combined effects of changes in grading as well as the shape of

the particular sands. Furthermore, it can be seen that the increase in the fineness of the grading for MFA of a particular mineralogy reduces the voids content. Marek (1992) and Hudson (1997) reported that the inclusions of higher amounts of fines improves the packing density of MFA, which is supported by these results.

If only the results from the NZFC and the information from the literature review regarding shape, surface texture and grading are taken into account, then it might be expected that all MFAs and the natural sand should show good consistency in concrete mixtures. However, there might be an increased water demand for the higher fines gradings of basalt and gritstone as these lie close to the area marked as "very fine, high water demand" in the NZFC plot. The quarry dust feeds, on the other hand, might be expected to exhibit poor consistency as these lie in the area marked as "very coarse".

3.5.3 High resolution images

Figure 3.5.7 contains the images of NS, G-A and B-A 4-2mm and 2-1mm sand fractions. Images of other size fractions are included in the Appendix A, but the shape and texture features of MFAs are the same as in the upper size classes. It can be seen from these that NS is very well rounded, with a smooth surface due to the natural attrition processes it has undergone over many years. The particles are sometimes flat and elongated as seen in the 4-2 mm fraction but this tendency decreases for smaller size fractions.

Size fraction	NS	Granite sand, G-A	Basalt sand, B-A
4-2 mm			
2-1 mm	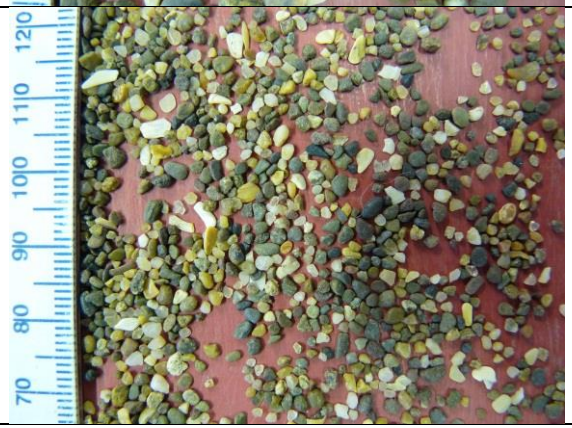	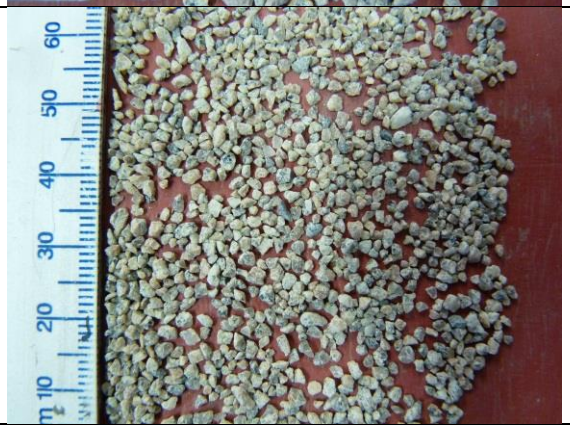	

Figure 3.5.7 Images of different size fractions

.

The two MFA shown in the Figure 3.5.7 exhibit both rough and angular surface features as expected. There is little difference between the shapes of the different MFA. However, it can be noted that by visual inspection the edges of basalt sand particles looks rounder than those of the granite sand which may be due to the different hardness, intrinsic crystalline structure and cleavage planes of the two rock types. These properties in combination with the rotor speed in the V7 plant affect the shape and fracture surface roughness. The MFA particles are relatively equi-dimensional in all size fractions. This also applies to the limestone and gritstone sands.

A comparison between granite quarry dust, granite MFA and natural sand in the 4 – 2 mm size fraction is shown in Figure 3.5.8. The quarry dust mostly consists of flaky, elongated, angular and rough particles whereas the reprocessed MFA contains few elongated or flaky particles as mentioned above. This means the V7 process has improved the shape of the particles and thus it may be expected that the water demand of the MFA will be less than that of the feed quarry dust. Smooth and rounded NS would be expected to outperform MFA in terms of water demand, however, a trade-off in compressive and flexural strength might be expected.

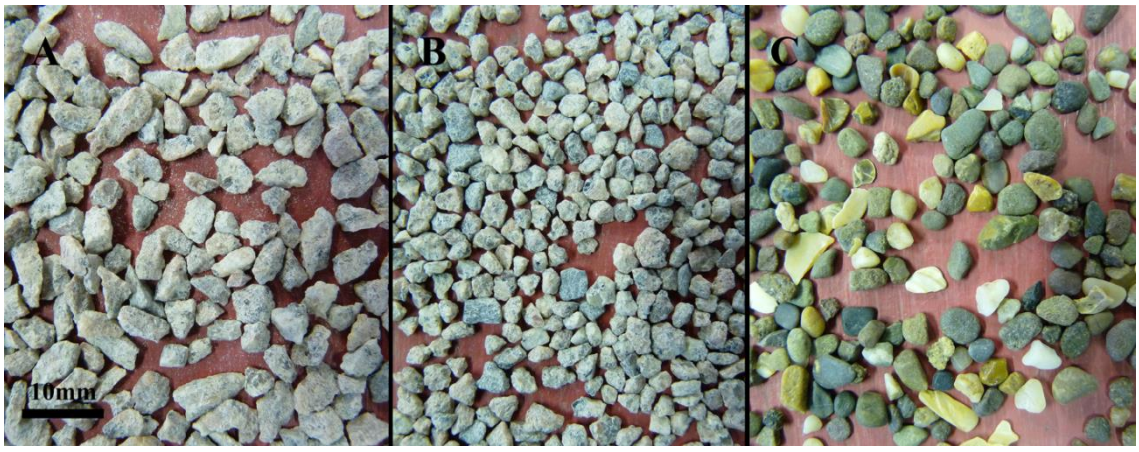

Figure 3.5.8 Images of 4-2 mm sand fractions, A: G-FEED, B: G-A, C: NS.

3.5.4 MBV and GMBV test results

Both methylene blue tests will be discussed in this section as they are based on the same principles – measuring the amount of MB solution required to cover all particle surface areas with a mono-molecular layer. These tests can indicate the presence of deleterious particles, and in particular clays, which are known for their large specific surface area, which consumes a larger quantity of the MB dye compared to the same size inert rock fines (Nikolaides et al. 2007).

Figure 3.5.9 shows the test results obtained for the fine aggregates used in this study and it can be seen that the natural, granite and limestone sands had MBV below 0.63 g/kg, whereas the basalt and gritstone sands had MBVs above 1.73 g/kg. As the MFA gradings were similar, the notable differences in MBV suggest that the latter sands contained clays and therefore would have an increased water and admixture demand when used in a concrete mix (Li et al. 2011b). However, the air classification stage during the V7 manufacturing process was able to remove a portion of the deleterious fines along with excess filler as indicated by the reduction in the MBV for all sands compared to their quarry dust counterparts. For the basalt and gritstone sands the MBV increases for finer gradings due to a greater quantity of clay particles in the sub 63 micron fraction, whereas for the granite and limestone sands the MBV exhibited just a marginal increase due to the small increase in the specific surface area.

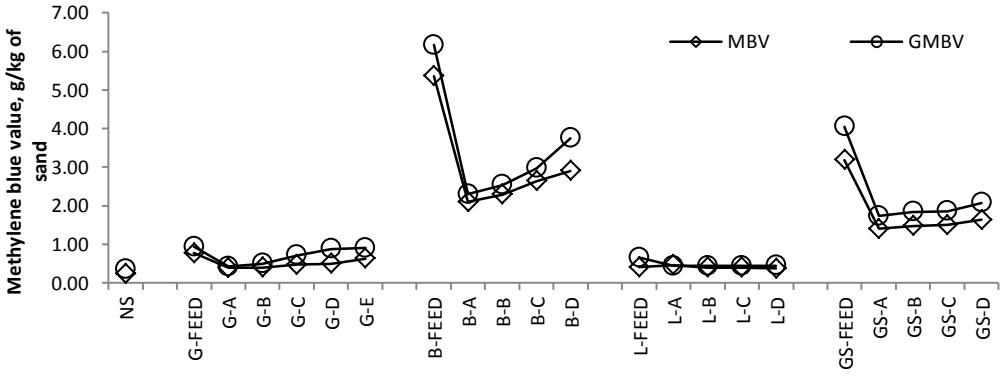

Figure 3.5.9 MBV and GMBV results

There are no specified upper values in PD 6682-1:2009 for the MBV test. As mentioned in Chapter 2, this is due to doubt concerning the accuracy of MBV test results and their correlation with concrete performance when different clays are present in the fine aggregate. Other countries impose specific requirements. For example, in France the MBV is required to be less than 1g/kg of sand for the 0/2 mm fraction (Nikolaides et al. 2007). However, such restrictions could prevent the use of fine aggregates that perform well within concrete even with high MBV values. Thus, in Australia, Thomas et al. (2007) proposed a limit on the multiple of the MBV value of sub 75 micron particles and the amount of fines in the whole sand sample. This would control both the volume of clay particles as well as their impact. Such a requirement would allow the use of a high fines MFA without clays as well as a low fines MFA which contain some clays. However, the MBV test employed in Australia tests the 0/0.075mm sand fraction as opposed to the standard BS EN 933-9 test which in general is carried out for the 0/2 mm sand fraction. Thus a direct evaluation of the proposal was not possible in this thesis.

One reason to include the GMBV test in the characterisation test suite was to address the doubts expressed about the standard MBV test, including its repeatability and accuracy (Koehler et al. 2009, PD 6682-1:2009). As described in section 3.4 the interpretation of when the endpoint of the MBV test has been reached can be subjective and vary from one operator to another. In this respect the GMBV test has the advantage that operator error in the estimation of MB solution consumption is minimised. The consumption of MB solution is directly estimated using a colorimeter which measures the concentration of the final solution. Furthermore, the time it takes to test all sands is the same as opposed to the standard MBV test which can take 20 to 30 minutes if the clay content is high.

Figure 3.5.10 shows a very clear correlation between the results of the MBV and GMBV confirming that they can be considered to be measuring the same property of the fine aggregate over a range of fine aggregate sources. Furthermore, this suggests that GMBV could be a viable replacement for the standard test.

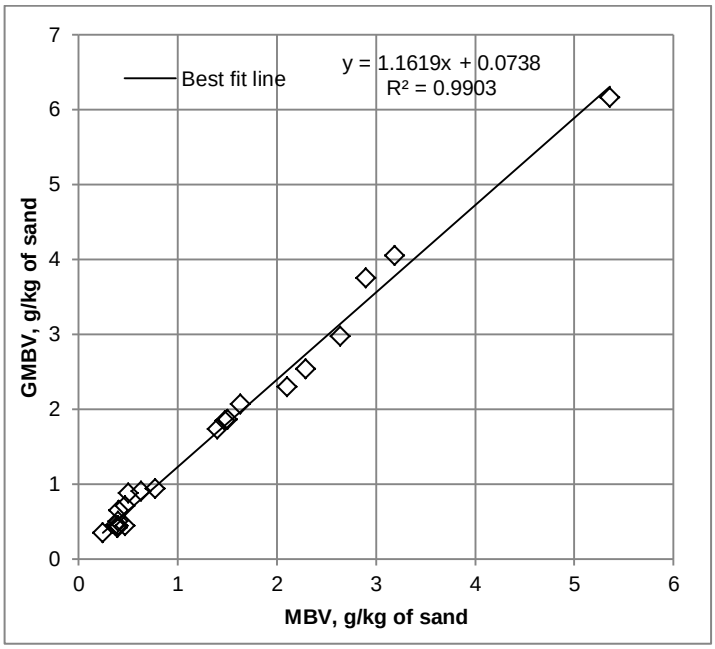

Figure 3.5.10 Correlation between MBV and GMBV results

3.5.5 Sand equivalent test

The sand equivalent test evaluates the proportion of clay and silt sized particles compared to the sand sized material. The higher the SE value, the lower the volume of clay sized material in the sample. Low SE values indicate a large proportion of clay sized material which can be potentially deleterious to concrete. As with the MBV test there are no specified values in the UK which restrict the use of a particular sand due to its SE value. However, it has been suggested for the Australian standards that the SE value is limited to 60 and used in conjunction with the limit on MBV multiplied by the fines percentage to screen for aggregates with potentially deleterious particles (Thomas et al. 2007). This suggested limit is indicated in Figure 3.5.11 along with the SE results.

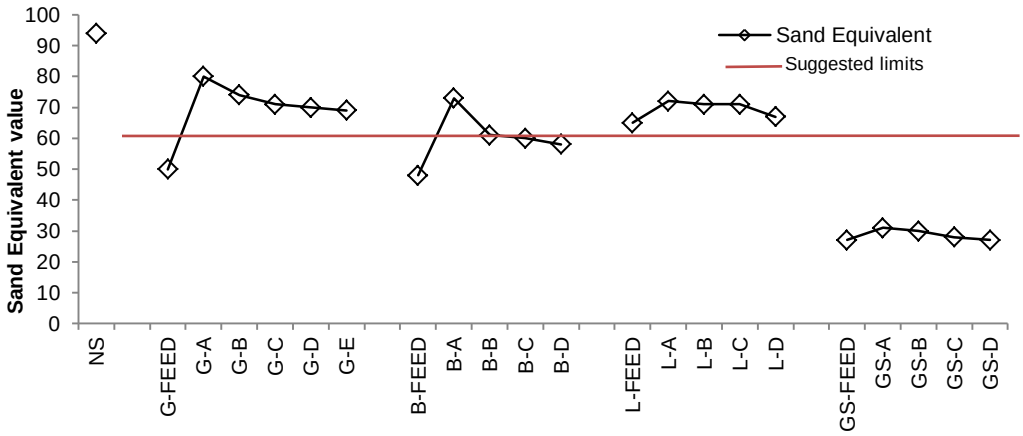

Figure 3.5.11 Sand equivalent values

As it can be seen from Figure 3.5.10 the natural sand had the highest SE value of 92 followed by the granite and limestone sands, which had SE values in the range of 67 to 80, basalt sands (58 to 73) and gritstone (from 27 to 31). As was the case for the MBV values, for a particular mineralogy of sand, the SE values decreased as the amount of fines increased. However, if all MBV and SE values are considered there is a wide scatter of results and only a weak trend of decreasing SE values corresponding to an increase in MBV as shown in Figure 3.5.12. Similar results are found by Nikolaides et al. (2007). This could be due to the SE test being more sensitive to a particular clay type, in this case, illite as identified by XRD analysis and reported by Thomas et al. (2008).

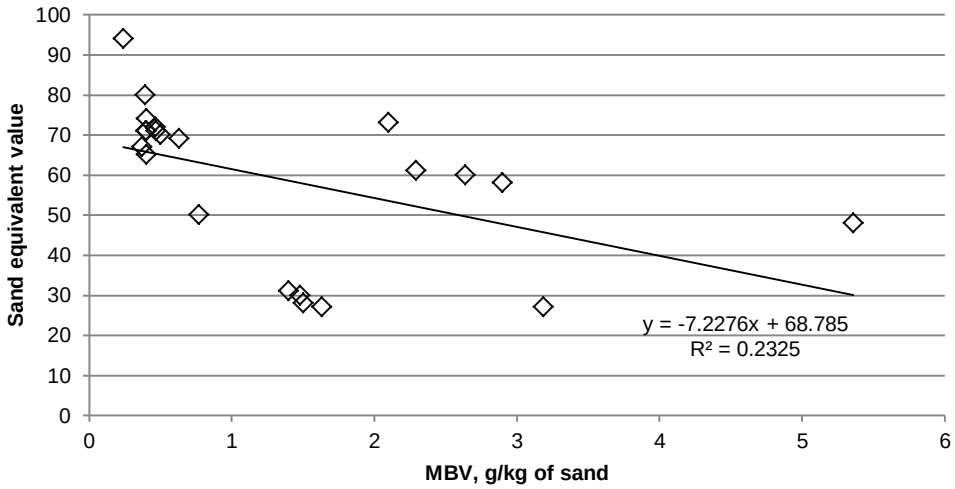

Figure 3.5.12 Sand equivalent values against MBV

In this study, if the suggested SE limit of 60 was adopted, all quarry dusts except for limestone, all gritstone MFA and the B-B, B-C and B-D sands would be deemed unfit for use in concrete applications. The feasibility and validity of this limitation will be discussed in conjunction with the concrete results in Chapter 4.

3.5.6 X-ray diffraction

It has been suggested that XRD analysis could be used to identify the presence of clays in fine aggregates for screening purposes (Thomas et al. 2007, Koehler et al. 2009). However, such an approach cannot be used in-situ as it requires sophisticated equipment as well as expertise to perform the test and analyse the results. Nevertheless, it can be a valuable tool for identifying the clay types present in aggregates. The mineralogical compounds of MFA are shown in Table 3.5.1. The XRD test was able to identify the clays present in the gritstone and basalt sands which gave the worst MBV and SE test results as well as the other major mineralogical constituents of the MFAs.

It was identified that gritstone sand contains illite clay, whereas basalt sand contains montmorillonite-chlorite. Basalt has been found to sometimes contain interstratified montmorrilonite like layers and chlorite like layers (Earley and Milne 1955). Fine aggregates containing illite clays have been shown to increase the water and admixture demand with little effect on compressive strength of concrete, whereas montmorillonite clay presence drastically increases the water/admixture demand and decreases the compressive strength (Norvell et al. 2007). While the XRD analysis provides the information of the type of the clay, it does not identify the actual amount of the clay present in the sample. Therefore other tests or methods should be used in combination with the XRD analysis that would allow to assess potential effects of the clay type and quantity as noted by Thomas et al. (2007).

Table 3.5.1 XRD identified compounds and their chemical formulas

Sample	Identified compounds	Chemical formula
GS	Quartz	SiO_2
	Illite	$(K,H_3O)(Al,Mg,Fe)_2(Si,Al)_4O_{10}[(OH)_2,(H_2O)]$
L	Ankerite	$CaFe_{0.6}Mg_{0.3}Mn_{0.1}(CO_3)_2$
	Coesite	SiO_2
B	Albite	$Na_{0.95}Ca_{0.05}Al_{1.05}Si_{2.95}O_8$
	Montmorillonite- chlorite	$NaCaAlSi_4O_{10}O$
	Magnessium iron alumosilicate	$Mg_{0.34}Fe_{1.66}Al_4Si_5O_{18}$
G	Quartz	SiO_2
	Albite, calcian	$(Na, Ca)Al(Si, Al)_3O_8$
	Biotite	$K(Mg_{1.48}Fe_{1.28}Ti_{0.24})\ (Al_{1.2}Si_{2.8}O_{10})\ (OH)_{1.4}F_{0.32}O_{0.28}$

Other mineralogical compounds that could be detrimental to concrete are amorphous forms of silicon dioxide that can cause alkali-aggregate reaction, however, none of those identified above fall in this category (Ferraris 1995).

3.5.7 Particle density and water absorption test

The particle density measurement was used in the voids calculation for the NZFC as well as to determine whether the aggregate should be classified as lightweight or normal and, thus, which standard should be adopted. The water absorption measurement is primarily used in concrete mix design in order to adjust the mix w/c ratios. However, high water absorption values can indicate porous aggregates and can therefore influence the concrete properties. All fine aggregates that were tested had oven dry densities above 2.0 Mg/m^3 thus they can be classified as normal weight aggregates and BS EN 12620:2002+A1:2008 can be used for corresponding requirements.

Table 3.5.2 Water absorption and dry density results

Sand	WA_{24}, %	ρ_{rd}, Mg/m^3
NS	1.04	2.63
G-FEED	0.58	2.62
Granite sands	0.58	2.61
B-FEED	1.92	2.83
Basalt sands	1.67	2.87
L-FEED	0.62	2.85
Limestone sands	0.45	2.85
GS-FEED	1.53	2.64
Gritstone sands	0.98	2.57

The water absorption of the quarry dusts was either higher or the same as that of the corresponding MFA as shown in Table 3.5.2. Processing of the quarry dust may have induced fracture of the particles through water accessible voids. This in turn could have reduced the number and volume of these voids which are measured by the water absorption test (Neville 1995). Furthermore, BS EN 933-1 states that the tested sands must be washed over a 63 micron sieve, but coatings like clays may not be readily removed by washing, resulting in higher absorption values for aggregates with initially higher fines contents. This assumption is supported by the highest water absorption values being measured for sands with high MBV. Dry density was found to be relatively constant for feed materials and the corresponding MFA.

3.6 Conclusions

It can be concluded that all MFA produced in the V7 plant conform to UK grading requirements and similar MFA gradings can be manufactured irrespective of rock type with modern processing equipment by removing excess filler while leaving particles in the 0.3 to 1 mm range which are usually deficient in MFAs.

The shape and grading of MFA has been improved in the reprocessing of quarry dusts as indicated by the NZFC results and high resolution imaging. The MFA particles are

relatively equi-dimensional but more angular and with rougher surfaces than NS that may be beneficial for flexural and compressive strength of concrete.

MBV and GMBV tests show good potential for indicating the presence of clays as confirmed by XRD analysis. Both MB test methods show very good correlation and GMBV could be used as a replacement for the standard method with the benefit that it minimises operator error. The SE test can be used to indicate the potential presence of clays; however, it seems to be more sensitive to the type of clay than the MBV test.

Based on the fine aggregate tests described here it can generally be concluded that quarry dusts followed by the corresponding MFA and then the NS would require a higher water content in concrete for constant consistency. In terms of deleterious fines, clays have been detected in the basalt and gritstone sands, thus a high water demand is expected for concrete mixes incorporating these sands when compared to granite and limestone MFA, especially those with higher fines gradings.

The characteristics of MFAs presented in this chapter and the corresponding conclusions will be used to give a better insight into the performance of concrete in the fresh and hardened states in the following chapters.

4 Concrete testing

4.1 Introduction

The aim of this chapter is to investigate fresh and hardened properties of concrete made using MFA. Therefore, the following subsections will cover the test procedures employed, concrete mix proportions and materials, results and discussion of constant slump and constant w/c ratio concretes, as well as the correlation with the fine aggregate characterisation test results.

4.2 Concrete test procedures, mix composition and materials

4.2.1 Fresh concrete tests

In order to evaluate fresh concrete performance several test procedures were employed. The concrete mixes were tested for slump two consecutive times according to BS EN 12350-2:2009, however, the slump values were recorded to the nearest 5 mm instead of 10 mm that are stated in the standard and the average value of the two test results was used throughout the thesis. Furthermore, additional observations were made during mixing, placing and finishing of the concrete specimens as the slump test alone does not fully characterise the workability of concrete mixes incorporating MFAs (Quiroga et al. 2006). In addition to this the mixes were tested for plastic density and air content according to BS EN 12350-6:2009 and BS EN 12350-7:2009 respectively. Brief protocol of the fresh concrete tests is given in paragraphs below:

Slump test (BS EN 12350-2:2009)

- Standard base plate and steel cone mould with funnel was dampened with a wet cloth.

- The cone was held on the base plate and filled with three approximately equal height layers of concrete. Each layer was compacted with 25 strokes of compacting rod.
- The funnel was removed and the concrete at the top of the cone was smoothed level with rolling motion of the compacting rod. The concrete stuck to the base plate and the outside of the cone was removed.
- The steel cone was lifted upwards in a slow motion. The slump value (the difference between the highest point of concrete cone and the height of the steel cone mould) was measured to the nearest 5 mm.
-

Plastic density (BS EN 12350-6:2009)

- A steel container of known volume (V) and mass (m_1) was filled with concrete in three equal height layers. Each layer was fully compacted using a vibrating table.
- The top of the container was smoothed level with a float and the excess concrete from the sides and edges removed with a cloth.
- The filled container was weighed and the mass recorded as m_2.
- The density of fresh concrete was calculated according to the Equation 4.2.1:

$$D = \frac{m_2 - m_1}{V} \qquad \text{Equation 4.2.1}$$

where: D is density of fresh concrete in kg/m^3, m_1 is mass of empty container in kg, m_2 is the mass of the container completely filled and compacted with concrete in kg and V is volume of the container in m^3.

Air content (BS EN 12350-7:2009)

- Air content was determined using the pressure gauge method and the apparatus described in the standard and shown in Figure 4.2.1.

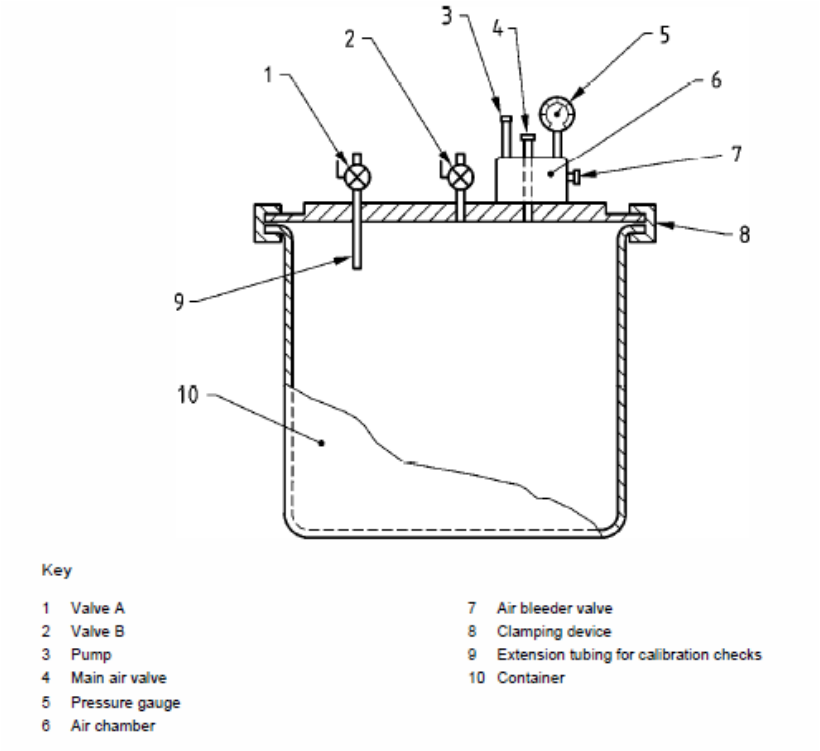

Figure 4.2.1 Pressure gauge method apparatus

- A container was filled in three layers with concrete and fully compacted using a vibrating table.
- The top of the concrete was smoothed level with a float and the rim and sides of the container were cleaned from excess concrete with a cloth.
- Cover assembly (1-7 in Figure 4.2.1) was clamped in place on top of the container, main air valve was closed and water was injected into the assembly through valve A until it emerged through valve B.
- The air bleeder valve was closed and the air was pumped in the air chamber and the pressure adjusted so that the pressure gauge was on initial pressure line.
- Valves A and B were closed and the main air valve was opened. The reading of entrained air was taken from the pressure gauge after light tapping.
- Valves A and B were opened to release the pressure before the cover assembly was removed.

4.2.2 Hardened concrete tests

Hardened concrete was tested for compressive strength at 1, 7 and 28 days according to BS EN 12390-3:2009 and flexural strength at 28 days according to BS EN 12390-5:2009. Brief descriptions of these procedures are given below:

Compressive strength (BS EN 12390-3:2009)

- Concrete cubes were removed from curing tank and the free water was wiped off with a cloth.
- The cube was put in the compression testing machine with the cast face towards the operator and aligned with steel plates at the top and bottom of the cube.
- Load was applied at a rate of 360±36 kN/minute which corresponds to 0.6 MPa/s until failure of the cube.
- The failure pattern was inspected and the load recorded.
- Compressive strength was calculated according to Equation 4.2.2.

$$f_c = \frac{F}{A_c} \qquad \text{Equation 4.2.2}$$

where: f_c is compressive strength in MPa, F is force in N and A_c is area in mm^2.

Flexural strength (BS EN 12390-5:2009)

- The concrete prisms 500 x 100 x 100 mm were taken from curing tank and dried off with a cloth.
- These were set up on rollers in a flexural strength testing machine as shown in Figure 4.2.2.
- A load at a rate of 125±12.5 N/s was applied until failure of the prism and the load was recorded.

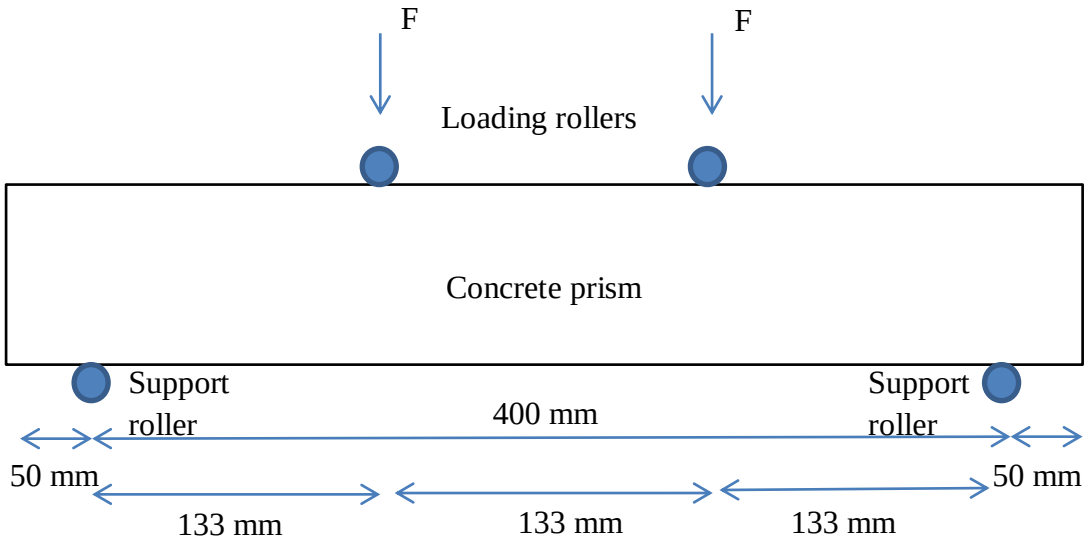

Figure 4.2.2 Setup for flexural strength testing

- The flexural strength of concrete was calculated according to the equation 4.2.3.

$$f_{t,fl} = \frac{F \cdot I}{d^3}$$ Equation 4.2.3

where: $f_{t,fl}$ is flexural strength in MPa, F is maximum load in N, I is distance between support rollers and d is lateral dimension of the prism.

4.2.3 Concrete mix composition

From the literature review in Chapter 2 it has been shown that the MFAs usually have a negative impact on concrete consistency, which is a primary factor dictating the suitability of a concrete mix for its intended use. Thus, if a MFA concrete is to be used, an appropriate consistency class for the particular mix has to be ensured. In the UK between 2011 and 2012, 71% of all concrete produced in ready-mix plants had a consistency class of either S2 or S3 which correspond to 50 to 150 mm slump (ERMCO 2013). Therefore, it was decided to design concrete mixes with an aim of achieving an S2 consistency class (50 to 90 mm slump) as this consistency is suitable for most concrete applications and would allow meaningful comparison between different fine aggregates.

Preliminary concrete mixes of 10 litre volume incorporating NS, B-D and G-FEED showed that due to variations in the fine aggregate gradings, geology and other properties it was impossible to make all mixes within the S2 consistency class slump range with the same w/c ratio and mix composition without the incorporation of a water reducing admixture. Thus, in order to minimize the number of variables and ensure better comparison between the different MFAs, two series of MFA concrete mixtures were created, those with constant slump and those with constant w/c ratio via the use of a plasticiser.

All MFA concrete mixes in the study had a volume of 40 litres. The first set of mixes was slump controlled and did not incorporate water reducing admixtures and in this thesis will be referred to as Stage I mixes. A control mix with natural sand was made with a view to achieving an S2 (50 – 90 mm) slump. For the MFA the -B graded sands were mixed to achieve the same S2 slump and the required w/c ratio recorded. This w/c ratio was then kept constant for the remaining gradings of the same quarry sand, recording the change in slump observed in each concrete mix.

In addition to the MFA sand mixes in Stage I, four mixes using the feed quarry dusts as the fine aggregate were made. These mixes were used to give an indication of quarry dust performance in concrete and to provide a comparison with MFA. However, the results should be treated with caution as the amount of quarry dusts was limited, therefore, these mixes had a volume of 10 litres and only slump and compressive strength were measured. These mixes were slump controlled with an aim to achieve the same S2 slump as in Stage I.

Following this, mixes incorporating various doses of water reducing agent to achieve an S2 slump whilst keeping the w/c ratio constant at 0.55 were made. These mixes in the thesis will be referred to as Stage II mixes. The w/c ratio was set to 0.55 as this is a common durability requirement set out in BS EN 206-1:2000 and covers the majority of commonly used concrete exposure classes. The limestone sand mixes achieved an S2 slump at a w/c ratio of 0.55 without admixtures, therefore the w/c ratio of these mixes was lowered to 0.50.

The mix proportions by weight are shown in Table 4.2.1. It was assumed in the mix design calculations shown in Appendix C that the density of the mix does not change when a different fine aggregate was used. This is not true as different aggregates will have different densities that result in change of mix volume if they are batched by weight. Therefore, for completeness the exact contents of the concrete components were recalculated using the densities of all components and are shown in Table 4.2.2.

Table 4.2.1 Concrete mix proportions by weight

Designation	Cement	FA	CA	w/c ratio	Admixture, l/m^3
Stage I	1	2.15	2.97	varies	-
Stage II	1	2.15	2.97	0.55 (0.5)[1]	varies

[1]for limestone mixes

Table 4.2.2 Concrete mix composition at SSD conditions

	Mix	Cement, kg/m^3	FA, kg/m^3	CA, kg/m^3	Water, kg/m^3	w/c
	Assumed	350	753	1040	varies	varies
Stage I	NS	368	792	1094	177	0.48
	G-series	354	762	1053	206	0.58
	B-series	352	758	1047	236	0.67
	L-series	367	790	1091	202	0.55
	GS-series	342	736	1016	229	0.67
	G-FEED	346	744	1027	228	0.66
	B-FEED	345	742	1025	248	0.72
	L-FEED	359	773	1068	219	0.61
	GS-FEED	335	721	996	251	0.75
Stage II	NS	359	772	1067	197	0.55
	G-series	358	770	1064	197	0.55
	B-series	368	792	1093	202	0.55
	L-series	374	805	1112	187	0.50
	GS-series	356	767	1059	196	0.55

Table 4.2.2 shows that there is slight variation in the mix composition per cubic meter due to the change of the fine aggregate, however, the ratios of aggregates to cement and coarse to fine aggregate by mass are constant. The cement contents of the 0.55 w/c ratio mixes, which were used for compressive strength comparison, range from 356 to 368 kg/m^3. It has been shown by Popovics and Ujhelyi (2008) and Zoran et al. (2010) that the effects of the variation of cement content in this range on compressive strength are small if the w/c ratio is constant. Therefore, the differences in compressive strength are attributable to the properties of the fine aggregate.

The fine aggregates produced in the V7 plant consisted of the basic V7 sand product and “skimmer” particles as discussed in Chapter 2. These were supplied in separate bags with corresponding production reports from the manufacturer. These components were mixed according to predefined proportions in order to ensure that the MFA sand gradings used in the concrete were consistent with the ones that were produced in the plant. The details of how this was achieved are given in Appendix B.

In all concrete mixes the weight of water and aggregate was adjusted according to their absorption capacity and corresponding water contents that were measured before the mixing in order to maintain a constant w/c ratio for each quarry sand. Exact calculations and records of these can be found in Appendix C, however, in short the adjustments were done in the following manner:

- The water content of aggregates was measured and the free water calculated according to Equation 4.2.4.

$$Free\ water, \% = Water\ content, \% - Absorption\ capacity, \% \quad \text{Equation 4.2.4}$$

where: *Absorption capacity* is water absorption capacity (WA_{24}) for the particular aggregate shown in Table 3.5.2.

- The weight correction for each aggregate due to moisture content difference from SSD conditions was then calculated according to Equation 4.2.5.

$$Correction, kg/m^3 = \frac{Free\ water,\%}{100} \times SSD\ weight, kg/m^3 \quad \text{Equation 4.2.5}$$

where: *SSD weight* is the weight of the aggregate at SSD conditions shown in tables in Appendix C.

- Then the corrected weight for each aggregate was determined using Equation 4.2.6.

$$Corrected\ Weight, kg/m^3 = SSD\ weight + Correction \quad \text{Equation 4.2.6}$$

- If a plasticiser was used, the additional water contained in the plasticiser that would contribute to the w/c ratio was calculated according to Equation 4.2.7.

$$Admixture\ water, L/m^3 = Admixture\ dosage \times \left(1 - \frac{solids,\%}{100}\right) \quad \text{Equation 4.2.7}$$

where: *solids,%* is the percentage of solids present in the plasticiser.

- Equation 4.2.8 was used to correct the mix water content:

$$Corrected\ water, l = SSD\ water - Admixture\ water - \sum Correction \quad \text{Equation 4.2.8}$$

where: *SSD water* is the initially assumed water content to be used in the mix if all aggregates were at SSD conditions.

4.2.4 Mixing sequence

The MFA concrete was mixed in a Belle Premier 200XT mixer which was wetted prior to the mixing with a thin film of water in order to minimise the loss of water which is usually experienced when a mixer is not pre-wetted. Table 4.2.3 shows the mixing sequence and corresponding duration of each stage.

Table 4.2.3 Concrete mixing sequence

Stage	Action	Mixing duration
1	Mix dry fine and coarse aggregates	1 min
2	Add half of mixing water	1 min
3	Add cement	1 min
4	Slowly add the rest of mixing water and plasticiser	1 min
5	Further mixing	1 min

The second stage of mixing is intended to saturate the aggregates before the cement is added since it may be possible that their water content is below SSD condition. By doing this the cement particles are limited in their ability to prevent or delay the absorption process in the aggregates, which would result in higher initial slump values if compared with aggregates which are already at SSD conditions (Lo et al. 2008).

The quarry dust mixtures described in section 4.2.3 were mixed in a smaller mixer due to the 10 litre volume of the mix, however, the procedures laid out in this section were observed.

4.2.5 Curing and specimen details

From each MFA concrete mix, nine 100 mm cubes for compressive strength tests and three 100 x 100 x 500 mm beams for flexural strength tests were cast. These were de-moulded after 16 hours and placed in a water tank at a temperature of 20 ± 3 °C until the testing age was reached.

4.2.6 Materials

All concrete mixes were prepared with the same cement, coarse aggregate and plasticiser in order to limit the number of variables and to allow the evaluation of fine aggregate effects on concrete properties. In addition to the fine aggregates described in Chapter 3 concrete mixes incorporated 4/20 mm crushed limestone coarse aggregate complying with BS EN 12620:2002, with water absorption of 0.66% and the grading shown in Figure 3.5.5. The cement chosen for the project was CEM I 52.5 N complying with EN 197-1 with a chemical composition given in Table 4.2.4. CEM I was used in order to avoid the inclusion of cement replacement materials such as PFA or GGBS, which are present in other cement types, which may have had an influence on the fresh and hardened concrete properties under consideration.

Table 4.2.4 Cement properties and oxide composition (wt. %)

Oxide	SiO_2	Al_2O_3	Fe_2O_3	CaO	MgO	SO_3	Cl^-	Free CaO	$Na_2O_{eq.}$[1]	LOI[2]
wt %	19.7	4.8	3.1	63.6	1.2	3.6	0.1	2.3	0.7	2.7

[1] Na_2O equivalent
[2] Loss of ignition

Potable tap water at a temperature of 20 ± 3 °C complying with BS EN 1008:2002 was used in the concrete mixes. Where necessary a mid-range water reducing agent (plasticiser) WRDA 90 supplied by GRACE Construction Products complying with BS EN 934-2 and with solids content of 50% was also incorporated.

4.3 Stage I results and discussion

This section will discuss the results of the Stage I concrete mixes and inspect the influence of the characterisation test results on the concrete properties. As these mixes are slump controlled with variations in w/c ratio, the main attention in this section will be focused on the factors that influence workability. Trend lines used in figures in this section are best fit lines intended for better indication of possible trends where not stated otherwise. If error bars are present in figures, then they represent minimum and maximum values for a given measurement with marked average value.

4.3.1 Workability

Table 4.3.1 shows the results of fresh and hardened concrete tests for Stage I concrete mixes. With regards to consistency, the basalt and sandstone sands required higher w/c ratios (0.67) than the granite and limestone sands (0.58 and 0.55 respectively) to achieve an S2 slump. This may be attributed to the presence of clay particles in the sands as indicated by the MBV and XRD tests discussed previously. Similarly Li et al. (2011) and Norvell et al. (2007) found that the presence of clays in the fine aggregate increases the water demand in concrete mixes for the same slump. Natural sand required the least water to cement ratio (0.48) to reach the S2 slump, as a result of the intrinsic roundness of the sand particles as well as a lack of fines which had been washed out in the dredging and screening process.

Table 4.3.1 Stage I concrete results

Mix	w/c	Slump, mm	Entrapped air, %	Plastic density, kg/m^3	Fines content, % of FA	Compressive strength, N/mm^2						Flexural strength, N/mm^2	
						1 day	COV, %	7 day	COV, %	28 day	COV, %	28 day	COV, %
NS-slump	0.48	95	0.50	2447	1.0	23.8	0.4	48.0	2.8	58.9	2.9	6.1	4.6
G-FEED[1]	0.66	80	-	-	13.0	12.5	1.9	30.3	0.0	39.1	3.5	-	-
G-A	0.58	120	0.45	2393	2.0	17.6	0.6	43.5	1.0	52.2	2.3	5.6	5.3
G-B	0.58	80	1.60	2375	2.9	17.0	1.6	40.2	1.6	49.9	1.9	5.6	5.4
G-C	0.58	80	0.90	2378	5.1	17.9	0.7	40.4	2.0	50.1	1.2	6.0	5.7
G-D	0.58	60	0.65	2393	6.5	19.3	1.9	42.2	2.1	52.3	1.4	5.8	7.3
G-E	0.58	60	0.78	2393	9.0	16.6	0.3	40.6	1.0	48.1	3.6	5.4	5.6
B-FEED[1]	0.72	70	-	-	10.0	9.3	2.4	25.8	0.4	35.5	0.9	-	-
B-A	0.67	70	0.50	2429	1.0	11.8	1.8	30.4	2.9	41.7	2.2	5.3	4.9
B-B	0.67	80	0.50	2423	2.9	12.9	2.1	31.3	4.5	43.7	1.7	5.5	5.1
B-C	0.67	62.5	0.45	2435	5.1	13.0	2.3	33.1	2.0	42.7	1.8	5.4	7.7
B-D	0.67	47.5	0.65	2410	7.4	13.2	2.3	35.2	0.4	45.6	2.6	5.6	3.2
L-FEED[1]	0.61	60	-	-	12.0	18.5	1.6	38.0	3.9	50.2	0.4	-	-
L-A	0.55	90	1.40	2444	2.8	18.0	2.5	44.3	2.8	55.7	3.1	6.6	4.3
L-B	0.55	70	1.50	2447	4.9	21.2	1.0	47.8	1.2	58.0	1.1	6.7	4.3
L-C	0.55	82.5	1.48	2456	7.1	22.7	4.2	46.2	3.2	56.2	3.6	6.1	8.0
L-D	0.55	65	1.38	2456	9.0	21.4	1.5	46.9	2.0	56.6	7.4	6.0	6.3
GS-FEED[1]	0.75	80	-	-	18.0	8.2	2.4	23.3	1.7	31.3	1.1	-	-
GS-A	0.67	85	1.40	2332	3.5	12.7	0.9	34.5	2.9	41.4	3.9	5.2	3.3
GS-B	0.67	75	0.78	2374	5.0	14.9	1.4	31.4	0.7	43.3	2.6	5.6	8.2
GS-C	0.67	97.5	1.00	2336	7.0	14.7	1.4	32.8	3.3	42.8	2.2	5.5	4.5
GS-D	0.67	75	1.20	2336	9.0	12.1	0.9	30.5	2.3	39.9	0.6	5.2	6.3

[1]Entrapped air and plastic density measurements missing due to 10 litre volume of the –FEED mixes.

The w/c ratio required to achieve an S2 slump for all quarry dust mixes was higher than for their MFA counterparts and the NS mix. This could be due to the inferior shape of the quarry dust as shown by the NZFC and high resolution images as well as the higher amount of fines in the quarry dusts when compared with the corresponding MFA. This may be seen as a beneficial influence of the MFA by allowing a lower w/c requirement for the same slump range from the same rock geology.

The results show a general trend of decreasing slump as the fines content increases as a result of an associated increase in the specific surface area of the sands. However, there are exceptions to this observation, for mixes GS-C, L-C and B-B in particular, where the slump values are higher than the expected trend. The GS-C and L-C sands contain 7.0 and 7.1% of fines whereas B-B only 2.9%. This could be attributed to the optimum packing or lubricating effect of the fines offsetting the negative effect of an increased specific surface area as suggested by Jones et al. (2003) and Wang et al. (2013). However, the geology, shape, grading and presence of clay particles in the fines affect the fines content required for optimum aggregate packing which would result in higher slump value. This is indicated by the different fines content of GS-C, L-C and B-B sands as well as the absence of unexpectedly higher slump value for any of the granite MFA mixes.

The classification of observations made during the mixing, handling and finishing of the concrete mixes is given in table 4.3.2 and the observations made for the Stage I mixes are presented in Table 4.3.3. According to the observations for the Stage I mixes a higher volume of fines in MFA concrete mixes is necessary to aid workability and finishability. For example, it can be seen in the G- series that the G-A mixture has a slump of 120 mm, but the concrete exhibits a harsh finish. As the fines content increases,

the slump reduces but the finishability improves. However, the G-E mixture with the fines content of 9% becomes sticky. Thus, it can be concluded that there is an optimum amount of fines for any particular combination of aggregates and cement to provide the required fresh concrete properties.

Table 4.3.2 Classification of observations

Observation	Classification	Description
Finishability	Easy	A smooth finish is easily achieved using a float.
	With effort	Considerable effort has to be exerted to make the finish smooth using a float.
	Harsh finish	The finished surface is rough as a result of angular aggregate edges protruding from the concrete surface.
Handling	Easy	Little effort is necessary to penetrate the fresh concrete with a scoop and fill it.
	Hard	Considerable effort is necessary to penetrate the fresh concrete with a scoop and fill it.
Cohesiveness	Sticky	Concrete adheres to the scoop and float and is not easily detached.
	Normal	A film of paste covers the scoop and float but is easily detached.
Other observations	Clumpy	During mixing clumps of aggregate and cement form.
	Dry	The paste is dry and the aggregate particles cannot float past each other.
	Segregating	Coarse aggregate detaches from paste and fine aggregate.

However, if limestone sands are considered which had the least water demand for an S2 slump and the least MBV of all MFA, then it can be seen from Table 4.3.3 that they finished with effort and showed a harsh finish even with slump values from 65 to 90 mm. This could be attributed to slightly more angular particles as indicated by the NZFC flow times which were slightly higher than those of other MFA.

The basalt sands which contained montmorillonite-chlorite clay required a w/c ratio of 0.67 to achieve an S2 slump. From Table 4.4.3 it can be seen that B-A, B-B and B-C mixtures were “a bit” sticky but still easy to handle and finish, whereas B-D mix lost workability immediately following mixing and was sticky. The cohesiveness along with the rapid loss of workability could be attributed to the increased presence of montmorillonite-chlorite clay in higher fines sands and the time dependent water absorption process of the clay particles. In B-A to B-C mixes the fines fill the voids, thus aiding workability and finishability and the clay content is low enough for the time dependant water absorption effect to be readily perceived, whereas in the B-D mix the clay concentration offset the positive influence of the fines on fresh concrete properties.

Sandstone sands required the same 0.67 w/c ratio as the basalt sands but showed slightly higher slump values than the B- series. Furthermore, all mixes were easy to work and finish at this w/c ratio. This could indicate the importance of the type of the clay which is present in the sand. Sandstone MFA contained illite clays whereas basalt MFA contained montmorillonite-chlorite as identified by the XRD analysis. These observations suggest that montmorillonite-chlorite is more detrimental to the fresh concrete properties than illite clay. The amount of the clay present in each sand is unknown, however, according to Norvell et al. (2007), at the same concentration, montmorillonite clays show a higher water and admixture demand than illite clays.

Table 4.3.3 Observations made during mixing and casting of Stage I concrete mixes

Mix	Observations
NS-slump	Finishability: easy, Handling: easy, Cohesiveness: Normal
G-FEED	Finishability: easy, Handling: easy, Cohesiveness: Normal, minor segregation
G-A	Finishability: with effort, harsh, Handling: easy, Cohesiveness: Normal
G-B	Finishability: easy, harsh, Handling: easy, Cohesiveness: Normal
G-C	Finishability: easy, Handling: easy, Cohesiveness: Normal
G-D	Finishability: easy, Handling: easy but harder than that of G-C, Cohesiveness: Normal
G-E	Finishability: easy, Handling: easy, Cohesiveness: Sticky
B-FEED	Finishability: easy, Handling: easy, Cohesiveness: Normal
B-A	Finishability: easy, Handling: easy, Cohesiveness: a bit sticky
B-B	Finishability: easy, Handling: easy, Cohesiveness: a bit sticky
B-C	Finishability: easy, Handling: easy, Cohesiveness: a bit sticky
B-D	Finishability: easy, Handling: easy right after mixing but rapidly becomes stiff, Cohesiveness: sticky, Dry
L-FEED	Finishability: with effort, Handling: hard, Cohesiveness: Normal, segregation
L-A	Finishability: with effort, harsh, Handling: easy, Cohesiveness: Normal
L-B	Finishability: with effort, harsh, Handling: easy, Cohesiveness: Normal
L-C	Finishability: with effort, harsh, Handling: easy, Cohesiveness: Normal
L-D	Finishability: harsh, Handling: hard, Cohesiveness: Normal
S-FEED	Finishability: easy, Handling: easy, Cohesiveness: Sticky
GS-A	Finishability: easy, Handling: easy, Cohesiveness: Normal
GS-B	Finishability: easy, Handling: easy, Cohesiveness: Normal
GS-C	Finishability: easy, Handling: easy, Cohesiveness: Normal
GS-D	Finishability: easy, Handling: easy, Cohesiveness: Normal

The effects of fine aggregate characteristics, in terms of the test results presented in Chapter 3, on the concrete workability were investigated for the –B sands, quarry dust feed materials and NS. These covered a range of sands with different mineralogy and physical characteristics while the mixes had slump values in the S2 range with different

w/c ratios. The trends of water demand were evaluated by observing the variation of w/c ratio requirement for an S2 slump with the aggregate characterisation test results.

Figure 4.3.1 shows a general trend of higher water demand for a constant slump range as the fines content of the fine aggregate is increased. Similar observations were made by Ahn and Fowler (2001), who reported that an increased w/c ratio is required for a constant MFA mortar flow as the fines content is increased in the aggregate. It can be seen from the R^2 value of 0.47 in Figure 4.31 that the trendline is a weak fit to the data. If the data points are grouped as shown in the Figure 4.3.1 then a general trend can be seen where natural fine aggregate requires the least w/c ratio and have the least fines followed by MFA and then quarry dusts. However, within the groups there is a significant variation of required w/c ratio for constant slump. Thus, the scatter of results suggests that there are other, more dominant factors influencing the water demand.

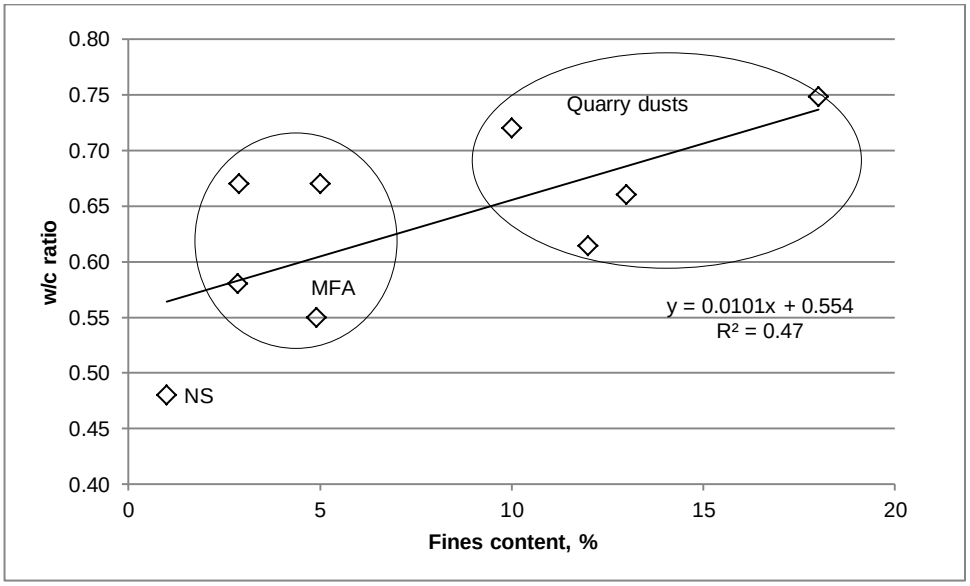

Figure 4.3.1 Variation of w/c ratio for constant slump due to fines content

Figure 4.3.2 shows the variation of w/c ratio with increase in MBV for a constant slump range and a non-linear best fit line for the data. It can be seen that clay free sands (as indicated by XRD tests) have a MBV below 1 g/kg and, in order to obtain concrete

mixes with slump in the S2 range using these fine aggregates, the required w/c ratio varies from 0.48 to 0.66. This suggests that below an MBV of 1 g/kg the water demand is governed by the grading, shape and texture of the fine aggregate. However, if the MBV exceeds 1 g/kg and the fine aggregate contains clays the required w/c ratio for an S2 slump is above 0.67 regardless of other properties of the aggregate. Similarly Li et al. (2011) found that limestone MFA aggregate with an MBV below 1.1 g/kg had little effect on consistency, however, a drastic decrease in consistency was observed when the MBV exceeded 1.45 g/kg due to addition of clay particles in the aggregate.

The Stage I results show that, while high MBV increases the water demand, the concrete mixes can be made workable by increasing the w/c ratio. Thus MFA with high MBV could be used in concrete applications where low compressive strength is required and there are no limitations on the w/c ratio due to exposure to aggressive environments.

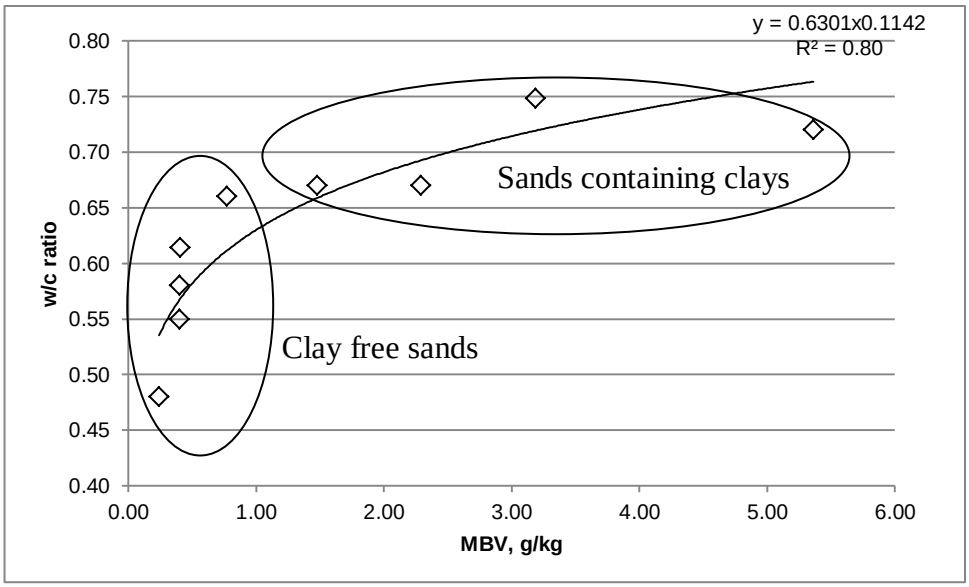

Figure 4.3.2 Variation of w/c ratio for constant slump due to MBV

Figure 4.3.3 shows the variation of water demand for constant slump with SE values. There is a prominent trend of decreased water demand when SE values exceed 65 and

the best fit line for the data was found with a 2nd order polynomial. It can be seen that the SE test performs worse compared to the MBV test when trying to distinguish between sands with and without clays as indicated by the overlapping marked areas in Figure 4.3.3.

The aim of the MBV and SE tests is to identify the presence of clays in an aggregate and in Figure 3.5.12 it was shown that there is a weak trend between SE and MBV values similarly to the results reported by Nikolaides et al. (2007). The differences in the ability of these tests to distinguish between sands containing clays and clay free sands could be attributed to the principle of the SE test which is to determine the proportion of clay sized particles in the whole sample. The clay sized particles (very fine stone dust) are marginally affecting water demand when compared to clays as shown by Norvell et al. (2007). However, given the relatively good trend between the water demand and both abovementioned tests as shown in Figures 4.3.2 and 4.3.3, it can be concluded that these tests are able to indicate presence of deleterious fines (clays) in fine aggregates through different mechanisms.

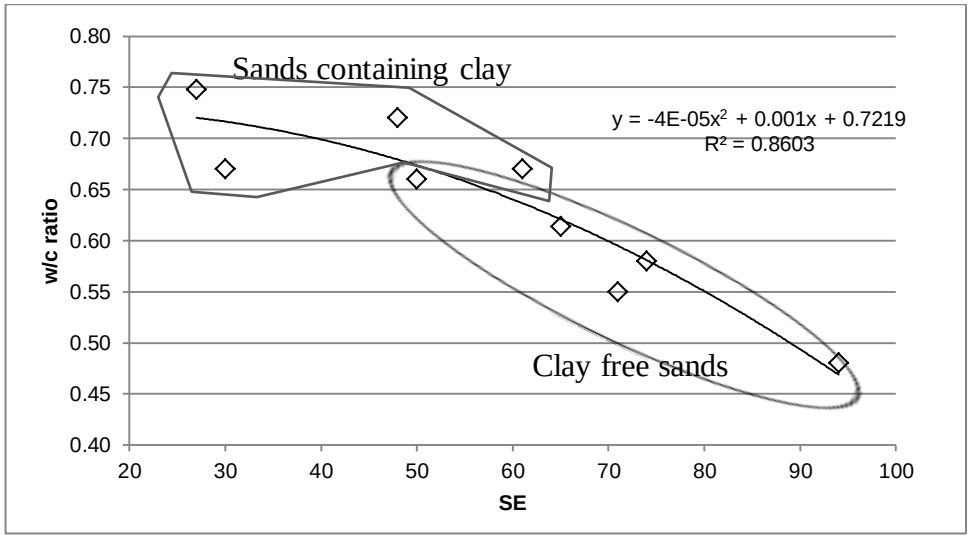

Figure 4.3.3 Variation of w/c ratio for constant slump due to SE values

If the NZFC results are considered, then it can be seen from Figure 4.3.4 that an increase in the un-compacted voids content of the fine aggregates generally results in an increased water demand. These observations are supported by the findings of Marek (1992) and Donza et al. (2002) who suggest that the more angular the aggregate particles, the higher the voids content for a particular grading and, thus, more cement paste is required to fill the voids and provide adequate workability.

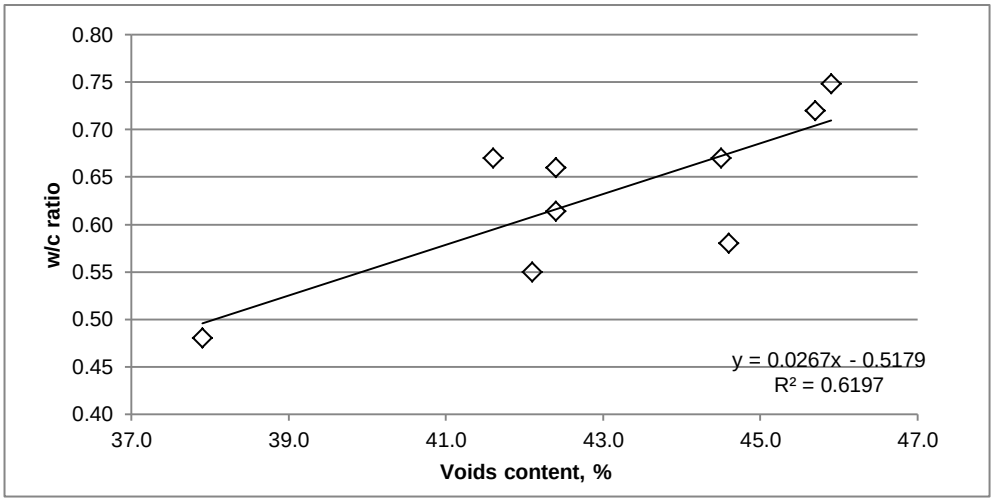

Figure 4.3.4 Variation of w/c ratio for constant slump due to voids content

A similar trend but with a larger scatter of data points between the water demand and flow time determined through the NZFC test is shown in Figure 4.3.5. The increase in flow time is associated with higher angularity of aggregate particles or coarser grading or both. A coarser grading would result in a decreased water demand due to the reduction in the specific surface area, while a higher angularity in contrast would increase the specific surface area of the fine aggregate, thus requiring a higher amount of paste and water to wet the surface. As the gradings for the sands plotted in Figure 3.4.5 are different, it is impossible to distinguish between the two theories mentioned above.

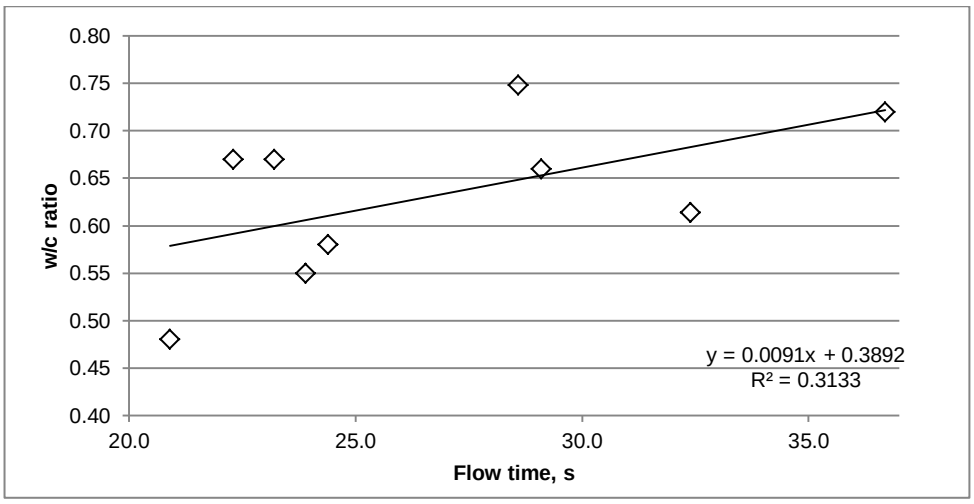

Figure 4.3.5 Variation of w/c ratio for constant slump due to flow time

From Figure 4.3.6 it can be seen that increase in absorption capacity of quarry dusts and MFA results in an increased water demand. This trend should be treated with caution since the water absorption results may have been influenced by the presence of clays that are not readily removed by washing during the water absorption test as noted in Chapter 3 and reported by Thomas et al. (2007). If that is the case, then the water absorption is an indication of the presence of clays in the MFA and as shown in Figures 4.3.2 and 4.3.3, this fine aggregate characteristic has a prominent effect on water demand. On the other hand, rougher particle surface and finer sands could result in higher specific surface area compared to smooth and coarsely graded sands, which leads to increased absorption capacity as well as increased water demand in fresh concrete.

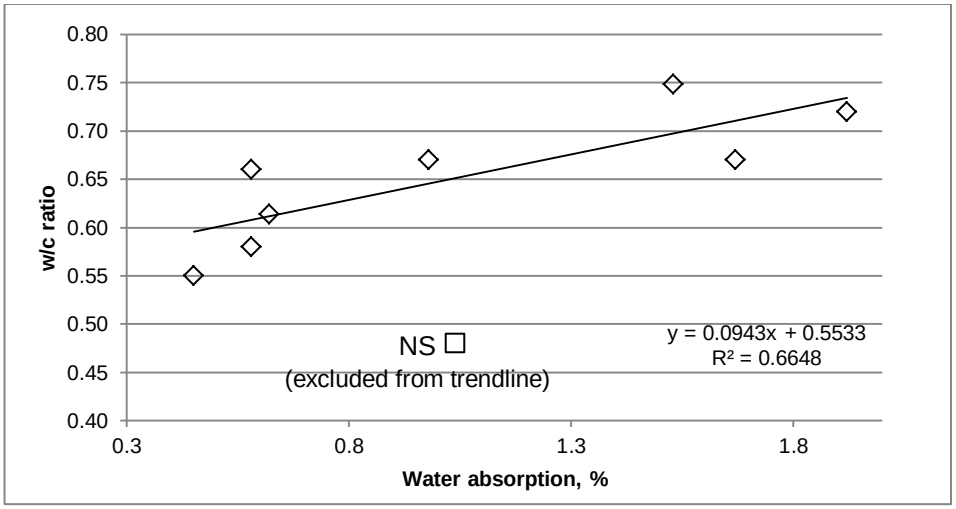

Figure 4.3.6 Variation of w/c ratio for constant slump due to water absorption

In terms of MFA concrete workability it can be concluded that the dominant factor affecting it is the presence of clays as indicated by the SE and MBV results. Other factors, shape, texture, grading, fines content affect the workability to a lesser extent as indicated by the test results, however, their influence is interconnected and can not be isolated from one another. Thus, the workability of concrete should be considered as a multi-variable non-linear problem. In order to aid the mix design and predictions of expected performance of fresh concrete made with different fine aggregates appropriate tools that are capable of dealing with non-linear multi-variable problems should be employed.

4.3.2 Compressive and flexural strength

Despite the presence of clay and a w/c ratio of 0.67 basalt and sandstone concretes produced workable concretes with 28 day compressive strengths in a range of 39.9 to 43.7 N/mm^2. Granite sands at 28 days reached compressive strength of 48.1 to 52.2 N/mm^2. Limestone sands yielded concrete with compressive strengths from 55.7 to 58.0 N/mm^2 which is comparable to the dredged sand control mix that had a strength of 58.9 N/mm^2.

The major factor influencing the compressive strength is the w/c ratio as shown in Figure 4.3.7: the lowest w/c ratio yielded the highest compressive strength and vice versa. In general it is agreed that compressive strength of concrete follows the Abrams' formula shown in Equation 4.3.1 (Neville 1995).

$$f_c = \frac{A}{B^{w/c}} \qquad \text{Equation 4.3.1.}$$

Where f_c is the compressive strength of concrete; *A* and *B* are experimental parameters for a given age, material and curing conditions; and *w/c* is water/cement ratio by mass.

In Figure 4.3.7 three of these equations have been fitted for 28 day compressive strength with different coefficients. It can be seen that NS, G-FEED and GS-FEED mixes fit

better to the line with coefficient B=12.5 whereas the –L and L-FEED are closer to B=9 line and the rest are somewhere in-between the two. Given that the difference in the mixes apart from the w/c ratio is the fine aggregate it can be seen that the properties of fine aggregate have a distinct influence on the compressive strength of concrete. For example, the limestone sands produced concretes with approximately the same strength as natural sand concrete but with a 0.07 higher w/c ratio. This could be attributed to the beneficial effects of MFA particle shape and texture on bond strength as reported by Donza et al. (2002) or the ability of limestone fines to act as nucleation sites for cement hydration products (Li et al. 2009).

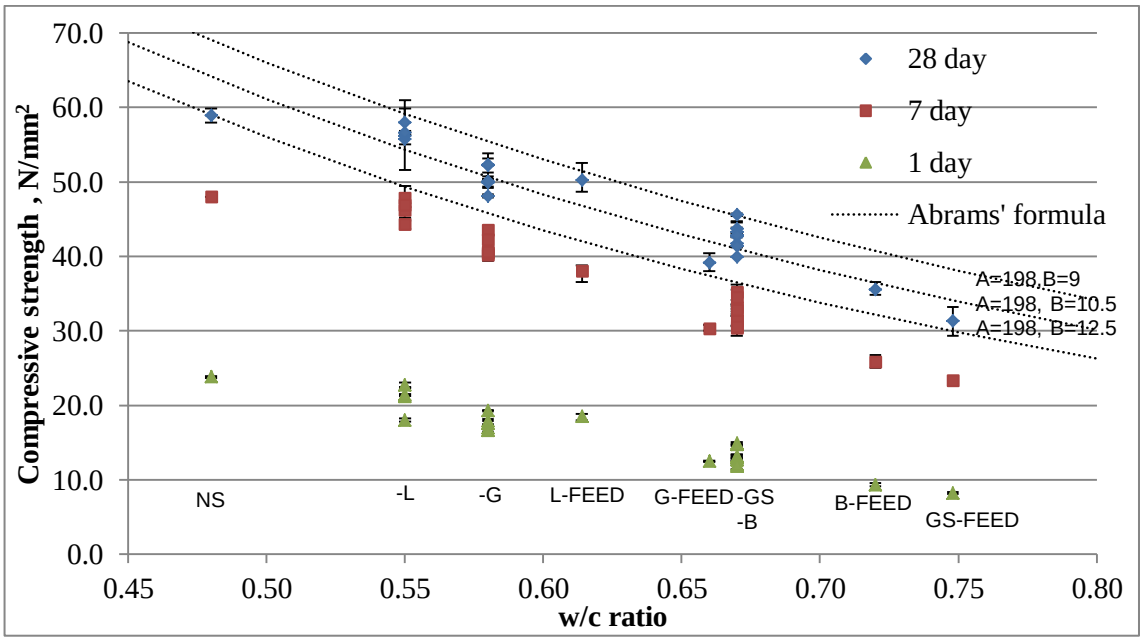

Figure 4.3.7 Variation of compressive strength with w/c ratio for Stage I mixes

The 28 day compressive strength of concretes made with quarry dust mixes is 5 to 10 N/mm^2 lower than that of corresponding MFA concretes. This is due to the elevated w/c ratios required to achieve the same slump. This suggests that the reprocessing of the quarry dusts in the V7 plant has yielded more suitable fine aggregate for concrete applications.

The coefficient of variation (CoV) for all compressive strength measurements is below 5% with the exception of the L-D mix at 28 days which had a CoV of 7.4%. This suggests that the concrete mixes were homogeneous and had been properly and consistently compacted and cured.

Figure 4.3.8 shows the 28-day compressive strength trends with respect to increasing fines content in each MFA series. It can be seen that there is no evident trend for different mineralogy sands as suggested in previous studies (Celik and Marar 1996, Topçu and Uurlu 2003, Li et al. 2009). The compressive strength variations do not show any trends and do not exceed 5 N/mm^2 and can be considered negligible in the 1 to 9 % fines content range. The lack of correlation could be attributed to the low level of fines content as other researchers have used fines contents as high as 30%. Furthermore, they have been replacing a part of fine aggregate with sub 63 micron particles, typically limestone fines. Whereas the difference in the MFAs used in this study is that they incorporated sub 63 micron particles as well as coarser ones of the same mineralogy. Thus it can be concluded that the fines content in the range from 1 to 9 % has only a limited effect on compressive strength for the tested MFA. This suggests that, if the compressive strength is considered, the highest fines content grading of the tested MFA should be used in concrete to ensure efficient use of materials and minimisation of waste. However, the limitation on the fines content will be imposed by the required fresh concrete properties due to the effect on water demand as discussed in the previous section.

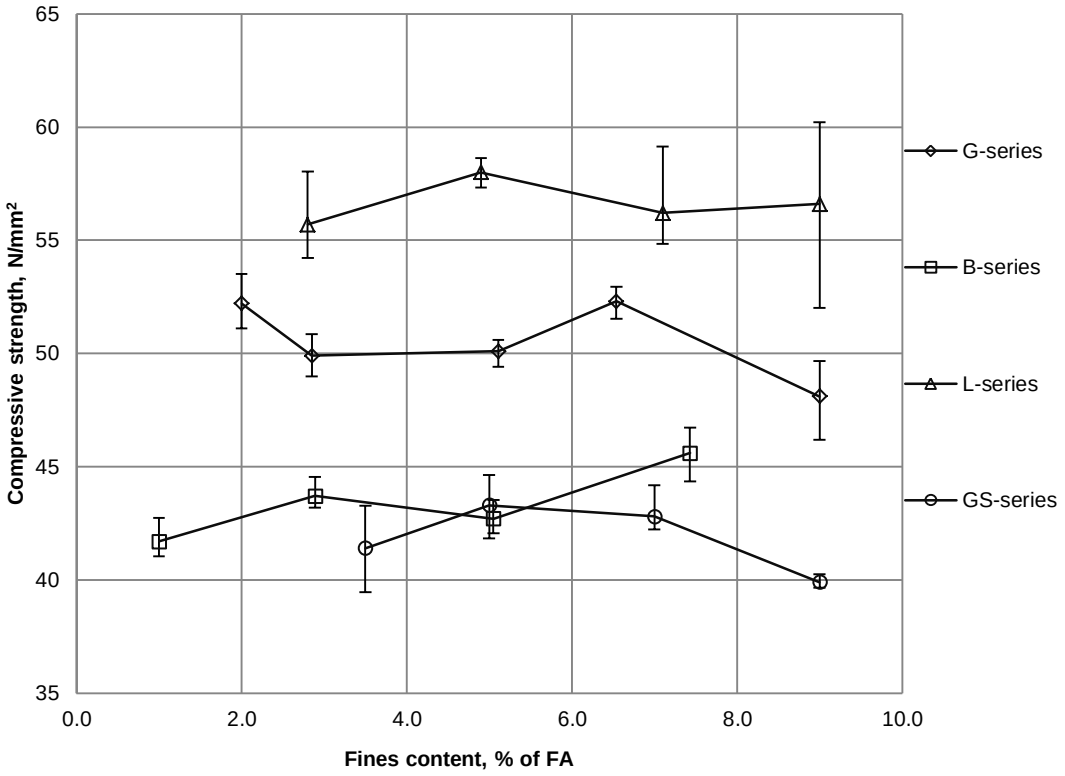

Figure 4.3.8 MFA concrete compressive strength versus fines content for Stage I mixes

The flexural strength of all concrete mixes was in the range of 5.2 to 6.7 N/mm^2 with the highest coefficient of variation of 8 %. The variation of the flexural strength with compressive strength, theoretical relationship from Eurocode 2 and its upper and lower bound values are shown in Figure 4.3.9. The flexural strength results show a good fit to the theoretical relationship from Eurocode 2 as all data points lie within the upper and lower bound values and are close to the corresponding mean flexural strength values.

Eurocode 2 provides a relationship for estimating the tensile strength from characteristic compressive strength of concrete and it is given in Equation 4.3.2 and 4.3.3.

$f_{ctm} = 0.3 \cdot (f_{ck})^{2/3}$ for concrete grades ≤C50/60 Equation 4.3.2

$f_{ctm} = 2.12 \cdot ln(1 + 0.1 \cdot (f_{ck} + \Delta f)$ for concrete grades >C50/60 Equation 4.3.3

Where: f_{ck} is characteristic compressive strength and Δf is 8 MPa.

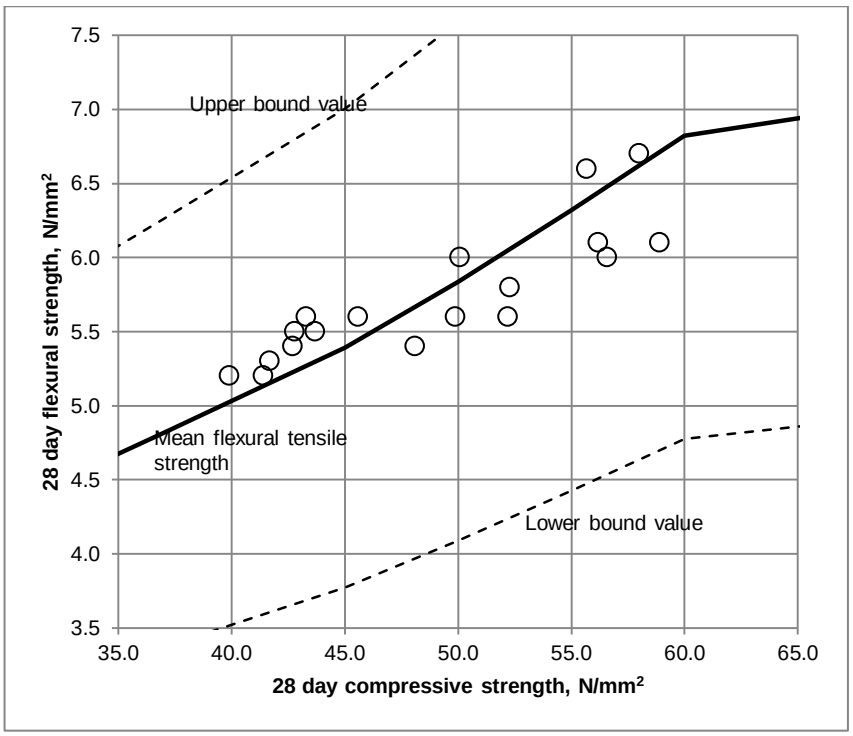

Figure 4.3.9 Flexural strength against compressive strength for Stage I mixes

It also provides an estimation of lower and upper bound values, $f_{ctk,0.05}$ and $f_{ctk,0.95}$ respectively, for characteristic tensile strength from the mean tensile strength as shown in Equations 4.3.4 and 4.3.5. These lower and upper bound values roughly correspond to 5% and 95% percentiles for the characteristic tensile strength.

$$f_{ctk,0.05} = 0.7 \cdot f_{ctm} \qquad \text{Equation 4.3.4}$$

$$f_{ctk,0.95} = 1.3 \cdot f_{ctm} \qquad \text{Equation 4.3.5}$$

It has to be noted that the relationship in Equation 4.3.1 and 4.3.2 uses cylinder compressive strength and estimates axial tensile strength while the test results in the thesis are cube compressive strength and flexural tensile strength. Eurocode 2 does not provide a direct relationship for converting cube compressive strength to cylinder compressive strength, however, discreet data points are provided when defining concrete strength classes and they can be found in Table 3.1 in Eurocode 2. Therefore, these were used to calculate the axial tensile strength and the lower and upper bound values for a range of cube compressive strength and used in the production of Figure

4.3.9. For converting axial tensile strength to flexural tensile strength a relationship suggested in Model Code 2010 (fib 2013) and shown in Equation 4.3.6 and 4.3.7 was used:

$$f_{ct,fl} = \frac{f_{ctm}}{A_{fl}} \qquad \text{Equation 4.3.6}$$

Where: $f_{ct,fl}$ is mean flexural strength, f_{ctm} is mean tensile strength, $A_{fl} = \frac{\alpha_{fl} h_b^{0.7}}{1+\alpha_{fl} h_b^{0.7}}$, h_b is beam depth in mm and α_{fl} is 0.06.

Given that beam depth was 100 mm, Equation 4.3.6 becomes:

$$f_{ct,fl} = \frac{f_{ctm}}{0.6} \qquad \text{Equation 4.3.7}$$

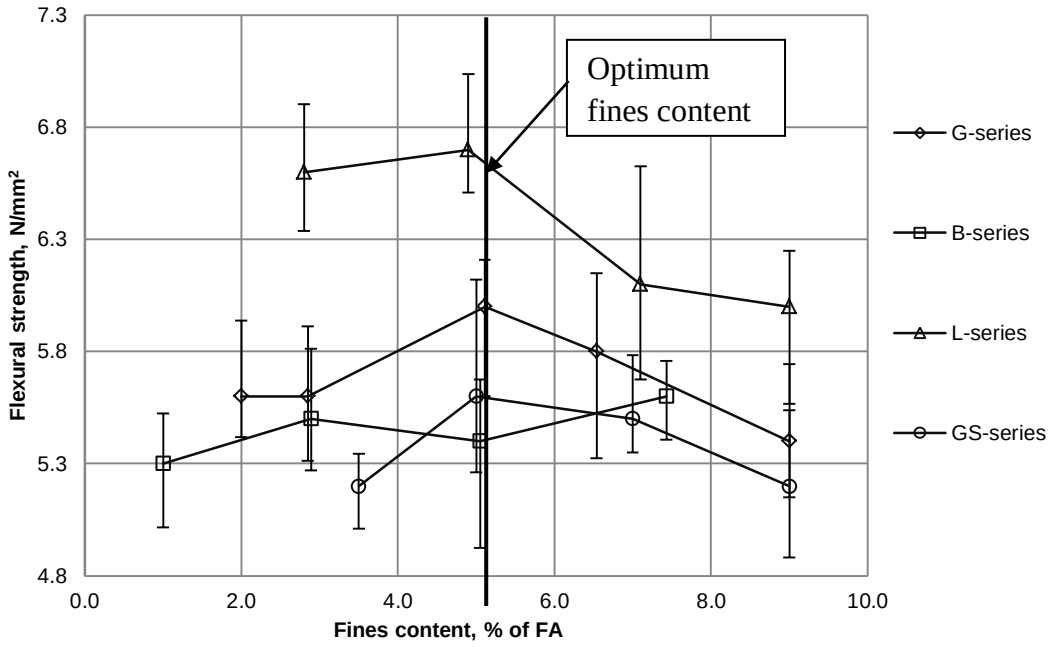

Figure 4.3.10 Flexural strength against fines content for Stage I mixes

Considering the effects of the fines on flexural strength, in contrast to the compressive strength, there is an optimum value which provides the highest flexural strength value as shown in Figure 4.3.10. For all MFA series except that of basalt sand, a 5% fines content yields the highest flexural strength. The usual explanation in the literature for this behaviour is that a particular fines content provides the optimum packing density of

the paste which results into a denser concrete and increased bond strength between the aggregates and the paste. If this is the case, then the flexural strength is affected by the bond strength to a greater degree than compressive strength and thus no apparent trend between fines content and compressive strength was observed. However, this optimum fines content value for flexural strength should vary for different mixture compositions and aggregate properties as shown by the differences observed in the B-series results. Furthermore, the difference in flexural strength at optimum fines content compared to other levels of fines for each sand series did not exceed 0.8 N/mm^2. Thus the potential benefit of slightly higher flexural strength when using MFA with optimum fines content should be considered concurrently with the potential sustainability benefits from utilizing the highest fines content MFA.

4.3.3 Plastic density and entrapped air

The plastic density of the fresh concrete mixes varied from 2332 kg/m^3 for the GS-A to 2456 kg/m^3 for the L-C and L-D mixes. Dry density, w/c ratio and entrapped air influence this measurement. In general, the higher the dry density of the fine aggregate, when in combination with a lower w/c ratio the higher the plastic density for concrete as can be seen in the L-series mixes. Within each sand series the density follows the inverse trend of entrapped air – the higher the volume of entrapped air, the lower the plastic density.

The entrapped air measurement ranges from 0.45 to 1.60 %. Within each MFA concrete series it is relatively constant with the exceptions of the G-B and GS-B mixes. This could be explained by excessive or insufficient vibration of these concrete samples. This is supported by correspondingly higher plastic density for the GS-B mix, and a lower for G-B mix.

4.4 Stage II results and discussion

This section will discuss the results of the Stage II concrete mixes and inspect the influence of the MFA characterisation test results on concrete properties. As these mixes are made with a constant w/c ratio, the main attention in this section will be focused on the influence on compressive and flexural strength since these two parameters should be affected only by the aggregate properties if the w/c ratio remains unchanged. Trend lines used in figures in this section are best fit lines intended for better indication of possible trends where not stated otherwise. If error bars are present in figures, then they represent minimum and maximum values for a given measurement with marked average value.

4.4.1 Workability

Stage II concrete results are shown in Table 4.4.1. It shows that the G- and L- series achieved the S2 slump with the aid of a water reducing admixture, whereas the B-B to B-D and GS-B to GS-D slump values were either at or below the lower S2 limit even with the highest recommended admixture dosages. This suggests that if a workable concrete mix with reasonable w/c ratio is required then the presence of clay in MFA is the first and foremost limiting factor.

The observations made during the mixing and casting are shown in Table 4.4.2 and it can be seen that in the clay free MFA mixes (G-series, L-series) the handling and finishability improves as the grading becomes finer. If the gradings in Figures 3.5.1 to 3.5.4 are considered, it can be concluded that for the MFA the clay free fines content along with particles smaller than 1 mm are important for providing adequate handling and finishing properties of concrete.

Table 4.4.1 Stage II concrete results

							Compressive strength, N/mm^2						Flexural strength, N/mm^2	
MIX	w/c	Slump, mm	Admixture, l/m^3	Entrapped air, %	Plastic density, kg/m^3	Fines, % of FA	1day	CoV, %	7 day	CoV, %	28 day	CoV, %	28day	CoV, %
NS-w/c	0.55	collapse	0	0.90	2457	1.0	13.2	1.9	39.0	2.3	50.5	0.6	5.3	10.4
G-A	0.55	65	0	1.50	2387	2.0	16.4	1.7	44.4	2.7	53.0	2.7	5.7	5.7
G-B	0.55	67.5	0	1.40	2388	2.9	20.1	1.4	46.1	1.6	59.2	2.2	5.8	9.6
G-C	0.55	70	1.25	1.30	2395	5.1	20.7	0.9	46.1	1.7	55.2	1.9	5.9	7.1
G-D	0.55	60	0.62	1.40	2387	6.5	19.4	3.1	48.3	1.3	58.6	1.7	5.5	2.7
G-E	0.55	85	1.00	1.40	2385	9.0	16.6	2.2	47.8	1.6	59.2	1.7	4.7	12.2
B-A	0.55	60	2.75	1.41	2470	1.0	14.5	2.8	48.2	1.1	57.6	2.5	6.1	4.2
B-B	0.55	30	2.75	1.60	2457	2.9	14.6	1.7	49.2	1.1	60.5	1.8	6.4	3.8
B-C	0.55	30	3.30	1.30	2475	5.1	17.9	2.7	48.4	1.5	59.4	2.4	6.1	1.0
B-D	0.55	25	3.30	1.80	2439	7.4	16.5	2.8	48.3	2.4	58.5	2.5	5.9	1.4
GS-A	0.55	60	2.45	1.28	2407	3.5	14.8	1.1	44.3	1.3	55.0	2.8	5.4	4.1
GS-B	0.55	50	2.75	1.30	2403	5.0	19.8	2.0	43.8	1.6	55.3	1.9	6.0	5.6
GS-C	0.55	50	2.75	1.35	2388	7.0	18.4	1.7	43.2	0.8	55.6	2.1	5.4	7.3
GS-D	0.55	45	2.75	1.56	2412	9.0	17.2	1.7	41.7	0.4	53.0	2.6	5.9	10.6
L-A	0.50	90	1.63	1.30	2482	2.8	23.9	0.7	52.5	1.8	64.3	5.5	6.1	3.6
L-B	0.50	90	1.10	1.30	2459	4.9	20.0	1.8	49.7	6.4	61.1	1.9	6.4	16.0
L-C	0.50	75	1.35	1.10	2467	7.1	23.2	0.8	51.1	2.6	63.0	3.0	6.1	23.1
L-D	0.50	65	1.10	0.80	2465	9.0	20.0	0.9	47.1	0.2	59.9	2.1	6.8	14.2

Table 4.4.2 Observations made during mixing and casting of Stage II concrete mixes

MIX	Observations
NS-w/c	Finishability: easy, Handling: easy, Cohesiveness: Normal, slump collapse and some segregation observed.
G-A	Finishability: harsh, Handling: easy, Cohesiveness: Normal.
G-B	Finishability: easy, Handling: easy, Cohesiveness: Normal.
G-C	Finishability: easy, Handling: easy, Cohesiveness: Normal.
G-D	Finishability: easy, Handling: easy, Cohesiveness: Normal.
G-E	Finishability: easy, Handling: easy, Cohesiveness: Normal.
B-A	Finishability: with effort, Handling:hard, Cohesiveness: Normal, dry mix.
B-B	Finishability: with effort, Handling:hard, Cohesiveness: Normal, dry mix.
B-C	Finishability: with effort, Handling:hard, Cohesiveness: Normal, dry and clumpy mix.
B-D	Finishability: with effort, Handling:hard, Cohesiveness: sticky, dry and clumpy mix.
GS-A	Finishability: with effort, Handling:easy, Cohesiveness: Normal, “dryish” mix.
GS-B	Finishability: with effort, Handling:easy, Cohesiveness: Normal, “dryish” mix.
GS-C	Finishability: with effort, Handling:easy, Cohesiveness: A bit sticky, “dryish” mix.
GS-D	Finishability: easy, Handling:hard, Cohesiveness: Sticky, “dryish” mix.
L-A	Finishability: harsh, with effort, Handling:hard, Cohesiveness: Normal, some segregation observed.
L-B	Finishability: with effort, Handling:easy, Cohesiveness: Normal.
L-C	Finishability: easy, Handling:easy, Cohesiveness: Normal.
L-D	Finishability: easy, Handling:easy, Cohesiveness: Normal..

The MFA (B-series, GS-series) with clays present at a w/c ratio of 0.55 were observed to be dry and hard to handle and finished with effort. Increasing the fineness of the sands (i.e. an increase in % fines content) decreased the consistency and mixes became sticky and hard to handle. Even the high plasticiser dosages could not remedy this

shortfall as there was insufficient free water left in the mixes following the absorptive action of the clays.

To address the presence of clays in MFA when a low w/c ratio mix is required with adequate slump several solutions could be adopted. The first would be using the lowest fines grading, thus reducing the clay content but meanwhile sacrificing the beneficial effects of fines in terms of handling and finishability of the fresh concrete. The other would be looking at different types of admixtures such as CLARENA™ developed by Grace Construction Products that is claimed to mitigate the negative effects of clays in aggregates. Another option would be to wash the fines out of the aggregates, however, as shown by the observations in Tables 4.4.1 and 4.4.2 in some cases this would be detrimental to the MFA performance and would add additional costs to the aggregate production.

From the Stage II results it can be concluded that presence of clays is the major factor negatively influencing concrete consistency and increasing admixture demand. This effect cannot always be counteracted by increasing the admixture dosage, as shown by the gritstone and basalt sand results.

There is a general trend of increased admixture demand/reduced slump due to finer MFA gradings. However, the handling and finishability properties are improved even with lower slump values by increased levels of fines, if they are free from clay particles, as observed with the granite and limestone sands. These observations support the conclusions of Quiroga et al. (2006) that the slump test alone does not provide adequate information about the fresh properties of MFA concrete. Thus, along with the slump test, it could be suggested that observations are made regarding the handling and finishing

during trial mixing as well as selecting MFA with higher fines gradings (3 – 7% fines content) if these have low MBV values (below 1g/kg) when designing MFA concrete.

4.4.2 Compressive and flexural strength

This section presents the results and discussion of compressive and flexural strength with respect to fine aggregate characteristics from the Stage II concrete mixes. In the Figures presented the average values with error bars showing maximum and minimum values are given along with the best fit lines for the data.

In the Stage II mixtures a mid-range plasticiser was used and one of the assumptions in its use was that it does not affect the compressive or flexural strength of concrete at 28 days and acts only as a workability aid. The extra water introduced by the admixture was deducted from the mixing water, thus eliminating the changes in w/c ratio which would otherwise occur. This is supported by the fact that the 7 and 28 day concrete strength results do not show a trend with the admixture dosage according to Figure 4.4.1. Slightly reduced 1 day compressive strength at a high admixture dosage could be caused by the delayed cement hydration caused by the influence of the admixture, as observed by Uchikawa et al. (1992).

As shown in Table 4.4.1 at the same w/c ratio of 0.55 the compressive strength of all MFA mixes was found to exceed that of the NS-w/c control which attained 50.5 N/mm^2 at 28 days. The compressive strength for all MFA mixes at a w/c ratio of 0.55 was in the range 53.0 to 60.5 N/mm^2 at 28 days, whereas the slump controlled NS mix (from Stage I) attained 58.9 N/mm^2 at 28 days. The compressive strength of the limestone mixes at a w/c ratio of 0.50 exceeded or were equal to that of the control NS mixtures. These results show the beneficial effects of MFA particle angularity with respect to the compressive strength of concrete.

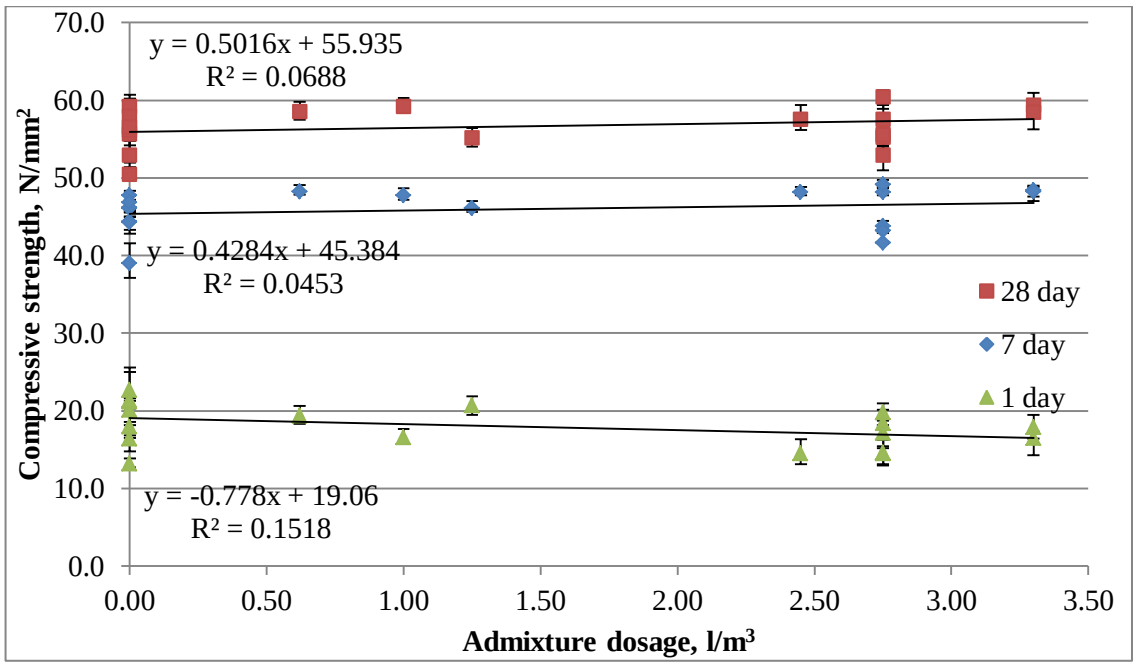

Figure 4.4.1 Compressive strength versus admixture dosage for 0.55 w/c ratio mixes

The coefficients of variation for all compressive strength measurements were below 5% except for the L-A and L-B mixtures with 5.5% at 28 days and 6.4% at 7 days respectively. This, similarly to the Stage I mixes, suggests that the concrete samples have been properly vibrated and cured and the variations in the measurements are not significant.

If all MFA and NS concrete mixes at a w/c ratio of 0.55 are considered, then there is a trend between fines content and compressive strength as shown in Figure 4.4.2. Typically the highest compressive strengths were found for fines contents in the range of 5 to 8%. However, low R^2 values for these trends suggest a scatter of data and that the fines content is not a major influencing factor on compressive strength at the levels considered and the changes in compressive strength might have been caused by other fine aggregate properties.

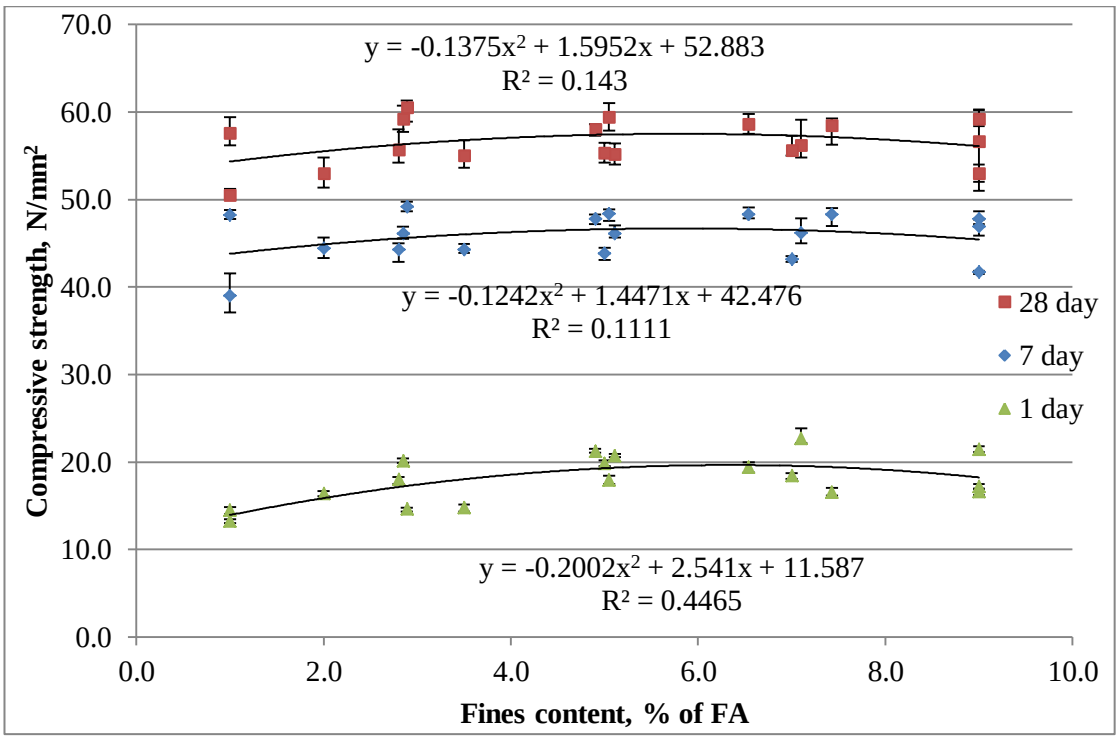

Figure 4.4.2 Compressive strength versus fines content for 0.55 w/c ratio mixes

Similarly, if the 28-day compressive strength variation with fines content is considered for each type of sand as shown in Figure 4.4.3, there is no evident trend or optimum value that results in the highest compressive strength. This contradicts the findings of a number of other researchers (Li et al. 2009, Li et al. 2011, Wang et al. 2013). Suggested explanations for the differences from the observations in literature include the low level of fines studied as well as the differences in the overall grading as is discussed in more detail in section 4.3.2.

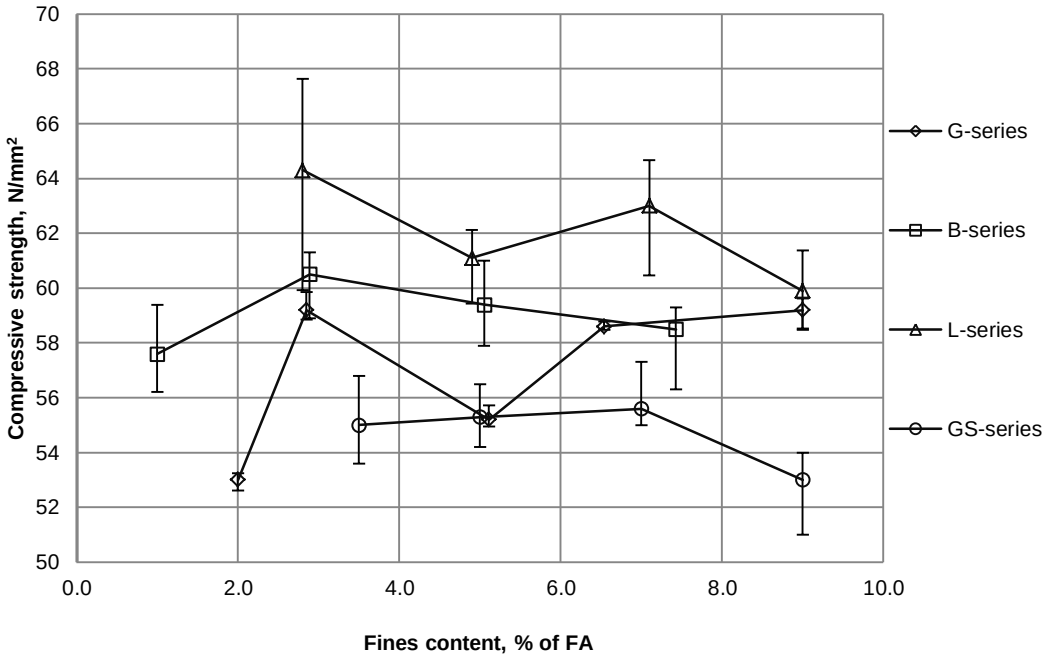

Figure 4.4.3 28-day compressive strength against fines content for Stage II mixes

The MBV results do not show a definite overall trend with compressive strength as shown in Figure 4.4.4. If the rate of strength gain of concrete relative to MBV value is considered as shown in Table 4.4.3, then it can be seen that basalt sand concretes exhibited lower 1-day strengths (25% from 28 day strength) whereas at 7 days it had gained 83% of the 28-day compressive strength. Gritstone sands showed similar rates of strength gain to the other sands. The behaviour of the basalt sand concretes can be explained by the high doses of water reducing agent that was employed to try to achieve an S2 slump range. Lower 1-day strength could be due to the delayed cement hydration reaction whereas the increase in the 7-day compressive strength could have been aided by better and more uniform distribution of cement particles within the concrete when compared to other Stage II mixes, which incorporated lower admixture dosages.

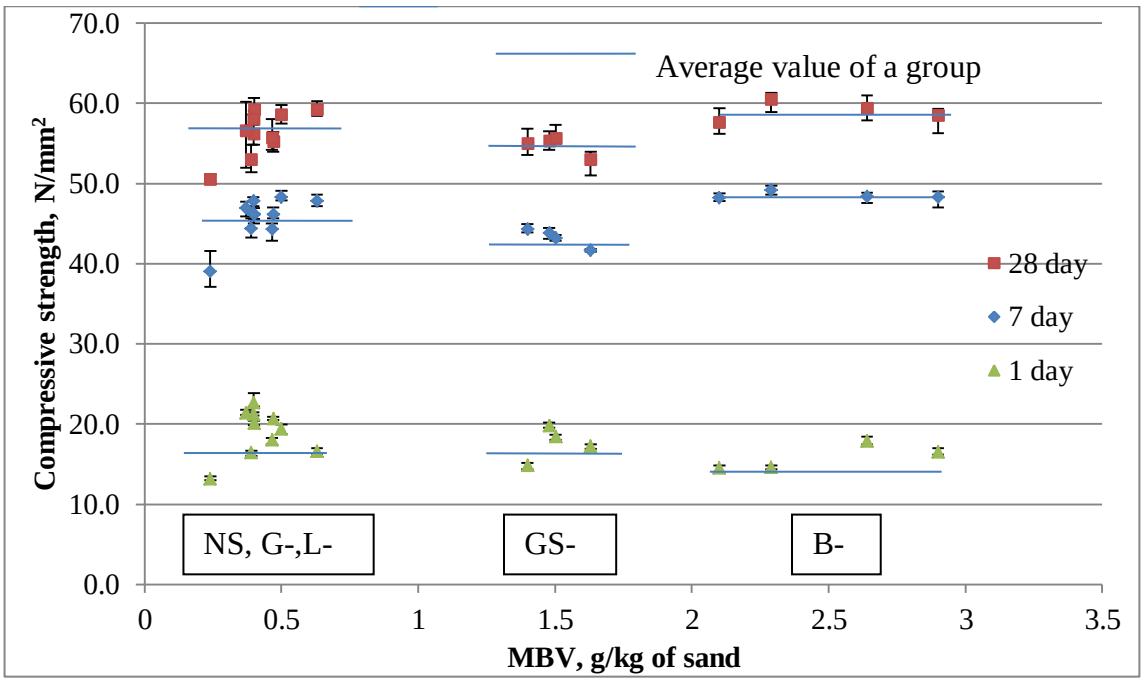

Figure 4.4.4 Compressive strength versus MBV for 0.55 w/c ratio mixes

Thus, it can be concluded that the clay types (illite and montmorillonite-chlorite) at given concentrations that were present in the sands do not affect the compressive strength up to 28 days. Similar findings were presented by Norvell et al. (2007) regarding illite clays, however, they found that concretes containing montmorillonite clay at a constant w/c ratio had significantly reduced compressive strengths. They could not explain whether this reduction was due to clays or excessive superplasticiser dosage. This suggests that MFA containing illite and montmorillonite-chlorite clays could be used in concrete without adverse effects on compressive strength if deficiencies in the fresh concrete properties can be tolerated.

Table 4.4.3 Compressive strength gain with increase in MBV for Stage II mixes

MBV, g/kg	0.5		1.5		2.5	
Compressive strength	N/mm^2	% of 28 day	N/mm^2	% of 28 day	N/mm^2	% of 28 day
28 day	57	100%	55	100%	59	100%
7 day	46	81%	43	78%	49	83%
1 day	18	32%	18	33%	15	25%

A trend between the SE values and compressive strength is shown in Figure 4.4.5. It shows that there is an optimum SE value around 60 that produces concretes with the highest compressive strength at all ages at the same w/c ratio. It has to be noted that literature does not report a correlation of sand equivalent test results with compressive strength.

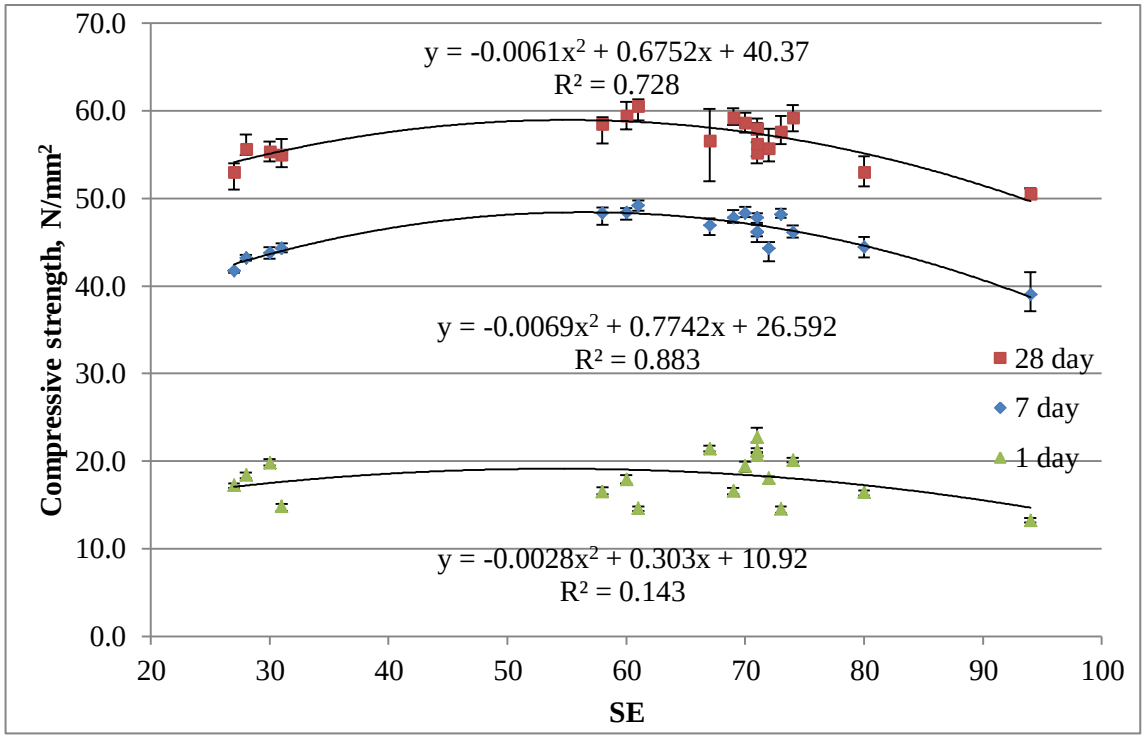

Figure 4.4.5 Compressive strength versus SE for 0.55 w/c ratio mixes

The SE test is intended to identify the presence of clay in the fine aggregate similarly to the MBV test. It was shown that the MBV as well as the clay types present in the MFAs do not influence the compressive strength of concrete whereas SE values show a trend with the strength. These observations suggest that the SE test measures other fine aggregate parameters that have an effect on concrete strength. Thomas et al. (2007) reported that the higher the SE value, the greater the proportion of sand-sized material or the lower the proportion of clay-sized materials in the fine aggregate. Thus, it can be

inferred that, to an extent, a proportion of clay-sized particles in a fine aggregate is beneficial to concrete strength although not necessarily clays.

If all mixtures at 0.55 w/c ratio are considered, then the un-compacted voids content from the NZFC test shows a non-linear trend with compressive strength as shown in Figure 4.4.6 where the 7 and 28-day compressive strength increases with the rise in voids content. As discussed in Chapter 3, the voids content is mainly influenced by the shape and grading of the aggregates. Marek (1992) noted that the more angular the particles, the higher the voids content in the fine aggregate. Higher angularity at the same w/c ratio will yield higher compressive strength concrete, however, angular and elongated particles can result in lower compressive strengths (Gonçalves et al. 2007, Donza et al. 2002). Thus, the slope of the trends decreases at higher NZFC voids ratios. The fine aggregate voids content is also influenced by the particle size distribution which in turn has been shown to have an effect on the compressive strength (Quiroga 2003). Thus it can be concluded that MFAs with un-compacted voids contents in the range of 43 – 45% produce the highest compressive strengths at a constant w/c ratio at 7 and 28 days. The trend for 1-day compressive strength shows an optimum value of voids content at 42% but has a large scatter of data as indicated by the lower coefficient of determination for that trendline. Therefore it can be implied that at an early age the shape, texture and grading of fine aggregate has limited effect on compressive strength and will be governed by the degree of hydration of the cement paste as reported by Donza et al. (2002).

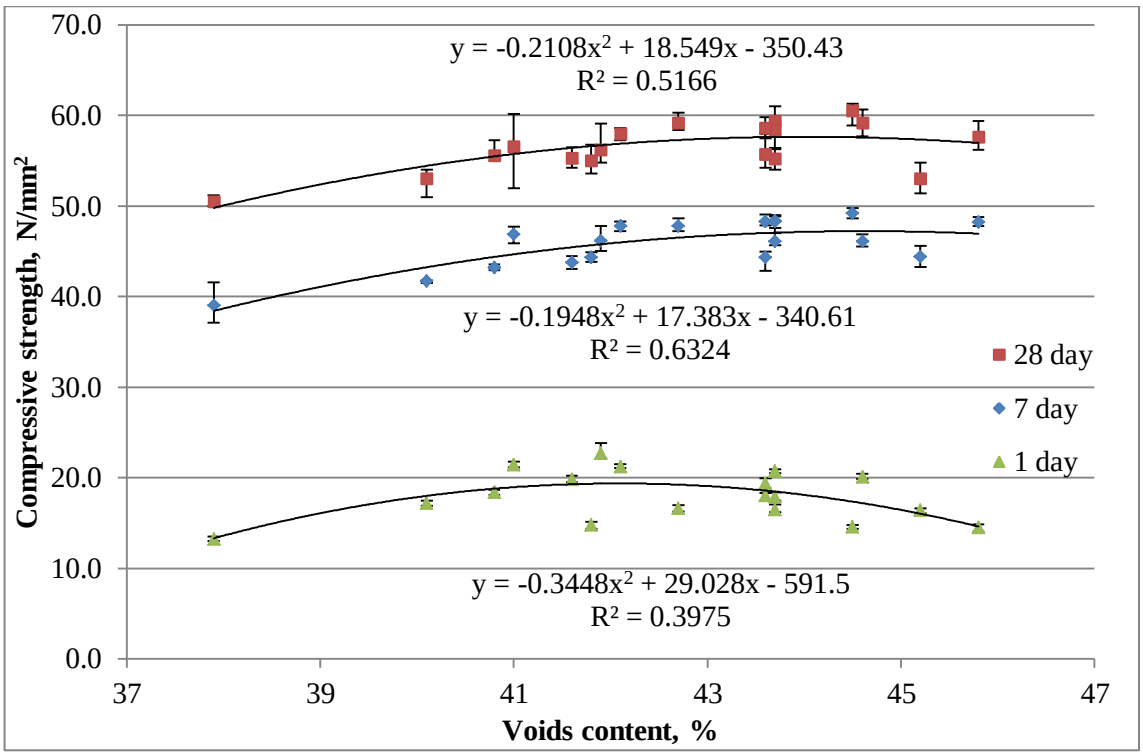

Figure 4.4.6 Compressive strength versus NZFC voids content for 0.55 w/c ratio mixes

The variation in the compressive strength with respect to the NZFC flow time is shown in Figure 4.4.7. It can be seen that there is an optimum range for NZFC flow time, of 23 to 24.5 seconds, that will produce concretes with the highest compressive strength at all ages. The flow time is mostly governed by the surface texture and grading of the particles (Goldsworthy 2005). It was observed by Li et al. (2011) that higher fine aggregate flow times with different aggregates of the same grading, produce concretes with higher compressive strengths as a result of an increased surface roughness of the particles. Quiroga (2003) noted that the particle size distribution influences the compressive strength, thus it can be concluded that the flow time is an indication of optimal grading with respect to compressive strength for a particular fine aggregate with a particular particle surface roughness.

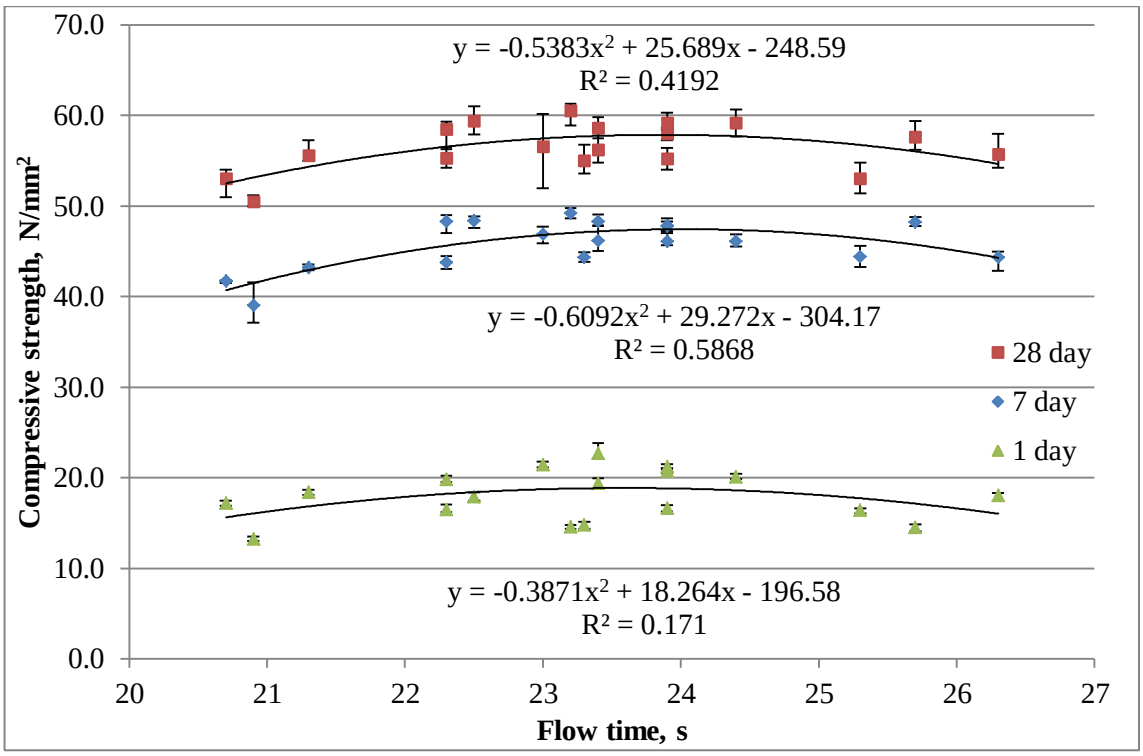

Figure 4.4.7 Compressive strength versus NZFC flow time for 0.55 w/c ratio mixes

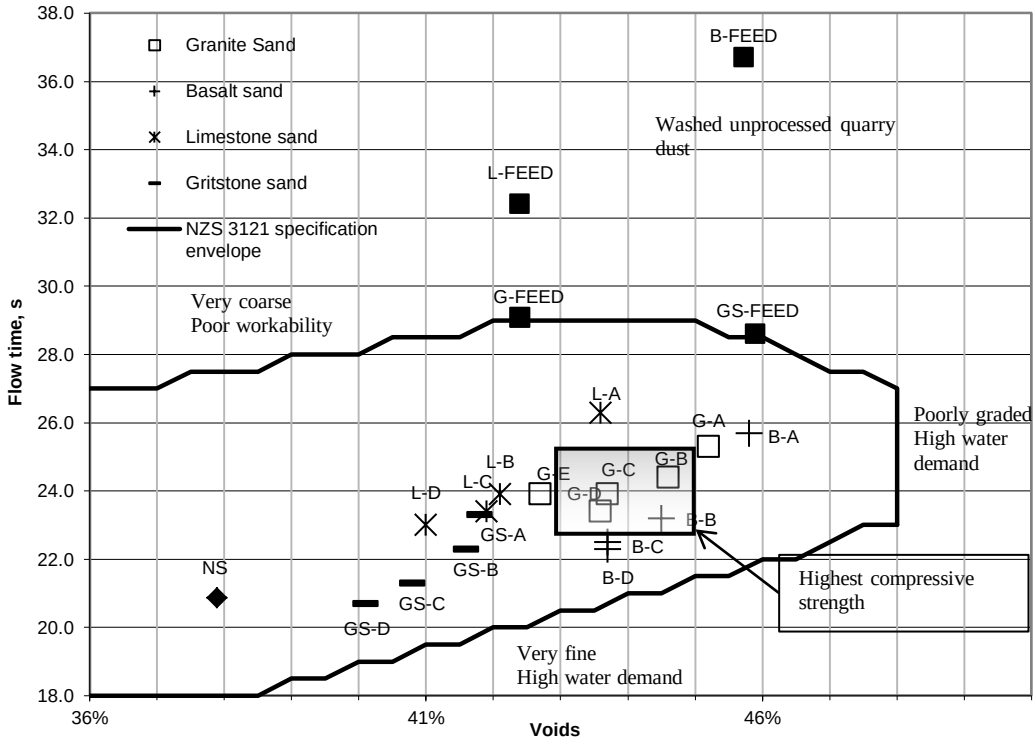

Figure 4.4.8 NZFC results with optimum range for highest compressive strength

The optimum ranges of NZFC flow time and voids content for the highest compressive strength along with the MFA results and standard envelope are shown in Figure 4.4.8. It

can be seen that the optimum ranges fall within the New Zealand standard envelope. Furthermore, it covers G-B, G-C, G-D and B-B sands suggesting that these have the combination of shape, texture and grading that should results in the highest compressive strength. If the mixes with the highest compressive strengths from Tables 4.3.1 and 4.4.1 with w/c ratio of 0.55 are considered it is evident that B-B, G-B and G-D sands are three out of five mixes with the highest compressive strengths.

Concrete flexural strength in Stage II varied from 4.7 to 6.8 N/mm^2 with the lowest found for the G-E mix. The coefficients of variation for Stage II flexural strength measurements were higher than in Stage I with the largest value of 23.1 % for the L-C mix. As shown in Figure 4.4.9 there is a general trend between the compressive and flexural strength at 28 days that follows the relationship suggested in Eurocode 2 and described in section 4.3.2. It seems that the reduction of the w/c ratio and subsequent loss of consistency which was remedied by the introduction of the water reducing admixture may have hindered proper compaction and homogenous distribution of mix components in the concrete samples thus resulting in the lower average flexural strength as indicated by the results falling below the theoretical mean flexural tensile strength.

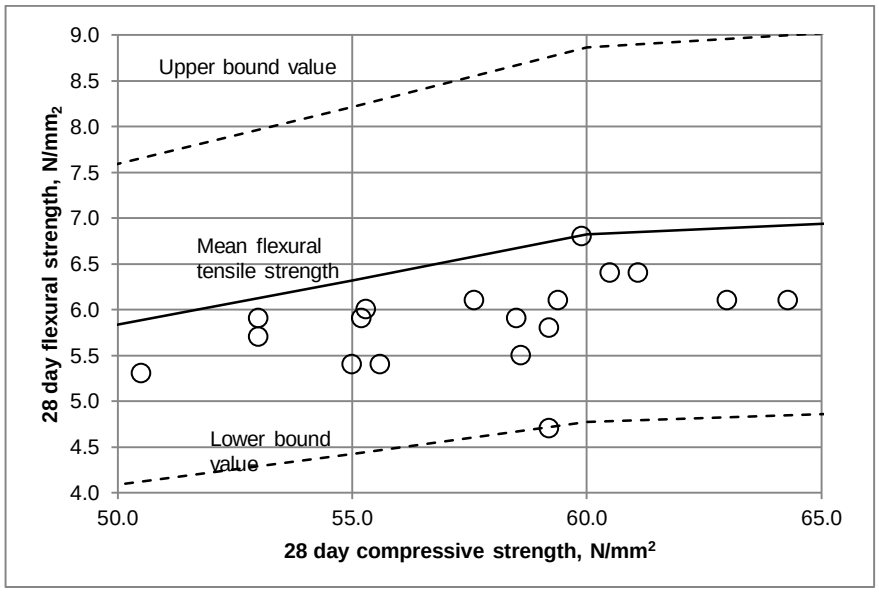

Figure 4.4.9 Flexural versus compressive strength for Stage II mixes

The change in flexural strength with fines content for Stage II mixes, shown in Figure 4.4.10, does not exhibit an optimum value for fines content, as was observed for the Stage I mixes. Furthermore, other significant correlations were not found between the fine aggregate characterisation test results and flexural strength. This could be attributed to the relatively high scatter of flexural strength measurements as indicated by the CoV values.

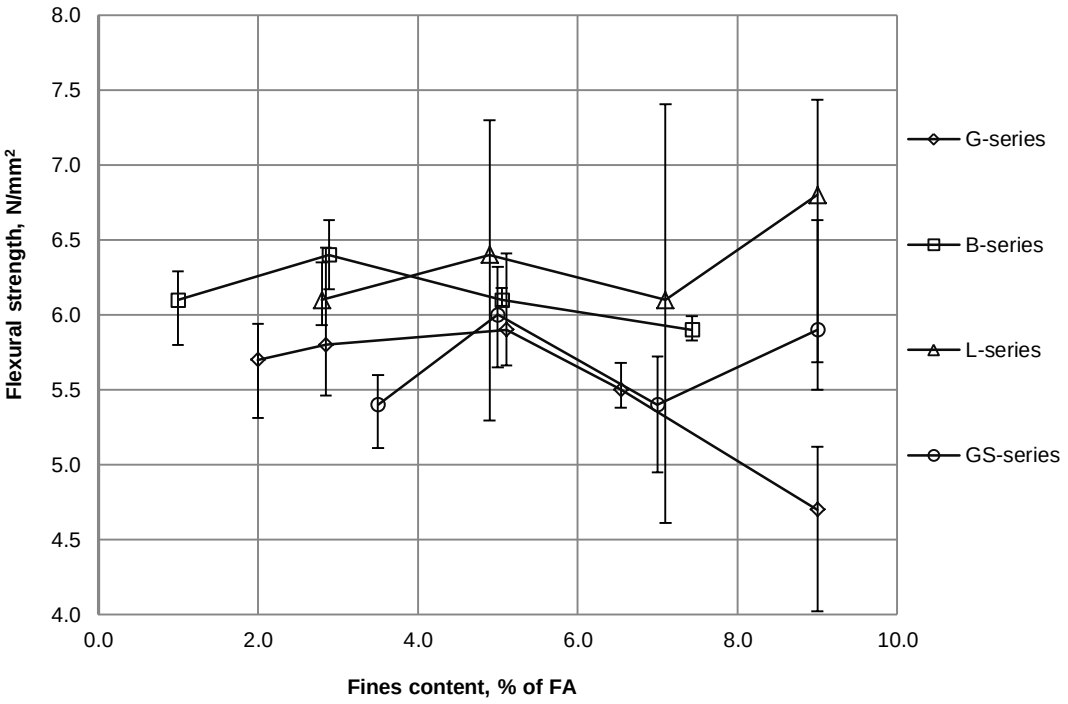

Figure 4.4.10 Flexural strength against fines content for Stage II mixes

4.4.3 Plastic density and entrapped air

The plastic density of the fresh concrete for Stage II mixes varies from 2385 kg/m^3 for the G-E mix to 2482 kg/m^3 for the L-A mix. Overall the densities are higher than for the Stage I mixes, which is as expected because the water content has been reduced in all mixes. Water has the lowest relative density of all concrete components and its volume has been replaced by denser materials, thus increasing the plastic density.

The entrapped air measurement ranges from 0.80 to 1.80 %. Within each MFA concrete series the measurement appears to be relatively constant and slightly elevated in comparison to Stage I results. This could be due to both the entrainment of air as a result of the incorporation of a plasticiser as well as due to reduced consistency, which may could result in a higher number of air voids in the hardened concrete.

4.5 Conclusions

The aim of this chapter was to investigate the fresh and hardened properties of concrete made using MFA with and without a water reducing agent and correlate these to the fine aggregate properties presented in Chapter 3. The findings of this chapter can be summarised as follows:

Properties of fresh concrete:

- Workable concretes were produced using 100% MFA as the fine aggregate at different w/c ratios. Basalt and gritstone sands, with high MB values required much higher w/c ratios to achieve an S2 slump than sands produced from granite and limestone quarry dusts. Feed quarry dusts required higher w/c ratios to achieve an S2 slump than corresponding MFAs.
- The MBV and SE values are good indicators of the potential presence of clays and an increased water/admixture demand in concrete mixes.
- The presence of clays in MFA can be a limiting factor in their use in concrete applications where high consistency and relatively low w/c ratios are specified, for example, highly reinforced load bearing structural elements.
- An increase in the fines content, un-compacted voids content and flow time (measured using NZFC) generally result in an increased water/admixture

demand. Thus reprocessing of quarry dusts yields more favourable fine aggregate with reduced flow time, voids and fines contents.

- Water reducing admixtures can be used to counteract the increase in water demand caused by the higher angularity of MFA when compared with dredged sand. However, if the sand is contaminated with clay, admixture effectiveness may be limited to fines contents below 3%.
- The slump test alone does not describe the consistency, handling and finishability parameters of fresh MFA concrete.
- MFA gradings containing 5-7 % fines are optimal for aiding the handling, placing and finishing of MFA concrete, provided that the fines are free from clay particles. However, the optimal fines content depends on the particular fine aggregate properties and concrete mix composition.

Properties of hardened concrete:

- At the same w/c ratio, compressive and flexural strengths of MFA concretes are higher than that of their natural sand counterparts. This is believed to be due to the angular shape of the material which has a positive effect on aggregate interlock, and hence leads to an improved bond between the cement and aggregate particles.
- No significant trend of concrete compressive strength with fines content was observed in the Stage I and the Stage II mixes in the 1 to 9% fines content range that was investigated. Thus, in order to maximise efficient use of materials higher fines content MFA gradings should be employed where the compressive strength of a mix is the governing factor.
- Stage I concretes exhibited an optimum fines content for the highest flexural strength at 5%, however no such trend could be observed in Stage II mixes. This

suggests that the optimum fines content regarding the flexural strength of concrete could depend on the mix composition.

- Presence of illite or montmorillonite-chlorite clay and correspondingly high MBV values do not affect the 28 day strength of concrete made with different MFA at the same w/c ratio. Therefore there is a potential for clay containing aggregates to be used in concrete that were previously discouraged.
- Shape, texture and grading of MFA influence the compressive strength of concrete as shown by the SE and NZFC tests.
- There is an optimum SE value around 60 at which the highest compressive strength was observed. This is due to the proportion of clay-sized particles in the fine aggregate.
- MFAs with an un-compacted voids content in the range of 43 – 45% and flow times in the range of 23 to 25 seconds produced the highest compressive strengths. Thus, there is an optimum grading for a particular particle shape and texture that results in the highest compressive strength that can be evaluated using the NZFC test.

The fresh and hardened properties of concrete depend on a variety of interdependent fine aggregate characteristics. It is extremely difficult to isolate and measure each of these characteristics as well as their influence on fresh and hardened concrete properties due to their complex interaction. Thus, a model which can analyse all parameters at the same time and predict fresh and hardened concrete properties would be valuable so that the performance of a particular aggregate in concrete could be estimated without lengthy trial and error based concrete lab trials.

Overall, it has been shown that workable concretes can be produced using reprocessed quarry dusts irrespective of mineralogy and with appropriate grading can exhibit good handling, finishing and placing properties. These concretes possess strength which is adequate for the majority of concrete applications and can surpass that of natural sand concrete.

5 Modelling of MFA concrete strength and consistency

5.1 Introduction

The aim of this chapter is to develop a model which predicts the compressive strength and consistency of MFA concrete mixes. In previous chapters it has been shown that the properties of MFA influence the resulting concrete performance, however, their effects are complex, interconnected and non-linear. Thus, the development of a model which accounts for MFA properties would help reduce the number of laboratory trials required to establish an appropriate mix design for a given MFA for a specific application.

The compressive strength and consistency of concrete can be considered as a multi-variable continuous function within certain boundaries based on the observations from literature and results presented in Chapter 3 and 4. According to Cybenko (1989) it is possible to approximate any continuous function with one layer feed forward neural network that uses continuous sigmoid transfer function. Furthermore, in Chapter 2 it was identified that artificial neural network (ANN) modelling is a suitable tool for predicting the compressive strength and consistency of various concretes based on the properties of the constituents, however, there is a lack of ANN models which use the characteristics of the fine aggregate as input variables for these predictions. Therefore, this chapter will describe the development of an ANN model that uses the MFA properties along with the mix design as input variables for the prediction of the compressive strength and consistency of such mixes.

The chapter will cover the general principles and types of ANN, the data and its selection, the parameters and topologies of the ANN models, the evaluation and

selection of the most accurate models, the validation of these models using trial mixes and a numerical evaluation of the model's predictions.

5.2 Artificial neural networks

This section will describe the basic concepts of ANN. In particular, the structure of the model and the principles of how it works.

5.2.1 The concept of neuron

The ANNs are based on the concept of human brains. Brain cells or neurons are heavily interconnected and send and receive messages. These form the central nervous system and allow humans to make decisions. Similarly, in the ANN concept, the basic processing unit is called a neuron and is defined as follows (Hill 2006):

a) It receives a number of inputs. Each input comes via a connection that has a strength (or weight); Each neuron also has a single threshold value (or bias). The weighted sum of the inputs is formed, and the threshold subtracted, to compose the *activation* of the neuron.

b) The activation signal is passed through an activation function (also known as a transfer function) to produce the output of the neuron.

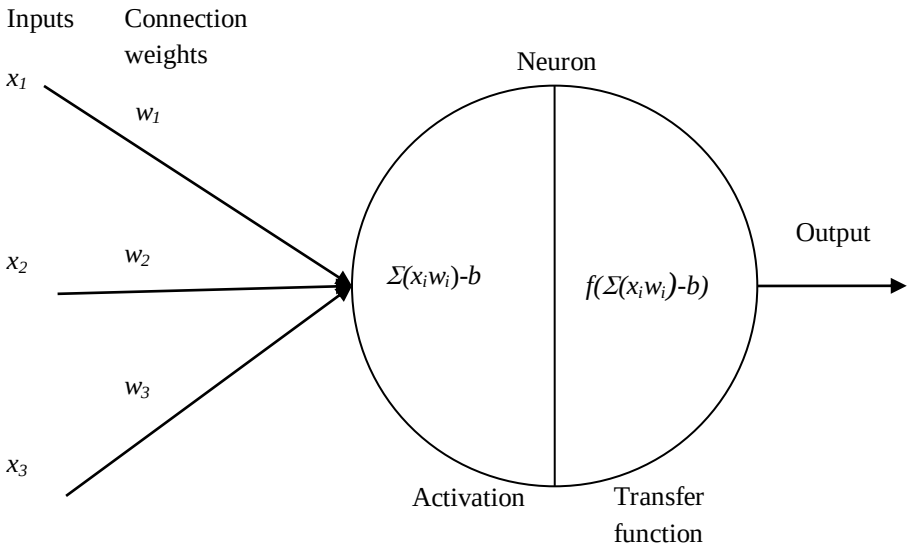

Figure 5.2.1 Schematic diagram of a neuron

A schematic representation of the neuron is shown in Figure 5.2.1. The choice of the transfer function will depend on the problem which is to be solved. In classification problems a step function which provides an output of 0 or 1 might be employed but for non-linear problems a sigmoid transfer function is used, the most common one is presented in Equation 5.2.1.

$$f(x) = \frac{1}{1+e^{-x}} \qquad \text{Equation 5.2.1.}$$

Equation 5.2.1 always produces an output in the range from 0 to 1 and is sensitive for inputs in a range not much larger than (-1;+1) as shown in Figure 5.2.2. Thus, the input values are usually linearly scaled to this range before being fed to the network for processing (Fausett 1994).

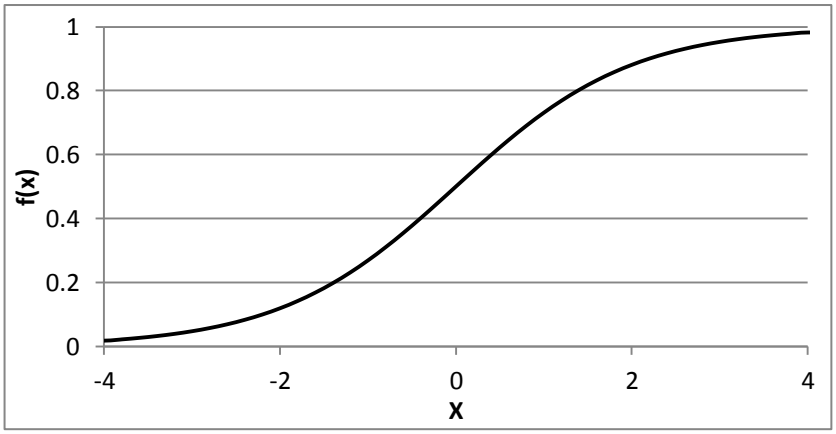

Figure 5.2.2 Sigmoid function plot

5.2.2 Neural network topology

In order to solve problems the neurons have to be arranged in an interconnected structure so that they can receive input data, process it and produce an output. There are several ways to create a network, but the most common structure for solving general problems is a fully connected feed forward network (Jadid and Fairbairn 1996) as shown in Figure 5.2.3. It consists of an input layer, one or more hidden layers and an output layer. The data is presented to the input layer, processed and passed on to the next one until an output is produced. Such a structure or topology of a neural network is

usually described in following manner: X-Y-…-Z where: X is the number of neurons in the input layer, Y the number of neurons in the first hidden layer and Z is the number of neurons in the output layer.

The choice of the number of hidden layers and neurons in each layer depends on the complexity of the problem, but there are no fixed guidelines in selecting this number, thus it is usually found by trial and error. A starting point, as suggested by Hill (2006), is one hidden layer with the number of neurons equal to the half of the sum of input and output neurons.

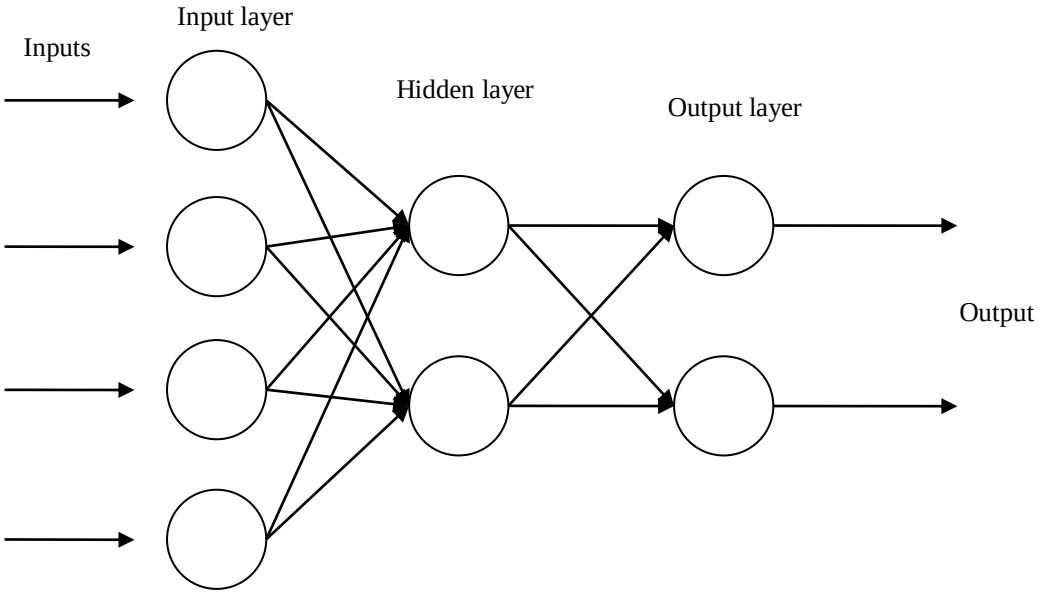

Figure 5.2.3 Feed forward neural network

5.2.3 Neural network training

If the network is to produce meaningful results, it has to be trained with some existing input and output data which represents the problem. The training process is concerned with adjusting the thresholds and connection weights so that the network prediction error is minimised and the model has learned the underlying relationship from the training data. For any possible configuration of *N* weights the error can be plotted in the *N*+1th dimension, forming an error surface. The objective of network training is to find

the lowest point in this many-dimensional surface. The most commonly used and reliable technique for training the network for complex non-linear relationships is a back-propagation algorithm (Jadid and Fairbairn 1996).

This algorithm has been described in-depth by Fausett (1994), but in summary the algorithm calculates the gradient vector of the error surface for the current network configuration. This vector points along the line of steepest descent towards the error surface minimum. The connection weights are incrementally updated corresponding to the slope of the error surface and the error is recalculated in an iterative process. These iterations are called *epochs* and the algorithm is stopped after an acceptable error is reached, the error stops improving or a prescribed number of epochs has been executed.

There are two terms introduced in the algorithm to accelerate its convergence – learning rate and momentum factor. The learning rate is a constant used to adjust the size of the increments of weights, while the momentum factor encourages the algorithm to move in a fixed direction, thus, allowing it to sometimes escape local minima and rapidly move over flat spots in the error surface (Moreira and Fiesler 1995).

The most desired property of a ANN is its ability to generalize to new cases, however, a common issue with network training is over-learning or over-fitting (Fausett 1994). It has been illustrated in Figure 5.2.4 where a simple $y=x^2+3$ function is shown with blue dots and the over-fitting with ANN in red. It means that the function modelled by ANN fits all data points presented to it, however, intermediate values do not correspond to the function that had to be modelled. Such phenomenon can be observed if the network error starts to increase during the training process. In such case, it is suggested to decrease the number of hidden neurons as the network is too powerful for the given

problem (Hill 2006). Furthermore, there should be a testing dataset that has not been used in the training of the network, which serves as an independent check of the progress of the learning algorithm.

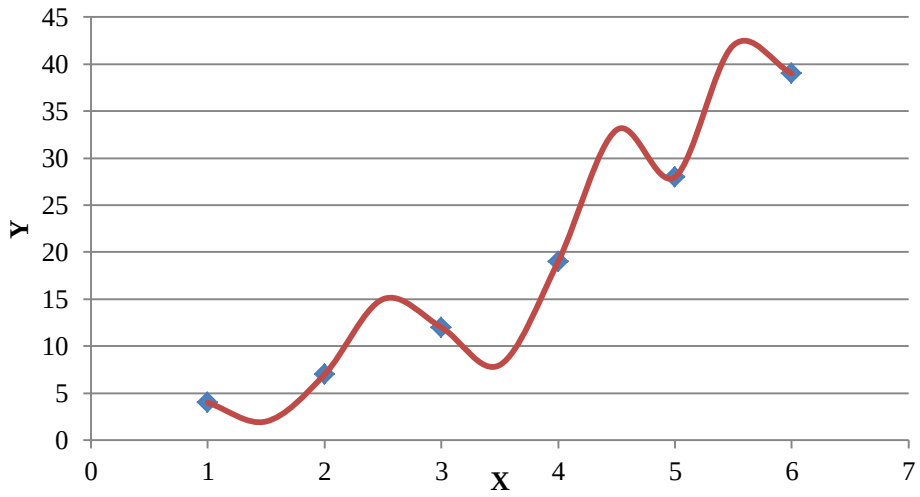

Figure 5.2.4 Example of ANN over-fitting

5.2.4 Data selection

As for any model, in order to make the ANN model accurate, the data needs to be representative of the underlying problem. Also the amount of data is of importance to ensure that it covers the range of input and output parameters. Hill (2006) lists the common problems which should be avoided when selecting data for ANN model training and validation:

- Outdated data – If the training data was acquired some time ago, one must be sure that it is still representative of the problem to be modelled as the relationships from the past might not be true for present circumstances.
- Range of data – The ANN models work well in the range of the data which was used to train them. One can not expect ANN model to make accurate predictions for out of range cases.
- ANN learns the easiest features – one should make sure that the data covers all aspects of the problem to be modelled.

- Unbalanced data sets – the network does not distinguish between “bad” or “good” data, it will be trained for minimal error according to the given data set. The data should be crafted so that it represents the distribution of the population.

Overall the developer and operator of the model should be aware of the possible errors with ANN, thus carefully evaluating the data which is used in the training and testing. Furthermore, validation of the model with new data can be used to control the performance of the neural network. In addition to that, one can validate the model by changing each variable in turn while keeping others constant and checking if that yields the desired or previously known effect on the predictions, for example, in the case of modelling concrete strength an increase in w/c ratio will decrease the compressive strength.

5.2.5 Summary of ANN models

Artificial neural network modelling is a technique that allows modelling of complex, multivariable problems. The model consists of units called neurons that are typically arranged in an interconnected, feed forward layered network structure. Each neuron contains an activation function, typically a sigmoid function. The sum of neuron output values of the previous layer are multiplied by the connection weights and are fed into the activation function of the current neuron which then provides an output value. The networks are trained using a dataset and an algorithm that adjusts the connection weights between neurons in order to minimise the network output error. The dataset usually is divided into two datasets, one for training and one for testing. A commonly used algorithm for training is a back-propagation algorithm.

5.3 Data selection

This and following sections of the chapter will describe the variables and parameters used in the development of the ANN model, and its evaluation. In the development of

the model the data presented in Chapters 3 and 4 were used. It includes the characterisation test results for MFAs, natural sand and quarry dusts along with the corresponding concrete test results.

5.3.1 Variable selection

Before the model could be developed it was necessary to select meaningful input and output variables from the data available. First of all, 28-day compressive cube strength and slump test results were selected as the relevant output variables representing the compressive strength and consistency. The slump test values (BS EN 12350-2:2009) can theoretically range from 0 to 300 mm which is the height of the concrete cone. However, according to the standard, if the slump collapses or shears, it is noted but no value recorded. In the experimental work several concrete mixes resulted in a slurry and collapse of the slump. Thus, in order to use these mix results in the modelling, the slump value of such mixes was taken as 300 mm.

As discussed in Chapter 2, it has been shown by other researchers that the composition of the mix affects the concrete properties. Thus, relevant mix proportion parameters should be selected as variables for the model. All concrete mixes had the same type and quantity of cement and coarse aggregate. Also the same amount of fine aggregate, thus these parameters can be excluded from the set of input variables for the particular dataset. However, w/c ratio and plasticiser dosage varied for different mixes, thus these were selected as input parameters representing the mix proportions.

The fine aggregate parameters that influence the concrete's properties can be considered under three broad categories – shape and texture, grading and presence of deleterious particles. The particle shape and texture was measured indirectly by the voids content

and flow time results of the NZFC test. Therefore, the shape and texture parameters were represented by these two input variables in the ANN model.

All of the fine aggregates used in the study were continuously graded over the 0/4 mm particle range. Thus, the major difference in the gradings under consideration was defined by the fines content, which was included in the set of input variables. The flow time and voids content measured in the NZFC test are influenced by the aggregate grading as noted by Thomas et al. (2007) and confirmed in Chapter 3, therefore these variables were also adopted as inputs for the proposed model.

The presence of deleterious particles (clays), sometimes also referred to as the quality of the fines, was measured by the SE, MBV and GMBV tests and, as highlighted in Chapter 4 had a profound effect on concrete consistency. It was also shown that the MBV and GMBV tests are directly correlated and measure the same aggregate property, therefore, only one of them is necessary as an input. It was decided to include the SE and GMBV tests in the input variable set. Another variable which could have a potential effect on the concrete properties and was measured in the MFA characterisation was the aggregate absorption capacity. This is influenced by the mineralogy of the rock and potential presence of deleterious fines, thus it was also added to the input parameters.

Overall there were 8 input and 2 output variables selected for the ANN model. These along with the parameters that they influence are listed in Table 5.3.1.

Table 5.3.1 Range of input and output variables and the parameter that they influence.

Variable	Minimum	Maximum	Influence
w/c ratio	0.48	0.75	Mix composition
Plasticiser, l/m^3	0	3.3	Mix composition
GMBV, g/kg of sand	0.35	6.16	Quality of fines
SE	27	94	Quality of fines
Water absorption, %	0.45	1.92	Quality of fines
Voids, %	37.9	45.9	Grading, shape and texture
Flow time, s	20.7	36.7	Grading, shape and texture
Fines, % of FA	1	18	Grading
28 day compressive strength, N/mm^2	31.3	64.3	Result
Slump, mm	25	300	Result

5.3.2 Dataset

The available data for the development of the model consisted of 44 entries. As noted in previous sections, the training of an ANN requires a portion of data to be allocated for testing the progress of the learning algorithm, therefore, the dataset was randomly divided into 35 training entries and 9 for testing. Table 5.3.1 shows the range of the input and output values used in the training dataset. The testing dataset variable values were all within the range of the values used in the model training. The full datasets can be found in Appendix D.

5.4 ANN parameters

The development and training of the ANN models was executed using the software package MBP version 2.2.4 that employs the backpropagation algorithm described in section 5.2.3. Once the connection weights and threshold values for trained networks were obtained from the software package, they were transferred to MS Excel sheets for evaluation.

5.4.1 Transfer function

In general, any continuous sigmoid transfer function could be used for approximating a continuous function with one layer feed forward neural network as proven by Cybenko (1989). The compressive strength and slump values are always positive and the effects of aggregate characteristics and mix proportions on them are non-linear as discussed in Chapter 4. In order to model such problems literature suggests the use of a sigmoid transfer functions (Fausett 1994, Hill 2006) with output values in range from 0 to 1. The most common sigmoid transfer function that is used in ANN modelling of concrete properties and that satisfies the positive output values is given in Equation 5.4.1.

$$f(x) = \frac{1}{1+e^{-x}}$$ Equation 5.4.1.

Furthermore, the function above is easy to differentiate, thus reducing the complexity of the network training process. Thus, the function in Equation 5.4.1 was adopted for the development of ANN networks.

5.4.2 Data scaling

As noted in section 5.2.1 the sigmoid transfer function is sensitive to input values in the range -1 to +1, thus the input data should be scaled to match this range. That was done according to equation 5.4.2 for all input variables, where: I_{scaled} is the scaled input variable, I_{actual} is the value of the variable to be scaled, I_{min} is the minimum value of the variable used in the training set, I_{max} is the maximum value of the variable used in the training set.

$$I_{scaled} = -1 + \frac{I_{actual} - I_{min}}{\left(\frac{I_{max} - I_{min}}{2}\right)}$$ Equation 5.4.2

This equation coupled with the transfer function explains why the ANN models might give poor estimates if the input values presented to the model are outside the range of the variables that it was trained with. If the range is exceeded, the scaled values will be

outside the sensitive (-1;+1) region of the transfer function and thus any extrapolation by the model is unlikely to be particularly accurate.

As the transfer function produces a value in the range 0 to 1, the output of the network has to be scaled as well and this is done using Equation 5.4.3, where: O_{scaled} is the scaled output value, O_{min} is the minimum value of the output in the training set, O_{max} is the maximum value of the output in the training set and $O_{newtork}$ is the unscaled neural network output. Therefore, the predicted values of the neural network will not exceed the ones it was trained with.

$$O_{scaled} = O_{min} + O_{network} \times (O_{max} - O_{min}) \qquad \text{Equation 5.4.3}$$

5.4.3 Topology

The optimal architecture of the neural network depends on the complexity of the problem and the input/output variables. It was determined that there are eight input and two output parameters. However, even with the same input variables the solution for compressive strength and consistency might differ, and thus would require different neural network topologies. As a result it was decided that for each output variable a separate network would be built.

This meant that for each slump and compressive strength model there would be 8 input variables in the input layer and 1 output variable in the output layer. It has been shown by researchers that one hidden layer is sufficient for predictions of concrete strength and consistency based on mix composition (Ni and Wang 2000, Siddique et al. 2011, Duan et al. 2013a). Therefore, one hidden layer structure was adopted for the development of the ANN model used in this study.

As noted in Section 5.2.2, the choice of the number of neurons in the hidden layer is a function of the problem complexity and is usually determined empirically. Researchers investigating ANN predictions of concrete properties tend to use networks with a hidden neuron number equal to or smaller than that of the sum of input and output parameters. Taking this into account it was decided to construct five models for each parameter to be modelled. These networks had 2, 4, 6, 8 and 10 neurons in the hidden layer. Afterwards the most accurate model was chosen by identifying that which had the smallest prediction error. Neural network models were designated according to the number of neurons in each layer in the form "input layer-hidden layer-output layer" and the output parameter considered e.g. strength or slump.

5.4.4 Other parameters

As discussed in section 5.2.3 there are three other criteria that have to be addressed for the back-propagation training algorithm – learning rate, momentum factor and epochs or number of cycles. These, in a similar fashion to the number of hidden neurons, are usually selected empirically. The literature shows a wide scatter of these parameters while still resulting in ANNs which perform well. Thus, preliminary training of an ANN with a range of these parameters was performed. The values of these parameters that showed a good training performance are given in the following paragraph and, therefore, were adopted for further ANN model training.

The initial learning rate was set to 0.7 and was decreased by 1% after each 7 learning cycles. The initial momentum factor was set to 0.7 and was decreased by 1% after each 500 cycles. The online training mode was used where the weights were updated after each training entry and the training data was presented in a random order. The training of each network was halted after 5000 cycles. It was observed that the training error (root mean squared error RMS) had stabilized for all networks after approximately

2000-3000 learning cycles. This implies that the combination of connection weights and biases corresponded to the minimum training error for a given topology and training dataset.

5.5 Evaluation of ANN models

Once the models were trained, the final connection weights and threshold values were transferred to MS Excel spredsheets. Using this software the evaluation of the ANN models was performed based on the prediction error for the testing data. Tables containing the connection weight values for all models are presented in Appendix D.

The predicted compressive strength values from all models for the testing data are plotted in Figure 5.5.1. It can be seen that irrespective of the hidden neuron count all models make relatively accurate predictions within a range of 5 to 10 N/mm^2. Similarly to the compressive strength predictions, the slump values in absolute terms have been plotted in Figure 5.5.2 and all five ANN models make predictions within a range of 30 mm from the actual test data values. It has been noted that the slump values are poorly distributed and are discussed in more depth in section 5.8. The small errors shown by different models could explain the variety of ANN model topologies that have been reported in literature that accurately predict concrete compressive strength and consistency based on mixture composition parameters.

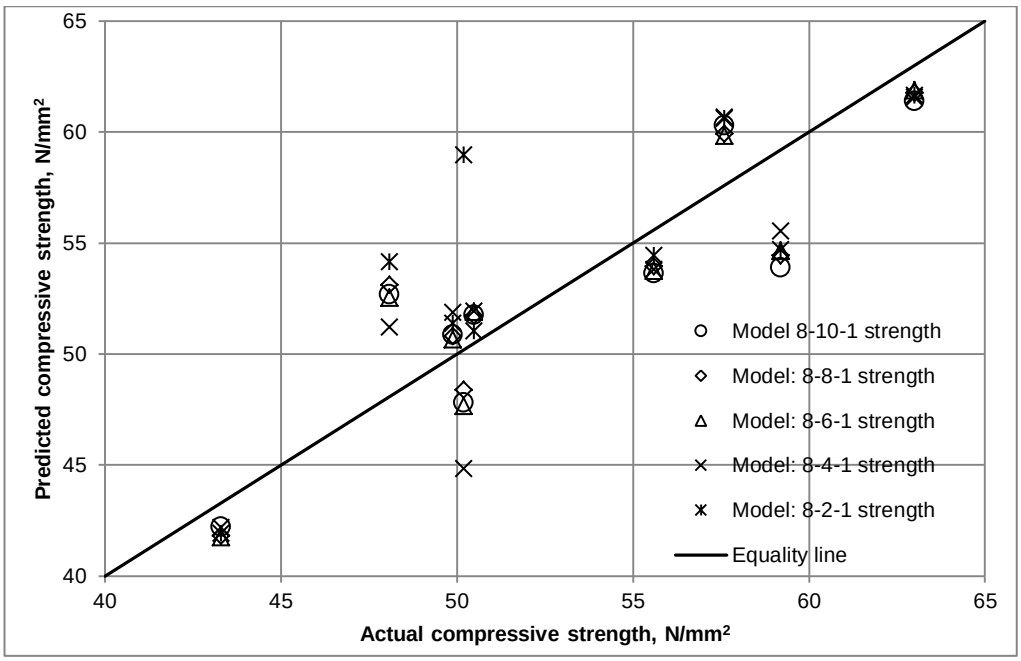

Figure 5.5.1 Predicted and actual compressive strength values of testing data

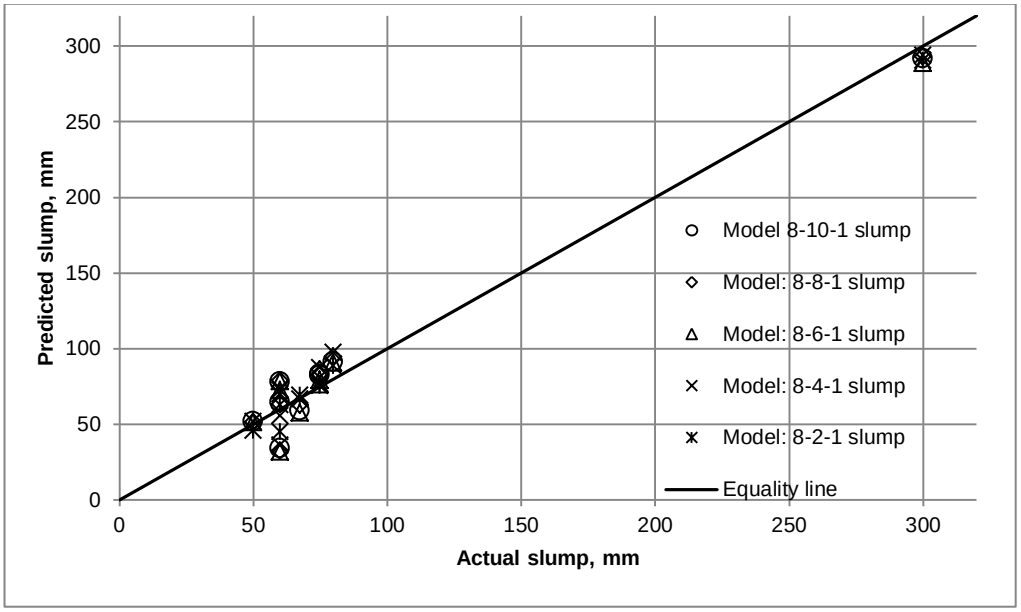

Figure 5.5.2 Predicted and actual slump values of testing data

The most accurate models for further validation and analysis were selected based on the overall prediction error, in this case the root mean square error (RMS), of the test data. The RMS of the models that were created is shown in Table 5.4.1. It can be seen that the least slump prediction error is for the 8-2-1 slump model, whereas for the strength prediction, the least error is obtained with the 8-6-1 strength model, and therefore these

were adopted as the most accurate for the given dataset. These results also support the decision to create separate models for compressive strength and consistency as different numbers of hidden neurons yielded the most accurate predictions for each concrete property.

Table 5.5.1 ANN model RMS errors for testing dataset.

Model	RMS, mm	Model	RMS, N/mm^2
8-10-1 slump	12.50	8-10-1 strength	2.83
8-8-1 slump	13.36	8-8-1 strength	2.70
8-6-1 slump	13.58	8-6-1 strength	**2.61**
8-4-1 slump	11.50	8-4-1 strength	2.87
8-2-1 slump	**7.97**	8-2-1 strength	4.09

5.6 Model validation with trial mixtures

In order to validate the prediction capabilities of the selected models four concrete mixes were made with the same fine, coarse aggregate and cement contents as detailed in Chapter 4 but with varying w/c and plasticiser dosage which were within the range of the training data. These mixes included a limestone quarry dust which was not used in the training or testing of the models, a natural sand, a granite sand without clays and a gritstone sand with clay particles. Thus, the validation mixes covered a range of fine aggregate and mix composition properties in the range of the training data, however, these did not match any of the training or test data inputs. The validation mix model input values are given in Table 5.6.1 and the full mix design sheets are presented in Appendix C.

Table 5.6.1 Validation mixture input values

Sample	w/c ratio	Plasticiser, l/m^3	GMBV, g/kg	SE	Voids, %	Flow time, s	WA_{24}, %	Fines, % of FA
Quarry dust	0.65	0	1.55	44	42.2	36.6	0.77	9.3
NS	0.51	0	0.35	94	37.9	20.9	1.04	1.0
G-C	0.60	0	0.71	71	43.7	23.9	0.58	5.1
GS-B	0.60	3	1.84	30	41.6	22.3	0.98	5.0

The predicted and actual slump and compressive strength values for the validation mixes are shown in Figures 5.6.1 and 5.6.2. It can be seen that the compressive strength predictions are relatively accurate with the highest percentage error being 13% and an RMS of 4.47 N/mm^2 for the 8-6-1 strength model. This error is comparable with those found by other researchers for ANN models that predict compressive strength (Ni and Wang 2000, Duan et al. 2013).

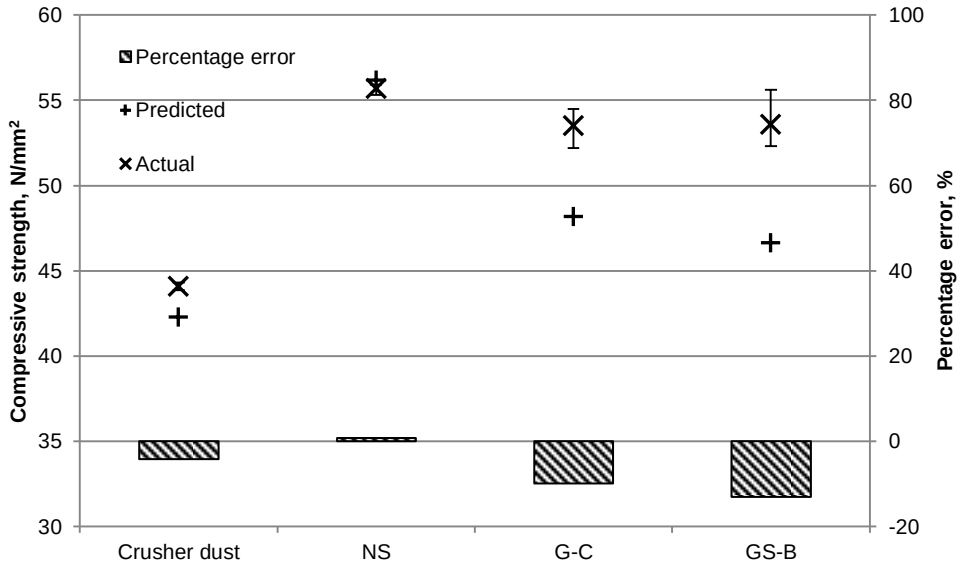

Figure 5.6.1 Predicted and actual compressive strength values for validation mixtures.

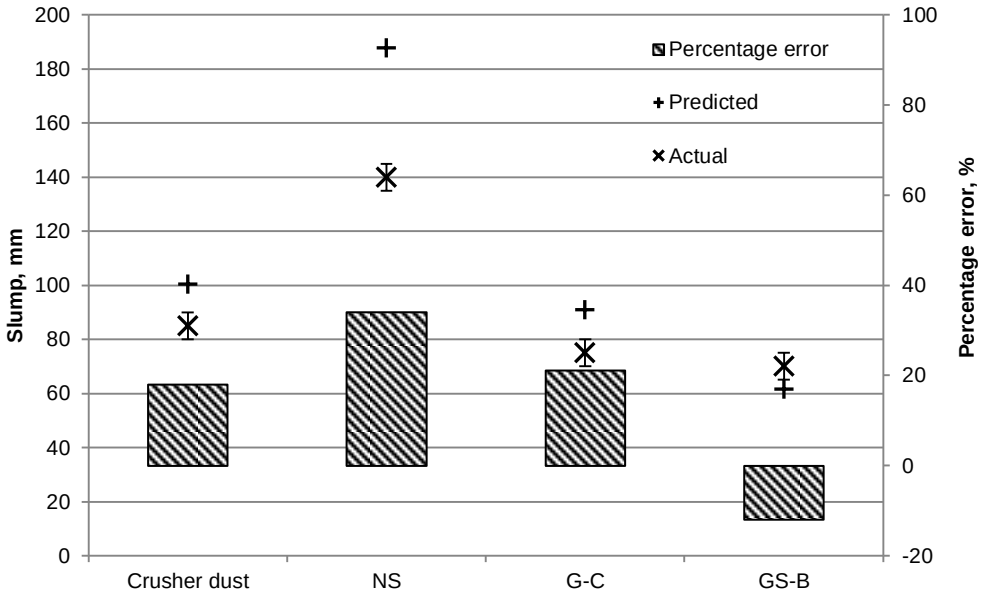

Figure 5.6.2 Predicted and actual slump values for validation mixtures

The 8-2-1 slump model had an RMS of 26.61 mm and the highest percentage error of 34% for the NS sand mix. It has to be noted that in the 50 – 100 mm slump range, where most of the training data was located, the percentage error does not exceed 21% (16 mm by absolute value) which is once again comparable to those found by others and claimed to be accurate (Öztaş et al. 2006). Furthermore, taking into account the artificial 300 mm value adopted for the slump collapse in the training data it might be expected that there would be an overestimation in the higher consistency mixes as in the NS validation mix. This is due to unbalanced slump value data as discussed in section 5.2.4.

The findings of this and the previous section demonstrate the ability of the ANN models to accurately predict the concrete compressive strength and consistency of concrete when the fine aggregate properties are used in combination with the mix composition parameters as input variables.

However, it has been noted in Section 5.2 that the ANN models will adjust the connection weights to minimize the error according to the training data. If the data is corrupt or, in other words, does not properly represent the relationship that is being modelled, then the resulting ANN predictions will be inadequate. Thus, numerical evaluation of the model can help to confirm that the ANN has actually learnt the underlying theoretical relationship as will be discussed in the next section.

5.7 Numerical evaluation

This section presents the results of a numerical evaluation of the adopted ANN models: 8-6-1 strength and 8-2-1 slump. Assuming that the ANN model has learnt the underlying trends from the training dataset, then, if one of the input variables is varied keeping all others constant, the output should change according to the input's influence. If the output changes according to the observations and trends found by researchers, then the ANN model can be considered to have picked up the correct trends from the training data.

In the models under consideration some of the input variables describing the fine aggregates are interconnected as they partially define the same property as shown in Table 5.3.1. For example, the shape and texture of the aggregates is measured by voids content and flow time, while the grading is described by voids content, flow time and fines content. This means that the result of a change in the flow time alone may not be able to be determined without knowing how the other two variables have changed as well. Another example is the quality of fines, where the GMBV and SE values have been shown in Chapter 3 to be inversely related to one another, albeit not by a direct relationship. This means that an increase in GMBV would require a decrease in SE in order to represent fine aggregate parameters that might be encountered in a real life situation.

While keeping in mind what has been discussed in the paragraphs above, three values of the input variables were chosen for numerical evaluation – maximum, minimum and average values of the training data range of each variable as shown in Table 5.7.1.

Table 5.7.1 Variable values for numerical evaluation

Variable	Minimum	Average	Maximum
w/c ratio	0.48	0.62	0.75
Plasticiser, l/m^3	0.00	1.65	3.30
GMBV, g/kg of sand	0.35	3.26	6.16
SE	27.00	60.50	94.00
Water absorption, %	0.45	1.19	1.92
Voids, %	37.90	41.90	45.90
Flow time, s	20.70	28.70	36.70
Fines, % of FA	1.00	9.50	18.00

The average values represent the properties of a fine aggregate which could be encountered and could be a 50:50 blend of dredged natural sand and clay contaminated quarry dust mixed in concrete with medium dosage of plasticiser and w/c ratio of 0.62. However, the maximum and minimum input values represent an implausible combination of fine aggregate properties but these still can be used to explore the model's potential regarding them as a stiff concrete mix for minimum values and fluid concrete mix for maximum values.

5.7.1 Mixture composition variables

The variation of the compressive strength predictions with respect to w/c ratio is shown in Figure 5.7.1. Compressive strength decreases non-linearly as the w/c ratio increases. Furthermore, the change in w/c ratio covers the whole range of the compressive strength domain of the ANN model. Thus, it can be concluded that the predictions correspond to

the views expressed in literature and that the w/c ratio is the dominant factor defining concrete strength.

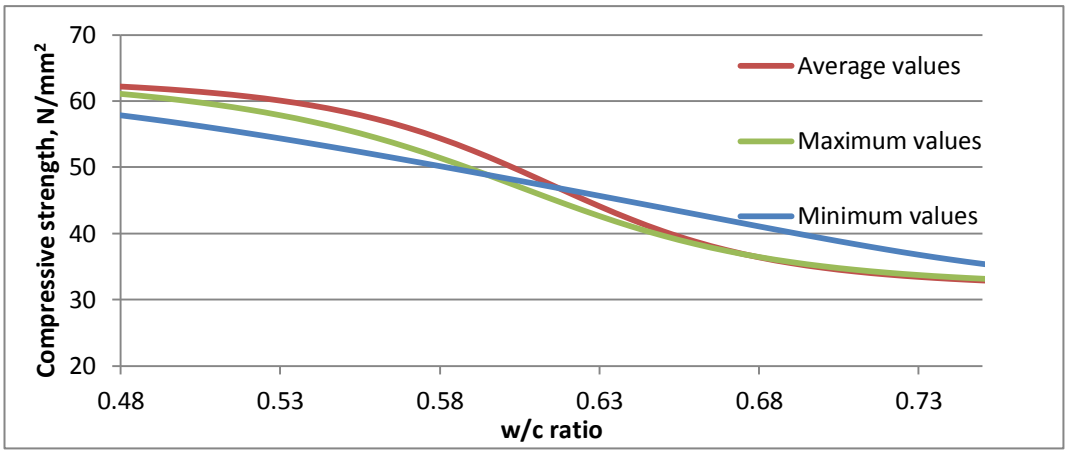

Figure 5.7.1 Variation of compressive strength predictions with w/c ratio

The predicted slump increases non-linearly with the rise in w/c ratio for all three cases under consideration covering the model's whole domain as shown in Figure 5.7.2. Thus, the effects correspond to the views expressed in the literature that the w/c ratio is one of the dominant factors affecting the consistency of concrete.

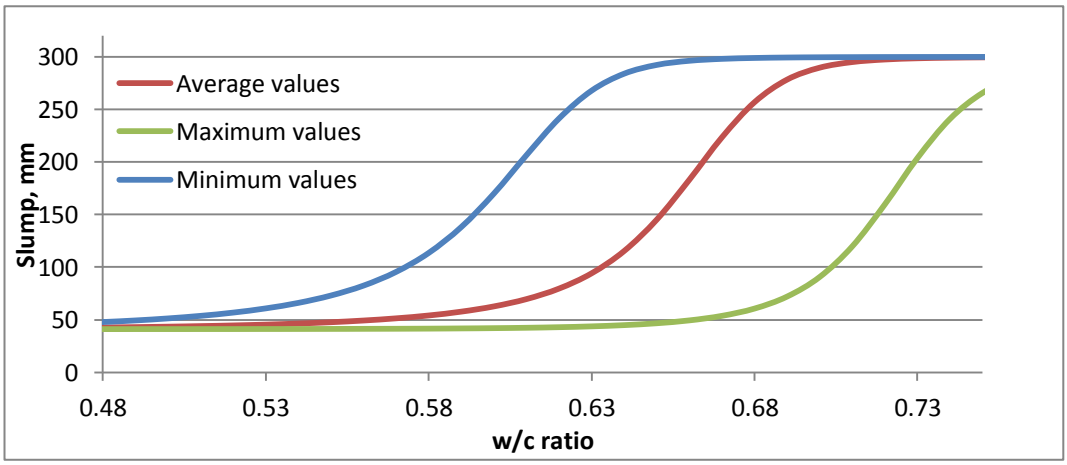

Figure 5.7.2 Variation of slump predictions with w/c ratio

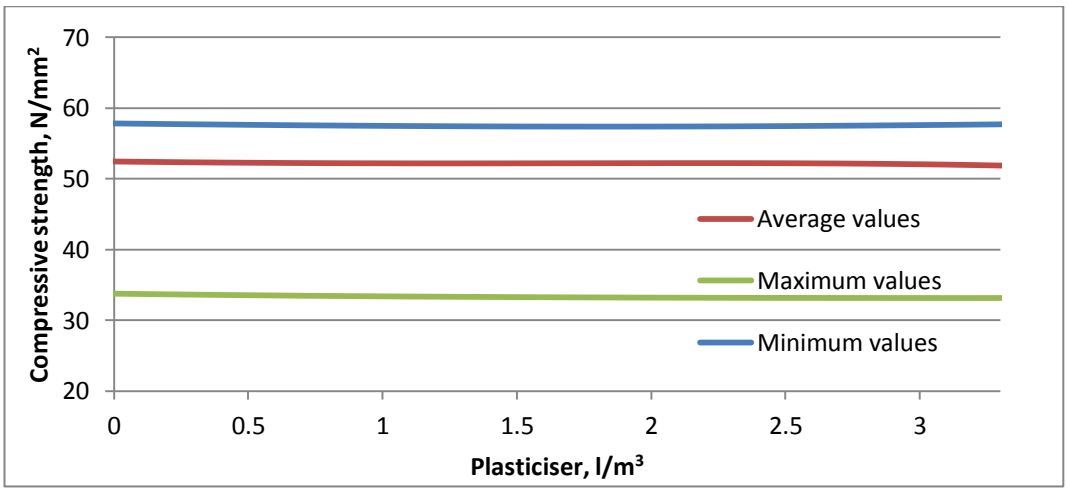

Figure 5.7.3 Variation of compressive strength predictions with plasticiser dosage

The influence of plasticiser dosage on compressive strength predictions is negligible as shown in Figure 5.7.3. However, there is a pronounced effect on the slump predictions for the minimum and average values with a less prominent effect for the maximum values as depicted in Figure 5.7.4. This corresponds to the expected effects of a plasticiser – to make stiff concrete mixes more workable and have very little to no influence on concrete strength within the recommended dosage range.

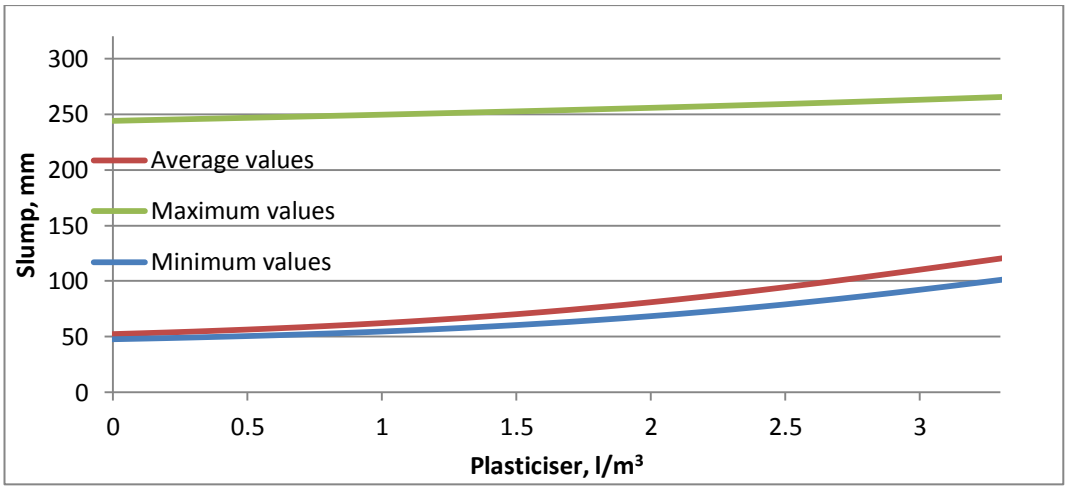

Figure 5.7.4 Variation of slump predictions with plasticiser dosage

It can therefore be concluded that the ANN predictions with respect to mix composition parameters are valid. Another thing to note and keep in mind for future reference is the

dominant role of the w/c ratio when considering concrete strength and the profound effect of the w/c ratio in combination with plasticiser dosage on concrete consistency. Thus, the minimum value line in the numerical evaluation figures corresponds to a very stiff high strength concrete mix, whereas the maximum value line represents a very fluid low strength concrete mix.

5.7.2 Quality of fines parameters

The quality of fines parameters are mainly related to the presence of clays in the fine aggregates and will be evaluated separately as well as in combination with each other due to their interconnected nature.

The compressive strength predictions are relatively constant with variations in GMBV for the maximum and minimum values, while average values exhibit a slight increase as shown in Figure 5.7.5. Small variations in compressive strength predictions due to change in SE values can be observed in Figure 5.7.6. It can be noted that for the average values the strength slightly rises until SE value of 50 is reached where it starts to drop similarly to the trend observed in Chapter 4 and shown in Figure 4.4.5. A slight drop in compressive strength predictions is observed due to the variation of water absorption for all values considered as shown in Figure 5.7.7. It has been noted by Neville (1995) and Lo et al. (2008) that a decrease of compressive strength might be expected for higher water absorption values.

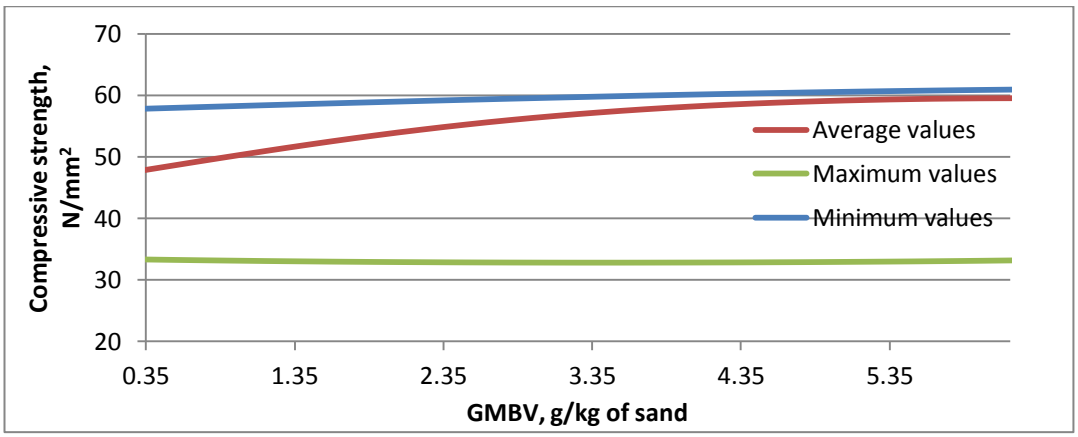

Figure 5.7.5 Variation of compressive strength predictions with GMBV

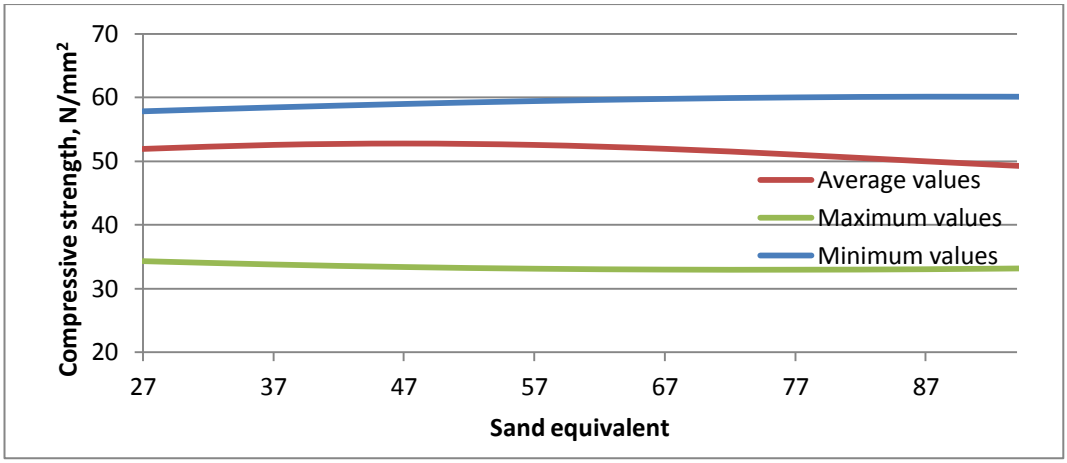

Figure 5.7.6 Variation of compressive strength predictions with SE

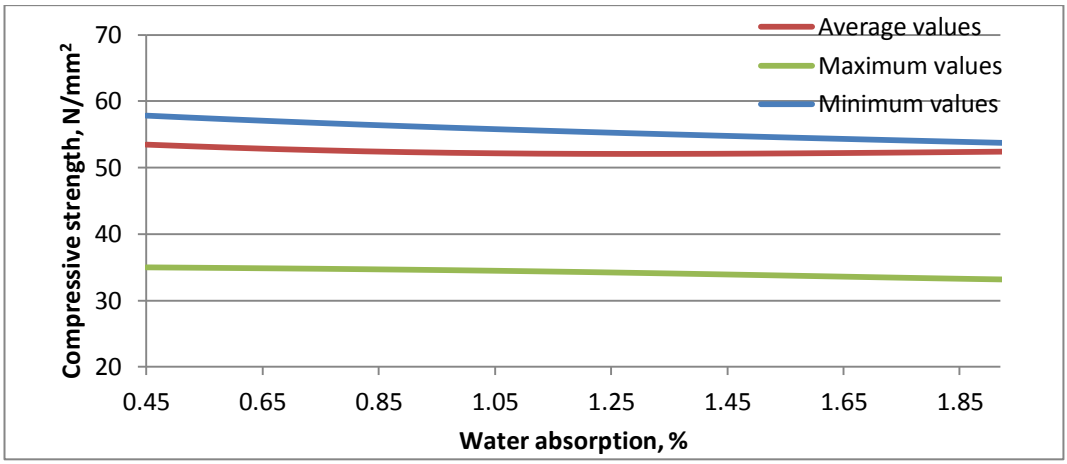

Figure 5.7.7 Variation of compressive strength predictions with water absorption

It might be expected that there would be either no effect or a decrease in compressive strength due to an increased presence of clays in the fine aggregate and a corresponding rise in the GMBV and a decrease in the SE values (Li et al. 2011b). However, that is not the case for the average values of GMBV and SE. This could be explained by the composition of the training dataset – it contains several NS mixtures that have the lowest GMBV and produce the lowest concrete strengths due to the rounded shape not due to the lack of clays, thus the ANN could have picked up this feature from the data and attributed that to GMBV values as discussed in section 5.2.4.

However, as mentioned at the beginning of this section, the fine aggregate parameters should be considered concurrently. Thus, Figure 5.7.8 shows the compressive strength variation due to both, SE and GMBV values, when all other properties are kept at average values from the training dataset. It was shown in Chapter 3 that there is a general trend between SE and GMBV values – an increase in GMBV value corresponds to a decrease of SE value. Thus, in Figure 5.7.8 realistic fine aggregate properties are represented by area around the grey dashed line. From Figure 5.7.8 it can be seen that for these realistic values when the w/c ratio is 0.7 the predictions are relatively constant whereas for w/c ratio of 0.6 and 0.5 there are optimum range of values for SE and GMBV that result in the highest compressive strength. It was discussed in Chapter 4 that the SE values represent the proportion of clay sized particles relative to the whole sand sample, which is indirect feature of aggregate grading, and it was observed that concrete reaches optimum compressive strength when the SE is around 60 similar to the trend shown in Figure 5.7.8. The effects of GMBV shown in Figure 5.7.8 on compressive strength could be attributed to the slightly biased composition of the dataset as mentioned above as such trends are not reported in literature.

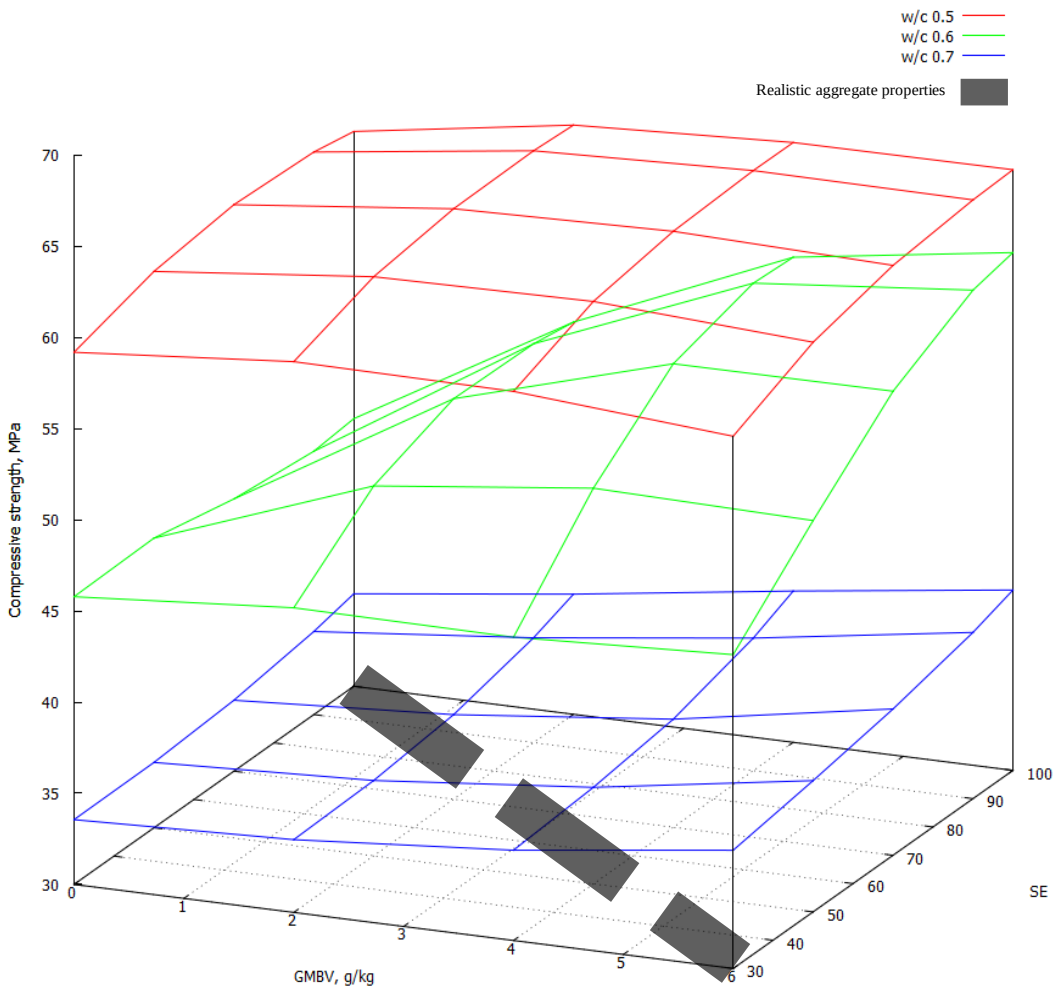

Figure 5.7.8 Variation of compressive strength predictions with change of SE and GMBV

It can be concluded that the ANN model's compressive strength predictions with respect to the quality of fines parameters follow the trends reported in literature or observed in the results presented in Chapter 4 with the exception of GMBV. However, the direct influence of clays on compressive strength in terms of GMBV, SE and water absorption over the range under consideration is relatively small for realistic aggregate properties.

As shown in Figure 5.7.9 the slump predictions decrease as the GMBV rises, whereas, the slump predictions increase significantly with a rise in SE value for all cases considered as it can be seen in Figure 5.7.10. The inverse trend between GMBV and SE values has been noted before but for clarification – a rise in GMBV corresponds to an

increase in the clay content of the fine aggregate and an increase in clay content corresponds to a decrease of the concrete consistency (Norvell et al. 2007), while an increase in SE values corresponds to a decrease in clay content.

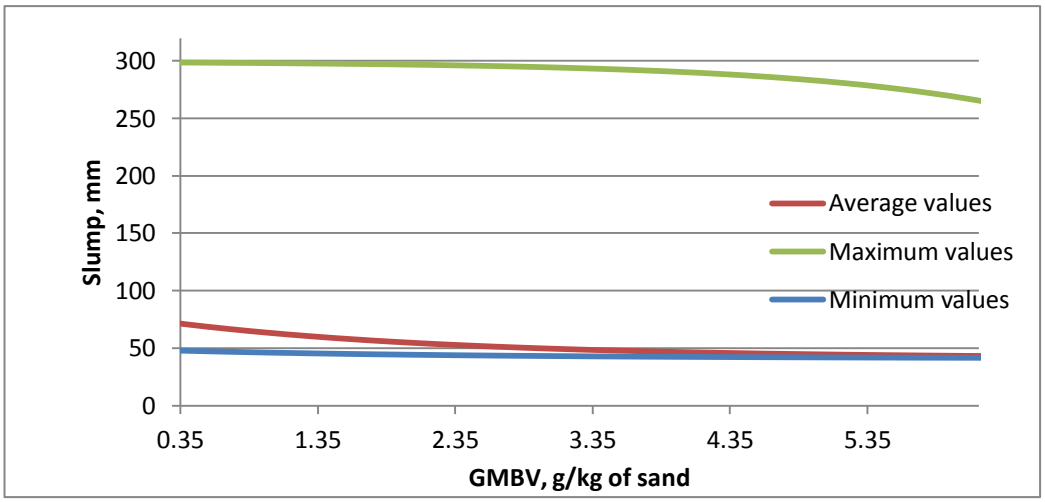

Figure 5.7.9 Variation of slump predictions with GMBV

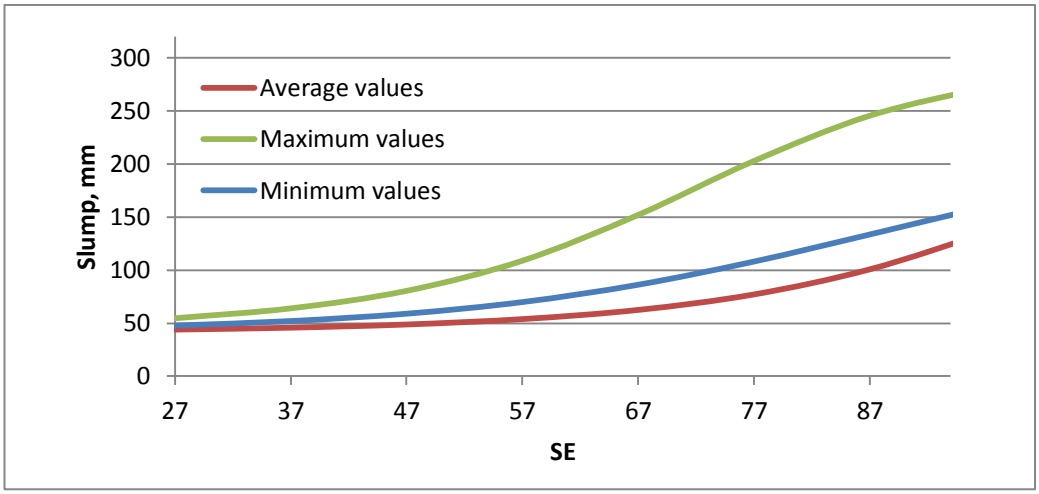

Figure 5.7.10 Variation of slump predictions with SE

Assuming that the water absorption of aggregates is related to the mineralogy and subsequently the clay content as discussed in Chapter 3 there should be a decrease in slump predictions as shown in Figure 5.7.11 for the average values. However, for the minimum values the predictions are relatively constant and a rise in slump is observed for maximum values only. This could be attributed to the time dependant water

absorption process meaning that high absorption capacity aggregates below SSD conditions yield higher initial slump values when the water content and absorption is taken into account in the mix design as observed by Alhozaimy (2009).

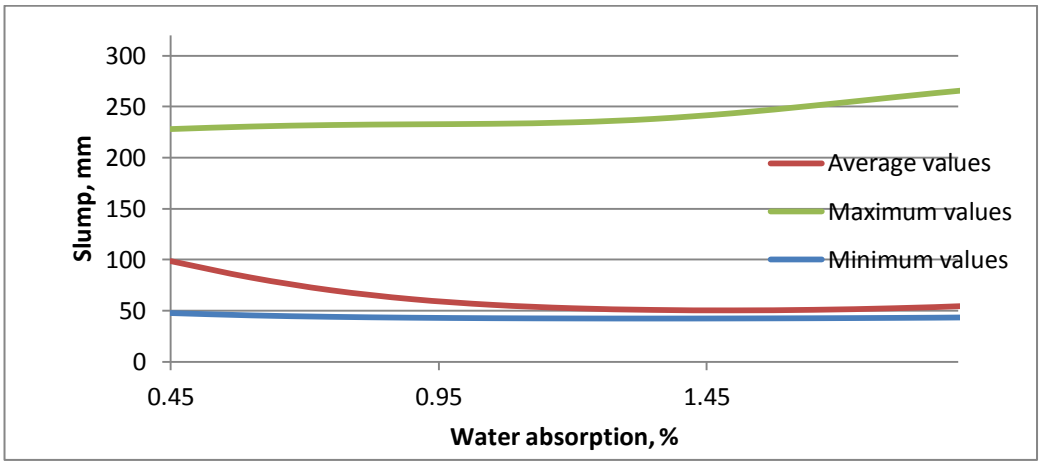

Figure 5.7.11 Variation of slump predictions with water absorption

Figure 5.7.12 shows the variation of slump predictions with SE and GMBV values and it can be seen that for fluid mixes with w/c ratio of 0.6 and 0.7 there is a prominent decrease in slump as the clay content increases. Whereas in stiff concrete represented by w/c 0.5 surface there is little effect on the slump predictions.

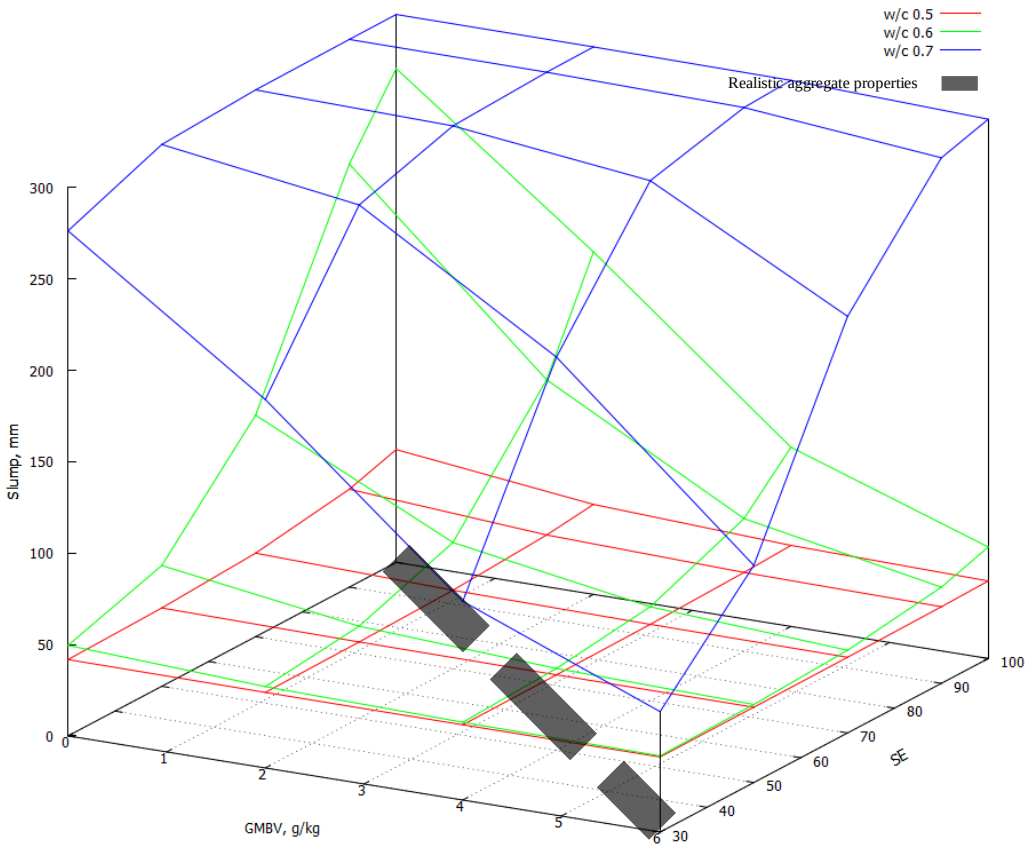

Figure 5.7.12 Variation of slump predictions with GMBV and SE values.

Taking the abovementioned into account it can be concluded that the presence of clays in terms of GMBV, SE and water absorption has a considerable influence on the concrete consistency and the ANN model's predictions follow the trends reported in literature and observed in the results of Chapter 4.

5.7.3 Shape, texture and grading parameters

If the fine aggregate grading is constant then a rise in the voids content is associated with higher angularity which improves the aggregate interlock in hardened concrete. In Figure 5.6.13 it can be observed that there is a rise in compressive strength predictions for average and minimum values as the voids content rises. However, a decrease in strength for the maximum values is observed.

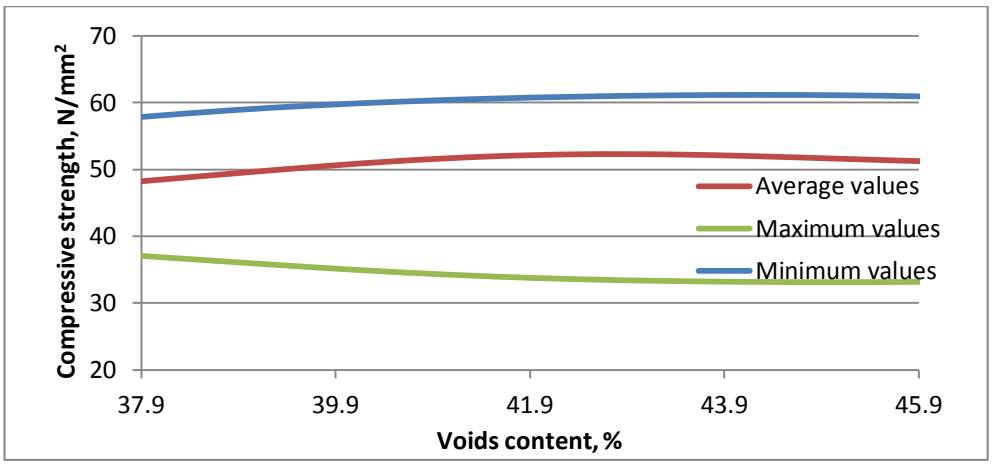

Figure 5.7.13 Variation of compressive strength predictions with voids content

Remembering that the w/c ratio is the dominant factor regarding concrete strength, the maximum value line corresponds to a high w/c ratio where the shape, texture or grading of the aggregate has little effect on compressive strength in contrast to high strength (low w/c ratio) concretes (Donza et al. 2002). The flow time is mainly defined by the grading and surface texture of the fine aggregate. It has been shown by Li et al. (2011) that if the grading is the same, then increased flow time indicates a rougher fine aggregate particle surface which increases the compressive strength. Such a trend is observed in Figure 5.7.14 for average and minimum values.

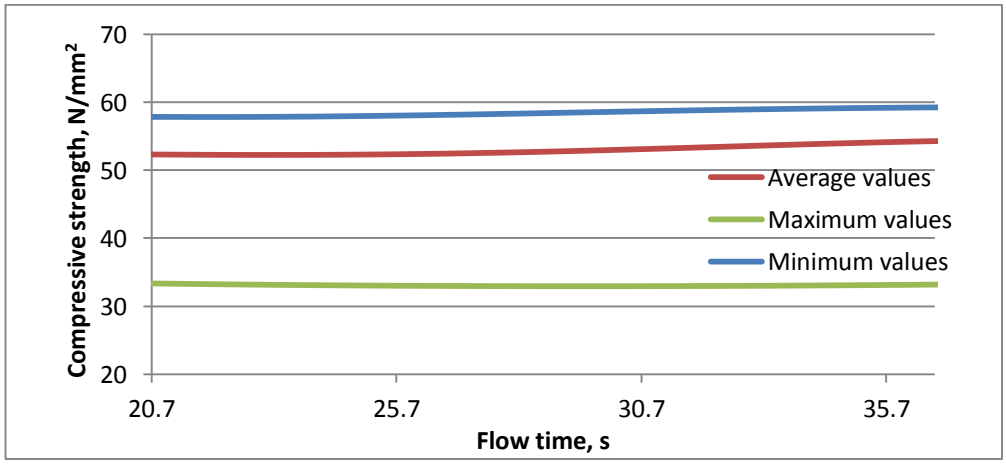

Figure 5.7.14 Variation of compressive strength predictions with flow time

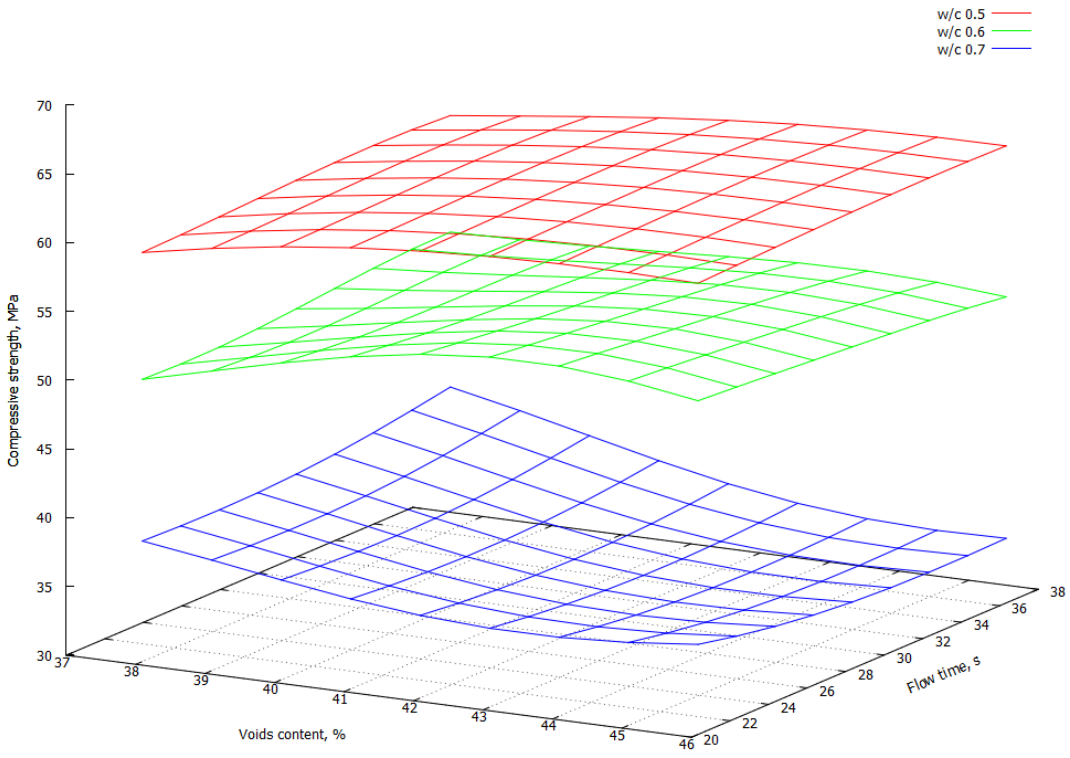

Figure 5.7.15 Compressive strength variation with flow time and voids content

Figure 5.7.15 shows that the variation of compressive strength with changes in the voids content and the flow time. It can be seen that the trends exhibited are the same as shown in Figures 5.7.13 and 5.7.14.

The fines content have a minor influence on concrete compressive strength at average and minimum values as shown in Figure 5.7.16. The effects of fines content on compressive strength are not fully understood and the views expressed in the literature vary. Furthermore, the results in Chapter 4 showed that there is no prominent trend between compressive strength and fines content, thus the minor trends observed could be attributed to natural variation in the training data.

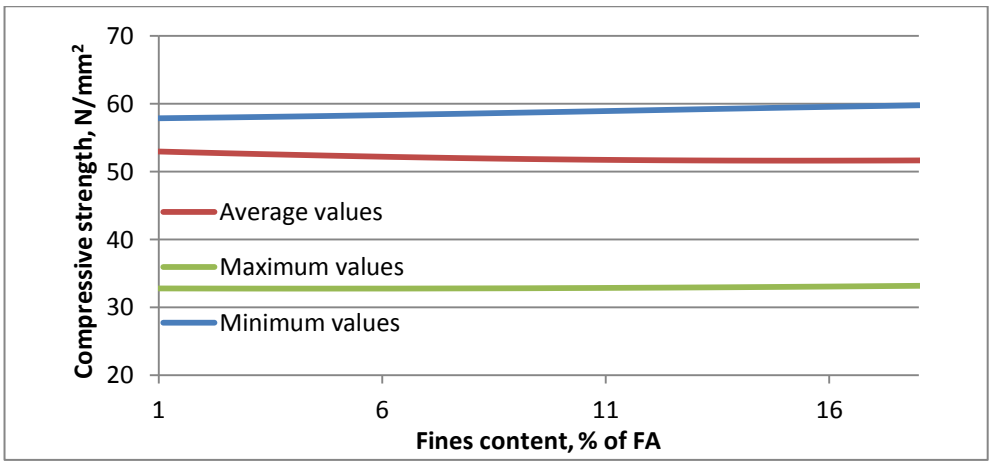

Figure 5.7.16 Variation of compressive strength predictions with fines content

The shape of the aggregate would have a minimal effect on concrete consistency in very fluid or extremely stiff mixes, whereas in mixes with medium w/c ratios the effects of shape should be more pronounced. This can be seen in Figure 5.7.17 where the average values show a pronounced drop in predicted slump as the voids content is increased. This is the relationship discussed in the literature which identified that more angular aggregates decrease the concrete consistency (Neville 1995, Gonçalves et al. 2007).

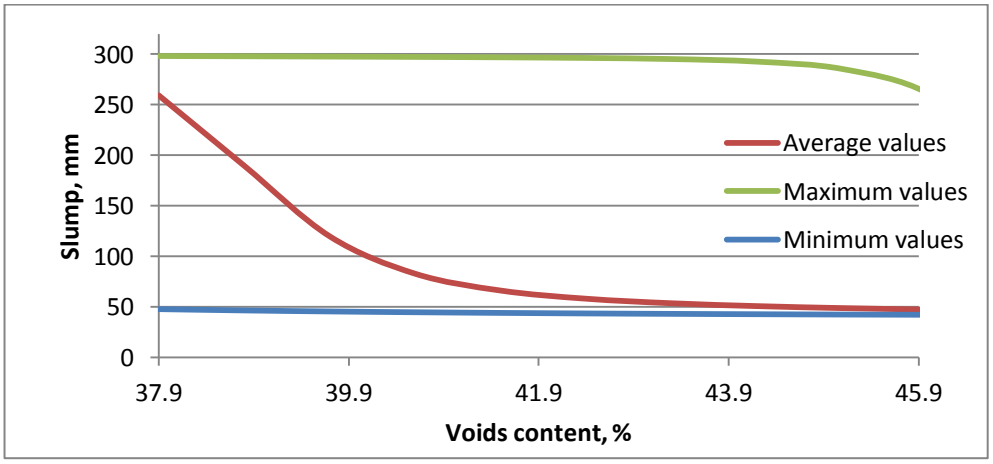

Figure 5.7.17 Variation of slump predictions with voids content

As depicted in Figure 5.7.18, there is a prominent rise in the slump predictions for high w/c ratio mixtures (maximum values line) as the flow time is increased, whereas for average values there is a slight increase and for minimum values there is no perceptible

effect. If Figure 3.5.6 of NZFC results is considered, it can be seen that the increase in the flow time corresponds to a decrease in fines content for MFAs. This subsequently means a reduction in the specific surface area of the fine aggregate, which corresponds to a reduced water demand in concrete for the same consistency (Fowler and Ahn 1999). Following this logic, an increase in fines content would correspond to a rise in the specific surface area of the aggregates, thus, decreasing the consistency of concrete. This can be seen in the slump variations shown in Figure 5.7.19 for average and maximum values. For stiff mixes, as represented by the minimum values lines, there is little effect. If the mix is dry and stiff with low slump value, changes in aggregate grading would not have a perceptible effect.

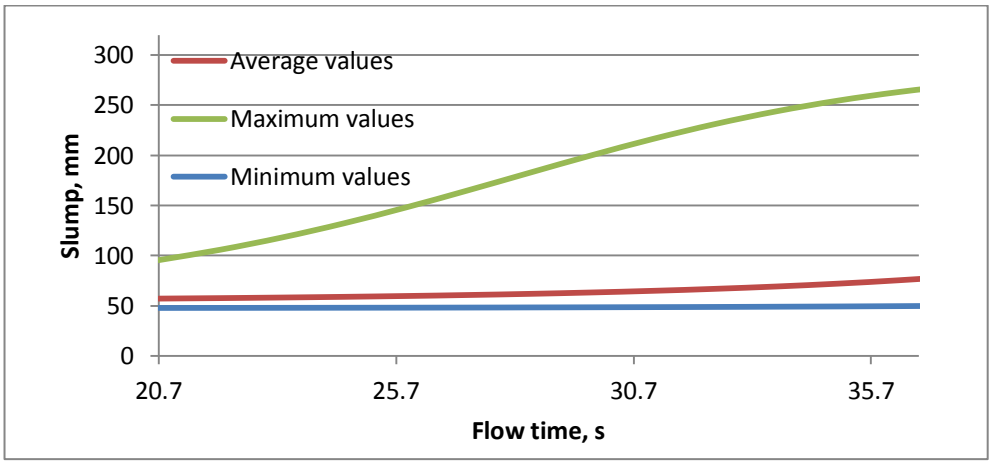

Figure 5.7.18 Variation of slump predictions with flow time

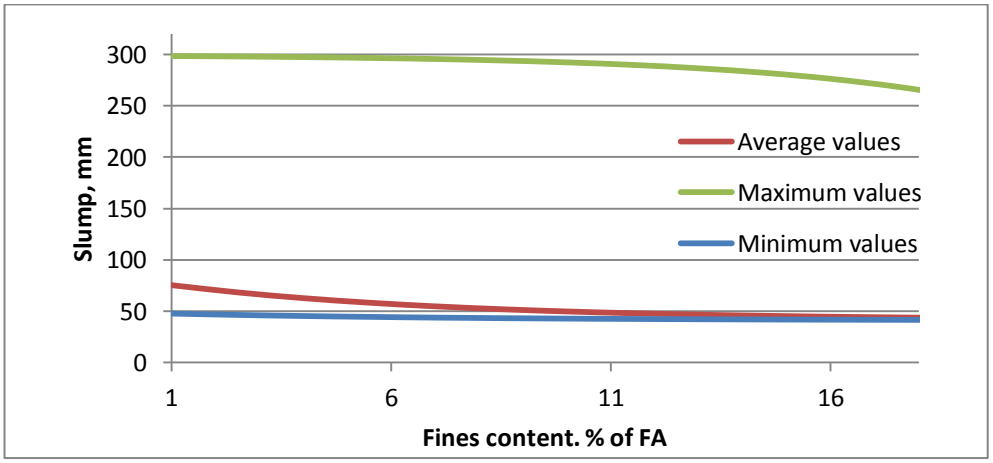

Figure 5.7.19 Variation of slump predictions with fines content

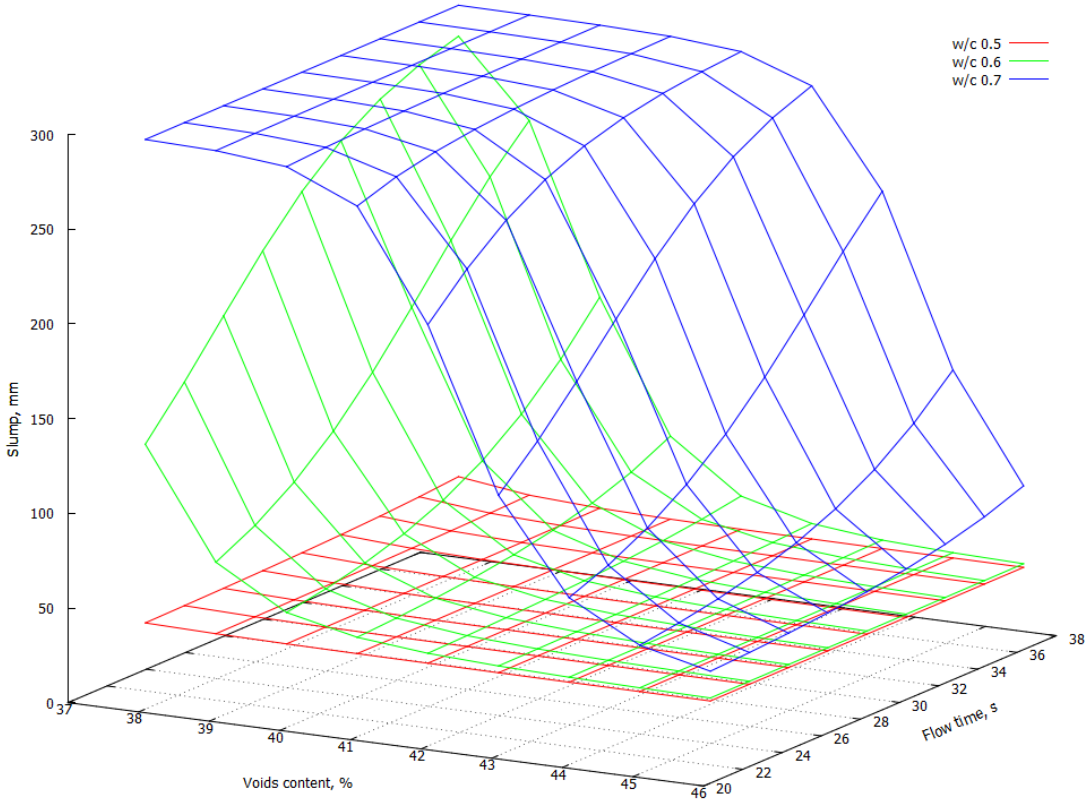

Figure 5.7.20 Variation of slump with voids content and flow time.

Figure 5.7.20 shows the slump predictions with changes in voids content and flow time and the trends are the same as described in Figures 5.7.17 and 5.7.18. For stiff mixes (0.5 w/c ratio) there is no effect of shape and grading on the slump whereas for fluid mixes (0.6 and 0.7 w/c ratio) the more angular the aggregate as indicated by increase in voids content the lower the slump, similarly the finer the grading as indicated by decrease in the flow time, the lower the predicted slump.

Taking into account the results and discussion of this section, it can be concluded that the ANN models predict compressive strength and slump according to the theoretical influence of aggregate shape, texture and grading.

5.7.4 Numerical evaluation summary

From the numerical evaluation exercise it can be concluded that the ANN models developed are valid and the predictions generally correspond to the theoretical relationships between the mix composition, fine aggregate parameters and concrete properties. It has been confirmed that the compressive strength predictions are mostly influenced by w/c ratio and voids content, whereas the slump predictions depend on all input parameters that were considered with the most dominant effects being these of w/c ratio, SE value and voids content.

5.8 Limitations

There are several limitations to the two models that have been developed. One is the lack of data for slump values outside the 30 to 120 mm range in combination with the artificial limit of 300 mm adopted for the slump of mixes which collapsed. This might have caused the relatively high prediction error for slump values above 120 mm as indicated by the NS validation mix results. Similarly, the compressive strength model's predictions range from 31 to 64 N/mm^2. In order to remedy these shortcomings, additional mix data that expands the output ranges could be used to retrain the models.

The fine aggregate grading was described by three input parameters and each of them only partially measures the particle size distribution. This could have increased the prediction error, thus an additional parameter, for example a fineness modulus as defined in BS EN 12620:2002+A1:2008 Annex B, could be introduced to account for the particle size distribution of the fine aggregate.

The models were developed using data that only accounted for the w/c ratio and plasticiser dosage as all other measures of the mix composition were kept constant. Therefore, the predictions are relevant only for the given cement and plasticiser type,

coarse aggregate type and content and fine aggregate content. However, the current models allow a comparison of expected performance of a range of fine aggregates with different properties as if they were used in the given concrete mix. As discussed in section 2.4, researchers have shown that mix composition parameters such as cement content, cement type, coarse aggregate content and properties, admixture type, fine aggregate content can be successfully used as input parameters for ANN models that predict concrete properties. Thus, the limitations of mix composition could be overcome by including mix design parameters along with the fine aggregate properties as input variables, expanding the training dataset and retraining the models. The optimal ANN topology would change as well, but the same development process described in this chapter could be applied.

5.9 Conclusions

The aim of the chapter was to develop and evaluate ANN models to predict concrete compressive strength and consistency based on fine aggregate properties and mix composition. This has been achieved and the 8-6-1 strength and 8-2-1 slump models that have been developed, have been validated and shown to be accurate with prediction error for test data (RMS) of 2.61 N/mm^2 and 7.97 mm respectively. They are also able to generalize within the range of data and input variables they were trained with. The numerical evaluation of the model has shown the potential of an ANN model to learn the underlying trends for compressive strength and consistency for a wide range of aggregate and mix composition parameters from few examples.

The models that have been developed can be used to predict and evaluate the consistency and compressive strength for different fine aggregates based on their characteristics. Thus, if a new fine aggregate is tested for its physical properties as detailed in Chapter 3, its expected performance can be evaluated and potentially

appropriate mix design selected based on the modelled results. This means that the number of laboratory trials required for comparison of various fine aggregates and selection of an appropriate mix composition can be reduced.

As encountered with any model, the ANN models that were developed have their limitations and these have been noted and potential remedies described in the previous section.

6 Geo-environmental application of excess rock filler

6.1 Introduction

As discussed in Chapter 1 and 2 the quarrying of coarse aggregates for construction purposes generates around 20 – 35 % of quarry waste or "quarry dust" (Harrison et al. 2000). This waste is often considered as inappropriate for use in construction due to its physical properties. However, it has been shown in Chapters 3 and 4 that this material can be reprocessed and used as the sole fine aggregate for concrete applications. The reprocessing creates usable aggregate by additional crushing and screening, however, it also generates further waste as a very fine rock powder. If a quarry is considered where all of the quarry dust is reprocessed into a fine aggregate using V7 process, then the final quarry waste will be a fine rock filler with a mass of 20 – 30% of the initial quarry waste.

In order to increase the sustainability and efficiency of the use of the resources in the quarrying industry and assuming that the initial quarry dust is being reprocessed, there is a need for an application for the waste rock filler. If the quarrying industry in the UK annually generates 55.1 million tonnes of quarry dust (Mitchell et al. 2008) then, assuming complete reprocessing of the quarry waste into fine aggregate, there is potentially 16.5 million tonnes of waste rock filler created in the UK per annum. This suggests that the potential applications of the rock filler should be able to consume large amounts of it and, preferably, should be employed near the quarries in order to minimize the environmental impact and costs of transportation.

If a specific rock type is considered, then limestone and dolomite has the widest range of applications. They are used in the production of cement, the steel industry as a flux in

the blast furnace, the pharmaceutical industry, as a filler for paints and putties and also for soil liming (BGS 2006a, BGS 2006b). These applications require high purity rock, except for liming where lower quality can be used and in 2011, 1.9 million tonnes of limestone, dolomite and chalk where produced for agricultural use in the UK (Bide et al. 2013). Given the amount of the rock material used in soil liming, it seems prudent to use this as a basis to investigate the feasibility of various rock fillers to increase the soil pH.

This Chapter therefore presents a literature review of soil liming, which is followed by characterisation of the rock fillers obtained in the sand manufacturing process according to a number of their chemical and physical properties. A laboratory soil incubation study evaluating the feasibility of the abovementioned rock fillers to be used to increase soil pH is then presented.

6.1.1 Soil pH

Whether a soil is classified as acidic or alkaline depends on the chemical elements present in the soil water and is measured by the activity of H^+ ions. The pH is the negative logarithm of the hydrogen concentration, expressed on a scale from 1 to 14 (Crozier and Hardy 2003). A pH of 7 is considered to be neutral, below as acidic and above as basic. For plant growth the soil pH generally should be near to neutral from 5.5 to 7.0 however, this is species specific. Some plants will grow in and prefer more acidic or basic soils (Crozier and Hardy 2003).

The soil pH is usually measured in a suspension of soil and water or other medium. Standard procedure BS ISO 10390:2005 states that the pH of soil is measured in 1:5 volume to volume suspension with water, 1 mol/l potassium chloride solution or in 0.01 mol/l calcium chloride solution. The results will differ depending on the medium used,

thus it is important to note which method was employed in order to compare and interpret the results.

When considering the pH of soil it should be noted that the soil cation exchange capacity (CEC) which is a result of negatively charged sites on the organic and inorganic matter in soil which can be occupied by positively charged ions such as H^+, Ca^{2+}, Mg^{2+}, K^+, Al^{3+}. In organic soils the CEC will be higher than for sandy soils, meaning that more cations can be stored on the surface of soil minerals and this in turn means that in order to change the pH of such soil larger amounts of liming material will be required (Crozier and Hardy 2003).

6.1.2 Effects of soil pH

As identified by Troug (1946) in Figure 6.1.1 the soil pH affects the availability of various macro and micro nutrients for the use of plants. Plants require specific amounts of macro and micro nutrients, and the availability of them is dictated by their presence in various chemical compounds within the soil as well as the pH of the soil. This suggests that the changes in pH can cause nutrient deficiency as well as toxicity if too much of one specific element is made available to the plant. This in turn can reduce the yield of the crops. Figure 6.1.1 shows that the macro nutrients (N, P, K) become less available to plants below pH of 6. Therefore, the optimum pH for soil in terms of nutrient availability is between 6.0 and 7.0 (Jacobs 2008) but it is species specific depending on the particular nutrients that a plant requires. Another point to note from Figure 6.1.1 is the illustration of the logarithmic nature of the pH scale, for example, a change of pH from 5 to 6 requires ten times higher reduction in H^+ ion concentration than that for a change of pH from 6 to 7.

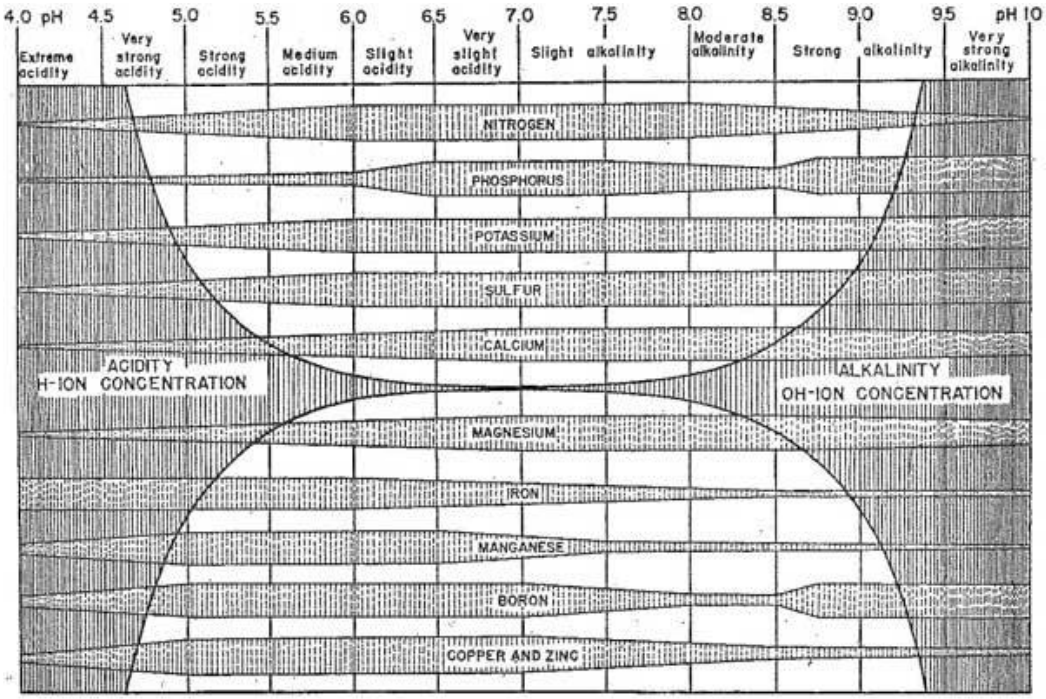

Figure 6.1.1 Plant nutrient availability depending on soil pH, reproduced from (Troug 1946).

Low soil pH can cause the toxicity of aluminium, iron and manganese as these become increasingly available to plants at low pH levels as shown in Figure 6.1.1. Aluminium toxicity is considered as the most limiting factor for plant growth in acidic soils as it inhibits the root growth and thus the nutrient uptake by plants (Hede et al. 2001). Furthermore, under acidic conditions minerals containing Al can dissolve releasing Al into the soil solution where it might be hydrolysed and increase the soil acidity (Hede et al. 2001). The relationship between Al availability and pH is depicted in Figure 6.1.2. where it can be seen that the availability of Al can be limited by increasing the soil pH to 5.5 or higher.

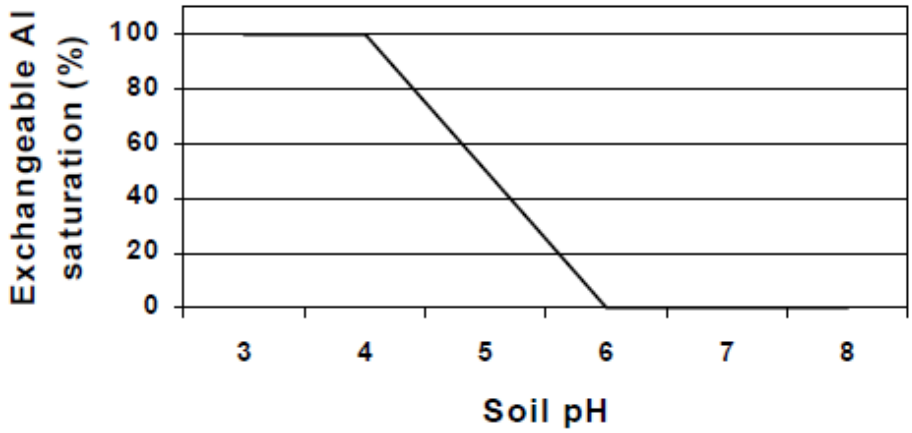

Figure 6.1.2 Exchangeable Al saturation versus pH, reproduced from (Crozier and Hardy 2003)

High pH above 6.5 -7.0 can induce deficiency of micronutrients as manganese and zinc in some plants, as well as reduce the availability of phosphates (Campbell 2008). Thus, it is evident that the pH of the soil should be controlled in order to avoid Al and other element toxicity at low pH or some nutrient deficiencies at high pH. It should be targeted to the optimum values for particular crop growth and nutrient availability, thus increasing plant yields.

6.1.3 Soil acidification

Many soils become acid over time for which there are several reasons, such as breakdown of organic matter, leaching of cations and fertiliser application. When organic matter is decomposed carbon dioxide and organic acids are produced. Furthermore, organic forms of nitrogen, phosphorus and sulphur are converted into inorganic species that can be utilised by plants. All these processes can increase the soil acidity by the release of H^+ ions in the soil solution (Hede et al. 2001).

Over time the highly mobile exchangeable bases Ca^{2+}, Mg^{2+}, K^+ and Na^+ are leached by rainwater out of the soil solution and replaced with H^+ and Al^{3+} ions which contribute to the soil acidity. It has to be noted that Al^{3+} ions act as acids in the soil interstitial water.

By reaction with water these form hydrogen as demonstrated in equation 6.1.1 (Campbell 2008; Crozier and Hardy 2003):

$$Al^{3+} + H_2O \leftrightarrow Al(OH)^{2+} + H^+ \qquad \text{Equation 6.1.1}$$

Application of ammonia based fertilizers will result in the release of H^+ ions due to the nitrification reaction of ammonium as shown in equation 6.1.2 (Crozier and Hardy 2003). Hence, the pH of soil will decrease as the concentration of H^+ ions rises in the soil water solution.

$$NH_4{}^+ + 1.5O_2 \rightarrow NO_3{}^- + 4H^+ \qquad \text{Equation 6.1.2}$$

6.1.4 Increasing soil pH

The most common method to increase soil pH to the required levels is to add a liming material. This agricultural liming material is a chemical compound containing calcium or magnesium and is capable of neutralizing acids. Most commonly these are limestone, dolomite, chalk, marl, burnt lime, wood ashes and various by-products (Mullins et al. 2009). The latter also state that liming materials are carbonates, oxides and hydroxides of calcium and magnesium. However, in principle these materials should dissolve releasing a base such as HCO_3^- or OH^- into the soil solution, which reacts with acid: H^+, Al^{3+}, thus increasing the soil pH (Crozier and Hardy 2003).

The effectiveness of a liming material is usually described by its calcium carbonate equivalent (CCE) or neutralizing value (NV). It represents how effective the liming material is in neutralizing acids expressed as a percentage of that which can be achieved with calcium carbonate. For pure $CaCO_3$ this number is 100% and it can be higher or lower for other liming materials depending on their chemical composition (Carey et al.

2006). For example, magnesium carbonate will have a CCE of 120% as the molecular mass of magnesium is lower than that of calcium, thus the same mass of $MgCO_3$ will neutralize more acid than $CaCO_3$. This means that the higher the neutralizing value of a material, the more acid it will neutralize with the same mass.

The CCE is determined in a laboratory according to the relevant standard. In the UK this is BS EN 12945:2008, however, the results according to the standard are expressed as a CaO equivalent rather than the more common $CaCO_3$ equivalent. This can be transformed into a $CaCO_3$ equivalent by multiplying it by the ratio of the molecular mass of $CaCO_3$ to CaO which is 1.8:1.

Liming materials dissolve relatively slowly in water, thus the CCE is not the only parameter defining their effectiveness. For limestone and dolomite it has been identified that the particle size and subsequently their surface area affect the rate of the neutralizing reaction. Particles passing a 150 micron sieve will react fully within one year, however majority of this size material will have reacted within a 2 – 4 week period. Whereas, particles coarser than 1mm are not expected to react within one year after its application to the field (Carey et al. 2006, Mullins et al. 2009).

This suggests that in order for rock dust to be effective in increasing soil pH, it must contain minerals soluble in water which are able to neutralize acid, preferably Ca and Mg, K and Na oxides, carbonates or hydroxides. Furthermore, they must be in a very finely divided form so that the reaction occurs rapidly due to the high specific surface area.

6.1.5 Rock dust and soil pH

There have been attempts to utilize rock dusts other than limestone and dolomite in order to increase the pH of the soil. However, the results have been variable and sometimes contradictory.

Hinsinger et al. (1995) investigated the effects of granite powder on soil pH and other properties during a 60 day soil incubation. It was found that at an application rate of approximately 20 t/ha gave an increase of 0.26 pH units in some samples. Similarly, Barral Silva et al. (2005) identified the potential of granite rock powder to increase soil pH, however, he noted that higher quantities would be required than if a limestone was used. In contrast Coroneos et al. (1995) concluded that there were no significant liming effects shown by granite powder in a sandy, acid podzol (an infertile acidic soil). Similarly, in a study by Campbell (2009), the use of basalt rock dust did not increase the pH of the soil in field trials over 3 years. It has to be noted that the crusher rock dust used by Campbell (2009) was up to 4 mm in diameter in contrast to other researchers who used finely ground powders, usually below 100 microns.

It was found by Gillman (1980) that soil pH was increased by crushed basalt in highly weathered soils. Higher application rates, incubation times and fineness of the material enhanced the effect. Similar results were found by Gillman et al. (2002) with basalt dust ground finer than 150 microns. It was concluded that fine basalt dust increased the pH of weathered soils, however, the application rates needed to be high (above 25 t/ha) to raise the pH above 5. Furthermore, in an soil incubation investigation by Silva et al. (2012) it was found that various ground silicate rocks with very low CCE values can increase the soil pH by up to 1 unit depending on the application rate and fineness.

The use of rock dusts as soil fertilizers have been researched and some conclusions regarding nutrient release in soil can also be drawn with respect to the the liming potential. Kleiv and Thornhill (2007) investigated the K-feldspars as potassium fertilizers and their efficiency when subjected to ultrafine grinding. They came to the conclusions that the grinding increased the reactivity of the material through the increased surface area of the particles as well as structural disordering caused by mechanical activation due to grinding. This phenomenon was also reviewed by Harley and Gilkes (2000) who concluded that more rapid dissolution of minerals could be achieved through smaller particles and the introduction of defects to the crystalline surface, thus increasing the reactivity of the silicate rocks. This suggests that the fine rock filler created in quarry dust reprocessing might have been mechanically activated in the crushing process and, therefore, could show increased dissolution rates for minerals and reactivity in soil, thus increasing the pH.

There seems to be evidence that silicate rock powders can be used to increase soil pH, however, the results will depend on the chemical composition and particle size of the rock dust as well as on the composition and parameters of the soil. The best results as indicated by the literature are achieved in highly weathered and acidic soils with high doses of dust. The high dosage should not be problem in terms of material availability if the quarries reprocess the quarry dusts, however, the distance from the quarry and transportation costs might be the limiting factors for the liming application of rock filler.

6.2 Laboratory techniques and materials

This section will describe the laboratory procedures employed in the testing of rock fillers and the evaluation of their liming potential. The rock fillers were supplied along with the MFAs used in this thesis except for the control limestone rock filler (R) which

was obtained by grinding high quality limestone aggregate in a puck mill. Table 6.2.1 shows the notation of the rock fillers that were tested.

Table 6.2.1 Notation of rock fillers

Description	Notation	Notes
Limestone	L	As supplied from sand manufacturer
Sandstone (gritstone)	GS	As supplied from sand manufacturer
Basalt	B	As supplied from sand manufacturer
Granite	G	As supplied from sand manufacturer
Reference limestone	R	Coarse aggregate limestone ground in puck mill

6.2.1 Test procedures

Soil/rock powder pH

The pH of rock powders and soil was measured according to BS ISO 10390:2005 in 1:5(volume:volume) powder(soil):water suspension. The volume of each soil or rock powder sample was 5ml mixed with 25 ml of deionised water. These were thoroughly mixed and the pH of the suspension measured after 16 hours with a 510 Eutech CyberScan pH meter freshly calibrated at pH 4 and 7 for soil, pH 7 and 10 for rock powders.

Elemental composition

The elemental composition of the samples in terms of 28 elements (Al, Ag, As, B, Ba, Be, Bi, Ca, Cd, Ci, Cr, Cu, Fe, K, Li, Mg, Mn, Mo, Na, Ni, Pb, Sb, Se, Si, Sr, Ti, Tl, V, Zn) was determined by inductively coupled plasma optical emission spectrometry (ICP-OES) using a Perkin Elmer Optima 2100 DV and an autosampler. The samples were prepared by acid digestion using a Multiwave 3000 microwave in the following manner:

- 0.1 g of sample was weighed into a clean dry polytetrafluoroethylene (PTFE) microwave tube.
- 2ml of hydrofluoric acid (HF) was added to the microwave tube, covered and allowed to stand overnight.

- 6ml of aqua regia (a 50/50 mix of nitric acid (HNO_3) and hydrochloric acid (HCl) was added to the microwave tube and allowed to stand for 30 minutes.
- The microwave tube was heated in microwave for 30 minutes and allowed to cool for 20 minutes.
- 6ml of saturated boric acid ($B(OH)_3$) was added to the tube to neutralise the HF
- The solution was re-heated in the microwave for 15 minutes and allowed to cool for 20 minutes
- The samples for testing were made up to 50ml using de-ionised distilled water in a graduated flask.

The Perkin Elmer Optima 2100 DV ICP was calibrated using a commercial 28 element standard solution diluted with distilled water at 0.1 ppm, 1.0 ppm, 10 ppm, 100 ppm. The samples were placed into an autosampler and tested after calibration of the ICP apparatus. The results of the ICP are a measure of the element content which requires converting to an oxide expressed as a percentage and calculated as follows:

$$Element, \% = \frac{R \times V}{W} \times 10000 \qquad \text{Equation 6.2.1}$$

where: *R* is the result of the analysis in mg/L, *V* is the sample volume after digestion in ml, *W* is the weight of the digested sample in grams. In order to obtain the oxide content the result of equation 6.2.1 is multiplied by the ratio of its elemental mass to the appropriate oxide mass. For example using calcium oxide, CaO:

$$CaO, \% = \frac{Ca+O}{Ca} \times Ca, \% \qquad \text{Equation 6.2.2}$$

where: *Ca* and *O* are the atomic masses in g/mol and *Ca,%* is obtained from equation 6.2.1 for calcium.

X-ray diffraction (XRD)

Mineral composition of the rock powders was analysed by X-ray diffraction using Philips PW1710 diffractometer with PW3830 Generator and the results were interpreted using X'pert Highscore software supplied by Panalytical. The best analysis results are

achieved with powdered samples, therefore as the samples were already in a powder form no additional grinding was necessary. The powder samples were placed in a sample holder, compacted and the sample holder fitted in the diffractometer. The power settings of the generator were set to 35kV and 40mA, the diffractometer settings were set as follows: scan angle range 2θ from 5° to 80°, step size 0.02°, scan step time 0.5 seconds. The diffractometer scan results were recorded as a peak and profile list. These results were compared with a database of peak patterns using the X'pert Highscore sftware in order to identify the minerals present in the samples.

Particle size distribution and specific surface area

The particle size distribution was measured by laser diffraction technique using a Malvern Mastersizer 3000 with Hydro EV sample dispersion unit and a computer with Malvern software. The refractive indices and particle densities of the rock filler materials and refractive index of the dispersing medium, in this case distilled water, were input into the software. The Mastersizer was flushed and calibrated with deionised water prior the testing of each rock filler sample. Following that a small amount of rock filler was transferred into the dispersion unit and circulated through the apparatus. During the circulation five particle size distribution measurements were taken. The final particle size distribution is the average of these five measurements. The specific surface area of the rock fillers was automatically calculated by the Malvern software from the rock filler grading results assuming spherical particles which is not true for crushed materials. However, for means of comparison between different rock fillers it should be a sufficiently accurate approximation.

Neutralizing value

The neutralizing value of the rock fillers was determined according to BS EN 12945-2008. It provides two methods (A and B) where A is designed for all liming materials except silicate liming materials and B is applicable to silicate liming materials. Thus

Method A was used for R and L rock fillers (low silica content), method B for silicate rock fillers (G,B,GS). According to the standard the NV is expressed as a CaO equivalent in %.

Reactivity

The reactivity of the rock fillers was tested according to BS EN 13971:2008. The standard states that the results are not used to declare a value, but to classify the different product groups according to the speed and effectiveness of the neutralizing potential of calcium carbonate and calcium magnesium carbonate liming materials.

6.2.2 Soil incubation

In order to test the rock filler effects on soil pH, a soil incubation experiment was set up. An acid loamy sand soil with a pH in water of 4.41 was sampled near Trefil in Wales (51.828776,-3.294747 latitude and longitude in decimal degrees). The soil field capacity according to the method provided in BS EN 14984:2006 Annex B was determined to be 19% by mass. The soil was dried at 40°C until constant mass was reached and then sieved through a 2 mm sieve. During the sieving it was observed that the soil contains root fragments and semi-decomposed stems of grass The dried and sieved soil was homogenized before the incubation by thorough mixing in a tray.

For each rock filler and application rate 500 grams of soil were incubated in a sealed plastic pot (1 litre volume, 100 mm internal diameter) at 20 ±3°C for 30 days., The rock filler dosage to be tested was set at 10 and 20 t/ha. The amount of rock filler required for a pot with 500 grams of soil corresponding to these application rates was calculated considering 15 cm of topsoil with a density of 1.5 t/m^3. This results in 2.2 and 4.4 g of rock filler per 500 g of soil for 10 and 20 t/ha dosage rates respectively. The soil samples were moistened to 70% of the field capacity at the beginning of the incubation which for 500g of soil required 66.5 g of deionised water. Four pH measurements

according to the procedure described in the previous section were taken for each soil sample, two at the beginning and two at the end of the incubation period.

The soil incubation procedure in a step by step manner is described below:

- Dry soil at 40^{o}C until constant mass reached.
- Sieve the dry soil through a 2 mm sieve.
- Thoroughly mix the soil in a tray.
- Weigh 500g of dry sieved soil into a plastic pot (1 litre volume, 100 mm internal diameter).
- Weigh dry rock filler (2.2 or 4.4 g) and add on top of the soil in the pot.
- Thoroughly mix the dry rock filler with the dry soil in the pot using a spatula.
- Add 66.5 g of deionised water to the soil and rock filler in the pot.
- Thoroughly mix the contents of the pot using a spatula.
- Take two 5 ml samples of the mixture in the pot for pH measurements using volumetric spoon.
- Seal the pot and leave at 20 ±3°C for 30 days.
- On the 30th day open the pot and thoroughly mix with a spatula.
- Take two 5 ml samples of the mixture in the pot for pH measurements using volumetric spoon.

6.3 Results and discussion

This section will present and discuss the results of rock filler testing and soil incubation. It will start with the rock filler characterisation tests and proceed to the incubation experiment results.

6.3.1 Rock filler test results

As shown in Table 6.3.1 all rock fillers that were investigated yielded basic pH in deionised water suspension. These ranged from 9.01 for sandstone to 10.25 for granite rock filler. This suggests that there are minerals within the rock fillers capable of dissociating into ions and increasing the pH. Similar observations were made by Gillman et al. (2002) and Grant (1969) regarding basalt and granite rocks when considering abrasion pH (pH in water suspension while grinding).

Table 6.3.1 Rock filler pH in suspension with water

Sample	L	GS	B	G	R
pH, water	9.36	9.01	9.40	10.25	9.30

The elemental compositions determined by ICP-OES expressed as oxides are shown in Table 6.3.2. The table shows the oxides which exceed 0.1% by mass, the full results can be found in Appendix E. In terms of liming potential the amount of calcium, magnesium, potassium and sodium are relevant as chemical compounds of these basic metals are capable of increasing the pH. It can be seen that two nominal limestones (L and R) contain a significant amount of calcium. When the calcium is expressed as $CaCO_3$ which should be present in limestones, it can be seen that R contains 90.1% of calcium carbonate, whereas L contains 46.9%. This suggests that these two rock fillers could have the potential to be liming materials. Furthermore, L contains 14.4% magnesium oxide which in dolomitic limestones can be present as magnesium carbonate, which is a well known liming material.

It can be seen that the basalt, granite and sandstone contains between 41.0 and 70.9% of silicon dioxide which is considered insoluble in crystalline form and does not exhibit liming potential (Krauskopf 1956). However, these three rock fillers contain the basic oxides in the range of 0.7 to 6.5%. This observation suggests that there could be a

liming potential for these siliceous rock fillers but at a much lower level when compared to the limestones.

Table 6.3.2 Elemental composition of rock fillers expressed as oxides

	Sample				
Oxide, %	L	GS	B	G	R
SiO_2	8.9	70.9	41.0	63.1	6.1
CaO ($CaCO_3$)	26.2 (46.9)	1.1	6.5	4.1	50.5 (90.1)
MgO	14.4	1.6	5.0	1.0	0.6
K_2O	0.3	3.3	1.1	4.1	0.1
Na_2O	0.2	0.7	2.6	3.9	0.1
Al_2O_3	1.1	12.8	9.8	13.4	0.4
Fe_2O_3	1.9	5.1	11.6	2.4	0.2
TiO_2	0.1	0.7	1.7	0.4	0.0
BaO	1.9	0.1	0.0	0.0	0.0

The ICP-EOS identifies the majority of the elements present within a sample, however, it does not identify the chemical compounds which are present. Thus X-ray diffraction (XRD) was used to identify the major mineral constituents in the rock fillers. The identified compounds are listed in Table 6.3.3. The major compound found in the reference limestone R was calcite, which is the most commonly used liming material. As for the rock filler L, it was found that it contains ankerite, which is a carbonate of calcium, iron, magnesium and manganese, and a form of silicon dioxide. In terms of liming potential ankerite contains basic metal carbonates and, thus, should exhibit liming properties. Minerals with chemical composition of SiO_2 found in the G, GS and L samples are considered insoluble in most cases and, thus are unlikely to be able to alter the pH of soil.

The B and G samples were identified as containing albite minerals. According to Chou and Wollast (1985) the dissolution of albite initially results in the release of basic ions such as Na^+ and Ca^{2+} which are replaced by H^+ ions, thus rock fillers containing this mineral could exhibit a liming potential. The granite contained biotite minerals and according to experiments carried out by Chae et al. (2006), dissolution of this mineral in water results in a continuous supply of calcium, sodium and potassium cations. Thus, it suggests that the dissolution of this mineral in soil has the potential to increase its pH.

Table 6.3.3 Chemical compounds identified in x-ray diffraction

Sample	Identified compounds	Chemical formula
L	Ankerite	$CaFe_{0.6}Mg_{0.3}Mn_{0.1}(CO_3)_2$
	Coesite	SiO_2
GS	Quartz	SiO_2
	Illite	$(K,H_3O)(Al,Mg,Fe)_2(Si,Al)_4O_{10}[(OH)_2,(H_2O)]$
B	Albite	$Na_{0.95}Ca_{0.05}Al_{1.05}Si_{2.95}O_8$
	Montmorillonite-chlorite	$NaCaAlSi_4O_{10}O$
	Magnesium iron aluminosilicate	$Mg_{0.34}Fe_{1.66}Al_4Si_5O_{18}$
G	Quartz	SiO_2
	Albite, calcian	$(Na,Ca)Al(Si,Al)_3O_8$
	Biotite	$K(Mg_{1.48}Fe_{1.28}Ti_{0.24})(Al_{1.2}Si_{2.8}O_{10})(OH)_{1.4}F_{0.32}O_{0.28}$
R	Calcite	$CaCO_3$

Other identified minerals such as illite in the GS rock filler and montmorillonite-chlorite and magnesium iron alumosilicate in the B rock filler are clay minerals. The dissolution of these minerals is complex and depends on the environment, whether there is water present or various organic acids (Huang and Keller 1971). Thus, it is only possible to speculate about the effects of these minerals on the soil pH.

The XRD results suggest that potentially the best liming effects could be expected from the R and L rock fillers, whereas the GS, B and G rock fillers may have a relatively low liming potential due to their mineral composition.

The particle size distribution along with the estimated specific surface area are presented in Table 6.3.4. It shows that all rock fillers are very fine and have 90% of particles smaller than 127 microns. The finest grading is for the L rock filler, followed by the R, GS, B and G rock fillers. In terms of specific surface area, the largest was found for R at 480.8 m^2/kg followed by L, GS, B and G with 157.4 m^2/kg. As discussed in the literature review, the particle size and surface area plays an important role in the rate of chemical reaction and the solubility of liming materials. One could expect faster reactions from finer rock fillers which possess larger specific surface area. However, the rate of reaction will also depend on the chemical composition of the rock fillers.

Table 6.3.4 Particle size distribution and surface area results

Sample	L	GS	B	G	R
Percent passing	Particle diameter, microns				
10	2.5	3.4	5.3	5.6	2.2
50	12.6	14.3	26.1	35.8	9.1
90	39.7	63.0	92.2	127.0	48.3
Specific surface area, m^2/kg	340.3	270.7	164.2	157.4	480.8

The main parameter which is quoted when discussing liming materials is the NV. The results of NV and reactivity tests for the rock fillers under consideration are presented in Table 6.3.5. The NV test involves dissolution of the samples in a known quantity and molarity of hydrochloric acid. The amount of neutralized acid is then determined by back titration with sodium hydroxide standard solution. This is a rapid test which evaluates the liming potential, however, the testing conditions are not representative of

the ones occurring in soil. Thus, the expected behaviour of multi-phase rocks such as granite or basalt as liming materials might not be obvious from such a test.

Table 6.3.5 Rock filler NV and reactivity

Sample	NV, CaO equivalent, %	NV, $CaCO_3$ equivalent, %	Reactivity %
L	43.4	78.2	54.8
GS	6.0	10.8	12.8
B	13.6	24.4	27.8
G	14.6	26.2	33.7
R	51.0	91.8	78.4

It can be seen from Table 6.3.5 that both the limestone R and L exhibited the highest NV of 51.0 and 43.4% respectively. This was expected due to their chemical composition identified in the ICP-OES and XRD tests. The B and G rock fillers showed much lower NVs, which were found to be 13.6 and 14.6%, respectively. These results correspond to the observations made from the mineralogical and elemental composition test results. The lowest NV was found for the GS rock filler, suggesting that the sandstone has very low liming potential.

Reactivity values show a direct correlation with the NV results (Figure 6.3.1). This suggests that the rate of reaction of the liming material depends on the concentration of the chemical compounds capable of increasing pH within the sample. This means that the rate of pH increase should be more rapid and efficient for carbonate liming materials when compared to silicate liming materials.

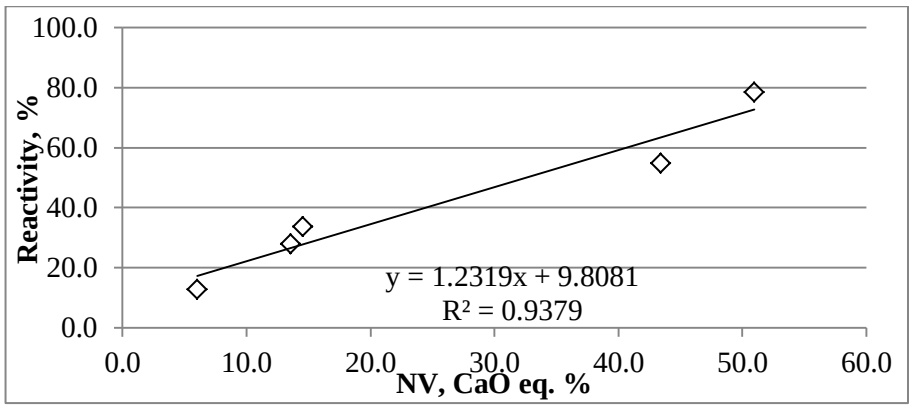

Figure 6.3.1 Reactivity versus neutralizing value

These results suggest that R, the reference limestone, will be the best in increasing soil pH closely followed by the rock filler L. Rock fillers B and G should yield similar results but with a lower increase in pH than for both limestones. The pH increase of the soil using the sandstone rock filler is expected to be lower than that of the G and B rock fillers on the basis of the NV results.

6.3.2 Soil incubation

The soil pH testing results for the incubation experiment are presented in Table 6.3.6, where numbers "10" and "20" next to the sample notation represent application rates of 10 and 20 t/ha respectively.

It has to be noted that the initial soil pH of the sieved, dried and homogenized soil was 4.41, whereas after a 30 day incubation it had increased to 5.75 without any additions (control pot). Such a phenomenon is explained by Bartlett and James (1980) as follows: "The behaviour of a dried sample immediately after adding water to it is different from that of the continuously moist soil. Remoistening for a longer period is followed by a microbiological explosion. The behaviour of the soil for an extended period, perhaps more than a month after rewetting, may be anomalous, or at least unpredictable." Furthermore, noting that the soil used in the incubation study contained root fragments and semi-decomposed stems of grass the increase in pH could be caused by

decomposition of organic matter as reported by Ritchie and Dolling (1985) in a 30 day incubation experiments with organic matter added to two different soils. They explained the pH increase with association of organic anions from the plant material with H^+ ions in the soil. They also went on to note the possibility of mineralization of organic anions to CO_2 and water thereby removing H^+ ions.

Table 6.3.6 Incubation soil pH results

	0 days			30 days			Difference from
Sample	pH 1	pH 2	Average	pH 1	pH 2	Average	control, pH unit
Control	4.39	4.43	4.41	5.74	5.75	5.75	0.00
R10	4.39	4.41	4.40	6.39	6.43	6.41	0.67
R20	4.39	4.41	4.40	6.66	6.67	6.67	0.92
B10	4.35	4.40	4.38	5.76	5.75	5.76	0.01
B20	4.39	4.36	4.38	5.90	5.98	5.94	0.20
GS10	4.38	4.41	4.40	5.94	5.89	5.92	0.17
GS20	4.45	4.42	4.44	5.92	5.96	5.94	0.19
G10	4.38	4.36	4.37	5.95	5.95	5.95	0.21
G20	4.42	4.42	4.42	5.98	6.00	5.99	0.25
L10	4.39	4.37	4.38	6.31	6.28	6.30	0.55
L20	4.39	4.38	4.39	6.37	6.42	6.40	0.65

It was assumed that the same increase in pH as recorded in the control pot would be observed in all soil pots, since consistent soil samples were used in each pot. Thus, any differences in the pH from the control soil after a 30 day incubation were attributed to the effects of rock filler addition.

The soil pH average values after 30 days incubation are plotted in Figure 6.3.2 and it can be seen that the R rock filler yielded the greatest pH increase at each application rate, 0.67 and 0.92 units above the control at 10 and 20 t/ha, respectively. The rise in pH was smaller for the L rock filler, 0.55 and 0.64 above the control at the two application

rates respectively. This observation correlates with the NV results as shown in Figure 6.3.3.

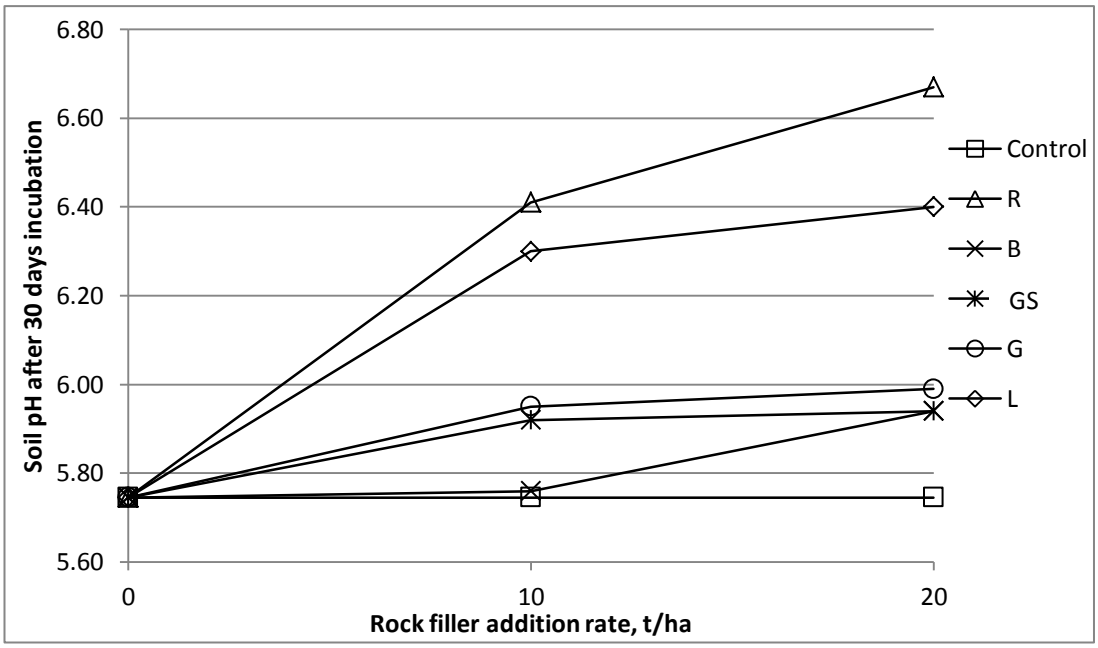

Figure 6.3.2 Soil pH after 30 day incubation versus the rock filler application rate

The G and GS rock fillers yielded similar soil pH increase at both application rates – in the range from 0.17 to 0.25 pH units above the control soil pH and only a slight difference in the results was observed for 10 and 20 t/ha application rates. This observation is interesting since the NV value of the GS rock filler is at least two times smaller than that of the G rock filler and it might be expected that a higher NV would yield a greater increase in soil pH value. However, this could be explained by the finer grading and larger surface area of the GS rock filler, which allows a faster reaction. This explanation is supported by the general correlation between the specific surface area and soil pH increase as shown in Figure 6.3.4. In such a case there should be a more prominent difference in the soil pH for the G rock filler in the longer term incubation experiments.

The B rock filler, with a similar NV value to the G rock filler at an application rate of 10 t/ha, showed negligible difference in the soil pH from the control soil. However, at the 20 t/ha application rate the increase of pH was 0.2 units above that of the control soil pH, which is comparable to the G and GS results.

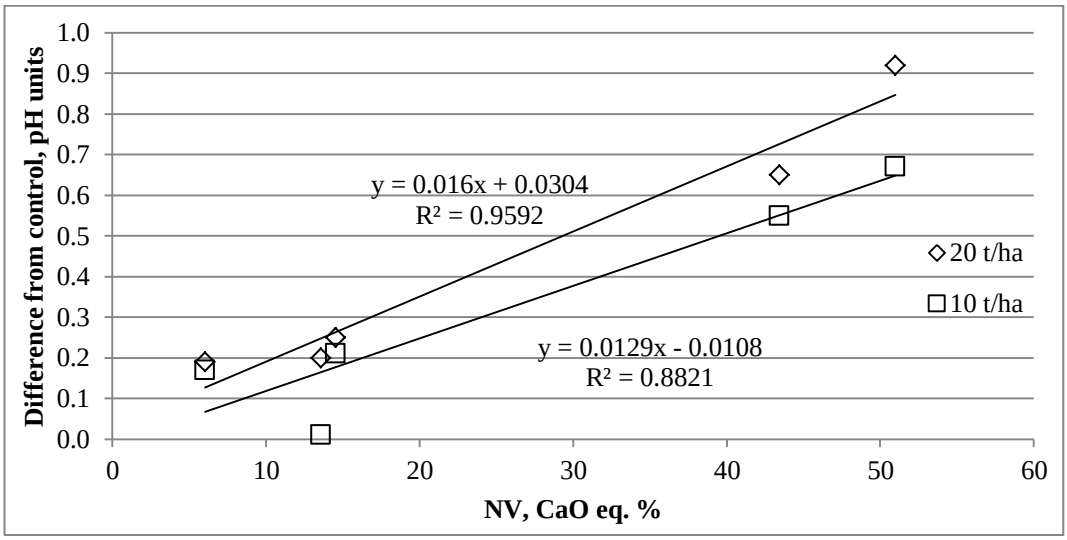

Figure 6.3.3 Difference from control pH versus NV

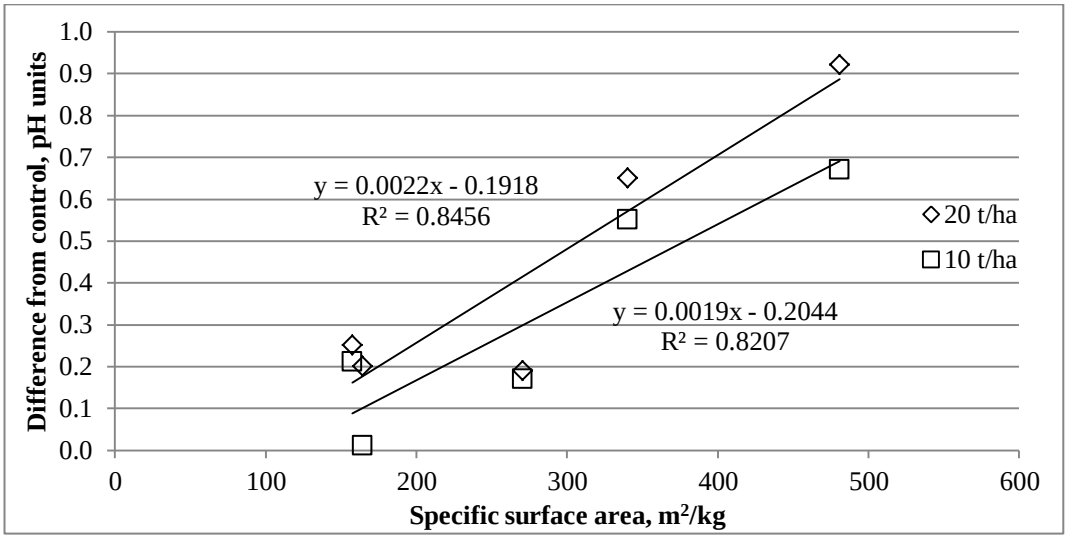

Figure 6.3.4 Difference from control pH versus specific surface area

Figures 6.3.4 and 6.3.3 illustrate that the change in soil pH depends on the neutralizing value and the specific surface area of the rock fillers. Higher R^2 coefficients are found for the correlations with neutralizing value, suggesting that the chemical composition, which influences the neutralizing value, is a more dominant factor with respect to pH

change than rock filler fineness. However, the specific surface area is shown to have an important effect as well and the liming potential of a low NV material could be increased by higher specific surface area (e.g. grinding). Furthermore, given the variations in the incubation experiment results for the B, G and GS rock fillers, which are not consistent with the expected performance based on the NV, it can be concluded that soil incubation experiments for silicate rock powders yields a better indication of their effect on soil pH than does the NV, particle size distribution and reactivity test results. Therefore, soil incubation studies or field trials in combination with the abovementioned tests should be employed when assessing silicate rock powder liming potential.

6.4 Conclusions and suggestions for future work

From the testing results presented in this chapter the following conclusions were drawn:

- Soil liming with rock fillers containing calcium and magnesium carbonates, with high NV (above 40% CaO equivalent) and with the majority of particles smaller than 127 micron is feasible and effective.
- Rock fillers of silicate origin can increase the soil pH even when their NV is as low as 6%. Their effectiveness is highly dependent on their chemical composition and fineness.
- When dealing with silicate rocks, soil incubation results yield a better indication of their liming performance than just NV, particle size distribution and reactivity testing.
- Elemental and XRD analysis can yield good information about expected rock filler performance as a liming material.

It has been shown that different mineralogy rock fillers can be used as liming materials, but silicate rock effectiveness is much lower than that of a good quality limestone. This

means that in order to increase the soil pH a much larger amount of the silicate rock filler is needed. This should not be a problem in terms of the quantity of the rock filler produced through the V7 sand manufacturing process discussed earlier. There could be sustainability benefits in changing the pH of acid soil using silicate rock fillers near quarries where transportation costs are low. The quarries could remove the rock fillers thus reducing the costs and effort of rock filler stockpile management enabling local farms to receive a cheap, local liming material.

However, before such actions, the long term effects of rock fillers on soil pH in different soils should be investigated by soil incubation experiments as well as field trials. Furthermore, there could be heavy metals present in the rock fillers which could be released in arable land by the rock filler application, thus this area also requires further investigation. Another point to consider would be the means of application of the rock fillers, whether ordinary farming equipment can be used or whether it requires some specialized tools or pre-treatment of the rock filler such as pelletizing.

7 Conclusions and suggestions for future work

7.1 Conclusions

This chapter summarises the main conclusions that have been drawn from the work presented in this thesis and proposes areas for future work in this research field. More detailed conclusions can be found at the end of each chapter.

There were four research objectives outlined in the introduction of this thesis and these along with the research undertaken to reach them and the corresponding main conclusions are presented below:

a) **Identify techniques that can be used to characterise physical and chemical properties of MFAs.**

   Seven test methods were identified that were easy to carry out and that can characterise fine aggregates with respect to particle size distribution, quality of fines, shape and texture. These were applied to sands manufactured by reprocessing quarry dusts of different mineralogy. The main conclusions drawn were:

   i. Reprocessing of quarry dusts in the V7 plant produced MFAs with improved particle size distribution that conformed to the UK grading requirements irrespective of mineralogy and grading of the feed material.

   ii. The shape of the MFAs was improved as indicated by the NZFC results and high resolution images. The MFA particles were relatively equi-dimensional but more angular and with rougher surfaces than the marine dredged natural sand control.

   iii. MBV, GMBV and SE tests showed good potential for the indication of presence of clays and XRD analysis allowed the identification of the clay type.

iv. MBV and GMBV test methods showed very good correlation, giving further credibility to the use of GMBV as a replacement for the standard method with the benefit that it minimises operator error.

b) Investigate MFA concrete fresh and hardened properties.

Two series of concrete mixes incorporating MFA were created. One where the w/c ratio was adjusted in order to achieve an S2 slump, the other where the w/c ratios of 0.55, 0.50 and a plasticiser were used to adjust the consistency as required to achieve an S2 slump. The fresh and hardened concrete properties were correlated to the characterisation test results of the MFA.

i. Workable concretes were produced using MFAs as the sole fine aggregate at different w/c ratios. Feed material quarry dusts required higher w/c ratios to achieve an S2 slump than corresponding MFA. The presence of clays in MFAs can be a limiting factor in their use in concrete applications where high consistency and relatively low w/c ratios are specified. Nevertheless adequate concrete incorporating MFA as sole fine aggregate can be made.

ii. An increase in fines content, MBV, SE, un-compacted voids content and flow time (measured using NZFC) generally resulted in an increased water/admixture demand.

iii. Water reducing admixtures can be used to counteract the increase in water demand caused by the higher angularity of MFA. However, if the sand is contaminated with clay, admixture effectiveness may be limited to fines contents below 3%.

iv. The slump test alone did not describe the workability of fresh MFA concrete. Thus, visual observations regarding the workability parameters e.g. handling, finishability and cohesiveness should be made during mixing or a rheometer

that measures yield stress and viscosity of concrete should be employed along with the slump test.

v. MFA gradings containing 5-7 % fines were optimal for aiding the handling, placing and finishing of MFA concrete, provided that the fines were free from clay particles. However, the optimal fines content depends on the particular fine aggregate properties and concrete mix composition.

vi. At the same w/c ratio, compressive and flexural strengths of MFA concretes are higher than that of their natural sand counterparts.

vii. The presence of illite or montmorillonite-chlorite clay and correspondingly high MBV values did not affect the 28 day strength of concrete at the same w/c ratio. Therefore there is a potential for clay containing aggregates to be used in concrete that were previously discouraged.

viii. The shape, texture and grading of MFA influenced the compressive strength of concrete as shown by SE and NZFC tests.

ix. An optimum SE value around 60 was observed at which the highest compressive strength was achieved. This was due to the proportion of clay-sized particles in the fine aggregate.

x. MFAs with un-compacted voids contents in the range of 43 – 45% and flow times in the range of 23 to 25 seconds produced the highest compressive strengths. Thus, there is an optimum grading for a particular particle shape and texture that results in the highest compressive strength that can be evaluated using the NZFC test.

xi. No significant trend of fines content and concrete compressive strength was observed in Stage I and Stage II mixes in the 1 to 9% fines content range that was investigated. Thus, in order to maximise the efficient use of materials,

higher fines content MFA gradings should be employed when compressive strength is the control property.

c) Develop a model which predicts compressive strength and consistency of MFA concrete mix.

Artificial neural network (ANN) models were developed that predict 28-day compressive strength and slump values of MFA concrete with a prediction error for test data of 2.6 N/mm^2 and 8 mm respectively. The predictions were based on the fine aggregate characterisation results from Chapter 3 and the concrete mix properties from Chapter 4.

i. The ANN models developed were accurate and were able to generalize within the range of data and input variables they were trained with.

ii. ANN models can be used to compare and analyse properties of concrete that is made with different MFA using their physical characteristics. This allows the selection of appropriate mix proportions for intended applications and reduction in the number of required concrete laboratory trials.

d) Identify and evaluate the feasibility of a geo-environmental application of waste rock filler.

Soil liming was identified as a feasible application for rock fillers generated during the quarry dust reprocessing. Rock fillers were characterised using a range of tests and tested for their potential for soil pH increase in a soil incubation study.

i. Soil liming with rock fillers containing calcium and magnesium carbonates, with high NV (above 40% CaO equivalent) and with the majority of particles smaller than 127 μm is feasible and effective. At 20 t/ha dosage at 28 days these rock fillers increased the soil pH by 0.65 and 0.92 units.

ii. Rock fillers of silicate origin can increase the soil pH even when their NV is as low as 6%. Silicate rock fillers at 20 t/ha dosage at 28 days had increased the soil pH by between 0.19 and 0.25 units. The effectiveness will be highly dependent on their chemical composition and fineness but generally a higher dosage will be required to achieve the same performance results when compared to agricultural lime.

iii. When dealing with silicate rocks, soil incubation results would yield more accurate predictions for field performance than just NV, particle size distribution and reactivity testing.

The work has shown that reprocessing of surplus quarry dust yields a fine aggregate that is suitable for use in concrete applications without blending with marine dredged sand and exhibits better compressive strength properties. The negative effects on water demand due to shape and the potential presence of clays can be counteracted by use of admixtures and selection of appropriate mix composition and MFA grading. Furthermore, the developed ANN models provide an opportunity to evaluate the MFA performance based on their physical properties and select an appropriate mix design reducing the number of laboratory trials required. Therefore, previously discouraged aggregate sources could potentially be used to diversify supply, increase the sustainability of quarrying and the construction industry and provide fine aggregates in locations where natural sand is scarce or depleted. Further economic and sustainability benefits could be gained through the utilisation of waste rock filler, which is generated during the quarry dust reprocessing, as a liming material.

7.2 Suggestions for future work

In this study MFA concretes were made using one type and content of cement, thus further investigation which would focus on MFA concrete properties with different types and contents of cements and cement replacement materials is necessary. This would show whether the observed trends for MFA hold true at different cement contents and types. Furthermore, such work should examine whether the higher fines contents of MFA are beneficial to the fresh and hardened properties of concrete at lower cement contents as observed by Kronlöf (1994) and Quiroga et al. (2006).

Concrete durability issues were not covered in this work, however, these typically are the cause for the necessity of repair works on concrete structures that result in high costs in terms of money, time and resources. In the thesis it has been shown that some clays do not affect the 28-day compressive strength, however, some researchers have observed an increase in drying shrinkage and permeability due to clays or high fines content in the fine aggregate (Norvell et al. 2007, Kenai et al. 2008). This can lead to shrinkage cracks and potentially corrosion of reinforcing steel. Therefore, a study which would concentrate on the effects of MFA on concrete shrinkage, permeability and other durability parameters would add to the knowledge about the MFA performance.

Noting the higher angularity and fines content when compared with marine dredged sand there could be potential concrete applications where maximum benefit of these properties could be observed. The angular and equi-dimensional shape could provide an improvement to the compressive strength and could be considered for use in high strength concrete. Furthermore, the combination of angularity and higher fines could prove to be beneficial in pumped and self-compacting concretes where the cohesion of the mix is of importance.

The concept of using fine aggregate parameters along with w/c ratio and plasticiser dosage for predictions of concrete 28 day compressive strength and consistency with ANN models was proved. The developed models did not account for other variations in mix composition, type of admixture and properties of coarse aggregates as these were constant in the study. Thus, the next step in improving the models is acquiring a dataset which includes all mixture composition parameters, different admixture types, coarse and fine aggregate parameters and covers a range of consistency and compressive strength results. ANN models trained and validated with this dataset could be used to investigate performance of MFAs in concrete based just on the aggregate properties. These models could then serve as tools for selecting optimal mixture composition for any given MFA and concrete application reducing the need for extensive laboratory trials.

In this thesis, soil liming was identified and investigated as a potential application for the rock filler created during the sand manufacturing process. For this particular application there is a need to conduct field trials as well as to look at other effects of the rock filler on soil properties that could potentially be detrimental to crop growth, animal and human health. The most important effect could be the leeching of heavy metals if they are present in the rock into the groundwater or their uptake by plants and animals and consequently humans. Also other areas of application of the rock fillers, for example, pelletizing and using as decorative elements for landscaping or as an aggregate for non-structural concrete applications should be investigated as not all rock fillers will have a liming potential.

References

Ahn, N. and Fowler, D.W. 2001. *An Experimental Study On The Guidelines For Using Higher Contents Of Aggregate Microfines In Portland Cement Concrete*. Austin, USA: International Centre For Aggregate Research. Research Report No. ICAR 102-1F.

Ahn, N., Phelan, T., Fowler, D.W. and Hudson, B. 2001. The Effects of High Fines on the Properties of Cement Mortar and Concrete. In: *International Center for Aggregates Research (ICAR) 9th Annual Symposium*. Austin, USA.

Alhozaimy, A.M. 2009. Effect of absorption of limestone aggregates on strength and slump loss of concrete. *Cement and Concrete Composites* 31(7), pp. 470–473.

Alshihri, M.M., Azmy, A.M. and El-Bisy, M.S. 2009. Neural networks for predicting compressive strength of structural light weight concrete. *Construction and Building Materials* 23(6), pp. 2214–2219.

American Association of State Highway and Transportation Officials. 2006. AASHTO TP57 Methylene Blue Value for Clays, Miner al Filler, and Fines.

American Concrete Institute and Committee 211 1997. *Standard practice for selecting proportions for normal, heavyweight, and mass concrete*. Detroit, Mich.: American Concrete Institute.

American Society for Testing and Materials. 2003. ASTM C 33 Standard Specification for Concrete Aggregates.

American Society for Testing and Materials. ASTM WK36804 Test Method for Rapid Determination of the Methylene Blue Value for Fine Aggregate and Mineral Filler

Al-Ansari, N.A., Mohammed, M.H., Pusch, R. and Knutsson, S. 2012. Optimization of Concrete by Minimizing Void Volume in Aggregate Mixture System. *Journal of Advanced Science and Engineering Research* 2(3), pp. 208–222.

Barral Silva, M.T., Silva Hermo, B., García-Rodeja, E. and Vázquez Freire, N. 2005. Reutilization of granite powder as an amendment and fertilizer for acid soils. *Chemosphere* 61(7), pp. 993–1002.

Bartlett, R. and James, B. 1980. Studying Dried, Stored Soil Samples — Some Pitfalls. *Soil Sci. Soc. Am. J.* 44(4), pp. 721–724.

BGS 2006. Mineral Planning Factsheet: Dolomite [Online]. Available at: http://www.bgs.ac.uk/downloads/start.cfm?id=1360 [Accessed: 14 August 2013].

BGS 2006. Mineral Planning Factsheet: Limestone [Online]. Available at: http://www.bgs.ac.uk/downloads/start.cfm?id=1361 [Accessed: 14 August 2013].

Bide, T., Brown, T.J. and Hobbs, S.F. 2013. *United Kingdom Minerals Yearbook 2012*. Keyworth, Nottingham: British Geological Survey.

British Standards Institution. 2000. BS EN 206-1: 2000 Concrete – Part 1: Specification, performance, production and conformity.

British Standards Institution. 1997. BS EN 933-1:1997 Determination of particle size distribution - sieving method.

British Standards Institution. 2001. BS EN 933-6:2001 Assessment of surface characteristics - flow coefficient of aggregates.

British Standards Institution. 2001. BS EN 933-6:2001 Assessment of surface characteristics - flow coefficient of aggregates.

British Standards Institution. 2004. BS EN 1992-1-1:2004 Eurocode 2: Design of concrete structures. General rules and rules for buildings.

British Standards Institution. 1999. BS EN 933-8:1999 Assessment of fines - sand equivalent test.

British Standards Institution. 1999. BS EN 933-9:1999 Assessment of fines - methylene blue test.

British Standards Institution. 2000. BS EN 934-2: 2001Admixtures for concrete, mortar and grout – Part 2: Concrete admixtures – Definitions, requirements, conformity, marking and labelling.

British Standards Institution. 2002.BS EN 1008:2002 Mixing water for concrete — Specification for sampling, testing and assessing the suitability of water, including water recovered from processes in the concrete industry, as mixing water for concrete.

British Standards Institution. 2000. BS EN 1097-6:2000 Determination of particle density and water absorption.

British Standards Institution. 2005. BS ISO 10390:2005 Soil quality – Determination of pH.

British Standards Institution. 2009. BS EN 12350-2:2009 Testing fresh concrete Part 2: Slump-test.

British Standards Institution. 2009. BS EN 12350-6:2009 Testing fresh concrete Part 6: Density.

British Standards Institution. 2009. BS EN 12350-7:2009 Testing fresh concrete Part 7: Air content – Pressure methods.

British Standards Institution. 2008. BS EN 12620:2002 + A1: 2008 Aggregates for concrete.

British Standards Institution. 2009. BS EN 12390-2:2009 Testing hardened concrete Part 2: Making and curing specimens for strength tests.

British Standards Institution. 2009. BS EN 12390-3:2009 Testing hardened concrete Part 3: Compressive strength of test specimens.

British Standards Institution. 2009. BS EN 12390-5:2009 Testing hardened concrete Part 5: Flexural strength of test specimens.

British Standards Institution. 2008. BS EN 12945:2008 Liming materials – Determination of neutralizing value – Titrimetric methods.

British Standards Institution. 2008. BS EN 13971:2008 Carbonate liming materials – Determination of reactivity – Potentometric titration method with hydrochloric acid.

British Standards Institution. 2006. BS EN 14984:2006 Liming materials – Determination of product effect on soil pH – Soil incubation method Annex B Determination of moisture at full soil water holding capacity

British Standards Institution. 2009. PD 6682-1:2009 Aggregates – Part 1: Aggregates for concrete – Guidance on the use of BS EN 12620.

Campbell, A. 2008. Soil Acidity and Liming [Online]. Available at: http://nzic.org.nz/ChemProcesses/soils/2C.pdf [Accessed: 18 August 2013].

Campbell, N.S. 2009. The Use of Rockdust and Composted Materials as Soil Fertility Amendments. PhD Thesis. Glasgow: University of Glasgow.

Carey, P., Ketterings, Q. and Hunter, M. 2006. Liming Materials, Fact Sheet #7 [Online]. Available at: http://nmsp.cals.cornell.edu/publications/factsheets/factsheet7.pdf [Accessed: 19 August 2013].

Celik, T. and Marar, K. 1996. Effects of crushed stone dust on some properties of concrete. *Cement and Concrete research* 26(7), pp. 1121–1130.

Cepuritis, R., Wigum, B.J., Garboczi, E.J., Mørtsell, E., Jacobsen, S. 2014. Filler from crushed aggregate for concrete: pore structure, specific surface, particle shape and size distribution. *Cement & Concrete Composites.* Article in press

Chae, G.-T., Yun, S.-T., Kwon, M.-J., Kim, Y.-S. and Mayer, B. 2006. Batch dissolution of granite and biotite in water: implication for fluorine geochemistry in groundwater. *Geochemical Journal* 40(1), pp. 95–102.

Chou, L. and Wollast, R. 1985. Steady-state kinetics and dissolution mechanisms of albite. *Am. J. Sci* 285(10), pp. 963–993.

Cibenko, G. 1989. Approximation by Superpositions of a Sigmoidal Function. *Math. Control Signals Systems* 2, pp. 303-314.

Coroneos, C., Hinsinger, P. and Gilkes, R.J. 1995. Granite powder as a source of potassium for plants: a glasshouse bioassay comparing two pasture species. *Fertilizer Research* 45(2), pp. 143–152.

Cortes, D.D., Kim, H.K., Palomino, A.M. and Santamarina, J.C. 2008. Rheological and mechanical properties of mortars prepared with natural and manufactured sands. *Cement and Concrete Research* 38(10), pp. 1142–1147.

Crozier, C. and Hardy, H.D. 2003. SoilFacts: Soil Acidity and Liming for Agricultural Soils [Online]. Available at: http://www.soil.ncsu.edu/publications/Soilfacts/AGW-439-50/SoilAcidity_12-3.pdf [Accessed: 14 August 2013].

Donza, H., Cabrera, O. and Irassar, E.F. 2002. High-strength concrete with different fine aggregate. *Cement and Concrete Research* 32(11), pp. 1755–1761.

Duan, Z.H., Kou, S.C. and Poon, C.S. 2013. Prediction of compressive strength of recycled aggregate concrete using artificial neural networks. *Construction and Building Materials* 40, pp. 1200–1206.

Duan, Z.H., Kou, S.C. and Poon, C.S. 2013. Using artificial neural networks for predicting the elastic modulus of recycled aggregate concrete. *Construction and Building Materials* 44, pp. 524–532.

Dumitru, I., Zdrilic, T. and Smorchevsky, G. 1999. The Use of Manufactured Quarry Fines in Concrete. In: *Proceedings of the 7th Annual ICAR Symposium*. Austin, USA.

Earley, J.W. and Milne, I.H. 1955. Regularly interstratified Montmorillonite-Chlorite in Basalt. *Clays and Clay Minerals* 4, pp. 381–384.

ERMCO 2013. Ready-mixed concrete industry statistics Year 2012 [Online]. Available at: http://www.ermco.eu/documents/ermco-documents/ermco-statistics-2012_final.pdf [Accessed: 15 September 2013].

Fausett, L.V. 1994. *Fundamentals of neural networks: architectures, algorithms, and applications*. Englewood Cliffs, NJ: Prentice-Hall.

FÉDÉRATION INTERNATIONALE DU BÉTON (fib). 2013. *Code-type models for structural behaviour of concrete: Background of the constitutive relations and material models in the fib Model Code for Concrete Structures 2010*. Lausanne, International Federation for Structural Concrete fib.

Fernandes, V.A., Purnell, P., Still, G.T. and Thomas, T.H. 2007. The effect of clay content in sands used for cementitious materials in developing countries. *Cement and Concrete Research* 37(5), pp. 751–758.

Ferraris, C.F. 1995. Alkali-silica reaction and high performance concrete [Online]. Available at: http://fire.nist.gov/bfrlpubs/build95/PDF/b95004.pdf [Accessed: 15 September 2013].

Gillman, G.P. 1980. The Effect of Crushed Basalt Scoria on the Cation Exchange Properties of a Highly Weathered Soil. *Soil Science Society of America Journal* 44(3), pp. 465-468.

Gillman, G.P., Burkett, D.C. and Coventry, R.J. 2002. Amending highly weathered soils with finely ground basalt rock. *Applied geochemistry* 17(8), pp. 987–1001.

Goldsworthy, S. 2005. Manufactured Sands in Portland Cement Concrete—The New Zealand Experience. In: *Proceedings of the 13th Annual ICAR Symposium*. Austin, USA.

Gonçalves, J.P., Tavares, L.M., Toledo Filho, R.D., Fairbairn, E.M.R. and Cunha, E.R. 2007. Comparison of natural and manufactured fine aggregates in cement mortars. *Cement and Concrete Research* 37(6), pp. 924–932.

Grant, W.H. 1969. Abrasion pH, an index of chemical weathering. *Clays and Clay Minerals* 17, pp. 151–155.

Grdić, Z., Topličić-Ćurčić, G., Stojić, N. 2010. Concrete aggregate and cement mass content effects on compressive strength. Facta universitatis - series: Architecture and Civil Engineering 8(4), pp. 413-423.

Harley, A.D. and Gilkes, R.J. 2000. Factors influencing the release of plant nutrient elements from silicate rock powders: a geochemical overview. *Nutrient Cycling in Agroecosystems* 56(1), pp. 11–36.

Harrison, D.J., Wilson, D., Henney, P.J. and Hudson, J.M. 2000. *Crushed Rock Sand In South Wales, A Reconnaissance Survey*. Nottingham, UK: British Geological Survey. Technical Report No. WF/00/3.

Hede, A.R., Skovmand, B. and López-Cesati, J. 2001. Acid Soils and Aluminum Toxicity. In: *Application of physiology in wheat breeding*. Mexixo: CIMMYT.

Highley, D.E., Hetherington, L.E., Brown, T.J., Harrison, D.J. and Jenkins, G.O. 2007. *The strategic importance of the marine aggregate industry to the UK*. British Geological Survey, Research Report No. OR/07/019.

Hill, T. 2006. *Statistics: methods and applications: a comprehensive reference for science, industry, and data mining*. Tulsa, OK: StatSoft.

Hinsinger, P., Bolland, M.D.A. and Gilkes, R.J. 1995. Silicate rock powder: effect on selected chemical properties of a range of soils from Western Australia and on plant growth as assessed in a glasshouse experiment. *Fertilizer Research* 45(1), pp. 69–79.

Huang, W.H. and Keller, W.D. 1971. Dissolution of Clay Minerals in Dilute Organic Acids at Room Temperature. *The American Mineralogist* 56(May-June), pp. 1082–1095.

Hudson, B. 1997. Manufactured Sand for Concrete. *The Indian concrete journal* 71(5), pp. 237–240.

Hudson, B. 1997. Manufactured Sand For Concrete. In: *Proceedings of the 5th Annual ICAR Symposium*. Austin, USA.

Jackson, N.M. and Brown, R.H. 1996. Use of higher fines contents in portland cement concrete. In: *Proceedings of the 4th Annual ICAR Symposium*.

Jacobs, L. 2008. *Micronutrients Needed by Crops.* MWEA Biosolids Conference, Bay City, Michigan.

Jadid, M.N. and Fairbairn, D.R. 1996. Neural-network applications in predicting moment-curvature parameters from experimental data. *Engineering Applications of Artificial Intelligence* 9(3), pp. 309–319.

Jones, M.R., Zheng, L. and Newlands, M.D. 2003. Estimation of the filler content required to minimise voids ratio in concrete. *Magazine of Concrete Research* 55(2), pp. 193-202.

Joudi-Bahri, I., Lecomte, A., Ouezdou, M.B. and Achour, T. 2012. Use of limestone sands and fillers in concrete without superplasticiser. *Cement and Concrete Composites* 34(6), pp. 771–780.

Kaya, T., Hashimoto, M. and Pettingell, H. 2009. The development of sand manufacture from crushed rock in Japan, using advanced VSI technology. In: *Proceedings of the 17th Annual ICAR Symposium*. Austin, USA.

Kenai, S., Menadi, B., Attar, A. and Khatib, J. 2008. Effect of Crushed Limestone Fines on Strength of Mortar and Durability of Concrete. In: *Proceedings of International Conference on Construction and Building Technology 2008*. Kuala Lumpur, Malaysia.

Kleiv, R.A. and Thornhill, M. 2007. Production of mechanically activated rock flour fertilizer by high intensive ultrafine grinding. *Minerals Engineering* 20(4), pp. 334–341.

Koehler, P.E., Jeknavorian, A., Chun, B. and Zhou, P. 2009. Ensuring Concrete Performance for Various Aggregates. In: *Proceedings of the 17th Annual ICAR Symposium*. Austin, USA.

Korjakins, A., Gaidukovs, S., Sahmenko, G., Bajare, D. and Pizele, D. 2008. Investigation of alternative dolomite filler properties and their application in concrete production.pdf. *Construction Sscience* 9, pp. 64–71.

Krauskopf, K.B. 1956. Dissolution and precipitation of silica at low temperatures. *Geochimica et Cosmochimica Acta* 10(1-2), pp. 1–26.

Kroh, T. 2010. Use of Manufactured Sand as a Replacement Material for dredged Sand in Mortar. MSc Dissertation. Cardiff University.

Kronlöf, A. 1994. Effect of very fine aggregate on concrete strength. *Materials and Structures* 27(1), pp. 15–25.

De Larrard, F. and Sedran, T. 2008. *BetonlabPro Logiciel de formulation des bétons*. France: LCPC.

De Larrard, F. and Sedran, T. 2002. Mixture-proportioning of high-performance concrete. *Cement and Concrete Research* 32(11), pp. 1699–1704.

LCPC 2004. *Essai de compacité des fractions granulaires à la table à secousses: mode opératoire.* (Compaction test for granular fractions using shaking table: operational manual) Paris: Laboratoire central des ponts et chaussées.

Li, B., Ke, G. and Zhou, M. 2011. Influence of manufactured sand characteristics on strength and abrasion resistance of pavement cement concrete. *Construction and Building Materials* 25(10), pp. 3849–3853. Available at: [Accessed: 12 September 2013].

Li, B., Wang, J. and Zhou, M. 2009. Effect of limestone fines content in manufactured sand on durability of low- and high-strength concretes. *Construction and Building Materials* 23, pp. 2846–2850.

Li, B., Zhou, M. and Wang, J. 2011. Effect of the Methylene Blue Value of Manufactured Sand on Performances of Concrete. *Journal of Advanced Concrete Technology* 9(2), pp. 127–132.

Lo, T.Y., Cui, H.Z., Tang, W.C. and Leung, W.M. 2008. The effect of aggregate absorption on pore area at interfacial zone of lightweight concrete. *Construction and Building Materials* 22(4), pp. 623–628.

Lusty, A. 2008. Sand industry leads revival of Japanese aggregates. *Quarry*, pp. 90–92.

Mangulkar, M.N. and Jamkar, S.S. 2013. Review of Particle Packing Theories Used For Concrete Mix Proportioning. *International Journal Of Scientific & Engineering Research* 4(5), pp. 143–148.

Manning, D. 2004. *Exploitation and Use of Quarry Fines*. Mineral Solutions Ltd. Report No. 087/MIST2/DACM/01.

Marek, C.R. 1995. Importance of fine aggregate shape and grading on properties of concrete. In: *Proceedings of the 3rd Annual ICAR Symposium*. Austin, USA.

Marek, C.R. 1992. Realistic Specifications for Manufactured Sand. In: *Proceedings of Materials Performance*. Atlanta, Georgia, pp. 245–260.

Meddah, M.S., Zitouni, S. and Belāabes, S. 2010. Effect of content and particle size distribution of coarse aggregate on the compressive strength of concrete. *Construction and Building Materials* 24(4), pp. 505–512.

Mitchell, C. 2007. GoodQuarry Production Technology. [Online]. Available at: http://nora.nerc.ac.uk/15899/1/GoodQuarry_Production_Technology.pdf [Accessed: 20 March 2013].

Mitchell, C.J., Mitchell, P. and Pascoe, R.D. 2008. Quarry fines minimisation: can we really have 10mm aggregate with no fines? In: *Proceedings of the 14th Extractive industry geology conference.* Walton, Geoffrey: EIG Conferences, pp. 37–44.

Mohammed, M.H., Emborg, M., Pusch, R. and Knutsson, S. 2012. Packing Theory for Natural and Crushed Aggregate to Obtain the Best Mix of Aggregate: Research and Development. In: *International Conference on Civil and Construction Engineering, Stockholm, Sweden*.

Moreira, M., Fiesler, E. 1995. *Neural networks with adaptive learning rate and momentum terms.* IDIAP Report No. 95-04.

Mullins, G.L., Alley, M.M. and Phillips, S.B. 2009. Sources of Lime for Acid Soils in Virginia [Online]. Available at: http://pubs.ext.vt.edu/452/452-510/452-510.html [Accessed: 18 August 2013].

Neville, A. 1995. *Properties of concrete*. 4th and final ed. Harlow: Longman Group.

Newman, J. and Choo, B.S. eds. 2003. *Advanced concrete technology*. Amsterdam: Elsevier.

Ni, H.-G. and Wang, J.-Z. 2000. Prediction of compressive strength of concrete by neural networks. *Cement and Concrete Research* 30(8), pp. 1245–1250.

Nikolaides, A., Manthos, E. and Sarafidou, M. 2007. Sand equivalent and methylene blue value of aggregates for highway engineering. *Foundations of civil and environmental engineering* 10, pp. 111–121.

Norvell, J., Stewart, J., Juenger, M. and Fowler, D. 2007. Effects of clays and clay-sized particles on concrete. In: *International Center for Aggregates Research (ICAR) 15th Annual Symposium*. Austin, USA.

Öztaş, A., Pala, M., Özbay, E., Kanca, E., Çagˇlar, N. and Bhatti, M.A. 2006. Predicting the compressive strength and slump of high strength concrete using neural network. *Construction and Building Materials* 20(9), pp. 769–775.

Özturan, T. and Cecen, C. 1997. Effect of coarse aggregate type on mechanical properties of concretes with different strengths. *Cement and Concrete Research* 27(2), pp. 165–170.

Parichatprecha, R. and Nimityongskul, P. 2009. Analysis of durability of high performance concrete using artificial neural networks. *Construction and Building Materials* 23(2), pp. 910–917.

Poon, C.S., Shui, Z.H., Lam, L., Fok, H. and Kou, S.C. 2004. Influence of moisture states of natural and recycled aggregates on the slump and compressive strength of concrete. *Cement and Concrete Research* 34(1), pp. 31–36.

Popovics, S., Ujhelyi, J. 2008. Contribution to the Concrete Strength versus Water-Cement Ratio Relationship. *Journal of Materials in Civil Engineering*, 20(7), pp. 459–463.

Quiroga, P.N. 2003. The effect of the aggregates characteristics on the performance of Portland cement concrete. PhD Thesis. University of Texas at Austin.

Quiroga, P.N., Ahn, N. and David W. Fowler 2006. Concrete Mixtures with High Microfines. *ACI Materials Journal* 103(4), pp. 258–264.

Rached, M., De Moya, M. and Fowler, D. 2009. *Utilizing Aggregates Characteristics to Minimize Cement Content in Portland Cement Concrete*. Austin, USA: International Centre For Aggregate Research. Research Report No. ICAR 401.

Ritchie, G.S.P. and Dolling, P.J. 1985. The role of organic matter in soil acidification. *Soil Research* 23(4), pp. 569–576.

Siddique, R., Aggarwal, P. and Aggarwal, Y. 2011. Prediction of compressive strength of self-compacting concrete containing bottom ash using artificial neural networks. *Advances in Engineering Software* 42(10), pp. 780–786.

Silva, D.R.G., Marchi, G., Spehar, C.R., Guilherme, L.R.G., Rein, T.A., Soares, D.A. and Ávila, F.W. 2012. Characterization and nutrient release from silicate rocks and influence on chemical changes in soil. *Revista Brasileira de Ciência do Solo* 36(3), pp. 951–962.

Standards Association of New Zealand. 1986. NZS 3111-1986 Methods of test for water and aggregate for concrete.

Teychenne, D.C., Franklin, R.E., Erntroy, H.C. and Building Research Establishment 1997. *Design of normal concrete mixes*. Watford: Building Research Establishment.

Thomas, T., Dumitru, I., van Koeverden, M., West, G., Basford, G., Lucas G., James W., Kovacs, T., Clarke, P., Guirguis, S. 2008. *Manufactured Sand Abrasion resistance and effect of manufactured sand on concrete mortar*. Australia: Cement Concrete & Aggregates Australia.

Thomas, T., Dumitru, I., van Koeverden, M., West, G., Basford, G., Lucas G., James W., Kovacs, T., Clarke, P., Guirguis, S. 2007. *Manufactured Sand National test methods and specification values*. Australia: Cement Concrete & Aggregates Australia.

Topçu, B. and Uurlu, A. 2003. Effect of the use of mineral filler on the properties of concrete. *Cement and Concrete Research* 33(7), pp. 1071–1075.

Troug, E. 1946. Soil reaction influence on availability of plant nutrients. *Soil Science Society of America Proceedings* 11, pp. 305–308.

Uchikawa, H., Hanehara, S., Shirasaka, T. and Sawaki, D. 1992. Effect of admixture on hydration of cement, adsorptive behavior of admixture and fluidity and setting of fresh cement paste. *Cement and Concrete Research* 22(6), pp. 1115 – 1129.

USGS 2013. USGS - Minerals Information: Cement [Online]. Available at: http://minerals.usgs.gov/minerals/pubs/commodity/cement/#links [Accessed: 9 September 2013].

Wang, Y., Jin, Z., Liu, S., Yang, L. and Luo, S. 2013. Physical filling effect of aggregate micro fines in cement concrete. *Construction and Building Materials* 41, pp. 812–814.

Yeh, I.-C. 2007. Modeling slump flow of concrete using second-order regressions and artificial neural networks. *Cement and Concrete Composites* 29(6), pp. 474–480.

Zollinger, G., Sarkar, S. 2001. *Framework for development of a classification procedure for use of aggregate fines in concrete.* International Centre For Aggregate Research. Report No. ICAR 101-2 F.

Appendix A Sand images

Size	NS sand	G-A sand	B-A sand
1- 0.5 mm		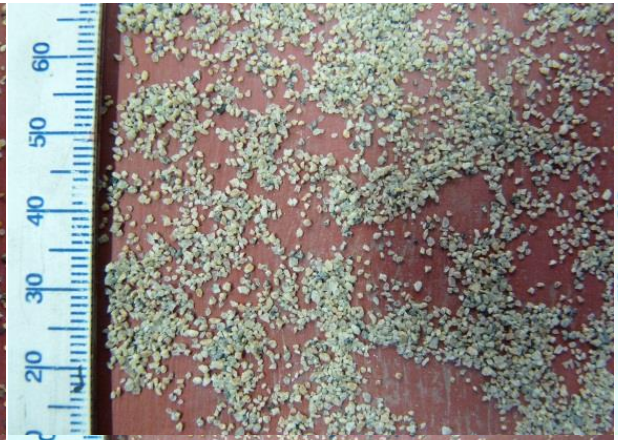	
0.5- 0.250mm	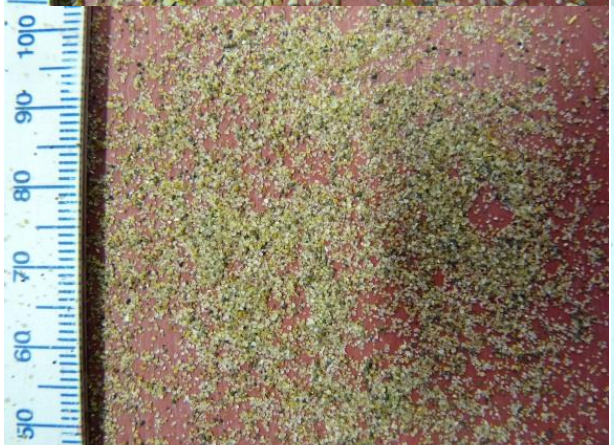	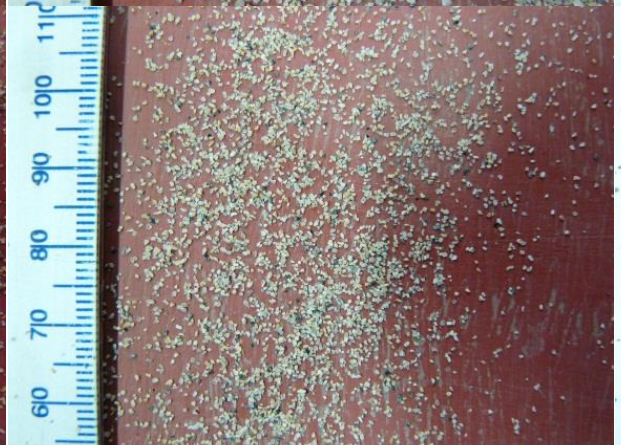	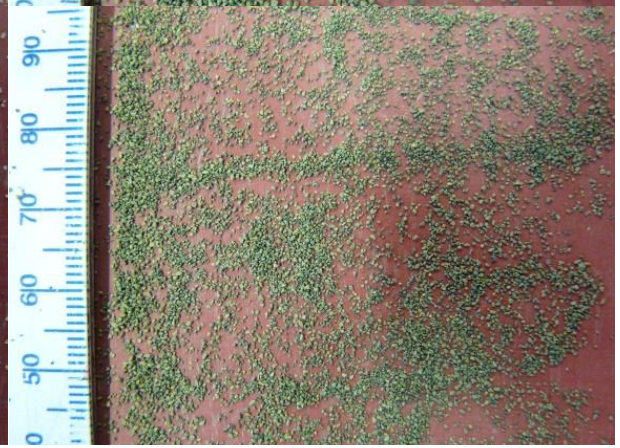

Size	NS sand	G-A sand	B-A sand
0.250-0.125mm	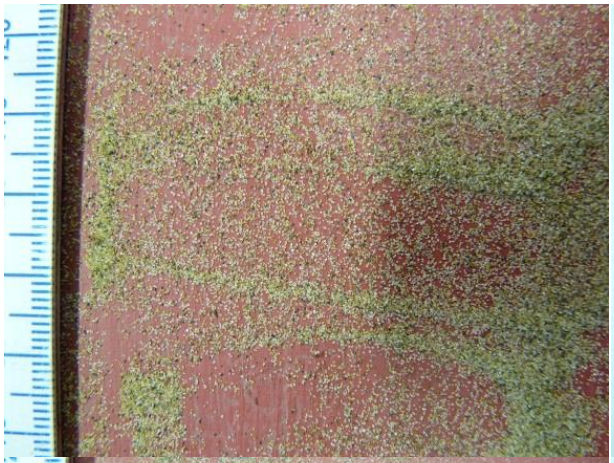	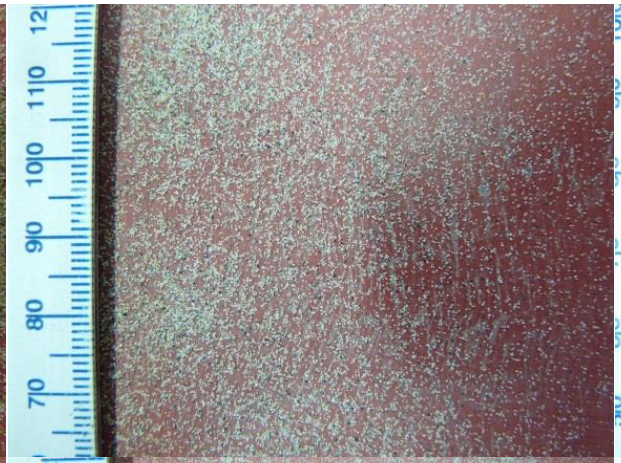	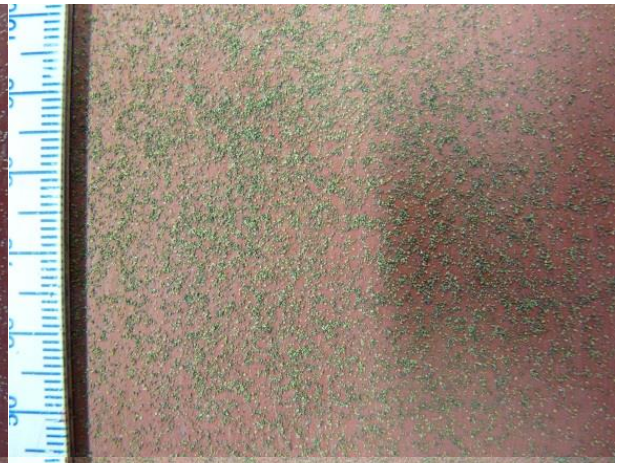
0.125 – 0.063mm	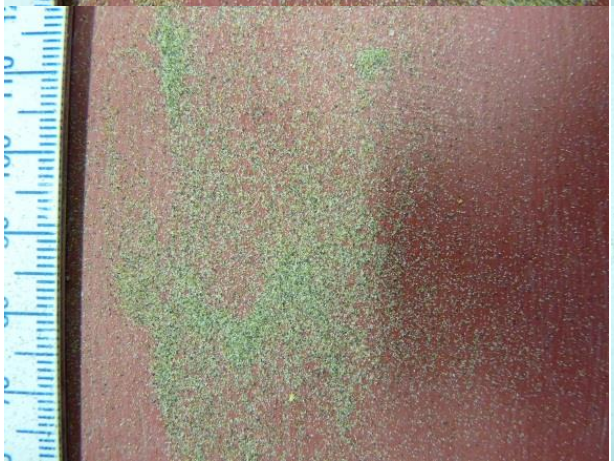	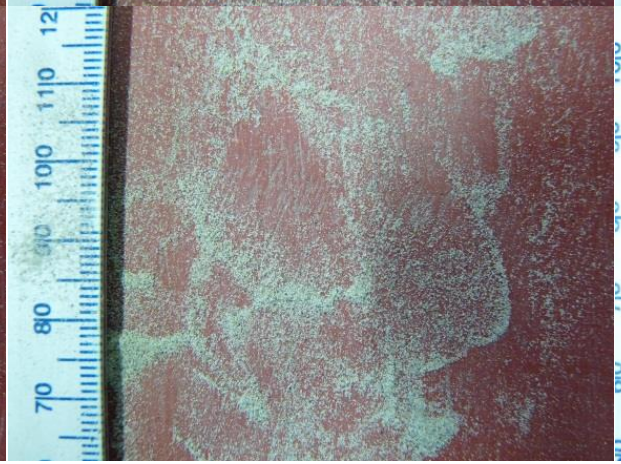	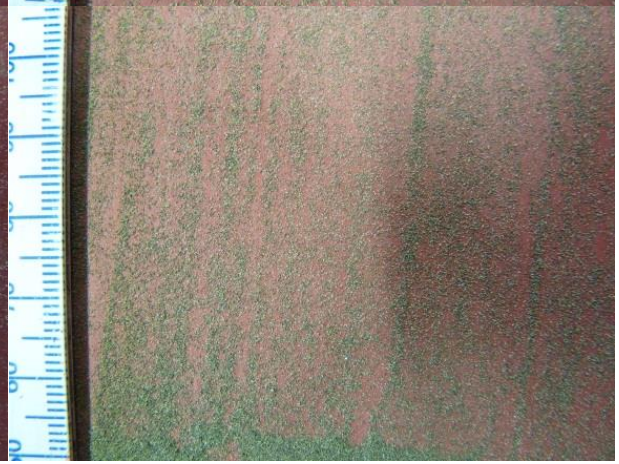

Appendix B Procedure for obtaining MFA sand gradings using production reports

The MFAs were supplied in separate bags with the V7 product and predusters (skimmers) along with a report of the manufacturing process. The proportions of a preduster or skimmer and V7 product, that have to be mixed in order to obtain the grading that was produced in the V7 plant, are determined based on the yield ratios of the plant. These are listed in the sand reports section "1) Test production flow" in table "d)". The sand reports are presented in the following pages of this appendix. Table A1 shows the notation used in the thesis, notation used in the reports and the notation of constituent materials for a particular sand grading.

Table A1 Notation of sands and constituent parts

Notation in thesis	Notation in sand reports	Constituents as coded in reports
G-A	V7-C	V7 product (before preduster) from Granite sands report
G-B	V7-CA	V7 product (before preduster) and PD-CA from Granite sands report
G-C	V7-CB	V7 product (before preduster) and PD-CB from Granite sands report
G-D	V7-CC	V7 product (before preduster) and PD-CC from Granite sands report
G-E	V7-CD	V7 product (before preduster) and PD-CD from Granite sands report
B-A	V7-C	V7 product (before preduster) from Basalt sands report
B-B	V7-CA	V7 product (before preduster) and PD-CA from Basalt sands report
B-C	V7-CB	V7 product (before preduster) and PD-CB from Basalt sands report
B-D	V7-CC	V7 product (before preduster) and PD-CC from Basalt sands report
GS-A	V7-C	V7 product (before Skimmer) from Gritstone sands report
GS-B	V7-CA	V7 product (before Skimmer) and SK-CA from Gritstone sands report
GS-C	V7-CB	V7 product (before Skimmer) and SK-CB from Gritstone sands report
GS-D	V7-CC	V7 product (before Skimmer) and SK-CC from Gritstone sands report
L-A	V7-C	V7 product (before Skimmer) from Limestone sands report
L-B	V7-CA	V7 product (before Skimmer) and SK-CA from Limestone sands

		report
L-C	V7-CB	V7 product (before Skimmer) and SK-CB from Limestone sands report
L-D	V7-CC	V7 product (before Skimmer) and SK-CC from Limestone sands report

For example, the G-C sand is obtained by mixing granite V7 product and PD-CB preduster. The yield ratios that are relevant in this case are the ones for V7-C of 66.9% and V7-CB of 81.9% taken from Granite sands report section 1) table d). Both of the components, the V7 product and the preduster, make up 100% of G-C sand. The percentage of preduster PD-CB in G-C sand is calculated as follows:

$$PD-CB,\% = \frac{(Yield\ ratio\ V7-CB)-(Yield\ ratio\ V7-C)}{Yield\ ratio\ V7-CB} \times 100 = \frac{81.9-66.9}{81.9} \times 100 = 18.31\%$$

The percentage of V7 product then is:

$$V7\ product,\% = (1-(PD-CB,\%)) \times 100 = (1-0.1831) \times 100 = 81.69\%$$

Then, the mass of each component to be mixed to obtain a known mass of G-C sand is determined by multiplying the percentage of each component with the required mass of G-C sand. Assuming the fine aggregate content of 753 kg/m^3 that was used in the concrete mixes, the required contents of each component at SSD conditions for G-C sand for 1 m^3 of concrete are:

$$PD-CB,kg = (D-CB,\%) \times 753 = 0.1831 \times 753 = 137.87kg$$

$$V7\ product,kg = (V7\ product,\%) \times 753 = 0.8169 \times 753 = 615.13\ kg$$

Granite sands report (G- series)

7. Test report for concrete

1) Test production flow.

a) Raw material
Granite Size : 6.7-0mm
Moisture content : 1.19%

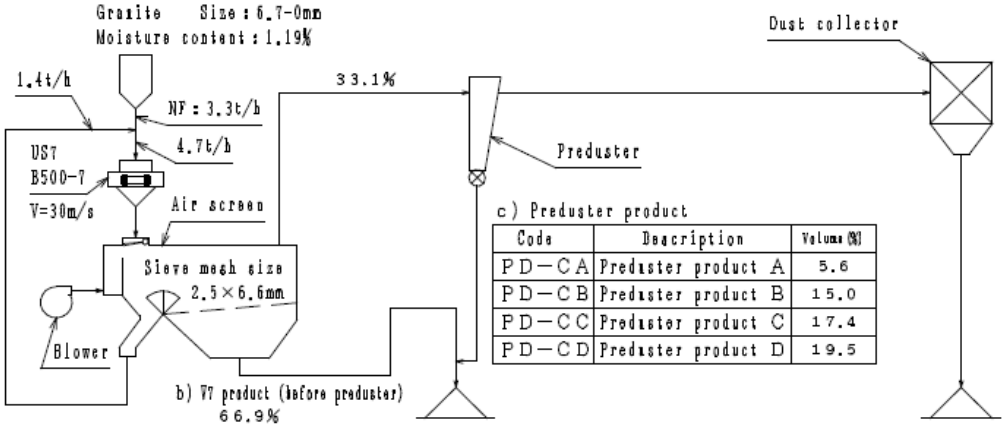

c) Preduster product

Code	Description	Volume (%)
PD−CA	Preduster product A	5.6
PD−CB	Preduster product B	15.0
PD−CC	Preduster product C	17.4
PD−CD	Preduster product D	19.5

Circulating load ratio
1.42

d) V7 product (with preduster product)

Code	Description	Yield ratio (%)
V7−C	V7 product (before preduster)	66.9
V7−CA	V7 product A (with PD-A)	72.5
V7−CB	V7 product B (with PD-B)	81.9
V7−CC	V7 product C (with PD-C)	84.3
V7−CD	V7 product D (with PD-CD)	86.4

e) Filler

Code	Description	Volume (%)
F−C	Filler	33.1
F−CA	Filler A	27.5
F−CB	Filler B	18.1
F−CC	Filler C	15.7
F−CD	Filler D	13.6

2) Grading

a) Raw material

Sieve size (mm)	Raw material	
	Retained (%)	Passed (%)
9.5～8	0.0	100.0
8～6.7	0.5	99.5
6.7～4	9.2	90.3
4～2	20.6	69.7
2～1	16.7	53.0
1～0.5	14.3	38.7
0.5～0.25	11.9	26.8
0.25～0.125	9.4	17.4
0.125～0.063	6.1	11.3
0.063～0	11.3	
total	100.0	

b) V7 product (before preduster)

Sieve size (mm)	V7−C : V7 product (before preduster)	
	Retained (%)	Passed (%)
9.5～8	0.0	100.0
8～6.7	0.0	100.0
6.7～4	0.0	100.0
4～2	11.6	88.4
2～1	26.8	61.6
1～0.5	25.9	35.7
0.5～0.25	20.4	15.3
0.25～0.125	11.3	4.0
0.125～0.063	2.1	1.9
0.063～0	1.9	
total	100.0	

c) Preduster product

Sieve size (mm)	PD−CA : Preduster product A		PD−CB : Preduster product B		PD−CC : Preduster product C		PD−CD : Preduster product D	
	Retained (%)	Passed (%)	Retained (%)	Passed (%)	Retained (%)	Passed (%)	Retained (%)	Passed (%)
6.7～4	0.0	100.0	0.0	100.0	0.0	100.0	0.0	100.0
4～2	0.2	99.8	0.3	99.7	0.4	99.6	0.5	99.5
2～1	2.5	97.3	2.0	97.7	1.5	98.1	1.1	98.4
1～0.5	5.3	92.0	4.2	93.5	3.6	94.5	3.0	95.4
0.5～0.25	11.1	80.9	9.3	84.2	8.2	86.3	7.2	88.2
0.25～0.125	31.8	49.1	28.6	55.6	26.1	60.2	23.9	64.3
0.125～0.063	35.2	13.9	34.4	21.2	34.0	26.2	33.5	30.8
0.063～0	13.9		21.2		26.2		30.8	
total	100.0		100.0		100.0		100.0	

d) V7 product (with preduster product)

Sieve size (mm)	V7−CA : V7 product A (with PD-CA)		V7−CB : V7 product B (with PD-CB)		V7−CC : V7 product B (with PD-CC)		V7−CD : V7 product C (with PD-CD)	
	Retained (%)	Passed (%)	Retained (%)	Passed (%)	Retained (%)	Passed (%)	Retained (%)	Passed (%)
6.7～4	0.0	100.0	0.0	100.0	0.0	100.0	0.0	100.0
4～2	10.7	89.3	9.5	90.5	9.3	90.7	9.1	90.9
2～1	24.9	64.4	22.3	68.2	21.5	69.2	20.9	70.0
1～0.5	24.3	40.1	21.9	46.3	21.3	47.9	20.8	49.2
0.5～0.25	19.7	20.4	18.4	27.9	17.9	30.0	17.4	31.8
0.25～0.125	12.9	7.5	14.5	13.4	14.4	15.6	14.2	17.6
0.125～0.063	4.7	2.8	8.0	5.4	8.7	6.9	9.2	8.4
0.063～0	2.8		5.4		6.9		8.4	
total	100.0		100.0		100.0		100.0	

Basalt sands report (B- series)

6. Test report for concrete

1) Test production flow.

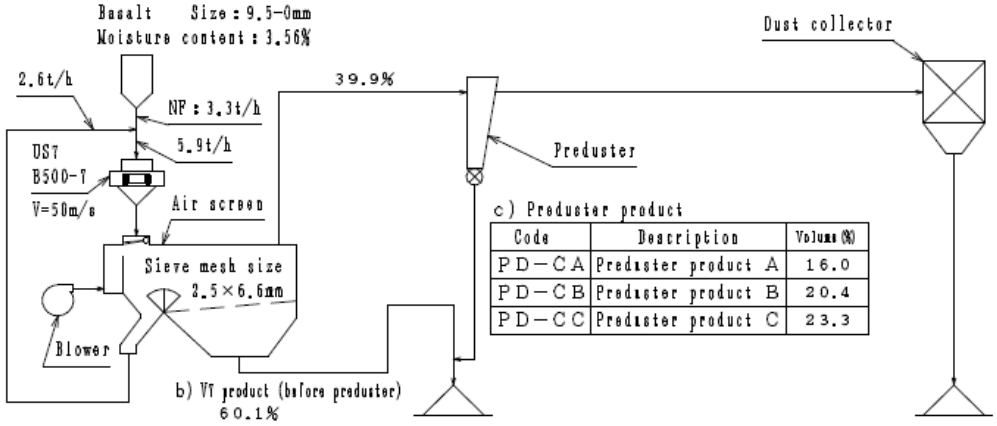

c) Preduster product

Code	Description	Volume (%)
PD−CA	Preduster product A	16.0
PD−CB	Preduster product B	20.4
PD−CC	Preduster product C	23.3

d) V7 product (with preduster product)

Code	Description	Yield ratio (%)
V7−C	V7 product (before preduster)	60.1
V7−CA	V7 product A (with PD-CA)	76.1
V7−CB	V7 product B (with PD-CB)	80.5
V7−CC	V7 product C (with PD-CC)	83.4

e) Filler

Code	Description	Volume (%)
F−C	Filler	39.9
F−CA	Filler A	23.9
F−CB	Filler B	19.5
F−CC	Filler C	16.6

Circulating load ratio
1.79

2) Grading

a) Raw material

Sieve size (mm)	Raw material	
	Retained (%)	Passed (%)
19～13.2	0.0	100.0
13.2～9.5	0.8	99.2
9.5～6.7	5.8	93.4
6.7～4	22.3	71.1
4～2	21.1	50.0
2～1	12.4	37.6
1～0.5	8.5	29.1
0.5～0.25	7.5	21.6
0.25～0.125	6.9	14.7
0.125～0.063	5.0	9.7
0.063～0	9.7	
total	100.0	

b) V7 product (before preduster)

Sieve size (mm)	V7−C : V7 product (before preduster)	
	Retained (%)	Passed (%)
19～13.2	0.0	100.0
13.2～9.5	0.0	100.0
9.5～6.7	0.0	100.0
6.7～4	0.0	100.0
4～2	11.7	88.3
2～1	29.1	59.2
1～0.5	22.8	36.4
0.5～0.25	18.0	18.4
0.25～0.125	12.0	6.4
0.125～0.063	2.7	3.7
0.063～0	3.7	
total	100.0	

c) Preduster product

Sieve size (mm)	PD−CA : Preduster product A		PD−CB : Preduster product B		PD−CC : Preduster product C	
	Retained (%)	Passed (%)	Retained (%)	Passed (%)	Retained (%)	Passed (%)
9.5～6.7	0.0	100.0	0.0	100.0	0.0	100.0
6.7～4	0.0	100.0	0.0	100.0	0.0	100.0
4～2	1.7	98.3	1.4	98.6	1.2	98.8
2～1	5.8	92.5	5.2	93.4	4.8	94.0
1～0.5	7.0	85.5	6.2	87.2	6.3	87.7
0.5～0.25	13.7	71.8	10.8	76.4	9.1	78.6
0.25～0.125	34.5	37.3	28.0	48.4	25.3	53.3
0.125～0.063	25.8	11.5	29.8	18.6	29.6	23.7
0.063～0	11.5		18.6		23.7	
total	100.0		100.0		100.0	

d) V7 product (with preduster product)

Sieve size (mm)	V7−CA : V7 product A (with PD-MA)		V7−CB : V7 product B (with PD-MB)		V7−CC : V7 product C (with PD-MC)	
	Retained (%)	Passed (%)	Retained (%)	Passed (%)	Retained (%)	Passed (%)
9.5～6.7	0.0	100.0	0.0	100.0	0.0	100.0
6.7～4	0.0	100.0	0.0	100.0	0.0	100.0
4～2	9.6	90.4	9.1	90.9	8.7	91.3
2～1	24.2	66.2	23.1	67.8	22.4	68.9
1～0.5	19.5	46.7	18.5	49.3	18.2	50.7
0.5～0.25	17.1	29.6	16.2	33.1	15.5	35.2
0.25～0.125	16.7	12.9	16.1	17.0	15.7	19.5
0.125～0.063	7.6	5.3	9.5	7.5	10.2	9.3
0.063～0	5.3		7.5		9.3	
total	100.0		100.0		100.0	

Limestone sands report (L- series)

7. Test report for concrete

1) Test production flow.

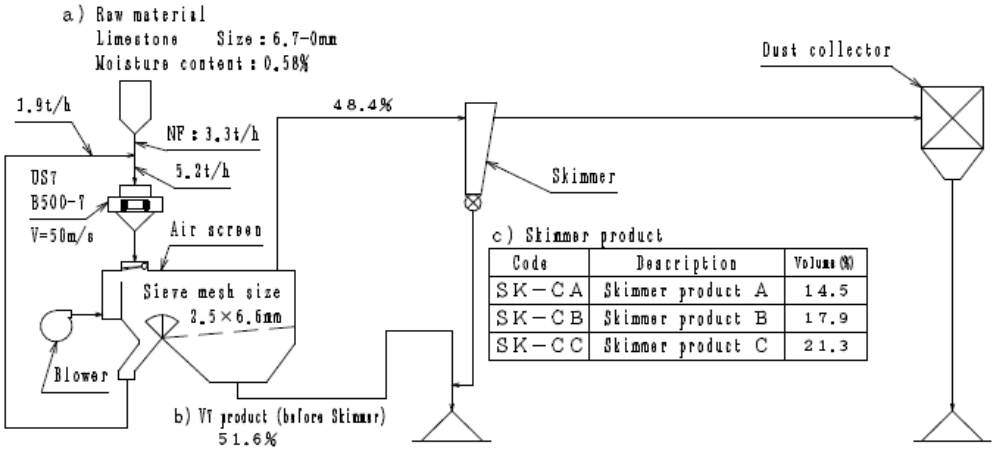

c) Skimmer product

Code	Description	Volume (%)
SK−CA	Skimmer product A	14.5
SK−CB	Skimmer product B	17.9
SK−CC	Skimmer product C	21.3

d) V7 product (with Skimmer product)

Code	Description	Yield ratio (%)
V7−C	V7 product (before Skimmer)	51.6
V7−CA	V7 product A (with SK-CA)	66.1
V7−CB	V7 product B (with SK-CB)	69.5
V7−CC	V7 product C (with SK-CC)	72.9

e) Filler

Code	Description	Volume (%)
F−C	Filler	48.4
F−CA	Filler A	33.9
F−CB	Filler B	30.5
F−CC	Filler C	27.1

Circulating load ratio
1.58

2) Grading

a) Raw material

Sieve size (mm)	Raw material	
	Retained (%)	Passed (%)
19～13.2	0.0	100.0
13.2～9.5	0.0	100.0
9.5～6.7	1.9	98.1
6.7～4	37.8	60.3
4～2	20.1	40.2
2～1	12.8	27.4
1～0.5	7.8	19.6
0.5～0.25	5.0	14.6
0.25～0.125	3.2	11.4
0.125～0.063	2.5	8.9
0.063～0	8.9	
total	100.0	

b) V7 product (before Skimmer)

Sieve size (mm)	V7−C : V7 product (before Skimmer)	
	Retained (%)	Passed (%)
19～13.2	0.0	100.0
13.2～9.5	0.0	100.0
9.5～6.7	0.0	100.0
6.7～4	0.0	100.0
4～2	20.0	80.0
2～1	32.3	47.7
1～0.5	21.0	26.7
0.5～0.25	12.5	14.2
0.25～0.125	7.8	6.4
0.125～0.063	3.6	2.8
0.063～0	2.8	
total	100.0	

c) Skimmer product

Sieve size (mm)	SK−CA : Skimmer product A		SK−CB : Skimmer product B		SK−CC : Skimmer product C	
	Retained (%)	Passed (%)	Retained (%)	Passed (%)	Retained (%)	Passed (%)
9.5～6.7	0.0	100.0	0.0	100.0	0.0	100.0
6.7～4	0.0	100.0	0.0	100.0	0.0	100.0
4～2	3.3	96.7	2.6	97.4	2.4	97.6
2～1	12.1	84.6	10.2	87.2	9.1	88.5
1～0.5	18.0	66.6	15.2	72.0	13.9	74.6
0.5～0.25	18.4	48.2	16.0	56.0	14.8	59.8
0.25～0.125	19.1	29.1	18.2	37.8	16.9	42.9
0.125～0.063	16.6	12.5	18.2	19.6	18.8	24.1
0.063～0	12.5		19.6		24.1	
total	100.0		100.0		100.0	

d) V7 product (with Skimmer product)

Sieve size (mm)	V7−CA : V7 product A (with SK-CA)		V7−CB : V7 product B (with SK-CB)		V7−CC : V7 product C (with SK-CC)	
	Retained (%)	Passed (%)	Retained (%)	Passed (%)	Retained (%)	Passed (%)
9.5～6.7	0.0	100.0	0.0	100.0	0.0	100.0
6.7～4	0.0	100.0	0.0	100.0	0.0	100.0
4～2	16.3	83.7	15.5	84.5	14.8	85.2
2～1	27.9	55.8	26.6	57.9	25.6	59.6
1～0.5	20.4	35.4	19.6	38.3	18.9	40.7
0.5～0.25	13.7	21.7	13.3	25.0	13.2	27.5
0.25～0.125	10.3	11.4	10.5	14.5	10.5	17.0
0.125～0.063	6.5	4.9	7.4	7.1	8.0	9.0
0.063～0	4.9		7.1		9.0	
total	100.0		100.0		100.0	

Gritstone sands report (GS- series)

7. Test report for concrete

1) Test production flow.

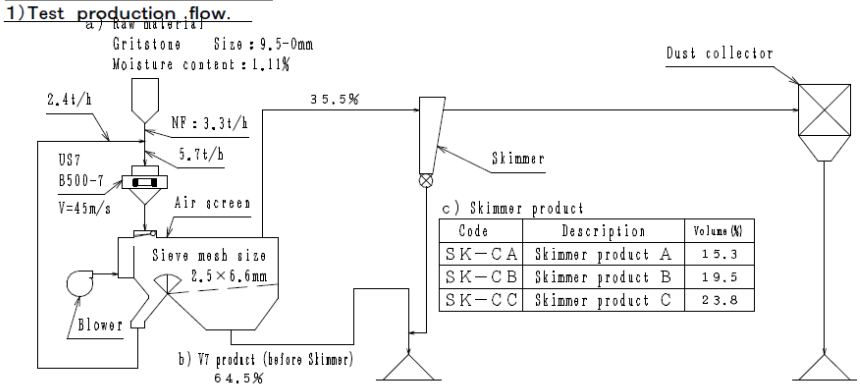

c) Skimmer product

Code	Description	Volume (%)
SK－CA	Skimmer product A	15.3
SK－CB	Skimmer product B	19.5
SK－CC	Skimmer product C	23.8

d) V7 product (with Skimmer product)

Code	Description	Yield ratio (%)
V7－C	V7 product (before Skimmer)	64.5
V7－CA	V7 product A (with SK-CA)	79.8
V7－CB	V7 product B (with SK-CB)	84.0
V7－CC	V7 product C (with SK-CC)	88.3

e) Filler

Code	Description	Volume (%)
F－C	Filler	35.5
F－CA	Filler A	20.2
F－CB	Filler B	16.0
F－CC	Filler C	11.7

Circulating load ratio
1.73

2) Grading

a) Raw material

Sieve size (mm)	Raw material	
	Retained (%)	Passed (%)
19～13.2	0.0	100.0
13.2～9.5	0.0	100.0
9.5～6.7	5.9	94.1
6.7～4	74.4	19.7
4～2	11.6	8.1
2～1	1.2	6.9
1～0.5	0.6	6.3
0.5～0.25	0.6	5.7
0.25～0.125	0.8	4.9
0.125～0.063	1.0	3.9
0.063～0	3.9	
total	100.0	

b) V7 product (before Skimmer)

Sieve size (mm)	V7－C：V7 product (before Skimmer)	
	Retained (%)	Passed (%)
19～13.2	0.0	100.0
13.2～9.5	0.0	100.0
9.5～6.7	0.0	100.0
6.7～4	0.0	100.0
4～2	14.0	86.0
2～1	28.6	57.4
1～0.5	20.9	36.5
0.5～0.25	16.8	19.7
0.25～0.125	12.5	7.2
0.125～0.063	3.7	3.5
0.063～0	3.5	
total	100.0	

c) Skimmer product

Sieve size (mm)	SK－CA：Skimmer product A		SK－CB：Skimmer product B		SK－CC：Skimmer product C	
	Retained (%)	Passed (%)	Retained (%)	Passed (%)	Retained (%)	Passed (%)
9.5～6.7	0.0	100.0	0.0	100.0	0.0	100.0
6.7～4	0.0	100.0	0.0	100.0	0.0	100.0
4～2	1.2	98.8	0.9	99.1	0.0	100.0
2～1	5.4	93.4	2.6	96.5	0.7	99.3
1～0.5	9.3	84.1	6.6	89.9	4.9	94.4
0.5～0.25	15.7	68.4	12.9	77.0	10.7	83.7
0.25～0.125	31.7	36.7	29.1	47.9	27.1	56.6
0.125～0.063	25.4	11.3	29.4	18.5	32.6	24.0
0.063～0	11.3		18.5		24.0	
total	100.0		100.0		100.0	

d) V7 product (with Skimmer product)

Sieve size (mm)	V7－CA：V7 product A (with SK-CA)		V7－CB：V7 product B (with SK-CB)		V7－CC：V7 product C (with SK-CC)	
	Retained (%)	Passed (%)	Retained (%)	Passed (%)	Retained (%)	Passed (%)
9.5～6.7	0.0	100.0	0.0	100.0	0.0	100.0
6.7～4	0.0	100.0	0.0	100.0	0.0	100.0
4～2	11.5	88.5	10.9	89.1	10.2	89.8
2～1	24.2	64.3	22.6	66.5	21.1	68.7
1～0.5	18.7	45.6	17.6	48.9	16.6	52.1
0.5～0.25	16.6	29.0	15.9	33.0	15.2	36.9
0.25～0.125	16.1	12.9	16.3	16.7	16.4	20.5
0.125～0.063	7.9	5.0	9.7	7.0	11.5	9.0
0.063～0	5.0		7.0		9.0	
total	100.0		100.0		100.0	

Appendix C Concrete data

The notation used in mix sheets: CEM I is cement, CA is coarse aggregate, FA 1 is the V7 product, FA 2 is corresponding preduster or skimmer as explained in Appendix B.

Series I mix sheets

Date:	01/09/2011							
Mix:	NS Slump Series I							
Volume:	40 l	Aggregate moisture		Design figures				
Materials	Absorption capacity, %	Total, %	Free, %	SSD, kg/m³	Moisture correction, kg/m³	Corrected, kg/m³	Trial Target, kg	Trial Actual, kg
CEM I				350	0.00	350.00	14.00	14.00
CA	0.66	0.27	-0.39	1040.00	-4.06	1035.94	41.44	41.44
FA 1	1.04	1.25	0.21	753.00	1.58	754.58	30.18	30.18
FA 2								
Water				167.00		169.47	6.78	6.76
Plasticiser				0.00	0.00	0.00	0.00	0.00
			Totals	2310.00	-2.47	2310.00	92.40	92.38

	SSD	Actual
W/C ratio	0.477	0.476

Entrapped air, %	0.50
Plastic Density, kg/m³	2447.20

Slump Test	
Test	Value(mm)
1	100
2	90
Mean	95

Date:	08/09/2011							
Mix:	G-A Series I							
Volume:	40 l	Aggregate moisture		Design figures				
Materials	Absorption capacity, %	Total, %	Free, %	SSD, kg/m³	Moisture correction, kg/m³	Corrected, kg/m³	Trial Target, kg	Trial Actual, kg
CEM I				350.00	0.00	350.00	14.00	14.00
CA	0.66	1.00	0.34	1040.00	3.54	1043.54	41.74	41.74
FA 1	0.58	1.50	0.92	753.00	6.93	759.93	30.40	30.40
FA 2								
Water				202.00	0.00	191.54	7.66	7.66
Plasticiser				0.00	0.00	0.00	0.00	0.00
			Totals	2345.00	10.46	2345.00	93.80	93.80

	SSD	Actual
W/C ratio	0.577	0.577

Entrapped air, %	0.45
Plastic Density, kg/m³	2393.00

Slump Test	
Test	Value(mm)
1	100
2	140
Mean	120

Date:	31/08/2011							
Mix:	G-B Series I							
Volume:	40 l	Aggregate moisture		Design figures				
Materials	Absorption capacity, %	Total, %	Free, %	SSD, kg/m³	Moisture correction, kg/m³	Corrected, kg/m³	Trial Target, kg	Trial Actual, kg
CEM I				350.00	0.00	350.00	14.00	14.00
CA	0.66	0.27	-0.39	1040.00	-4.06	1035.94	41.44	41.44
FA 1	0.58	1.44	0.86	694.84	5.98	700.81	28.03	28.03
FA 2	0.58	3.58	3.00	58.16	1.74	59.91	2.40	2.40
Water				202.00		198.34	7.93	7.92
Plasticiser				0.00	0.00	0.00	0.00	0.00
			Totals	2345.00	3.66	2345.00	93.80	93.79

	SSD	Actual
W/C ratio	0.577	0.577

Entrapped air, %	1.60
Plastic Density, kg/m³	2375.50

Slump Test	
Test	Value(mm)
1	80
2	80
Mean	80

Date:	01/09/2011							
Mix:	G-C Series I							
Volume:	40 l	Aggregate moisture		Design figures				
Materials	Absorption capacity, %	Total, %	Free, %	SSD, kg/m³	Moisture correction, kg/m³	Corrected, kg/m³	Trial Target, kg	Trial Actual, kg
CEM I				350.00	0.00	350.00	14.00	14.00
CA	0.66	0.27	-0.39	1040.00	-4.06	1035.94	41.44	41.44
FA 1	0.58	1.44	0.86	615.09	5.29	620.38	24.82	24.82
FA 2	0.58	3.67	3.09	137.91	4.26	142.17	5.69	5.69
Water				202.00		196.50	7.86	7.86
Plasticiser				0.00	0.00	0.00	0.00	0.00
			Totals	2345.00	5.50	2345.00	93.80	93.80

	SSD	Actual
W/C ratio	0.577	0.578

Entrapped air, %	0.90
Plastic Density, kg/m³	2378.00

Slump Test	
Test	Value(mm)
1	80
2	80
Mean	80

Date:	07/09/2011							
Mix:	G-D Series I							
Volume:	40 l	Aggregate moisture		Design figures				
Materials	Absorption capacity, %	Total, %	Free, %	SSD, kg/m³	Moisture correction, kg/m³	Corrected, kg/m³	Trial Target, kg	Trial Actual, kg
CEM I				350.00	0.00	350.00	14.00	14.00
CA	0.66	0.73	0.07	1040.00	0.73	1040.73	41.63	41.63
FA 1	0.58	1.50	0.92	597.58	5.50	603.07	24.12	24.12
FA 2	0.58	3.48	2.90	155.42	4.51	159.93	6.40	6.40
Water				202.00		191.27	7.65	7.65
Plasticiser				0.00	0.00	0.00	0.00	0.00
			Totals	2345.00	10.73	2345.00	93.80	93.80

	SSD	Actual
W/C ratio	0.577	0.578

Entrapped air, %	0.65
Plastic Density, kg/m³	2393.50

Slump Test	
Test	Value(mm)
1	60
2	60
Mean	60

Date:	07/09/2011							
Mix:	G-E Series I							
Volume:	40 l	Aggregate moisture		Design figures				
Materials	Absorption capacity, %	Total, %	Free, %	SSD, kg/m³	Moisture correction, kg/m³	Corrected, kg/m³	Trial Target, kg	Trial Actual, kg
CEM I				350.00	0.00	350.00	14.00	14.00
CA	0.66	0.73	0.07	1040.00	0.73	1040.73	41.63	41.63
FA 1	0.58	1.50	0.92	583.05	5.36	588.42	23.54	23.54
FA 2	0.58	3.43	2.85	169.95	4.84	174.79	6.99	6.99
Water				202.00		191.06	7.64	7.64
Plasticiser				0.00	0.00	0.00	0.00	0.00
			Totals	2345.00	10.94	2345.00	93.80	93.80

	SSD	Actual
W/C ratio	0.577	0.577

Entrapped air, %	0.78
Plastic Density, kg/m³	2392.70

Slump Test	
Test	Value(mm)
1	60
2	60
Mean	60

Date:	26/07/2012							
Mix:	G-FEED Series I							
Volume:	10 l	Aggregate moisture		Design figures				
Materials	Absorption capacity, %	Total, %	Free, %	SSD, kg/m³	Moisture correction, kg/m³	Corrected, kg/m³	Trial Target, kg	Trial Actual, kg
CEM I				350.00	0.00	350.00	14.00	14.00
CA	0.66	0.44	-0.22	1040.00	-2.29	1037.71	10.38	10.38
FA 1	0.58	1.80	1.22	753.00	9.19	762.19	7.62	7.62
FA 2			0.00	0.00	0.00	0.00	0.00	0.00
Water				210.00		203.10	2.03	2.24
Plasticiser				0.00	0.00	0.00	0.00	0.00
			Totals	2353.00	6.90	2353.00	23.53	23.74

	SSD	Actual
W/C ratio	0.600	0.660

Entrapped air, %	-
Plastic Density, kg/m³	-

Slump Test	
Test	Value(mm)
1	80
2	80
Mean	80

Date:	24/08/2011							
Mix:	B-A Series I							
Volume:	40 l	Aggregate moisture		Design figures				
Materials	Absorption capacity, %	Total, %	Free, %	SSD, kg/m³	Moisture correction, kg/m³	Corrected, kg/m³	Trial Target, kg	Trial Actual, kg
CEM I				350.00	0.00	350.00	14.00	14.00
CA	0.66	0.55	-0.11	1040.00	-1.14	1038.86	41.55	41.55
FA 1	1.67	3.79	2.12	753.00	15.96	768.96	30.76	30.76
FA 2								
Water				234.00		219.18	8.77	8.77
Plasticiser				0.00	0.00	0.00	0.00	0.00
			Totals	2377.00	14.82	2377.00	95.08	95.08

	SSD	Actual
W/C ratio	0.669	0.670

Entrapped air, %	0.50
Plastic Density, kg/m³	2429.88

Slump Test	
Test	Value(mm)
1	70
2	70
Mean	70

Date:	24/08/2011							
Mix:	B-B Series I							
Volume:	40 l	Aggregate moisture		Design figures				
Materials	Absorption capacity, %	Total, %	Free, %	SSD, kg/m³	Moisture correction, kg/m³	Corrected, kg/m³	Trial Target, kg	Trial Actual, kg
CEM I				350.00	0.00	350.00	14.00	14.00
CA	0.66	0.55	-0.11	1040.00	-1.14	1038.86	41.55	41.55
FA 1	1.67	3.79	2.12	594.68	12.61	607.29	24.29	24.29
FA 2	1.67	4.34	2.67	158.318	4.22	162.54509	6.5018037	6.5018037
Water				234.00		218.31	8.73	8.74
Plasticiser				0.00	0.00	0.00	0.00	0.00
			Totals	2377.00	15.69	2377.00	95.08	95.09

	SSD	Actual
W/C ratio	0.669	0.670

Entrapped air, %	0.50
Plastic Density, kg/m³	2422.94

Slump Test	
Test	Value(mm)
1	80
2	80
Mean	80

Date:	25/08/2011
Mix:	B-C Series I

Volume:	40 l	Aggregate moisture		Design figures				
Materials	Absorption capacity, %	Total, %	Free, %	SSD, kg/m³	Moisture correction, kg/m³	Corrected, kg/m³	Trial Target, kg	Trial Actual, kg
CEM I				350.00	0.00	350.00	14.00	14.00
CA	0.66	0.50	-0.16	1040.00	-1.66	1038.34	41.53	41.53
FA 1	1.67	3.79	2.12	562.18	11.92	574.10	22.96	22.96
FA 2	1.67	4.39	2.72	190.82236	5.19	196.01273	7.8405091	7.8405091
Water				234.00		218.56	8.74	8.74
Plasticiser				0.00	0.00	0.00	0.00	0.00
			Totals	2377.00	15.44	2377.00	95.08	95.08

	SSD	Actual
W/C ratio	0.669	0.669

Entrapped air, %	0.45
Plastic Density, kg/m³	2434.81

Slump Test	
Test	Value(mm)
1	65
2	60
Mean	62.5

Date:	25/08/2011							
Mix:	B-D Series I							
Volume:	40 l	Aggregate moisture		Design figures				
Materials	Absorption capacity, %	Total, %	Free, %	SSD, kg/m³	Moisture correction, kg/m³	Corrected, kg/m³	Trial Target, kg	Trial Actual, kg
CEM I				350.00	0.00	350.00	14.00	14.00
CA	0.66	0.50	-0.16	1040.00	-1.66	1038.34	41.53	41.53
FA 1	1.67	3.79	2.12	542.63	11.50	554.13	22.17	22.17
FA 2	1.67	5.22	3.55	210.37	7.47	217.84	8.71	8.71
Water				234.00		216.69	8.67	8.67
Plasticiser				0.00	0.00	0.00	0.00	0.00
			Totals	2377.00	17.31	2377.00	95.08	95.08

	SSD	Actual
W/C ratio	0.669	0.670

Entrapped air, %	0.65
Plastic Density, kg/m³	2410.19

Slump Test	
Test	Value(mm)
1	50
2	45
Mean	47.5

Date:	26/07/2012
Mix:	B-FEED Series I

Volume:	10 l	Aggregate moisture		Design figures				
Materials	Absorption capacity, %	Total, %	Free, %	SSD, kg/m³	Moisture correction, kg/m³	Corrected, kg/m³	Trial Target, kg	Trial Actual, kg
CEM I				350.00	0.00	350.00	14.00	14.00
CA	0.66	0.44	-0.22	1040.00	-2.29	1037.71	10.38	10.38
FA 1	1.92	3.77	1.85	753.00	13.93	766.93	7.67	7.67
FA 2			0.00	0.00	0.00	0.00	0.00	0.00
Water				210.00		198.36	1.98	2.40
Plasticiser				0.00	0.00	0.00	0.00	0.00
			Totals	2353.00	11.64	2353.00	23.53	23.95

	SSD	Actual
W/C ratio	0.600	0.720

Entrapped air, %	-
Plastic Density, kg/m³	-

Slump Test	
Test	Value(mm)
1	70
2	70
Mean	70

Mix:	GS-A Series I							
Volume:	40 l	Aggregate moisture		Design figures				
Materials	Absorption capacity, %	Total, %	Free, %	SSD, kg/m³	Moisture correction, kg/m³	Corrected, kg/m³	Trial Target, kg	Trial Actual, kg
CEM I				350.00	0.00	350.00	14.00	14.00
CA	0.66	0.62	-0.04	1040.00	-0.42	1039.58	41.58	41.58
FA 1	0.98	2.55	1.57	753.00	11.82	764.82	30.59	30.59
FA 2								
Water				235.00		223.59	8.94	8.94
Plasticiser				0.00	0.00	0.00	0.00	0.00
			Totals	2378.00	11.41	2378.00	95.12	95.12

	SSD	Actual
W/C ratio	0.671	0.672

Entrapped air, %	1.40
Plastic Density, kg/m³	2332.19

Slump Test	
Test	Value(mm)
1	85
2	85
Mean	85

Date:	23/05/2012							
Mix:	GS-B Series I							
Volume:	40 l	Aggregate moisture		Design figures				
Materials	Absorption capacity, %	Total, %	Free, %	SSD, kg/m³	Moisture correction, kg/m³	Corrected, kg/m³	Trial Target, kg	Trial Actual, kg
CEM I				350.00	0.00	350.00	14.00	14.00
CA	0.66	0.62	-0.04	1040.00	-0.42	1039.58	41.58	41.58
FA 1	0.98	2.55	1.57	608.63	9.56	618.18	24.73	24.73
FA 2	0.98	3.64	2.66	144.37	3.84	148.21	5.93	5.93
Water				235.00		222.02	8.88	8.88
Plasticiser				0.00	0.00	0.00	0.00	0.00
			Totals	2378.00	12.98	2378.00	95.12	95.12

	SSD	Actual
W/C ratio	0.671	0.672

Entrapped air, %	0.78
Plastic Density, kg/m³	2373.69

Slump Test	
Test	Value(mm)
1	75
2	75
Mean	75

Date:	24/05/2012
Mix:	GS-C Series I

Volume:		Aggregate moisture		Design figures				
Materials	Absorption capacity, %	Total, %	Free, %	SSD, kg/m³	Moisture correction, kg/m³	Corrected, kg/m³	Trial Target, kg	Trial Actual, kg
CEM I				350.00	0.00	350.00	14.00	14.00
CA	0.66	0.62	-0.04	1040.00	-0.42	1039.58	41.58	41.58
FA 1	0.98	2.55	1.57	578.20	9.08	587.27	23.49	23.49
FA 2	0.98	3.75	2.77	174.80	4.84	179.65	7.19	7.19
Water				235.00		221.50	8.86	8.86
Plasticiser				0.00	0.00	0.00	0.00	0.00
			Totals	2378.00	13.50	2378.00	95.12	95.12

	SSD	Actual
W/C ratio	0.671	0.672

Entrapped air, %	1.00
Plastic Density, kg/m³	2335.94

Slump Test	
Test	Value(mm)
1	100
2	95
Mean	97.5

Date:	24/05/2012							
Mix:	GS-D Series I							
Volume:		Aggregate moisture		Design figures				
Materials	Absorption capacity, %	Total, %	Free, %	SSD, kg/m³	Moisture correction, kg/m³	Corrected, kg/m³	Trial Target, kg	Trial Actual, kg
CEM I				350.00	0.00	350.00	14.00	14.00
CA	0.66	0.62	-0.04	1040.00	-0.42	1039.58	41.58	41.58
FA 1	0.98	2.55	1.57	550.04	8.64	558.68	22.35	22.35
FA 2	0.98	3.61	2.63	202.96	5.34	208.30	8.33	8.33
Water				235.00		221.44	8.86	8.86
Plasticiser				0.00	0.00	0.00	0.00	0.00
			Totals	2378.00	13.56	2378.00	95.12	95.12

	SSD	Actual
W/C ratio	0.671	0.672

Entrapped air, %	1.20
Plastic Density, kg/m³	2335.94

Slump Test	
Test	Value(mm)
1	75
2	75
Mean	75

Date:	26/07/2012							
Mix:	GS-FEED Series I							
Volume:	10 l	Aggregate moisture		Design figures				
Materials	Absorption capacity, %	Total, %	Free, %	SSD, kg/m³	Moisture correction, kg/m³	Corrected, kg/m³	Trial Target, kg	Trial Actual, kg
CEM I				350.00	0.00	350.00	14.00	14.00
CA	0.66	0.44	-0.22	1040.00	-2.29	1037.71	10.38	10.38
FA 1	1.53	3.37	1.84	753.00	13.86	766.86	7.67	7.67
FA 2			0.00	0.00	0.00	0.00	0.00	0.00
Water				210.00		198.43	1.98	2.50
Plasticiser				0.00	0.00	0.00	0.00	0.00
			Totals	2353.00	11.57	2353.00	23.53	24.05

	SSD	Actual
W/C ratio	0.600	0.748

Entrapped air, %	-
Plastic Density, kg/m³	-

Slump Test	
Test	Value(mm)
1	80
2	80
Mean	80

Date:	02/05/2012							
Mix:	L-A Series I							
Volume:	40 l	Aggregate moisture		Design figures				
Materials	Absorption capacity, %	Total, %	Free, %	SSD, kg/m³	Moisture correction, kg/m³	Corrected, kg/m³	Trial Target, kg	Trial Actual, kg
CEM I				350.00	0.00	350.00	14.00	14.00
CA	0.66	2.20	1.54	1040.00	16.02	1056.02	42.24	42.24
FA 1	0.45	2.14	1.69	753.00	12.73	765.73	30.63	30.63
FA 2								
Water				194.00		165.26	6.61	6.62
Plasticiser				0.00	0.00	0.00	0.00	0.00
			Totals	2337.00	28.74	2337.00	93.48	93.49

	SSD	Actual
W/C ratio	0.554	0.556

Entrapped air, %	1.40
Plastic Density, kg/m³	2443.94

Slump Test	
Test	Value(mm)
1	90
2	90
Mean	90

Date:	02/05/2012							
Mix:	L-B Series I							
Volume:	40 l	Aggregate moisture		Design figures				
Materials	Absorption capacity, %	Total, %	Free, %	SSD, kg/m³	Moisture correction, kg/m³	Corrected, kg/m³	Trial Target, kg	Trial Actual, kg
CEM I				350.00	0.00	350.00	14.00	14.00
CA	0.66	2.20	1.54	1040.00	16.02	1056.02	42.24	42.24
FA 1	0.45	2.14	1.69	587.82	9.93	597.75	23.91	23.91
FA 2	0.45	3.42	2.97	165.18	4.91	170.09	6.80	6.80
Water				194.00		163.14	6.53	6.52
Plasticiser				0.00	0.00	0.00	0.00	0.00
			Totals	2337.00	30.86	2337.00	93.48	93.47

	SSD	Actual
W/C ratio	0.554	0.555

Entrapped air, %	1.50
Plastic Density, kg/m³	2447.06

Slump Test	
Test	Value(mm)
1	70
2	70
Mean	70

Date:	03/05/2012							
Mix:	L-C Series I							
Volume:	40 l	Aggregate moisture		Design figures				
Materials	Absorption capacity, %	Total, %	Free, %	SSD, kg/m³	Moisture correction, kg/m³	Corrected, kg/m³	Trial Target, kg	Trial Actual, kg
CEM I				350.00	0.00	350.00	14.00	14.00
CA	0.66	2.20	1.54	1040.00	16.02	1056.02	42.24	42.24
FA 1	0.45	2.14	1.69	559.06	9.45	568.51	22.74	22.74
FA 2	0.45	3.48	3.03	193.94	5.88	199.81	7.99	7.99
Water				194.00		162.66	6.51	6.51
Plasticiser				0.00	0.00	0.00	0.00	0.00
			Totals	2337.00	31.34	2337.00	93.48	93.48

	SSD	Actual
W/C ratio	0.554	0.556

Entrapped air, %	1.48
Plastic Density, kg/m³	2456.81

Slump Test	
Test	Value(mm)
1	80
2	85
Mean	82.5

Date:	03/05/2012							
Mix:	L-D Series I							
Volume:	40 l	Aggregate moisture		Design figures				
Materials	Absorption capacity, %	Total, %	Free, %	SSD, kg/m³	Moisture correction, kg/m³	Corrected, kg/m³	Trial Target, kg	Trial Actual, kg
CEM I				350.00	0.00	350.00	14.00	14.00
CA	0.66	2.20	1.54	1040.00	16.02	1056.02	42.24	42.24
FA 1	0.45	2.14	1.69	532.99	9.01	542.00	21.68	21.68
FA 2	0.45	3.42	2.97	220.01	6.53	226.55	9.06	9.06
Water				194.00		162.44	6.50	6.49
Plasticiser				0.00	0.00	0.00	0.00	0.00
			Totals	2337.00	31.56	2337.00	93.48	93.47

	SSD	Actual
W/C ratio	0.554	0.555

Entrapped air, %	1.38
Plastic Density, kg/m³	2455.94

Slump Test	
Test	Value(mm)
1	65
2	65
Mean	65

Date:	26/07/2012							
Mix:	L-FEED Series I							
Volume:	10 l	Aggregate moisture		Design figures				
Materials	Absorption capacity, %	Total, %	Free, %	SSD, kg/m³	Moisture correction, kg/m³	Corrected, kg/m³	Trial Target, kg	Trial Actual, kg
CEM I				350.00	0.00	350.00	14.00	14.00
CA	0.66	0.44	-0.22	1040.00	-2.29	1037.71	10.38	10.38
FA 1	0.62	1.29	0.67	753.00	5.05	758.05	7.58	7.58
FA 2								
Water				210.00		207.24	2.07	2.12
Plasticiser				0.00	0.00	0.00	0.00	0.00
			Totals	2353.00	2.76	2353.00	23.53	23.58

	SSD	Actual
W/C ratio	0.600	0.614

Entrapped air, %	-
Plastic Density, kg/m³	-

Slump Test	
Test	Value(mm)
1	55
2	65
Mean	60

Series II mix sheets

Date:	23/01/2012
Mix:	NS w/c Series II

Volume:	40 l	Aggregate moisture		Design figures				
Materials	Absorption capacity, %	Total, %	Free, %	SSD, kg/m³	Moisture correction, kg/m³	Corrected, kg/m³	Trial Target, kg	Trial Actual, kg
CEM I				350	0.00	350.00	14.00	14.00
CA	0.66	0.13	-0.53	1040.00	-5.51	1034.49	41.38	41.38
FA 1	1.04	0.41	-0.63	753.00	-4.74	748.26	29.93	29.93
FA 2								
Water				192.00		202.26	8.09	8.11
Plasticiser				0.00	0.00	0.00	0.00	0.00
			Totals	2335.00	-10.26	2335.00	93.40	93.42

	SSD	Actual
W/C ratio	0.549	0.550

Entrapped air, %	0.90
Plastic Density, kg/m³	2457.19

Slump Test	
Test	Value(mm)
1	Collapse
2	Collapse
Mean	Collapse

Date:	23/01/2012
Mix:	G-A Series II

Volume:	40 l	Aggregate moisture		Design figures					
Materials	Absorption capacity, %	Total, %	Free, %	SSD, kg/m³	Moisture correction, kg/m³	Corrected, kg/m³	Trial Target, kg	Trial Actual, kg	
CEM I				350.00	0.00	350.00	14.00	14.00	
CA	0.66	0.13	-0.53	1040.00	-5.51	1034.49	41.38	41.38	
FA 1	0.58	1.72	1.14	753.00	8.58	761.58	30.46	30.46	
FA 2				0.00	0.00	0.00	0.00	0.00	
Water				192.00		188.93	7.56	7.54	Plasticiser water, kg
Plasticiser				0.00		0.00	0.00	0.00	0.00
			Totals	2335.00	3.07	2335.00	93.40	93.38	

	SSD	Actual
W/C ratio	0.549	0.549

Entrapped air, %	1.40
Plastic Density, kg/m³	2387.19

Slump Test	
Test	Value(mm)
1	65
2	65
Mean	65

Date:	14/02/2012
Mix:	G-B Series II
Volume:	32 l

		Aggregate moisture		Design figures					
Materials	Absorption capacity, %	Total, %	Free, %	SSD, kg/m³	Moisture correction, kg/m³	Corrected, kg/m³	Trial Target, kg	Trial Actual, kg	
CEM I				350.00	0.00	350.00	14.00	14.00	
CA	0.66	0.29	-0.37	1040.00	-3.85	1036.15	33.16	33.16	
FA 1	0.58	2.83	2.25	694.84	15.63	710.47	22.74	22.74	
FA 2	0.58	2.83	2.25	58.16	1.31	59.47	1.90	1.90	
Water				192.00		178.91	5.72	5.72	Plasticiser water, kg
Plasticiser				0.00		0.00	0.00	0.00	0.00
			Totals	2335.00	13.09	2335.00	74.72	74.72	

	SSD	Actual
W/C ratio	0.549	0.549

Entrapped air, %	1.40
Plastic Density, kg/m³	2388.40

Slump Test	
Test	Value(mm)
1	70
2	65
Mean	67.5

Date:	26/01/2012								
Mix:	G-C Series II								
Volume:	40 l	Aggregate moisture		Design figures					
Materials	Absorption capacity, %	Total, %	Free, %	SSD, kg/m³	Moisture correction, kg/m³	Corrected, kg/m³	Trial Target, kg	Trial Actual, kg	
CEM I				350.00	0.00	350.00	14.00	14.00	
CA	0.66	1.98	1.32	1040.00	13.73	1053.73	42.15	42.15	
FA 1	0.58	1.72	1.14	615.09	7.01	622.10	24.88	24.88	
FA 2	0.58	4.57	3.99	137.91	5.50	143.41	5.74	5.74	
Water				192.00		165.76	6.63	6.61	Plasticiser water, kg
Plasticiser				1.25		1.25	0.05	0.05	0.03
			Totals	2336.25	26.24	2336.25	93.45	93.43	

	SSD	Actual
W/C ratio	0.549	0.550

Entrapped air, %	1.30
Plastic Density, kg/m³	2395.30

Slump Test	
Test	Value(mm)
1	70
2	70
Mean	70

Date:	14/02/2012
Mix:	G-D Series II
Volume:	32 l

		Aggregate moisture		Design figures					
Materials	Absorption capacity, %	Total, %	Free, %	SSD, kg/m³	Moisture correction, kg/m³	Corrected, kg/m³	Trial Target, kg	Trial Actual, kg	
CEM I				350.00	0.00	350.00	14.00	14.00	
CA	0.66	0.35	-0.31	1040.00	-3.22	1036.78	41.47	41.47	
FA 1	0.58	1.41	0.83	597.58	4.96	602.54	19.28	19.28	
FA 2	0.58	3.16	2.58	155.42	4.01	159.43	5.10	5.10	
Water				192.00		186.25	5.96	5.95	Plasticiser water, kg
Plasticiser				0.62		0.62	0.02	0.02	0.01
			Totals	2335.62	5.75	2335.62	74.74	74.73	

	SSD	Actual
W/C ratio	0.549	0.549

Entrapped air, %	1.40
Plastic Density, kg/m³	2387.20

Slump Test	
Test	Value(mm)
1	60
2	60
Mean	60

Date:	14/02/2012
Mix:	G-E Series II
Volume:	40 l

		Aggregate moisture		Design figures					
Materials	Absorption capacity, %	Total, %	Free, %	SSD, kg/m³	Moisture correction, kg/m³	Corrected, kg/m³	Trial Target, kg	Trial Actual, kg	
CEM I				350.00	0.00	350.00	14.00	14.00	
CA	0.66	0.35	-0.31	1040.00	-3.22	1036.78	41.47	41.47	
FA 1	0.58	1.41	0.83	583.05	4.84	587.89	23.52	23.52	
FA 2	0.58	4.12	3.54	169.95	6.02	175.96	7.04	7.04	
Water				192.00		184.37	7.37	7.37	Plasticiser water, kg
Plasticiser				1.00		1.00	0.04	0.04	0.02
			Totals	2345.00	10.94	2345.00	93.80	93.80	

	SSD	Actual
W/C ratio	0.549	0.550

Entrapped air, %	1.40
Plastic Density, kg/m³	2384.70

Slump Test	
Test	Value(mm)
1	85
2	85
Mean	85

Date:	18/01/2012
Mix:	B-A Series II
Volume:	40 l

		Aggregate moisture		Design figures					
Materials	Absorption capacity, %	Total, %	Free, %	SSD, kg/m³	Moisture correction, kg/m³	Corrected, kg/m³	Trial Target, kg	Trial Actual, kg	
CEM I				350.00	0.00	350.00	14.00	14.00	
CA	0.66	0.13	-0.53	1040.00	-5.51	1034.49	41.38	41.38	
FA 1	1.67	4.00	2.33	753.00	17.54	770.54	30.82	30.82	
FA 2				0.00	0.00	0.00	0.00	0.00	
Water				192.00		179.97	7.20	7.17	Plasticiser water, kg
Plasticiser				2.75		2.75	0.11	0.11	0.06
			Totals	2337.75	12.03	2337.75	93.51	93.48	

	SSD	Actual
W/C ratio	0.549	0.552

Entrapped air, %	1.41
Plastic Density, kg/m³	2469.90

Slump Test	
Test	Value(mm)
1	60
2	60
Mean	60

Date:	02/02/2012								
Mix:	B-B Series II								
Volume:	40 l	Aggregate moisture		Design figures					
Materials	Absorption capacity, %	Total, %	Free, %	SSD, kg/m³	Moisture correction, kg/m³	Corrected, kg/m³	Trial Target, kg	Trial Actual, kg	
CEM I				350.00	0.00	350.00	14.00	14.00	
CA	0.66	0.85	0.19	1040.00	1.98	1041.98	41.68	41.68	
FA 1	1.67	3.95	2.28	594.68	13.56	608.24	24.33	24.33	
FA 2	1.67	4.33	2.66	158.32	4.21	162.53	6.50	6.50	
Water				192.00		172.25	6.89	6.84	Plasticiser water, kg
Plasticiser				2.75		2.75	0.11	0.11	0.06
			Totals	2337.75	19.75	2337.75	93.51	93.46	

	SSD	Actual
W/C ratio	0.549	0.550

Entrapped air, %	1.60
Plastic Density, kg/m³	2457.19

Slump Test	
Test	Value(mm)
1	30
2	30
Mean	30

Date:	19/01/2012								
Mix:	B-C Series II								
Volume:	40 l	Aggregate moisture		Design figures					
Materials	Absorption capacity, %	Total, %	Free, %	SSD, kg/m³	Moisture correction, kg/m³	Corrected, kg/m³	Trial Target, kg	Trial Actual, kg	
CEM I				350.00	0.00	350.00	14.00	14.00	
CA	0.66	0.13	-0.53	1040.00	-5.51	1034.49	41.38	41.38	
FA 1	1.67	4.00	2.33	562.18	13.10	575.28	23.01	23.01	
FA 2	1.67	6.82	5.15	190.82	9.83	200.65	8.03	8.03	
Water				192.00		174.59	6.98	6.93	Plasticiser water, kg
Plasticiser				3.30		3.30	0.13	0.13	0.07
			Totals	2338.30	17.41	2338.30	93.53	93.48	

	SSD	Actual
W/C ratio	0.549	0.552

Entrapped air, %	1.30
Plastic Density, kg/m³	2475.19

Slump Test	
Test	Value(mm)
1	30
2	30
Mean	30

Date:	19/01/2012								
Mix:	B-D Series II								
Volume:	40 l	Aggregate moisture		Design figures					
Materials	Absorption capacity, %	Total, %	Free, %	SSD, kg/m³	Moisture correction, kg/m³	Corrected, kg/m³	Trial Target, kg	Trial Actual, kg	
CEM I				350.00	0.00	350.00	14.00	14.00	
CA	0.66	0.13	-0.53	1040.00	-5.51	1034.49	41.38	41.38	
FA 1	1.67	4.00	2.33	542.63	12.64	555.27	22.21	22.21	
FA 2	1.67	6.95	5.28	210.37	11.11	221.48	8.86	8.86	
Water				192.00		173.76	6.95	6.87	Plasticiser water, kg
Plasticiser				3.30		3.30	0.13	0.13	0.07
			Totals	2338.30	18.24	2338.30	93.53	93.45	

	SSD	Actual
W/C ratio	0.549	0.550

Entrapped air, %	1.80
Plastic Density, kg/m³	2439.44

Slump Test	
Test	Value(mm)
1	25
2	25
Mean	25

Date:	30/05/2012
Mix:	GS-A Series II

Volume:	40 l	Aggregate moisture		Design figures					
Materials	Absorption capacity, %	Total, %	Free, %	SSD, kg/m³	Moisture correction, kg/m³	Corrected, kg/m³	Trial Target, kg	Trial Actual, kg	
CEM I				350.00	0.00	350.00	14.00	14.00	
CA	0.66	0.26	-0.40	1040.00	-4.16	1035.84	41.43	41.43	
FA 1	0.98	2.55	1.57	753.00	11.82	764.82	30.59	30.59	
FA 2				0.00	0.00	0.00	0.00	0.00	
Water				192.00		184.34	7.37	7.33	Plasticiser water, kg
Plasticiser				2.45		2.45	0.10	0.10	0.05
			Totals	2337.45	7.66	2337.45	93.50	93.45	

	SSD	Actual
W/C ratio	0.549	0.550

Entrapped air, %	1.41
Plastic Density, kg/m³	2469.90

Slump Test	
Test	Value(mm)
1	60
2	60
Mean	60

Date:	07/08/2012								
Mix:	GS-B Series II								
Volume:	40 l	Aggregate moisture		Design figures					
Materials	Absorption capacity, %	Total, %	Free, %	SSD, kg/m³	Moisture correction, kg/m³	Corrected, kg/m³	Trial Target, kg	Trial Actual, kg	
CEM I				350.00	0.00	350.00	14.00	14.00	
CA	0.66	0.49	-0.17	1040.00	-1.77	1038.23	41.53	41.53	
FA 1	0.98	2.61	1.63	608.63	9.92	618.55	24.74	24.74	
FA 2	0.98	3.55	2.57	144.37	3.71	148.08	5.92	5.92	
Water				192.00		180.14	7.21	7.17	Plasticiser water, kg
Plasticiser				2.75		2.75	0.11	0.11	0.06
			Totals	2337.75	11.86	2337.75	93.51	93.47	

	SSD	Actual
W/C ratio	0.549	0.551

Entrapped air, %	1.30
Plastic Density, kg/m³	2403.06

Slump Test	
Test	Value(mm)
1	50
2	50
Mean	50

Date:	07/08/2012								
Mix:	GS-C Series II								
Volume:	40 l	Aggregate moisture		Design figures					
Materials	Absorption capacity, %	Total, %	Free, %	SSD, kg/m³	Moisture correction, kg/m³	Corrected, kg/m³	Trial Target, kg	Trial Actual, kg	
CEM I				350.00	0.00	350.00	14.00	14.00	
CA	0.66	0.49	-0.17	1040.00	-1.77	1038.23	41.53	41.53	
FA 1	0.98	2.61	1.63	578.20	9.42	587.62	23.50	23.50	
FA 2	0.98	3.50	2.52	174.80	4.41	179.21	7.17	7.17	
Water				192.00		179.94	7.20	7.17	Plasticiser water, kg
Plasticiser				2.75		2.75	0.11	0.11	0.06
			Totals	2337.75	12.06	2337.75	93.51	93.48	

	SSD	Actual
W/C ratio	0.549	0.551

Entrapped air, %	1.35
Plastic Density, kg/m³	2388.44

Slump Test	
Test	Value(mm)
1	50
2	50
Mean	50

Date:	07/08/2012								
Mix:	GS-D Series II								
Volume:	40 l	Aggregate moisture		Design figures					
Materials	Absorption capacity, %	Total, %	Free, %	SSD, kg/m³	Moisture correction, kg/m³	Corrected, kg/m³	Trial Target, kg	Trial Actual, kg	
CEM I				350.00	0.00	350.00	14.00	14.00	
CA	0.66	0.49	-0.17	1040.00	-1.77	1038.23	41.53	41.53	
FA 1	0.98	2.61	1.63	550.04	8.97	559.01	22.36	22.36	
FA 2	0.98	3.66	2.68	202.96	5.44	208.40	8.34	8.34	
Water				192.00		179.36	7.17	7.15	Plasticiser water, kg
Plasticiser				2.75		2.75	0.11	0.11	0.06
			Totals	2337.75	12.64	2337.75	93.51	93.49	

	SSD	Actual
W/C ratio	0.549	0.552

Entrapped air, %	1.56
Plastic Density, kg/m³	2412.19

Slump Test	
Test	Value(mm)
1	45
2	45
Mean	45

Date:	08/08/2012
Mix:	L-A Series II

Volume:	40 l	Aggregate moisture		Design figures					
Materials	Absorption capacity, %	Total, %	Free, %	SSD, kg/m³	Moisture correction, kg/m³	Corrected, kg/m³	Trial Target, kg	Trial Actual, kg	
CEM I				350.00	0.00	350.00	14.00	14.00	
CA	0.66	0.49	-0.17	1040.00	-1.77	1038.23	41.53	41.53	
FA 1	0.45	1.88	1.43	753.00	10.77	763.77	30.55	30.55	
FA 2				0.00	0.00	0.00	0.00	0.00	
Water				192.00		184.34	7.37	7.33	Plasticiser water, kg
Plasticiser				1.63		1.63	0.07	0.07	0.03
			Totals	2319.63	9.00	2319.63	92.79	92.76	

	SSD	Actual
W/C ratio	0.500	0.501

Entrapped air, %	1.30
Plastic Density, kg/m³	2482.19

Slump Test	
Test	Value(mm)
1	90
2	90
Mean	90

Date:	08/08/2012								
Mix:	L-B Series II								
Volume:	40 l	Aggregate moisture		Design figures					
Materials	Absorption capacity, %	Total, %	Free, %	SSD, kg/m³	Moisture correction, kg/m³	Corrected, kg/m³	Trial Target, kg	Trial Actual, kg	
CEM I				350.00	0.00	350.00	14.00	14.00	
CA	0.66	0.49	-0.17	1040.00	-1.77	1038.23	41.53	41.53	
FA 1	0.45	1.88	1.43	587.82	8.41	596.22	23.85	23.85	
FA 2	0.45	2.30	1.85	165.18	3.06	168.24	6.73	6.73	
Water				175.00		165.31	6.61	6.58	Plasticiser water, kg
Plasticiser				1.10		1.10	0.04	0.04	0.02
			Totals	2319.10	9.69	2319.10	92.76	92.73	

	SSD	Actual
W/C ratio	0.500	0.500

Entrapped air, %	1.30
Plastic Density, kg/m³	2458.69

Slump Test	
Test	Value(mm)
1	90
2	90
Mean	90

Date:	09/08/2012
Mix:	L-C Series II
Volume:	40 l

		Aggregate moisture		Design figures					
Materials	Absorption capacity, %	Total, %	Free, %	SSD, kg/m³	Moisture correction, kg/m³	Corrected, kg/m³	Trial Target, kg	Trial Actual, kg	
CEM I				350.00	0.00	350.00	14.00	14.00	
CA	0.66	0.49	-0.17	1040.00	-1.77	1038.23	41.53	41.53	
FA 1	0.45	1.88	1.43	559.06	7.99	567.06	22.68	22.68	
FA 2	0.45	3.86	3.41	193.94	6.61	200.55	8.02	8.02	
Water				175.00		162.16	6.49	6.46	Plasticiser water, kg
Plasticiser				1.35		1.35	0.05	0.05	0.03
			Totals	2319.35	12.84	2319.35	92.77	92.75	

	SSD	Actual
W/C ratio	0.500	0.501

Entrapped air, %	1.10
Plastic Density, kg/m³	2467.19

Slump Test	
Test	Value(mm)
1	75
2	75
Mean	75

Date:	09/08/2012								
Mix:	L-D Series II								
Volume:	40 l	Aggregate moisture		Design figures					
Materials	Absorption capacity, %	Total, %	Free, %	SSD, kg/m³	Moisture correction, kg/m³	Corrected, kg/m³	Trial Target, kg	Trial Actual, kg	
CEM I				350.00	0.00	350.00	14.00	14.00	
CA	0.66	0.49	-0.17	1040.00	-1.77	1038.23	41.53	41.53	
FA 1	0.45	1.88	1.43	532.99	7.62	540.61	21.62	21.62	
FA 2	0.45	3.67	3.22	220.01	7.08	227.10	9.08	9.08	
Water				175.00		162.06	6.48	6.45	Plasticiser water, kg
Plasticiser				1.10		1.10	0.04	0.04	0.02
			Totals	2319.10	12.94	2319.10	92.76	92.73	

	SSD	Actual
W/C ratio	0.500	0.500

Entrapped air, %	0.80
Plastic Density, kg/m³	2465.94

Slump Test	
Test	Value(mm)
1	65
2	65
Mean	65

ANN model validation mix sheets

Date:	11/12/2012								
Mix:	validation LS dust								
Volume:	10 l	Aggregate moisture		Design figures					
Materials	Absorption capacity, %	Total, %	Free, %	SSD, kg/m³	Moisture correction, kg/m³	Corrected, kg/m³	Trial Target, kg	Trial Actual, kg	
CEM I				350.00	0.00	350.00	14.00	14.00	
CA	0.66	0.05	-0.61	1040.00	-6.34	1033.66	10.34	10.34	
FA 1	0.77	0.02	-0.75	753.00	-5.65	747.35	7.47	7.47	
FA 2									
Water				228.00		239.99	2.40	2.39	Plasticiser water, kg
Plasticiser				0.00		0.00	0.00	0.00	0.00
			Totals	2371.00	-11.99	2371.00	23.71	23.70	

	SSD	Actual
W/C ratio	0.651	0.649

Entrapped air, %	-
Plastic Density, kg/m³	-

Slump Test	
Test	Value(mm)
1	85
2	
Mean	85

Date:	11/12/2012								
Mix:	Validation NS								
Volume:	10 l	Aggregate moisture		Design figures					
Materials	Absorption capacity, %	Total, %	Free, %	SSD, kg/m³	Moisture correction, kg/m³	Corrected, kg/m³	Trial Target, kg	Trial Actual, kg	
CEM I				350.00	0.00	350.00	14.00	14.00	
CA	0.66	0.05	-0.61	1040.00	-6.34	1033.66	10.34	10.34	
FA 1	1.04	0.03	-1.01	753.00	-7.61	745.39	7.45	7.45	
FA 2									
Water				179.00		192.95	1.93	1.92	Plasticiser water, kg
Plasticiser				0.00		0.00	0.00	0.00	0.00
			Totals	2322.00	-13.95	2322.00	23.22	23.21	

	SSD	Actual
W/C ratio	0.511	0.509

Entrapped air, %	-
Plastic Density, kg/m³	-

Slump Test	
Test	Value(mm)
1	140
2	
Mean	140

Date:	12/12/2012								
Mix:	Validation G-C								
Volume:	10 l	Aggregate moisture		Design figures					
Materials	Absorption capacity, %	Total, %	Free, %	SSD, kg/m³	Moisture correction, kg/m³	Corrected, kg/m³	Trial Target, kg	Trial Actual, kg	
CEM I				350.00	0.00	350.00	14.00	14.00	
CA	0.66	0.05	-0.61	1040.00	-6.34	1033.66	10.34	10.34	
FA 1	0.58	1.73	1.15	615.09	7.07	622.16	6.22	6.22	
FA 2	0.58	3.48	2.90	137.91	4.00	141.91	1.42	1.42	
Water				210.00		205.27	2.05	2.05	Plasticiser water, kg
Plasticiser				0.00		0.00	0.00	0.00	0.00
			Totals	2353.00	4.73	2353.00	23.53	23.53	

	SSD	Actual
W/C ratio	0.600	0.600

Entrapped air, %	-
Plastic Density, kg/m³	-

Slump Test	
Test	Value(mm)
1	75
2	
Mean	75

Date:	12/12/2012								
Mix:	Validation GS-B								
Volume:	10 l	Aggregate moisture		Design figures					
Materials	Absorption capacity, %	Total, %	Free, %	SSD, kg/m³	Moisture correction, kg/m³	Corrected, kg/m³	Trial Target, kg	Trial Actual, kg	
CEM I				350.00	0.00	350.00	14.00	14.00	
CA	0.66	0.05	-0.61	1040.00	-6.34	1033.66	10.34	10.34	
FA 1	0.98	2.49	1.51	608.63	9.19	617.82	6.18	6.18	
FA 2	0.98	5.29	4.31	144.37	6.22	150.59	1.51	1.51	
Water				210.00		200.93	2.01	1.99	Plasticiser water, kg
Plasticiser				3.00		3.00	0.03	0.03	0.02
			Totals	2356.00	9.07	2356.00	23.56	23.54	

	SSD	Actual
W/C ratio	0.600	0.600

Entrapped air, %	-
Plastic Density, kg/m³	-

Slump Test	
Test	Value(mm)
1	70
2	
Mean	70

Series I hardened concrete test data

		G-A Series I			G-B Series I			G-C Series I			G-D Series I			G-E Series I		
Cube	Age	Compressive Strength, N/mm²	Average	CoV, %	Compressive Strength, N/mm²	Average	CoV, %	Compressive Strength, N/mm²	Average	CoV, %	Compressive Strength, N/mm²	Average	CoV, %	Compressive Strength, N/mm²	Average	CoV, %
1	1	17.64	17.56	0.64	16.80	17.00	1.56	17.96	17.88	0.68	19.40	19.30	1.87	16.60	16.57	0.35
2	1	17.43			17.30			17.94			18.90			16.60		
3	1	17.60			16.90			17.74			19.60			16.50		
4	7	43.30	43.50	1.00	40.71	40.17	1.60	41.33	40.44	1.96	42.57	42.20	2.07	41.04	40.61	0.96
5	7	44.00			40.34			40.16			41.20			40.50		
6	7	43.20			39.46			39.82			42.82			40.28		
7	28	52.00	52.20	2.32	50.90	49.94	1.87	49.41	50.10	1.24	51.50	52.27	1.36	46.19	48.09	3.65
8	28	53.50			49.03			50.30			52.90			49.65		
9	28	51.10			49.88			50.60			52.40			48.43		
Beam	Age	Flexural Strength, N/mm²	Average	CoV, %	Flexural Strength, N/mm²	Average	CoV, %	Flexural Strength, N/mm²	Average	CoV, %	Flexural Strength, N/mm²	Average	CoV, %	Flexural Strength, N/mm²	Average	CoV, %
1	28	5.40	5.58	5.26	5.56	5.59	5.38	5.62	6.01	5.74	5.36	5.83	7.30	5.78	5.44	5.64
2	28	5.92			5.30			6.20			6.18			5.19		
3	28	5.42			5.90			6.22			5.96			5.35		

		NS Slump Series I			B-A Series I			B-B Series I			B-C Series I			B-D Series I		
Cube	Age	Compressive Strength, N/mm²	Average	CoV, %	Compressive Strength, N/mm²	Average	CoV, %	Compressive Strength, N/mm²	Average	CoV, %	Compressive Strength, N/mm²	Average	CoV, %	Compressive Strength, N/mm²	Average	CoV, %
1	1	23.74	23.76	0.45	11.66	11.77	1.84	13.04	12.89	2.06	13.29	13.04	2.29	12.97	13.16	2.26
2	1	23.87			12.02			13.04			13.12			13.50		
3	1	23.66			11.63			12.58			12.71			13.00		
4	7	46.54	47.97	2.76	31.32	30.38	2.88	32.94	31.34	4.52	32.50	33.07	2.01	35.10	35.23	0.43
5	7	49.15			30.22			30.82			32.90			35.20		
6	7	48.23			29.59			30.25			33.80			35.40		
7	28	58.10	58.87	2.86	42.70	41.67	2.17	44.53	43.69	1.68	42.54	42.73	1.75	44.32	45.57	2.62
8	28	57.70			41.02			43.18			42.09			46.70		
9	28	60.80			41.29			43.35			43.55			45.70		
Beam	Age	Flexural Strength, N/mm²	Average	CoV, %	Flexural Strength, N/mm²	Average	CoV, %	Flexural Strength, N/mm²	Average	CoV, %	Flexural Strength, N/mm²	Average	CoV, %	Flexural Strength, N/mm²	Average	CoV, %
1	28	5.84	6.13	4.61	5.03	5.32	4.88	5.23	5.46	5.15	5.66	5.39	7.68	5.80	5.65	3.16
2	28	6.40			5.54			5.78			5.59			5.68		
3	28	6.16			5.38			5.38			4.91			5.45		

		GS-A Series I			GS-B Series I			GS-C Series I			GS-D Series I		
Cube	Age	Compressive Strength, N/mm²	Average	CoV, %	Compressive Strength, N/mm²	Average	CoV, %	Compressive Strength, N/mm²	Average	CoV, %	Compressive Strength, N/mm²	Average	CoV, %
1	1	12.63	12.72	0.89	14.72	14.88	1.44	14.77	14.74	1.37	12.02	12.13	0.91
2	1	12.69			14.79			14.52			12.24		
3	1	12.85			15.12			14.92			12.14		
4	7	31.15	31.41	0.75	34.36	34.45	2.94	32.04	32.82	3.27	30.26	30.47	2.26
5	7	31.61			35.51			32.37			31.24		
6	7	31.46			33.49			34.04			29.91		
7	28	40.81	41.35	3.94	43.51	43.32	2.65	42.27	42.83	2.17	39.83	39.91	0.64
8	28	43.23			43.27			44.22			39.89		
9	28	39.41			41.85			42.42			39.65		
10	28	41.95			44.64			42.40			40.26		
Beam	Age	Flexural Strength, N/mm²	Average	CoV, %	Flexural Strength, N/mm²	Average	CoV, %	Flexural Strength, N/mm²	Average	CoV, %	Flexural Strength, N/mm²	Average	CoV, %
1	28	5.22	5.18	3.33	6.08	5.56	8.24	5.38	5.53	4.47	4.88	5.20	6.32
2	28	4.99			5.22			5.82			5.18		
3	28	5.32			5.38			5.40			5.54		

		L-A Series I			L-B Series I			L-C Series I			L-D Series I		
Cube	Age	Compressive Strength, N/mm²	Average	CoV, %	Compressive Strength, N/mm²	Average	CoV, %	Compressive Strength, N/mm²	Average	CoV, %	Compressive Strength, N/mm²	Average	CoV, %
1	1	18.29	17.97	2.53	21.47	21.23	1.03	23.84	22.74	4.21	21.13	21.40	1.54
2	1	18.17			21.18			22.22			21.77		
3	1	17.45			21.04			22.15			21.31		
4	7	44.97	44.30	2.82	47.82	47.77	1.18	45.73	46.19	3.16	47.70	46.88	2.00
5	7	45.08			47.19			47.82			45.86		
6	7	42.86			48.31			45.01			47.08		
7	28	56.00	55.68	3.12	58.00	57.97	1.12	59.10	56.15	3.57	52.00	56.58	7.44
8	28	54.20			57.30			55.00			60.10		
9	28	54.50			58.60			54.80			54.00		
10	28	58.00						55.70			60.20		
Beam	Age	Flexural Strength, N/mm²	Average	CoV, %	Flexural Strength, N/mm²	Average	CoV, %	Flexural Strength, N/mm²	Average	CoV, %	Flexural Strength, N/mm²	Average	CoV, %
1	28	6.93	6.63	4.29	6.53	6.72	4.34	5.97	6.07	7.97	5.55	5.98	6.28
2	28	6.59			7.06			6.60			6.16		
3	28	6.37			6.58			5.64			6.23		

		G-FEED			B-FEED			GS-FEED			L-FEED		
Cube	Age	Compressive Strength, N/mm²	Average	CoV, %	Compressive Strength, N/mm²	Average	CoV, %	Compressive Strength, N/mm²	Average	CoV, %	Compressive Strength, N/mm²	Average	CoV, %
1	1	12.71			9.16			8.01			18.26		
2	1	12.38	12.55	1.86	9.48	9.32	2.43	8.29	8.15	2.43	18.69	18.48	1.65
3	7	30.29			25.90			22.98			36.95		
4	7	30.28	30.29	0.02	25.77	25.84	0.36	23.54	23.26	1.70	39.06	38.01	3.93
5	28	38.08			35.69			31.52			50.30		
6	28	40.02	39.05	3.51	35.26	35.48	0.86	31.03	31.28	1.11	50.00	50.15	0.42

Series II hardened concrete test data

		G-A Series II			G-B Series II			G-C Series II			G-D Series II			G-E Series II		
Cube	Age	Compressive Strength, N/mm²	Average	CoV, %	Compressive Strength, N/mm²	Average	CoV, %	Compressive Strength, N/mm²	Average	CoV, %	Compressive Strength, N/mm²	Average	CoV, %	Compressive Strength, N/mm²	Average	CoV, %
1	1	16.07	16.36	1.74	20.40	20.09	1.40	20.91	20.69	0.94	18.78	19.41	3.08	16.24	16.62	2.18
2	1	16.37			20.00			20.53			19.97			16.66		
3	1	16.64			19.86			20.64			19.49			16.96		
4	7	44.13	44.35	2.66	45.54	46.10	1.56	47.03	46.14	1.68	47.86	48.34	1.31	48.65	47.77	1.61
5	7	43.30			45.84			45.66			49.06			47.20		
6	7	45.63			46.91			45.72			48.11			47.47		
7	28	52.50	52.98	2.69	59.80	59.23	2.20	56.40	55.15	1.88	57.50	58.63	1.75	60.30	59.20	1.66
8	28	51.40			57.70			55.50			58.10			58.90		
9	28	53.20			58.70			54.00			59.10			58.40		
10	28	54.80			60.70			54.70			59.80					
Beam	Age	Flexural Strength, N/mm²	Average	CoV, %	Flexural Strength, N/mm²	Average	CoV, %	Flexural Strength, N/mm²	Average	CoV, %	Flexural Strength, N/mm²	Average	CoV, %	Flexural Strength, N/mm²	Average	CoV, %
1	28	5.81	5.68	5.70	6.45	5.81	9.60	5.66	5.93	7.06	5.38	5.53	2.68	4.82	4.66	12.21
2	28	5.31			5.46			5.71			5.52			5.12		
3	28	5.92			5.51			6.41			5.68			4.02		

		NS w/c Series II			B-A Series II			B-B Series II			B-C Series II			B-D Series II		
Cube	Age	Compressive Strength, N/mm²	Average	CoV, %	Compressive Strength, N/mm²	Average	CoV, %	Compressive Strength, N/mm²	Average	CoV, %	Compressive Strength, N/mm²	Average	CoV, %	Compressive Strength, N/mm²	Average	CoV, %
1	1	13.47	13.20	1.87	14.65	14.51	2.81	14.33	14.61	1.69	17.98	17.95	2.68	16.18	16.48	2.78
2	1	12.99			14.05			14.70			18.41			16.26		
3	1	13.13			14.83			14.80			17.45			17.01		
4	7	41.56	39.05	5.84	47.78	48.21	1.11	49.28	49.22	1.13	48.88	48.39	1.48	47.00	48.32	2.37
5	7	38.47			48.03			49.75			47.57			48.99		
6	7	37.11			48.81			48.64			48.72			48.98		
7	28	51.20	50.47	1.27	56.70	57.60	2.51	60.60	60.45	1.77	57.90	59.35	2.44	59.20	58.48	2.48
8	28	50.20			58.10			58.90			61.00			59.30		
9	28	50.00			59.40			61.30			58.40			59.10		
10	28				56.20			61.00			60.10			56.30		
Beam	Age	Flexural Strength, N/mm²	Average	CoV, %	Flexural Strength, N/mm²	Average	CoV, %	Flexural Strength, N/mm²	Average	CoV, %	Flexural Strength, N/mm²	Average	CoV, %	Flexural Strength, N/mm²	Average	CoV, %
1	28	5.08	5.29	10.43	6.18	6.09	4.16	6.30	6.37	3.76	6.18	6.13	0.98	5.83	5.90	1.42
2	28	4.88			5.80			6.63			6.06			5.88		
3	28	5.92			6.29			6.17			6.13			5.99		

		GS-A Series II			GS-B Series II			GS-C Series II			GS-D Series II		
Cube	Age	Compressive Strength, N/mm²	Average	CoV, %	Compressive Strength, N/mm²	Average	CoV, %	Compressive Strength, N/mm²	Average	CoV, %	Compressive Strength, N/mm²	Average	CoV, %
1	1	14.57	14.75	1.08	19.57	19.76	1.96	18.69	18.40	1.69	16.91	17.23	1.68
2	1	14.84			19.51			18.07			17.48		
3	1	14.85			20.21			18.43			17.29		
4	7	43.99	44.26	1.27	43.93	43.83	1.59	42.90	43.23	0.75	41.82	41.66	0.41
5	7	43.88			44.47			43.55			41.48		
6	7	44.90			43.09			43.24			41.69		
7	28	56.80	55.00	2.83	55.70	55.28	1.86	55.00	55.55	2.13	54.00	52.98	2.63
8	28	53.30			54.20			57.30			51.00		
9	28	54.20			56.50			55.20			53.90		
10	28	55.70			54.70			54.70			53.00		
Beam	Age	Flexural Strength, N/mm²	Average	CoV, %	Flexural Strength, N/mm²	Average	CoV, %	Flexural Strength, N/mm²	Average	CoV, %	Flexural Strength, N/mm²	Average	CoV, %
1	28	5.17	5.36	4.06	5.65	6.00	5.64	4.95	5.37	7.31	5.61	5.91	10.57
2	28	5.60			6.02			5.72			5.50		
3	28	5.30			6.32			5.44			6.63		

		L-A Series II			L-B Series II			L-C Series II			L-D Series II		
Cube	Age	Compressive Strength, N/mm²	Average	CoV, %	Compressive Strength, N/mm²	Average	CoV, %	Compressive Strength, N/mm²	Average	CoV, %	Compressive Strength, N/mm²	Average	CoV, %
1	1	23.98	23.92	0.74	20.38	19.98	1.76	23.39	23.19	0.79	20.18	20.04	0.89
2	1	24.06			19.82			23.16			20.10		
3	1	23.72			19.73			23.03			19.84		
4	7	51.50	52.53	1.77	47.98	49.71	6.43	49.76	51.09	2.58	47.01	47.07	0.25
5	7	52.80			47.76			52.40			46.99		
6	7	53.30			53.40			51.10			47.20		
7	28	59.90	64.28	5.48	61.30	61.08	1.91	64.70	63.03	2.95	59.50	59.93	2.05
8	28	66.60			61.50			64.10			61.40		
9	28	67.60			62.10			60.50			58.50		
10	28	63.00			59.40			62.80			60.30		
Beam	Age	Flexural Strength, N/mm²	Average	CoV, %	Flexural Strength, N/mm²	Average	CoV, %	Flexural Strength, N/mm²	Average	CoV, %	Flexural Strength, N/mm²	Average	CoV, %
1	28	5.92	6.08	3.62	6.59	6.38	15.95	4.60	6.09	23.10	7.31	6.83	14.23
2	28	6.00			7.28			7.40			7.47		
3	28	6.33			5.28			6.27			5.71		

ANN model validation hardened concrete test data

		Validation LS dust			Validation NS			Validation G-C			Validation GS-B		
Cube	Age	Compressive Strength, N/mm²	Average	CoV, %	Compressive Strength, N/mm²	Average	CoV, %	Compressive Strength, N/mm²	Average	CoV, %	Compressive Strength, N/mm²	Average	CoV, %
1	7	34.62	34.88	1.27	44.03	44.49	0.90	40.51	41.19	1.86	42.69	42.39	0.94
2	7	34.63			44.78			42.02			42.54		
3	7	35.39			44.65			41.04			41.94		
4	28	44.32	44.12	0.53	55.90	55.70	0.62	54.50	53.50	2.20	52.30	53.63	3.24
5	28	44.18			55.30			53.80			55.60		
6	28	43.86			55.90			52.20			53.00		

Appendix D ANN model data

Training dataset

w/c	Admixture dosage, l/m^3	GMBV, g/kg	SE	Voids, %	Flow time, s	WA, %	Fines, %	Compressive strength, N/mm^2	Slump, mm
0.58	0.00	0.42	80.00	45.20	25.30	0.58	2.00	52.20	120.00
0.55	0.62	0.88	70.00	43.60	23.40	0.58	6.54	58.60	60.00
0.55	3.30	3.75	58.00	43.70	22.30	1.67	7.43	58.50	25.00
0.55	0.00	0.44	71.00	42.10	23.90	0.45	4.90	58.00	70.00
0.67	0.00	3.75	58.00	43.70	22.30	1.67	7.43	45.60	47.50
0.67	0.00	2.54	61.00	44.50	23.20	1.67	2.89	43.70	80.00
0.55	0.00	0.44	72.00	43.60	26.30	0.45	2.80	55.70	90.00
0.67	0.00	2.07	27.00	40.10	20.70	0.98	9.00	39.90	75.00
0.67	0.00	2.30	73.00	45.80	25.70	1.67	1.00	41.70	70.00
0.55	3.30	2.97	60.00	43.70	22.50	1.67	5.05	59.40	30.00
0.67	0.00	1.86	28.00	40.80	21.30	0.98	7.00	42.80	97.50
0.67	0.00	1.73	31.00	41.80	23.30	0.98	3.50	41.40	85.00
0.55	0.00	0.44	71.00	41.90	23.40	0.45	7.10	56.20	82.50
0.55	1.00	0.90	69.00	42.70	23.90	0.58	9.00	59.20	85.00
0.50	1.63	0.44	72.00	43.60	26.30	0.45	2.80	64.30	90.00
0.58	0.00	0.88	70.00	43.60	23.40	0.58	6.54	52.30	60.00
0.66	0.00	0.94	50.00	42.40	29.10	0.58	13.00	39.10	80.00
0.75	0.00	4.05	27.00	45.90	28.60	1.53	18.00	31.30	80.00
0.48	0.00	0.35	94.00	37.90	20.90	1.04	1.00	58.90	95.00
0.50	1.10	0.45	67.00	41.00	23.00	0.45	9.00	59.90	65.00
0.67	0.00	0.35	94.00	37.90	20.90	1.04	1.00	34.90	300.00
0.55	2.75	2.54	61.00	44.50	23.20	1.67	2.89	60.50	30.00
0.55	1.25	0.71	71.00	43.70	23.90	0.58	5.11	55.20	70.00
0.55	0.00	0.42	80.00	45.20	25.30	0.58	2.00	53.00	65.00
0.55	2.75	1.84	30.00	41.60	22.30	0.98	5.00	55.30	50.00
0.58	0.00	0.71	71.00	43.70	23.90	0.58	5.11	50.10	80.00
0.67	0.00	0.35	94.00	37.90	20.90	1.04	1.00	35.90	300.00
0.55	2.45	1.73	31.00	41.80	23.30	0.98	3.50	55.00	60.00
0.55	0.00	0.35	94.00	37.90	20.90	1.04	1.00	50.50	300.00
0.67	0.00	2.97	60.00	43.70	22.50	1.67	5.05	42.70	62.50
0.50	1.10	0.44	71.00	42.10	23.90	0.45	4.90	61.10	90.00
0.55	0.00	0.45	67.00	41.00	23.00	0.45	9.00	56.60	65.00
0.55	2.75	2.07	27.00	40.10	20.70	0.98	9.00	53.00	45.00
0.72	0.00	6.16	48.00	45.70	36.70	1.92	10.00	35.50	70.00
0.58	0.00	0.35	94.00	37.90	20.90	1.04	1.00	48.70	300.00

Testing dataset

w/c	Admixture dosage, l/m^3	GMBV, g/kg	SE	Voids, %	Flow time, s	WA, %	Fines, %	Compressive strength, N/mm^2	Slump, mm
0.58	0.00	0.50	74.00	44.60	24.40	0.58	2.85	49.90	80.00
0.55	2.75	2.30	73.00	45.80	25.70	1.67	1.00	57.60	60.00
0.61	0.00	0.65	65.00	42.40	32.40	0.62	12.00	50.20	60.00
0.55	0.00	0.35	94.00	37.90	20.90	1.04	1.00	50.50	300.00
0.58	0.00	0.90	69.00	42.70	23.90	0.58	9.00	48.10	60.00
0.67	0.00	1.84	30.00	41.60	22.30	0.98	5.00	43.30	75.00
0.55	2.75	1.86	28.00	40.80	21.30	0.98	7.00	55.60	50.00
0.55	0.00	0.50	74.00	44.60	24.40	0.58	2.85	59.20	67.50
0.50	1.35	0.44	71.00	41.90	23.40	0.45	7.10	63.00	75.00

ANN model weights

8-10-1 slump model weights

	from the input layer								
to the 1th hidden layer	bias	1th neuron	2th neuron	3th neuron	4th neuron	5th neuron	6th neuron	7th neuron	8th neuron
1th neuron	-1.8325	2.60594	1.68788	-0.75925	0.524125	-2.16847	-0.67903	0.27133	-1.40317
2th neuron	1.31745	-3.96221	0.484051	0.784313	-2.30523	0.211121	0.484442	-1.61697	0.308449
3th neuron	-1.0813	2.3922	0.625613	0.522801	2.49452	-2.36598	0.840879	0.329819	0.19454
4th neuron	-0.07282	-0.93425	-2.06761	1.30308	-0.50987	0.114656	1.34357	1.18559	1.13968
5th neuron	-1.13144	-0.48626	0.881727	-0.05701	-0.02292	0.640026	0.199067	0.15944	-0.14031
6th neuron	-0.92063	-1.31292	-0.10889	-0.11267	-0.61114	-0.36942	-0.12197	0.61463	0.21655
7th neuron	0.945502	1.06214	-0.9376	-0.94591	-1.13588	-0.29552	0.55545	-0.78649	0.246737
8th neuron	-0.06521	-1.03333	0.850154	1.18778	0.304966	0.54693	-1.18994	1.42724	-1.26727
9th neuron	0.845712	-0.82606	-2.15312	0.321239	-1.50194	0.699416	-0.98329	2.10501	1.4351
10th neuron	-0.21266	0.209885	-0.15057	-0.48165	-0.6705	0.358612	0.481611	-0.73044	0.612024

	from the 1th hidden layer										
to the output layer	bias	1th neuron	2th neuron	3th neuron	4th neuron	5th neuron	6th neuron	7th neuron	8th neuron	9th neuron	10th neuron
1th neuron	1.60549	3.21196	-3.31622	3.14891	-1.76079	0.221025	-0.49642	1.91909	-2.03667	-2.54666	0.801018

8-8-1 slump model weights

	from the input layer								
to the 1th hidden layer	bias	1th neuron	2th neuron	3th neuron	4th neuron	5th neuron	6th neuron	7th neuron	8th neuron
1th neuron	-0.92649	1.00336	-0.53613	-0.7522	-1.15805	0.040265	-0.20739	-0.47417	-0.67306
2th neuron	0.360571	-0.94245	-1.8403	0.555388	-1.29755	0.691297	-1.35484	1.91745	1.04944
3th neuron	0.147002	0.401574	-0.48359	0.476535	-0.05571	-0.40458	-0.42172	0.579492	0.252822
4th neuron	-1.26807	4.12846	-1.12972	0.113406	1.059	-0.25124	-0.32033	1.27461	-1.50471
5th neuron	-1.93977	4.32531	1.25044	0.285295	2.91099	-3.26447	0.7378	0.032918	-1.03921
6th neuron	0.712685	-0.87062	-1.19491	0.959709	0.439932	1.04618	0.733305	0.903463	-0.48382
7th neuron	0.79658	1.46631	-0.72335	0.904136	-1.2317	1.77262	0.891283	1.72095	0.693916
8th neuron	-0.53002	1.27427	-0.07825	-0.79632	0.438717	0.573895	0.712458	-0.35385	1.23951

	from the 1th hidden layer								
to the output layer	bias	1th neuron	2th neuron	3th neuron	4th neuron	5th neuron	6th neuron	7th neuron	8th neuron
1th neuron	-0.93685	1.11305	-2.27051	-0.04461	3.325	5.10101	-1.12739	-2.21136	1.63112

8-6-1 slump model weights

	from the input layer								
to the 1th hidden layer	bias	1th neuron	2th neuron	3th neuron	4th neuron	5th neuron	6th neuron	7th neuron	8th neuron
1th neuron	-0.04083	-1.90485	-1.25531	0.628235	-0.33512	0.862673	-0.4218	0.0121	0.851097
2th neuron	1.29411	-2.1427	-1.60371	0.834582	-1.67642	1.45107	-0.95732	1.17387	1.12021
3th neuron	-1.42747	2.28091	-0.16385	-1.06714	0.621544	-0.73945	-0.16441	1.42868	0.612258
4th neuron	0.300243	-5.31017	0.580201	-0.12191	-2.29893	0.754063	-0.56626	-1.24345	1.11926
5th neuron	-1.29204	-2.19352	0.652048	-1.96334	0.509076	-1.48726	-1.8124	-1.54131	-0.61407
6th neuron	0.340673	0.400306	-0.22429	-0.33826	-0.03046	-0.27724	1.10641	-1.72684	0.995308

	from the 1th hidden layer						
to the output layer	bias	1th neuron	2th neuron	3th neuron	4th neuron	5th neuron	6th neuron
1th neuron	1.08007	-1.6287	-3.22279	2.03827	-4.21074	4.00616	1.75834

8-4-1 slump model weights

	from the input layer								
to the 1th hidden layer	bias	1th neuron	2th neuron	3th neuron	4th neuron	5th neuron	6th neuron	7th neuron	8th neuron
1th neuron	-0.91222	5.10214	-0.44447	-1.20743	0.718769	-0.64854	0.150342	0.967643	-1.1486
2th neuron	0.96354	1.24866	0.602777	-0.4928	-1.35082	0.24792	0.665164	-1.35365	-0.42904
3th neuron	-1.20047	-0.75032	1.92277	-1.67115	1.87222	-1.08877	-0.10002	-2.17129	-0.76048
4th neuron	2.3792	-4.54525	-1.21271	0.184525	-2.7318	3.30446	0.226892	-0.24461	0.491099

	from the 1th hidden layer				
to the output layer	bias	1th neuron	2th neuron	3th neuron	4th neuron
1th neuron	-1.1391	3.74779	1.85487	3.70236	-5.31559

8-2-1 slump model weights

	from the input layer								
to the 1th hidden layer	bias	1th neuron	2th neuron	3th neuron	4th neuron	5th neuron	6th neuron	7th neuron	8th neuron
1th neuron	2.18607	-2.53397	-1.15596	1.26969	-1.56863	0.828079	-0.00688	2.09768	1.20227
2th neuron	-2.75768	5.17629	0.104102	-1.08621	1.44942	-3.39779	0.988899	1.18217	-0.98075

	from the 1th hidden layer		
to the output layer	bias	1th neuron	2th neuron
1th neuron	0.416596	-3.19873	6.69102

8-10-1 strength model weights

	from the input layer								
to the 1th hidden layer	bias	1th neuron	2th neuron	3th neuron	4th neuron	5th neuron	6th neuron	7th neuron	8th neuron
1th neuron	0.182768	1.86466	0.474815	-0.105633	-0.544298	-0.386643	1.15113	0.397583	-0.0564747
2th neuron	-0.301026	1.15385	0.605286	-0.684454	0.973304	-0.477415	-0.213985	0.412754	1.58497
3th neuron	0.901502	-1.95093	0.946588	-0.363215	-1.66065	-2.49083	0.413408	-0.457164	0.529712
4th neuron	-0.832207	-1.07401	0.8235	0.41249	0.940952	0.763619	0.194413	-0.598394	0.698796
5th neuron	0.266004	0.749553	1.78494	0.485004	-1.51839	-1.30222	0.563407	0.314282	0.796206
6th neuron	0.212646	0.567443	1.11103	0.407642	0.777352	-1.52595	0.653701	0.436038	-0.595083
7th neuron	-0.507508	2.38199	0.145351	0.337424	0.188714	-0.562027	1.2255	0.0430504	0.21585
8th neuron	-1.36917	-1.06175	0.717579	0.0903482	0.50234	0.611406	1.52481	-1.24137	0.695038
9th neuron	0.170618	-1.64284	0.951406	2.41224	0.205633	-0.0395722	-0.422722	1.53222	-0.0874216
10th neuron	-0.494839	0.265092	0.0324215	0.509502	0.340272	-0.476638	-0.687891	0.462701	-0.387656

	from the 1th hidden layer										
to the output layer	bias	1th neuron	2th neuron	3th neuron	4th neuron	5th neuron	6th neuron	7th neuron	8th neuron	9th neuron	10th neuron
1th neuron	0.0361337	-1.28774	-1.64625	1.80445	0.97892	-1.96707	-0.950866	-1.81036	1.98313	2.61299	-0.0679819

8-8-1 strength model weights

	from the input layer								
to the 1th hidden layer	bias	1th neuron	2th neuron	3th neuron	4th neuron	5th neuron	6th neuron	7th neuron	8th neuron
1th neuron	-0.688788	-1.86687	-0.214331	-0.417682	0.783852	-0.821429	1.19629	-0.258637	0.0621492
2th neuron	-0.562721	0.952034	0.844459	0.604754	0.426118	-2.40489	0.263004	-0.631269	0.569353
3th neuron	-0.5694	1.33941	-1.31349	-1.8134	-0.479444	-0.197991	0.0989537	-0.905969	-0.592361
4th neuron	-0.158852	-1.78242	-1.18114	0.196221	-0.752573	-0.158442	-0.425276	-0.432669	-0.487909
5th neuron	-1.02911	0.438216	1.73706	0.275593	-2.11875	1.07373	1.3832	0.187844	1.06862
6th neuron	0.0373895	-2.5077	0.490065	-0.377677	-0.167805	-1.86977	0.0259747	0.116616	0.844739
7th neuron	0.208452	-1.65638	1.20315	1.56683	0.343616	0.0642322	0.704044	-0.173131	0.449555
8th neuron	-0.523161	-0.728222	-0.60901	0.114071	-1.18913	1.52733	-0.423225	-0.561496	-0.663168

	from the 1th hidden layer								
to the output layer	bias	1th neuron	2th neuron	3th neuron	4th neuron	5th neuron	6th neuron	7th neuron	8th neuron
1th neuron	-0.931786	1.38025	-1.92782	-2.1577	1.44486	-3.27471	1.56707	2.1448	1.30384

8-6-1 strength model weights

	from the input layer								
to the 1th hidden layer	bias	1th neuron	2th neuron	3th neuron	4th neuron	5th neuron	6th neuron	7th neuron	8th neuron
1th neuron	-0.69716	1.33696	1.10796	1.46984	-1.29267	0.487983	0.923899	-0.280654	0.52268
2th neuron	-0.699079	-0.60181	0.609676	-0.169277	0.281904	-0.0717677	1.34252	-1.55985	0.88846
3th neuron	0.830143	-1.03657	1.28694	1.30756	0.704259	0.297506	0.693111	0.288332	0.674896
4th neuron	-0.897675	-1.39077	-0.469818	0.0956759	-0.503522	1.57664	-0.435563	-0.55236	-0.477337
5th neuron	-1.43744	2.52196	-0.0695127	-1.34626	1.44491	1.86836	-0.214905	-0.695308	0.441229
6th neuron	-0.37065	-1.8996	-0.44792	0.844947	1.03445	1.05416	-0.718608	0.103952	0.00536353

	from the 1th hidden layer						
to the output layer	bias	1th neuron	2th neuron	3th neuron	4th neuron	5th neuron	6th neuron
1th neuron	-1.17801	-2.33029	1.87954	1.22785	1.87361	-2.54536	1.81966

8-4-1 strength model weights

	from the input layer								
to the 1th hidden layer	bias	1th neuron	2th neuron	3th neuron	4th neuron	5th neuron	6th neuron	7th neuron	8th neuron
1th neuron	-0.38178	1.6935	0.221113	-0.0655989	1.3098	-0.783548	-0.878921	0.125095	0.90548
2th neuron	0.588847	-1.12785	1.26167	0.493821	-1.6224	0.10645	0.127402	-1.32559	-0.924451
3th neuron	-0.895273	3.18653	-0.131168	-1.22493	0.803841	1.4578	0.728069	-1.22745	-0.279586
4th neuron	0.228287	-2.27971	-1.64129	0.531646	2.29215	1.42518	-1.14711	-0.771911	0.363993

	from the 1th hidden layer				
to the output layer	bias	1th neuron	2th neuron	3th neuron	4th neuron
1th neuron	-0.935873	-2.3851	1.6637	-2.36941	3.01377

8-2-1 strength model weights

	from the input layer								
to the 1th hidden layer	bias	1th neuron	2th neuron	3th neuron	4th neuron	5th neuron	6th neuron	7th neuron	8th neuron
1th neuron	1.50173	-4.5182	-0.723734	1.20446	-0.110281	0.994987	-1.69958	-0.65845	-0.425947
2th neuron	-0.0379658	3.45186	-0.304848	0.146015	-0.316773	-0.0172784	-2.44531	-0.591053	-1.32258

	from the 1th hidden layer		
to the output layer	bias	1th neuron	2th neuron
1th neuron	-0.774623	4.59408	-3.82128

Appendix E ICP-OES results

Table E1 ICP-OES sample mass and volume

Sample	Mass, g	Volume, ml
G	0.1082	50
B	0.1007	50
R	0.1006	50
L	0.1066	50
GS	0.1053	50

Table E2 ICP-OES results

Sample	B	G	R	L	GS	B	G	R	L	GS
Element	Concentration, mg/L					Oxide, %				
Ag	0.0	0.0	0.0	0.0	0.0	0.0	0.0	0.0	0.0	0.0
Al	111.9	142.8	4.1	12.8	143.0	9.8	13.4	0.4	1.1	12.8
As	0.0	0.0	0.0	0.0	0.0	0.0	0.0	0.0	0.0	0.0
Ba	0.5	2.6	0.0	35.9	1.4	0.0	0.1	0.0	1.9	0.1
Be	0.0	0.0	0.0	0.0	0.0	0.0	0.0	0.0	0.0	0.0
Bi	0.0	0.0	0.0	0.0	0.0	0.0	0.0	0.0	0.0	0.0
Ca	100.6	59.5	726.0	400.0	16.4	6.5	4.1	50.5	26.3	1.1
Cd	0.0	0.0	0.0	0.0	0.0	0.0	0.0	0.0	0.0	0.0
Co	0.1	0.0	0.0	0.0	0.1	0.0	0.0	0.0	0.0	0.0
Cr	0.1	0.1	0.0	0.0	0.2	0.0	0.0	0.0	0.0	0.0
Cu	0.2	0.0	0.0	0.0	0.1	0.0	0.0	0.0	0.0	0.0
Fe	176.2	33.6	2.6	27.9	74.5	11.6	2.4	0.2	1.9	5.1
K	19.0	67.8	1.4	5.6	58.2	1.1	4.1	0.1	0.3	3.3
Li	0.0	0.1	0.0	0.0	0.1	0.0	0.0	0.0	0.0	0.0
Mg	64.7	12.7	7.1	185.0	19.7	5.0	1.0	0.6	14.4	1.6
Mn	2.4	0.9	0.4	2.6	1.7	0.1	0.1	0.0	0.2	0.1
Mo	0.0	0.0	0.0	0.0	0.0	0.0	0.0	0.0	0.0	0.0
Na	42.5	58.6	2.0	3.0	10.7	2.6	3.9	0.1	0.2	0.7
Ni	0.1	0.0	0.0	0.0	0.1	0.0	0.0	0.0	0.0	0.0
Pb	0.0	0.0	0.1	0.2	0.1	0.0	0.0	0.0	0.0	0.0
Sb	0.0	0.0	0.0	0.0	0.0	0.0	0.0	0.0	0.0	0.0
Se	0.0	0.0	0.0	0.0	0.0	0.0	0.0	0.0	0.0	0.0
Si	414.9	593.6	56.9	88.2	698.2	41.0	63.1	6.1	8.9	70.9
Sr	0.8	0.9	0.5	0.7	0.2	0.0	0.1	0.0	0.0	0.0
Ti	22.0	4.9	0.2	0.7	8.4	1.7	0.4	0.0	0.1	0.7
Tl	0.0	0.0	0.0	0.1	0.0	0.0	0.0	0.0	0.0	0.0
V	0.6	0.1	0.0	0.0	0.2	0.0	0.0	0.0	0.0	0.0
Zn	0.3	0.1	0.1	0.4	0.7	0.0	0.0	0.0	0.0	0.0